Optimisation-based retrofit of heat-integrated distillation systems

A thesis submitted to The University of Manchester for the degree of

Doctor of Philosophy

in the Faculty of Engineering and Physical Sciences

2016

Víctor Manuel Enríquez Gutiérrez

School of Chemical Engineering and Analytical Science

Contents

List of Figures

List of Tables

Abbreviations

ANN	Artificial neural networks
CDU	Crude oil distillation unit
DFO	Derivative free optimiser
FOQUS	Framework for optimisation and quantification of uncertainty and sensitivity
FUA	Fractional utilization of area
FUG	Fenske-Underwood-Gilliland
GS	Global search
HEN	Heat exchanger network
HETP	Height equivalent of a theoretical plate, m
HRAT	Heat recovery approach temperature
LP	Linear programming
MESH	Mass, equilibrium, summation and heat equations (rigorous methods)
MINLP	Mixed integer non-linear programming
NLP	Non-linear programming
SA	Simulated annealing
SQP	Successive quadratic algorithm

Symbols

a	Packing surface area, $m^2\ m^{-3}$
A_{ac}	Tray active area, m^2
A_{acnew}	Increase in active area due sloped downcomers, m^2
A_{DC}	Downcomer area, m^2
A_{DCbtm}	Active area gained at the bottom downcomer, m^2
A_{DCtop}	Top downcomer area, m^2
$A_{flooding}$	Constant used in Eqs. 2.24 and 2.26
A_T	Cross sectional area, m^2
$B_{flooding}$	Constant used in Eqs. 2.25 and 2.27
CF	Vapour capacity factor
$CP_{flooding}$	Capacity parameter at flooding conditions
C_{sb}	Operational capacity factor (C-factor)

$C_{sb,flooding}$	Capacity factor at flooding conditions
C_{xy}	Effect of the area of inclination
D_c	Distillation column diameter, m
$\dot{F}$	Molar flow rate of the feed, kmol s^{-1}
F_{lv}	Flow parameter
F_p	Packing factor, m^{-1}
%Flooding	Approach to jet flooding in Eq. 2.6; flooding in Eq. 2.19
h	Molar enlthalpy, kJ $kmol^{-1}$ K^{-1}
H_{cl}	Downcomer clearance, m
K	Constant of equilibrium
$\dot{L}$	Molar flow rate of the side stream of a distillation column, kmol s^{-1}
L_w	Liquid weir load, m^3 m^{-1} h^{-1}
l_w	Weir length, m
N_p	Number of passes per tray
P	Pressure, bar
Q	Heat flow rate, kJ $kmol^{-1}$
$\dot{S}$	Molar flow rate of the side stream of a distillation column, kmol s^{-1}
T	Temperature, K
T_{FL}	Tray flow path length
T_s	Tray spacing, m
v_{DCdes}	Downcomer design velocity, m s^{-1}
v_{DCexit}	Downcomer exit velocity, m s^{-1}
$\dot{V}$	Molar flow rate of the vapour phase, kmol s^{-1}
V_G	Volumetric vapour load, m^3 s^{-1}
V_L	Volumetric liquid load, m^3 s^{-1}
V_{load}	Vapour load factor, m^3 s^{-1}
x	Molar fraction of the liquid phase
y	Molar fraction of the vapour phase
z	Molar fraction of the feed

Greek letters

ρ_G	Vapour density, kg m^{-3}
ρ_L	Liquid density, kg m^{-3}
θ	Downcomer slope angle relative to the vertical, degrees (in Eq. 2.17)
μ_L	Liquid viscosity, kg m^{-1} s^{-1}

$\Delta P_{flooding}$	Flooding pressure drop, Pa m^{-1}
σ	Surface tension, mN m^{-1}

Optimisation-based retrofit of heat-integrated distillation systems

Victor Manuel Enríquez Gutiérrez

The University of Manchester

2016

Abstract — PhD in Chemical Engineering and Analytical Sciences

Distillation systems consist of one or more distillation columns, in which a mixture is separated into higher-value products, and a heat exchanger network (HEN) that recovers and reuses heat within the system. For example, crude oil distillation systems comprise crude oil distillation units (CDU), in which crude oil is distilled into products for downstream processing, a HEN and a furnace. Heat-integrated distillation systems present complex interactions between the distillation columns and HEN. These interactions, together with the many degrees of freedom and process constraints, make it challenging to retrofit or modify the operating conditions of existing distillation processes to accommodate changes in process operating conditions.

Retrofit designs aim to re-use existing equipment when process objectives change, for example to increase throughput, improve product quality, or reduce energy consumption or environmental impact. To achieve these retrofit objectives, operational, structural and/or flowsheet modifications to the overall system (distillation columns and HEN) may be considered, subject to specifications and system constraints. This work proposes an optimisation-based approach to retrofit design for the capacity expansion of heat-integrated distillation systems, with a particular focus on crude oil distillation systems.

Existing retrofit approaches found in the open research literature consider operational optimisation, replacing column internals, adding preflash or prefractionation units and HEN retrofit to increase the capacity of existing systems. Constraints considered usually relate to the distillation column hydraulic limits, product quality specifications and heat exchanger performance (e.g. minimum temperature approach and, pressure drop). However, no existing methodologies consider these possible modifications simultaneously; thus, beneficial interactions between flowsheet modifications, operational changes, heat integration and equipment modifications may be missed.

In this work, retrofit design solutions for crude oil distillation are developed using a stochastic optimisation framework implemented in MATLAB to optimise the system operating parameters and to propose flowsheet, column and HEN modifications. Within the framework, the optimiser can propose addition of a preflash unit, modifications to the CDU internals and changes to its operating conditions; the separation system is then simulated using Aspen HYSYS (via the MATLAB interface) and the hydraulic performance of the column is analysed using published hydraulic correlations. The optimiser also proposes modifications to the HEN (i.e. installed heat transfer area, HEN structure and operating conditions), which is then simulated to evaluate heating and cooling utility demand. Either simulated annealing and global search optimisation algorithms are applied to identify the optimal design and operating conditions that meet the production requirements and product specifications.

Industrially relevant case studies demonstrate the effectiveness and benefits of using the proposed retrofit approach. The case studies illustrate that combined structural and operational modifications can be effectively and systematically identified to debottleneck an existing crude oil distillation system with a relatively short payback time, while simultaneously reducing energy consumption per barrel of crude oil processed.

Declaration

No portion of the work referred to in the thesis has been submitted in support of an application for another degree or qualification of this or any other university or other institute of learning.

Victor Manuel Enríquez Gutiérrez

Copyright Statement

i. The author of this thesis (including any appendices and/or schedules to this thesis) owns certain copyright of related rights in it (the “Copyright”) and s/he has given The University of Manchester certain rights to use such Copyright, including for administrative purposes.

ii. Copies of this thesis, either in full or in extracts and whether in hard or electronic copy, may be made **only** in accordance with the Copyright, Designs and Patents Act 1988 (as amended) and regulation issued under it or, when appropriate, in accordance with licensing agreements which the University has from time to time. This page much form part of any such copies made.

iii. The ownership of certain Copyright, patents, designs, trade marks and other intellectual property (the “Intellectual Property”) and any reproductions of copyright works in the thesis, for example graphs and tables (“Reproductions”), which may be described in this thesis, may not be owned by the author and may be owned by third parties. Such Intellectual Property and Reproductions cannot and must not be made available for use without the prior written permission of the owner (s) of the relevant Intellectual Property and/or Reproductions.

iv. Further information on the conditions under which disclosure, publication and commercialisation of this thesis, the Copyright and any Intellectual Property and/or Reproductions described in it may take place in available in the University IP Policy (see http://documents.manchester.ac.uk/DocuInfo.aspx?DocID=487), in any relevant Thesis restriction declarations deposited in the University Library, The University Library’s regulations (see http://www.library.manchester.ac.uk/aboutus/regulations) and in The University’s policy on Presentation of Theses.

Acknowledgement

First of all, I would like to express my very great appreciation to Dr. Megan Jobson for her patience guidance, enthusiastic encouragement and constructive suggestions during the planning and development of this research work. Her willingness to give her time so generously to provide feedback for the reports, presentations, posters and this Thesis has been very much appreciated.

My grateful thanks are also extended to Prof. Robin Smith for sharing his vast industrial and academic experience to enrich this work. I would also like to thank him for giving me the opportunity of presenting my work at the “Processes Integration Research Consortium” and for the help and feedback provided to prepare the presentations. Both Dr. Megan Jobson and Prof. Robin Smith have been a great source of inspiration.

I wish to acknowledge the financial support of the Mexican National Council of Science and Technology (CONACyT no 333680/215899) and the Roberto Rocca Education Program. Thank you for making this dream come true.

I would also like to thank my friends and colleagues from the Centre for Process Integration (CPI). Many thanks for the laughs, foods and drinks we have shared. Special thanks are extended to my very good friends Lluvia, María, Mary, Gbemi and Katerina for their great support and contributions to this work, and all the hours we have spent talking and laughing. I will always carry you in my hearts.

To my friends back in Mexico and here in Manchester Marthita, Frida, Gaby, Andrés, Laura, Maialen and Arkatiz for giving me their honest and true friendship. I could not ask for better friends. My special thanks to Miguel for his company, love and support throughout my PhD. Thank you very much for making my life better.

Finally, I would like to thank my parents, my sister, my aunts, uncles and cousins for their words of encouragement and love. Without your unconditional support throughout my whole life, I would probably not be here.

Dedication

To my parents, Victor and Silvia, for their unconditional love, support and for always believe in me. I cannot express with words how much I love you and how grateful I am for all the sacrifices you have done for me.

To my sister Marisa, for her love and for always knowing how to make me laugh. I love you with all my heart.

Chapter 1 Introduction

Distillation is one of the most commonly used separation units (Rapoport et al., 1994). However, it is one of the most energy intensive processes in the chemical industries. To reduce the energy demand of distillation columns, heat integration can be applied to recover heat between the streams needing cooling and heating (Smith, 2005, Ch. 14). These types of systems are known as heat-integrated distillation systems.

Crude oil distillation is an example of a heat-integrated distillation system, where the crude oil is pre-heated using product and process streams, resulting in a complex system with strong interactions between the crude oil distillation unit (CDU) and its associated heat exchanger network (HEN).

To stay competitive in the market, processes need constant improvement through retrofit (Uerdingen et al., 2003). Retrofit aims to exploit existing assets, and may also include changes to the flow sheet and/or equipment structure (e.g. adding separation equipment, replacing column internals) (Rapoport et al., 1994).

Increasing the throughput, reducing the operating cost and/or the environmental impact, changing feedstock and increasing product yields and quality are examples of retrofit objectives that can increase the profitability of a process (Liu and Jobson, 2004).

The retrofit of heat-integrated distillation systems is a complex problem with many degrees of freedom and constraints, since any operating or structural modification of the distillation column will have an impact on the associated heat recovery system (Gadalla, 2003).

This work presents a retrofit approach for the capacity expansion of heat-integrated distillation systems in order to increase their profitability; the main focus is on crude oil distillation systems.

This approach builds on existing methods for simulation and hydraulic analysis of distillation columns, HEN retrofit and optimisation and aims to overcome the limitations of existing retrofit approaches for heat-integrated distillation systems.

Section 1.1 presents a review and discussion of the features of existing retrofit approaches for heat-integrated distillation systems found in the open literature, in order to motivate this work and support its objectives.

1.1 Retrofit approaches for heat-integrated distillation systems

Retrofit methodologies aim to find design solutions that overcome the physical and operating constraints (e.g. the maximum capacity of the equipment, the quality specification of the products) that limit an existing process. These limits are also known as bottlenecks. Existing retrofit methodologies for heat-integrated distillation systems can be classified into two categories: sequential and simultaneous approaches. Sequential approaches analyse and debottleneck the distillation column and HEN separately until the retrofit objective is reached, while simultaneous approaches aim to find the optimum conditions that satisfy the retrofit objective (Gadalla et al., 2013). In this work, the retrofit objective is to enhance production capacity.

1.1.1 Sequential approaches

Gadalla (2003) proposes a systematic retrofit approach for heat-integrated crude oil distillation systems capable of increasing capacity, reducing energy consumption, reducing CO_2 emissions, increasing profit and maximising product yield. In this approach, the CDU is simulated using shortcut models (Gadalla et al., 2003b), the hydraulic performance of the CDU is assessed in terms of the required diameter, estimated using Fair's correlation for jet flooding (Fair, 1961), the HEN is simulated in SPRINT (Department of Process Integration, 2002), and an area-energy curve, constructed using network pinch analysis (Asante and Zhu, 1997), is used to analyse beneficial modifications for HEN retrofit. The retrofit modifications considered to achieve the objectives include CDU operating parameters (i.e. furnace outlet temperature, stripping steam flow rates, and pumparound duties and temperature drops) and HEN structure modifications (i.e. adding, deleting, resequencing and repiping heat exchangers). Practical constraints are imposed during the optimisation (i.e. hydraulic constraints, product quality specifications, HEN constraints).

Gadalla (2003) formulates the optimisation as a non-linear programming (NLP) problem; thus, structural design decisions are not included in the optimisation. However, Gadalla (2003) presents methodologies to systematically assess replacing column internals and adding preflash. The main drawbacks of this approach are that the downcomer hydraulics

are not accounted for, which may lead to unfeasible column designs, and that the costs associated with HEN retrofit are not considered, which may overestimate the profitability of the system (Chen, 2008). Also, heat capacities are assumed to be constant with temperature, which is an unrealistic approach for crude oil (Chen, 2008).

Thernesz et al. (2010) presents a sequential retrofit methodology for increasing the processing capacity and/or changing the crude type of crude oil distillation systems. This approach (Thernesz et al., 2010) uses commercial simulation software to simulate the system and to analyse its constraints: PRO/II (Invensys Process Systems, 2005) is used to simulate the CDUs, KG-Tower (Koch-Glitsch, 2005) and SULCOL (Sulzer Chemtech, 2005) are used to assess the hydraulic performance of the CDUs and SUPERTARGET (KBC Energy Services, 2005) is used to simulate and to retrofit the HEN. The modifications permitted to the CDUs and HEN are replacing column internals with high-capacity trays and/or structured packings, and adding, deleting and resequencing heat exchangers.

The advantage this retrofit methodology (Thernesz et al., 2010) is that it uses a high level of detail to simulate the system and to assess the retrofit scenarios. However, it requires significant engineering effort, since commercial simulation software cannot work together and each retrofit scenario needs to be analysed separately. The structural design decisions (i.e. replacing column internals and HEN modifications) are taken based on observation and experience. This work does not consider operational optimisation.

Wang et al. (2011) propose a methodology to systematically find the best predistillation scheme (i.e. adding preflash or prefractionator before the furnace) to retrofit a CDU that process heavy crude oils. Wang et al. (2011) use rigorous simulation to simulate the CDU, preflash and prefractionator. The criterion to determine the best retrofit design is based on exergy analysis.

In this methodology (Wang et al., 2011), neither operational optimisation nor HEN retrofit are considered due to lay-out constraints. The drawback of this methodology is that it requires significant engineering time and effort to analyse different predistillation schemes, including the structural design decisions associated with these designs (e.g. the flashed vapour feed location). Also, exergy analysis does not reflect the effect of the proposed modifications on the CDU hydraulics or on the quality and yield of the products; thus, unfeasible design may be obtained.

Gadalla et al. (2015) develop a simulation-based procedure for reducing the energy consumption and CO_2 emissions of existing crude oil distillation columns. The procedure

(Gadalla et al., 2015) can be summarised as follows: i) the CDU and the crude oil pre-heat train are simulated in Aspen HYSYS, ii) composite curves are generated from the simulation results to estimate the energy targets and, iii) based on this analysis, operational (i.e. furnace outlet temperature, reflux flow rate, pumparound duties and temperature drops, side-stripper flow rates), structural (i.e. adding pumparounds, adding heat transfer area, repiping and resequencing existing heat exchangers, adding new heat exchangers) and flow sheet (i.e. adding a preflash unit) modifications are proposed until the energy targets are met. Jet flooding only is estimated to avoid unfeasible designs.

The drawbacks of this approach (Gadalla et al., 2015) is that it does not consider operational optimisation, neglects the downcomer hydraulics and relies on trial and error to propose retrofit modifications. Also, it requires significant engineering effort and time to analyse multiple retrofit scenarios.

1.1.2 Simultaneous approaches

Chen (2008) proposes an optimisation-based retrofit approach for increasing the profitability of heat-integrated distillation systems. This approach (Chen, 2008) divides the problem into two levels. In the first level, simulated annealing is used to change the CDU operating parameters (i.e. furnace outlet temperature, stripping steam flow rates, and pumparound duties and temperature drops), and then the CDU is simulated using shortcut methods (based on those of Suphanit (1999) and Gadalla et al. (2003b)). In the second level, the HEN is simulated and retrofitted using an optimisation-based retrofit approach based on network pinch analysis (Asante and Zhu, 1997). Practical constraints are imposed during the optimisation, such as column jet flooding, product quality specifications and minimum temperature approach constraints. The HEN retrofit approach, further published by Smith et al. (2010b), does account for the dependence of the heat capacities of the crude oil and its products on temperature.

The advantage of the approach of Chen (2008) is that it captures the interactions between the CDU and the HEN, since the whole system is optimised simultaneously. However, the downcomer hydraulics are not accounted for. The drawback of this approach is that shortcut models do not provide the stage wise information needed to perform a hydraulic analysis of the CDU. Replacing column internals and/or adding preflash are not considered.

López C. et al. (2013) present an approach to optimise the operating conditions and crude oil blending for a crude oil distillation unit in order to increase its profitability. The approach

is formulated as a non-linear programming (NLP) model; thus structural design decisions, such as replacing internals and/or adding a preflash unit are not considered. To simulate the CDU, second-order polynomial equations regressed from results of rigorous simulations are used. These equations, also known as metamodels, correlate the relationships between the input variables (i.e. crude oil flow rates, input and output furnace temperatures, condenser temperature and pressure, pumparound flow rates and temperature drops, stripping steam flow rates) with the product yields and quality specifications. Practical constraints are imposed during the optimisation.

The advantage of the approach of López C. et al. (2013) is that it is computationally inexpensive, as deterministic models can be used for optimisation. However, representing integer variables (e.g. replacing column internals, finding flashed vapour feed location) with metamodels can be hard, since it might be difficult to obtain representative simulations for all the possible combinations (Ochoa-Estopier et al., 2014).

Ochoa-Estopier et al. (2015b) propose a framework for the operational optimisation of heat-integrated crude oil distillation systems. Similar to Chen (2008), the approach is divided into two levels. In the first level, SA is used to change the CDU operating conditions, and the CDU is simulated using artificial neural network (ANN) models regressed from rigorous simulations (Ochoa-Estopier and Jobson, 2015a). In the second level, the HEN is retrofitted using a retrofit approach based on that one of Chen (2008), in which the HEN structure is represented using the principles of graph theory (de Oliveira Filho et al., 2007) instead of the network pinch concept (Asante and Zhu, 1997). The objective of the optimisation is to increase the profitability of the system; practical constraints related to column jet flooding, product quality specifications and HEN practical constraints are accounted for.

The advantage of the optimisation framework of Ochoa-Estopier et al. (2015b) is that it is capable of exploiting the interactions between the CDU and the HEN, as the system is optimised simultaneously. However, the use of metamodels to simulate the CDU limits the capability of the approach to include structural design decisions within the optimisation. Furthermore, the metamodels do not provide stage-by-stage information to perform a hydraulic analysis of the CDU.

Chen et al. (2015) propose a simultaneous process optimisation and heat integration approach that aims to find the design parameters and operating conditions of a process that maximise or minimise an objective function. In the case studies presented, the approach is applied to maximise the profit of a methanol production process, to minimise

the operating costs of a separation process for benzene and to maximise the net power efficiency of a supercritical coal power plant with carbon capture and compression.

The simultaneous approach of Chen et al. (2015) takes advantage of the capability of some rigorous simulation software (e.g. Aspen Plus, Aspen HYSYS, Aspen Custom Modeller, gPROMS) to be linked with equation-based modelling environments (e.g. GAMS, MATLAB). In this approach, data is transferred between a derivative free optimiser (DFO), rigorous simulation software, a heat integration module and a system performance evaluator.

The DFO used to propose new values for the decision variables (i.e. design parameters or operating conditions) is the Covariance Matrix Adaptation Evolutionary Strategy, a global search optimisation method suitable for nonlinear nonconvex problems in continuous domains (Hansen, 2006). The decision variables are used as inputs for rigorous simulation software (i.e. Aspen Plus, Aspen Custom Modeller, gPROMS) where the process is modelled. Once the simulation model is converged, data are extracted (i.e. stream temperatures and heating and cooling loads) and sent to the heat integration module. The heat integration module, coded in GAMS, is based on the linear programming (LP) transhipment model for a given heat recovery approach temperature (HRAT) of Papoulias and Grossmann (1983), which predicts the minimum utility cost, and the LP area target model proposed by Jeżowski et al. (2003), which predicts the minimum heat exchanger area target based on the results of the minimum utility cost. The results from the process simulation and the heat integration module are returned to the DFO to evaluate the objective function. This process is repeated until the objective function is satisfied or the maximum number of iterations is reached. The optimisation framework, the process simulation and the heat integration module are implemented within Python using the Framework for Optimization and Quantification of Uncertainty and Sensitivity (FOQUS) (Miller et al., 2014).

The advantages of the approach of Chen et al. (2015) are that it is ‘easy’ to implement and that it uses high-fidelity models directly, since rigorous simulation software is used to model the process that is desired to optimise. The drawback of the approach is that it does not consider structural changes to the distillation column (e.g. replacing column internals and/or adding a preflash unit) or the HEN (e.g. adding, deleting, repiping, and resequencing heat exchangers). The approach of Chen et al. (2015) has not been implemented in the context of retrofitting heat-integrated crude oil distillation systems in order to increase their processing capacity.

The approaches of Chen (2008), Ochoa-Estopier et al. (2015b) and Chen et al. (2015) provide useful guidance on how to exploit the interactions between the CDU and the HEN.

1.1.3 Retrofit approaches — summary and conclusions

In summary, most of the existing retrofit approaches for heat-integrated crude oil distillation systems have neglected the downcomer hydraulics and do not include structural design decisions, such as replacing column internals and adding a preflash unit, within the optimisation. Thus, unfeasible column designs might not be avoided and heat integration opportunities may be neglected.

Three methods are used in the existing retrofit methodologies to simulate the distillation columns: shortcut methods (Gadalla, 2003; Chen, 2008), rigorous methods (Thernesz et al., 2010; Wang et al., 2011; Gadalla et al., 2015; Chen et al., 2015) and metamodels (López C. et al., 2013; Ochoa-Estopier et al., 2015b). Of these three methods, only rigorous methods provide the stage-wise information needed to perform a hydraulic analysis of the distillation column and to date have been only rigorous models implemented within optimisation environments that include structural design decisions (Caballero et al., 2005).

An extensive literature review was performed and a retrofit methodology for crude oil distillation systems that include structural design decisions within the optimisation was not found. Only the design methodology of Caballero et al. (2005) include this option.

The design approach of Caballero et al. (2005) proposes using a superstructure-based optimisation algorithm to find the optimal column configuration (i.e. number of stages, feed location) and column operating conditions (i.e. reflux ratio, condenser and reboiler heat loads). The approach divides the problem into two: in the first sub-problem, the optimal number of trays is found, and in the second sub-problem, the optimal operating conditions (i.e. entrainer-to-feed ratio, reflux ratio, molar composition in the product streams) are found using an external NLP solver. This is accomplished by connecting a process simulator (Aspen HYSYS) with an external solver developed in MATLAB. The design approach is applied for the extractive distillation of ethanol using ethylene glycol as entrainer, but its application to column design or retrofit has not been reported.

HEN retrofit methodologies that consider structural modifications to the HEN and temperature-dependent heat capacities for the crude oil and its products, and that can be included within optimisation environments are available (Chen, 2008; Ochoa-Estopier et al., 2015a). However, none of these HEN retrofit approaches have been used together

with rigorous simulation-based models for distillation system design, retrofit or optimisation.

Optimisation-based approaches are more suitable for the retrofit of these types of systems than the approaches that analyse each unit individually (i.e. first the distillation column, then the HEN or vice versa), since they require less engineering effort to analyse multiple retrofit scenarios and can capture interactions between the CDU and the HEN. However, the approaches of Chen (2008) and Ochoa-Estopier et al. (2015b) are computationally expensive. SA has been successfully used to optimise both, the distillation column operating parameters and the HEN structure (Chen, 2008; Ochoa-Estopier et al., 2015b).

In conclusion, in order to exploit the capacity of existing heat-integrated distillation systems, an optimisation-based retrofit approach that includes structural design decisions is needed. To date, structural design decisions have only been implemented using rigorous simulation of the distillation column. Rigorous simulation provides stage-wise information for column hydraulic analysis; however a methodology to consider constraints related with both jet and downcomer flooding is lacking. Optimisation-based HEN retrofit approaches are available, but these need to be adapted to be used together with column rigorous simulation.

1.2 Heat-integrated crude oil distillation systems technology overview

The main focus of this work is the capacity expansion of heat-integrated crude oil distillation systems. This section summarises the features of these types of systems.

Crude oil is a mixture of hydrocarbons with a small amount of other components (e.g. sulphur, oxygen, nitrogen, metals) (Treese et al., 2015). From the refining of crude oil, several products with a high commercial value are produced, such as gasoline, diesel, jet fuel, etc. (Gary, 2007).

The first unit operation that is found in a refinery is the crude oil distillation unit. Figure 1.1 illustrates an example of a crude oil distillation system. Before entering the crude oil distillation unit (CDU), the crude oil is preheated to around 370°C using a HEN formed with the product and process streams and a fired heating furnace (Treese et al., 2015).

The CDU has a complex structure. It consists of a main fractionator and side-strippers from where the distillation products are produced, pumparounds that recover heat from the system and increase the reflux and a condenser. Usually, the main fractionator uses live steam as stripping agent, and the side-strippers can used steam or reboilers.

Crude oil distillation systems are energy intensive. It is estimated that their energy consumption is equivalent to 1-2% of the crude oil processed (Errico et al., 2009); some authors estimate 7-15% (Szklo and Schaeffer, 2007).

Retrofit methodologies to increase the profitability of crude oil distillation systems are commonplace. These methodologies aim to exploit the interactions between the CDU and the HEN in order to enhance the profitability of the system. However, the retrofit of this type of systems is a non-trivial problem with many degrees of freedom and constraints.

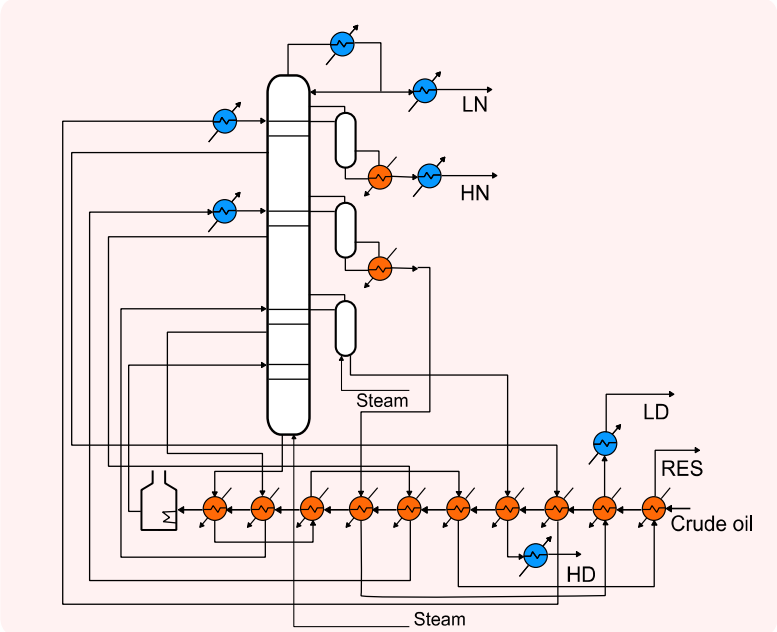

Figure 1.1 Crude oil distillation system

1.3 Motivation and objectives of this work

This work is motivated by the need for a retrofit approach for the capacity expansion of heat-integrated distillation systems that overcomes the limitations of existing approaches. Thus, the overall objective of this work is to develop such approach. This work is mainly focussed on crude oil distillation systems, as this process is widely used and important in petroleum refining.

To overcome the limitations of current practice and approaches presented in the research literature, an effective approach needs to consider operational optimisation, replacing column internals with high-capacity trays and structured packings, adding a preflash unit and HEN retrofit. Practical constraints need to be considered, such as the hydraulic performance of the distillation column, product quality specifications and HEN constraints (i.e. minimum temperature approach, target temperatures, existing heat transfer area).

The specific objectives of this work are to:

1. Develop a methodology to assess the hydraulic performance of distillation columns using rigorous simulation and to analyse replacing column internals with high-capacity trays and/or structured packings.
2. Apply a HEN retrofit approach to ensure adequate heat transfer and to account for interactions between the distillation column and HEN, and potentially a new preflash unit.
3. Propose a methodology to include rigorous simulation of distillation columns, hydraulic analysis of distillation columns and HEN retrofit within an optimisation environment, using suitable optimisation algorithms.
4. Include a methodology within the optimisation environment to evaluate the option of replacing column internals.
5. Include a methodology within the optimisation environment to evaluate the option of adding a preflash unit.
6. Demonstrate the effectiveness of the approach through industrially-relevant case studies.

1.4 Overview of this work

This thesis is organised in six chapters using the 'Alternative Format' of the University of Manchester, incorporating papers published or to be submitted for publication. It is acknowledged that there is some overlap and repetition within the Thesis, especially related to the reviews of research literature; this is necessary to allow each paper to stand alone.

Chapter 1 presents a brief discussion of retrofit approaches for heat-integrated distillation systems from the open research literature and an overview of heat-integrated crude oil distillation systems technology, in order to establish the objectives of this work.

Chapter 2 presents a literature review of modelling of distillation columns, hydraulics of distillation columns, HEN design and retrofit and optimisation. This chapter aims to support the literature review of the publications presented in the following chapters.

Chapter 3 presents a retrofit methodology to assess replacing column internals when increasing the processing capacity of heat-integrated distillation systems. An industrially relevant case study shows that using the proposed methodology reduces the engineering time and effort when exploring different retrofit scenarios.

Chapter 4 presents an optimisation-based retrofit approach for heat-integrated crude oil distillation systems. The approach incorporates the methodology described in Chapter 3 into an optimisation framework that uses stochastic optimisation to propose changes to the column operating and the HEN structure, in order to increase the profitability of a system when increasing its processing capacity. An industrially relevant case study shows the benefits of using the proposed approach.

Chapter 5 extends the optimisation-based retrofit approach presented in Chapter 4 by including structural design decisions (i.e. replacing column internals and adding a preflash unit) within the optimisation environment. The chapter is divided in two parts. The first part presents the approach proposed for replacing column internals, the second part the approach proposed for adding a preflash unit. Industrially relevant case studies show the capability of the approach to explore and to assess operational, structural and flowsheet modifications simultaneously.

Chapter 6 summarises the main contributions of this work, discusses the assumptions of the proposed retrofit approach, and recommends some future work.

Chapter 2 Literature review

This section aims to complement the literature reviews of the papers presented in Chapters 3 to 5 and in Appendix A (Enríquez-Gutiérrez et al., 2014; Enríquez-Gutiérrez et al., 2015; Enríquez-Gutiérrez and Jobson, 2016a; Enríquez-Gutiérrez and Jobson, 2016b; Enríquez-Gutiérrez and Jobson, 2016c).

2.1 Modelling of distillation columns

Existing retrofit approaches for heat-integrated crude oil distillation systems found in the open literature have used three methods to simulate distillation columns: shortcut methods, rigorous simulation and metamodels. This section explains and discusses the features of each method.

2.1.1 Shortcut methods

The Fenske-Underwood-Gilliland (FUG) method is a commonly applied shortcut method to design distillation columns. This method is based on the work of Fenske (1932), Underwood (1948) and Gilliland (1940).

The FUG method assumes constant molar flow within each column section and constant relative volatility throughout the column (Smith, 2005). These assumptions are only valid for relatively ideal mixtures. For multi-component and non-ideal mixtures these assumptions do not apply to the whole column (Smith, 2005). However, shortcut methods can be used to estimate the input values for more rigorous calculations.

Suphanit (1999) extends the FUG shortcut method by no longer assuming constant molar flows in the column. Instead, the Underwood equation is only used to calculate the vapour flow rates in the 'pinch' zones, i.e. the regions with constant compositions (Smith et al., 2010b), and enthalpy balances around the condenser and the reboiler are used to estimate the vapour flows at the top and the bottom of the column.

Suphanit (1999) modifies the FUG method to be applicable for steam-stripped columns, columns with thermal coupling, columns with side heat exchangers and crude oil distillation columns. In this method, complex columns are decomposed into thermodynamically equivalent sequences of columns (Carlberg and Westerberg, 1989; Liebmann et al., 1998). For distillation columns with pumparounds, only one location is permitted: just below the side-stripper draw stage.

Gadalla (2003) extends these shortcut methods to be applicable for retrofit. Also, Gadalla (2003) introduces a method (which needs rigorous simulation calculations) to express product specifications of crude oil distillation columns in terms of key components and their corresponding recoveries.

Rastogi (2006) extends the methods of Gadalla (2003) and Suphanit (1999) by accounting for pressure drop in crude oil distillation columns and by allowing flexibility of pump-around location (i.e. the pumparound location is no longer restricted to be just below the side-stripper draw stage).

Chen (2008) overcomes the limitations of the works of Gadalla (2003) and Rastogi (2006) by developing a method to identify key components and associated recoveries without needing rigorous simulation and by accounting for the effect of changing the pumparound locations on the separations.

The advantage of using shortcut models for the retrofit of heat-integrated distillation systems is that they can be incorporated within an optimisation environment that considers HEN retrofit, as in the works of Gadalla (2003) and Chen (2008). Thus, heat integration opportunities can be exploited.

However, shortcut methods do not provide the stage-by-stage information needed to perform a hydraulic analysis of the distillation column. Therefore, unfeasible column designs can be obtained. Also, the modified FUG models are normally difficult to initialise and solve and are not very compatible with conventional engineering/design approaches.

Section 2.1.2 explains and discusses the features of rigorous methods for designing and simulating distillation columns and cites examples of how these methods have been applied for the retrofit of heat-integrated crude oil distillation systems.

2.1.2 Rigorous simulation methods

Rigorous simulation methods allow more accuracy than shortcut methods. These methods are based on mass and enthalpy balances and equilibrium relations equations for a

simple equilibrium stage. Together with the summation equations, these equations are known as mass, equilibrium, summation and heat (MESH) equations. Rigorous simulation methods assume each stage is in equilibrium (Stichlmair, 1998).

Figure 2.1 illustrates an equilibrium stage.

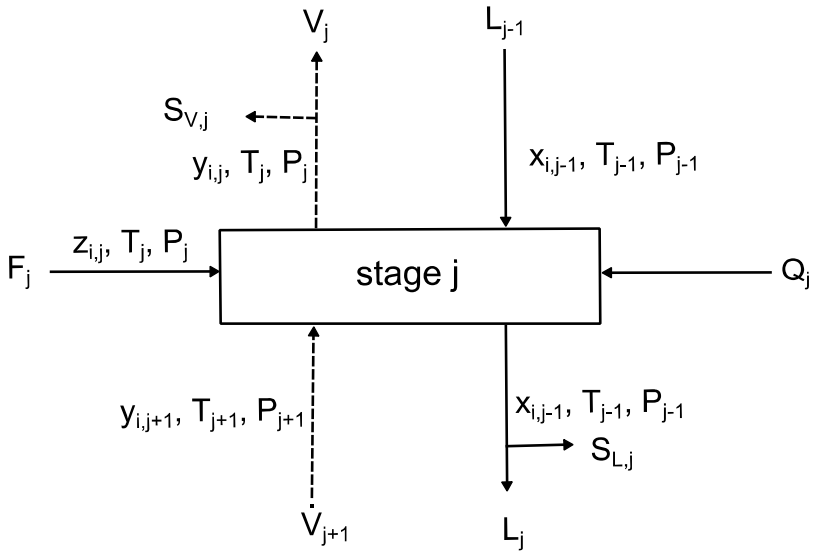

Figure 2.1 Equilibrium stage for MESH equations (Stichlmair, 1998, p. 171)

The MESH equations for a stage *j* are (Stichlmair, 1998, p. 171):

- Material balance for i = 1 … k components:

$$\dot{L}_{j-1}x_{i,j-1} + \dot{V}_{j+1}y_{i,j+1} + \dot{F}_j z_{i,j} - \left(\dot{L}_j + \dot{S}_{L,j}\right)x_{i,j} - \left(\dot{V}_j + \dot{S}_{V,j}\right)y_{i,j} = 0 \qquad (2.1)$$

- Equilibria for i = 1 … k components:

$$y_{i,j} - K_{i,j}x_{i,j} = 0 \quad \text{with} \quad K_{i,j} = f\left(T_j, P_j, x_{i,j}, y_{i,j}\right) \qquad (2.2)$$

- Summation of mole fraction in liquid and in vapour phase for i = 1 … k components:

$$\sum_{i=1}^{k} x_{j,i} - 1 = 0 \qquad (2.3)$$

$$\sum_{i=1}^{k} y_{j,i} - 1 = 0 \tag{2.4}$$

- Heat balance:

$$\dot{L}_{j-1}h_{L,j-1} + \dot{V}_{j+1}h_{V,j+1} + \dot{F}_j h_{F,j} - \left(\dot{L}_j + \dot{S}_{L,j}\right)h_{L,j} - \left(\dot{V}_j + \dot{S}_{V,j}\right)h_{V,j} + Q_j = 0 \tag{2.5}$$

Where *j* runs from *j = 1* to *j = n*; *n* being the number of stages. $\dot{L}$, $\dot{V}$, $\dot{F}$ and $\dot{S}$ are the molar flow rates of the liquid phase, the vapour phase, the feed and the side streams, respectively; $\dot{Q}$ indicates the heat flow; *x*, *y* and *z* refer to the molar fractions of the liquid phase, the vapour phase and the feed, respectively; *h* represents the molar enthalpy; and *K* is the equilibrium constant at a certain temperature *T* and pressure *P*. Consistent units should be used in these equations.

To solve these equations, the following information is required (Kister, 1992, p. 136):

- Flow rate, composition, and vapour fraction of each feed
- Number of stages
- The stage number of each feed, product, heat exchanger and pumparound draws and returns
- Column pressure profiles
- Type of reboiler and condenser

This information is usually estimated solving the Fenske-Underwood-Gilliland method, using plant data or by trial and error.

To solve the MESH equations, iterative methods are needed; such as the 'bubble point' method, the 'sum-of-rates' method, the '*2N* Newton' method and the 'global Newton of simultaneous correction' method (Kister, 1992, p. 144). These methods are already included in many commercial simulation software, such as Aspen HYSYS, Aspen Plus and Pro\II.

In practice, simulation models are used for design, to support control system design, troubleshooting and for retrofit design since they can provide a realistic representation of the system if properly modelled.

In the research literature, some of the retrofit approaches for heat-integrated crude oil distillation systems have used commercial simulation software to simulate the CDU.

Liu and Jobson (2004) use results from rigorous simulations to assess the hydraulic performance of distillation columns in terms of the fractional utilization of area (FUA), a parameter that represents the ratio between the required area and the available area of a distillation column, when increasing throughput and/or modifying the column topology. Rigorous simulation allows estimation of the FUA stage-by-stage. Thus, the location of bottlenecks (i.e. physical and operating constraints that limit the system) can be easily identified. However, FUA only accounts for the effects of jet flooding.

Errico et al. (2009) use rigorous simulation to assess the impacts of adding a preflash unit to an existing CDU. Rigorous simulation permits the assessment of proposed structural modifications to the distillation column (e.g. adding a flashed vapour feed stream) and analysing the impacts on the separation performance and the product quality. However, each proposed modification needs to be analysed individually, making the process time consuming.

Thernesz et al. (2010) use rigorous simulation to assess the capability of an existing crude oil distillation unit (CDU) to accommodate more throughput and/or process different types of crude oil. In their work, the results of rigorous simulations are exported to internals design software (e.g. KG-Tower and SULCOL) and to HEN design software (e.g. SUPERTARGET) in order to determine whether if the column internals need to be replaced and to identify whether if the HEN meets the energy targets. However, commercial software cannot work simultaneously (i.e. the results of one software are fed manually to another software package). Thus, the approach requires significant engineering time and effort.

Wang et al. (2011) extract stage-wise results from rigorous simulations to evaluate exergy losses and exergy efficiency in order to determine the best “predistillation” scheme to process a heavy crude oil. Exergy profiles do not reflect the effect of adding predistillation on the CDU hydraulics and/or the product quality; therefore, the methodology does not include checks for feasibility of retrofit solutions. Also, this approach requires significant engineering time, since each “predistillation” scheme should be analysed separately.

Gadalla et al. (2015) present a simulation-based retrofit approach for heat integrated crude oil distillation systems in which rigorous simulation is used to simulate both the existing CDU and its associated preheat train. In this approach, the impacts of modifying the CDU operating parameters (i.e. coil outlet temperature, reflux flow rate, pump-around duties and temperature drops, side-stripper draw and return flow rates) and the column structure (i.e. adding pumparounds, adding preflash) on the heat recovery system can be assessed. Results from rigorous simulations are used to estimate, stage-by-stage, the

required diameter in order to ensure hydraulic feasibility. The drawbacks of this approach are that no optimisation is included in the approach, which limits the exploration of heat integration opportunities, and that the method used to estimate the required diameter only accounts for jet flooding, neglecting the downcomer hydraulics.

Rigorous simulation software can be connected with external numerical solvers (e.g. MATLAB, Visual Basic, FORTRAN). This option has permitted the use of rigorous simulation in optimisation environments that include structural design decisions (Caballero et al., 2005) and data collection to build metamodels (López C. et al., 2013; Ochoa-Estopier and Jobson, 2015b).

In summary, rigorous simulation methods have been used to systematically assess beneficial retrofit modifications to crude oil distillation systems. Rigorous simulation methods are usually applied using commercial simulation software. Stage-by-stage information can be extracted from the results of the rigorous simulations, which can be used to estimate hydraulic parameters (e.g. FUA, required column diameter). However, the downcomer hydraulics is usually neglected. Rigorous simulation has not been included within optimisation algorithms that also address HEN retrofit.

Section 2.1.3 discusses the features and characteristics of metamodels, and presents a review on how these methods have been used for the retrofit of crude oil distillation systems.

2.1.3 Metamodels

Metamodels, or surrogate models, represent the relationship between variables in the form of mathematical or probability functions (Zobel and Keeling, 2008). The procedure to build a metamodel, typically consists of three steps (Ochoa-Estopier, 2014):

- data collection
- regression
- validation

Data collection is a key process to build metamodels. Firstly, the degrees of freedom (i.e. the independent variables that can be changed) need to be specified. The degrees of freedom are typically selected based on experience or sensitivity analysis. Secondly, the method to collect the samples is selected. This step depends on the scope of model (i.e. operational optimisation, control, retrofit) and whether real plant data are available (Ochoa-Estopier, 2014).

The regression of the data is typically carried out using a metamodel technique. A metamodel technique can be defined as an optimisation algorithm that estimates the parameters of the regressed function that minimise the error between the data collected and the model predictions (Ochoa-Estopier et al., 2014). Examples of metamodel techniques are Artificial Neural Networks (ANN) (Zobel and Keeling, 2008), Radial-Basis Function networks and Support Vector Machines (SVM's) (Sathyanarayanamurthy and Chinnam, 2009). In this step, it is also important to perform a sensitivity analysis in order to determine which of the input variables affect the most the variability of the outputs (Sathyanarayanamurthy and Chinnam, 2009).

In the validation step, the metamodel is compared against a new set of data in order to confirm the consistency of the predictions (Ochoa-Estopier, 2014).

For the retrofit of heat-integrated distillation systems, a few approaches have used metamodels to represent the CDUs (López C. et al., 2013; Ochoa-Estopier et al., 2015b).

López C. et al. (2013) use data generated from rigorous simulations to build second-order polynomial functions; Ochoa-Estopier et al. (2015b) use ANN to regress data from rigorous simulations. In both cases, the metamodels are used for operational optimisation in order to maximise the net profit (i.e. revenue minus operational costs).

The advantage of using metamodels to simulate complex systems is that are computational inexpensive (Sathyanarayanamurthy and Chinnam, 2009). However, setting up the metamodels can be time consuming.

2.1.4 Modelling of distillation columns — summary

In summary, three methods have been used in existing retrofit approaches to simulate distillation columns:

- Shortcut methods
- Rigorous methods
- Metamodels

Shortcut methods have been used in retrofit approaches for heat-integrated crude oil distillation systems. However, they are difficult to initialise and solve. Shortcut methods do not provide stage wise information needed to assess a hydraulic feasibility of the retrofitted distillation column.

Rigorous simulation software can be connected with external numerical solvers; therefore, it can be used for operational optimisation. Also, structural modifications can be easily modelled (i.e. adding a preflash unit) using rigorous simulation. Rigorous simulation does support hydraulic analysis, as it provides stage-by-stage information.

Metamodels have the advantages of being robust and computationally inexpensive once set up. However, the process to build them can be time consuming. No studies have shown them to be suitable for retrofit problems that include structural modifications.

For these reasons, this work uses rigorous simulation to model distillation columns. In Chapter 3 , results from rigorous simulations (generated using Aspen HYSYS v7.3) are used to assess the feasibility and viability of replacing column internals when increasing the processing capacity of a heat-integrated crude oil distillation system.

In Chapter 4 , rigorous simulation (in Aspen HYSYS v7.3) is incorporated in an a retrofit approach that optimises the column operating conditions and assesses replacing the column internals when increasing the throughput of a heat-integrated crude oil distillation system.

In Chapter 5 , rigorous simulation in Aspen HYSYS v7.3 is use in an optimisation-based retrofit approach that simultaneously assesses replacing the column internals, adding a preflash unit and optimising the column when increasing the processing capacity of heat-integrated crude oil distillation systems.

2.2 Hydraulics of distillation columns

Distillation is based on the concept of a vapour-liquid separation stage where vapour and liquid loads are in contact. In a real distillation column, contact between the two phases occurs in the column internals. Internals can be divided into two categories: trays and packings (Kister, 1992, Ch. 6).

This section presents the basic features of distillation columns containing trays and packings. A summary is provided for hydraulic correlations that can be used to predict the approach to jet and downcomer flooding, liquid weir load and downcomer exit velocity for conventional and high-capacity trays with sloped downcomers and, for structured packings, the approach to flooding.

Also, this section compares predictions obtained by applying the hydraulic correlations used in Chapters 3 to 5 and those obtained by using Aspen HYSYS (Aspen Tech, 2012)

and KG-Tower (Koch-Glitsch, 2014b) for conventional trays, high-capacity trays and structured packings in order to demonstrate their suitability and accuracy.

2.2.1 Hydraulics of trayed columns

Figure 2.2 illustrates the operational principles of trayed distillation columns. Liquid coming from a tray above enters the tray through the downcomer and contacts the vapour coming from a tray below. The vapour enters the tray through open areas (perforations, valves, bubble caps, etc.) and bubbles into the liquid forming a two-phase froth (where the mass transfer occurs). As the froth moves horizontally across the tray deck area, vapour disengages from the liquid and flows to the stage above. The liquid leaves the tray flowing over the weir and down the downcomer, where the rest of the vapour disengages, allowing 'clear' liquid to flow to the tray below (Stichlmair, 1998, Ch. 8; Smith, 2005). Trays can be classified as conventional and high-capacity trays (Smith, 2005, Ch. 9).

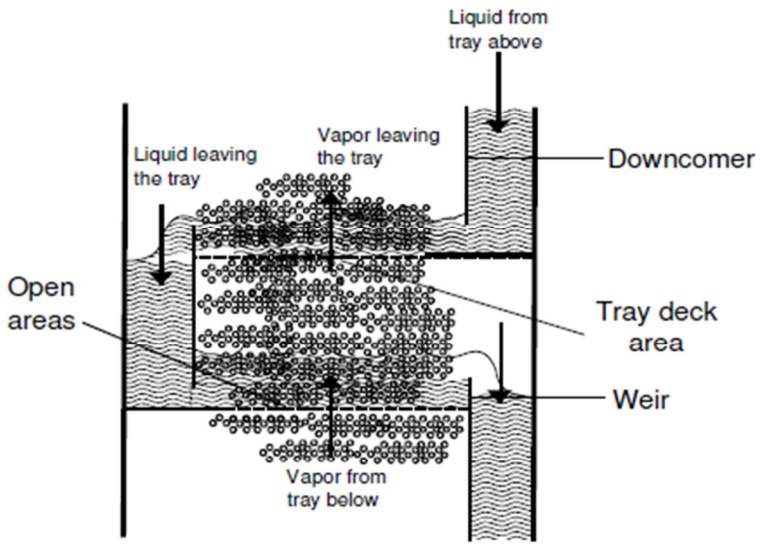

Figure 2.2 Operational principles of trays (adapted from Smith, 2005, Ch. 9.1)

2.2.1.1 Conventional trays

Table 2.1 lists the characteristics of the most common types of conventional trays: sieve trays and valve trays. Sieve trays, illustrated in Figure 2.3a, consist of perforated plates with downcomers in which the vapour velocity prevents the liquid from weeping, resulting in a relatively low turndown (ratio between the liquid and vapour rate), compared to valve

trays. Valve trays, illustrated in Figure 2.3b, allow a higher turndown because the valves prevent the liquid from weeping by reducing the open area (Kister, 1992, Ch. 6.1).

In general, sieve and valve trays present similar characteristics, but sieve trays are less expensive. Other examples of conventional trays are bubble-cap trays and dual-flow trays; they are only used for very specific applications (Kister, 1992, Ch. 6.1).

Table 2.1 Characteristics of sieve and valve trays (Kister, 1992, Ch. 6.1)

Parameter	Sieve trays	Valve trays
Maximum capacity, %	100	105
Turndown	2:1	4:1
Efficiency*, %	100	110
Pressure drop*, %	100	110
Fouling capacity	Moderate	Moderate to high
Vapour load capacity	Low to high	Low to high
Liquid load capacity	Moderate to high	Low to high
Cost*	100	120

* Relative to sieve trays performance

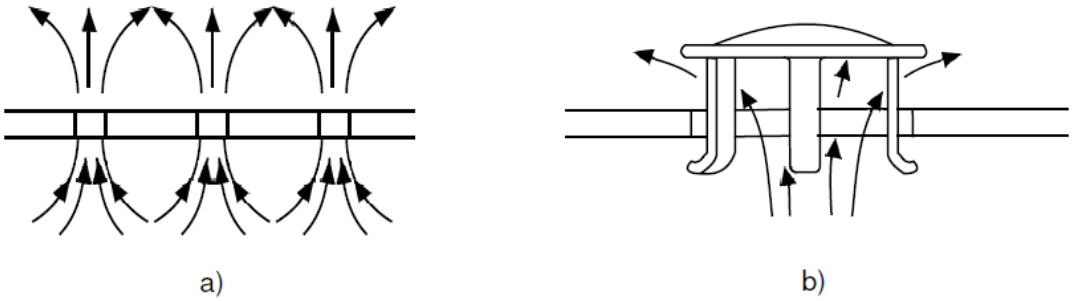

Figure 2.3 Conventional trays. a) Sieve tray; b) Valve tray (Kister, 1992, Ch. 6.1)

2.2.1.2 Hydraulic analysis of conventional trays

Figure 2.4 illustrates the flow limits at which trays can operate efficiently. High vapour loads may carry over liquid to the stage above; causing a phenomenon known as jet flooding. Entrainment is when droplets of liquid start being carried to the stage above (Stichlmair, 1998, Ch. 8.2). In practice, both of these phenomena are prevented by designing the distillation columns with an approach to jet flooding of 80-85% (Branan, 2011). Low vapour loads may cause weeping, i.e. when the vapour is no longer able to

prevent the liquid from leaking through holes to the stage below (Stichlmair, 1998, Ch. 8.2).

Eq. 2.6 can be used to predict the approach to jet flooding. This equation is known as 'Equation 13', and can be found in the "Ballast tray design manual" (Koch-Glitsch, 2013). Resetarits (2014) mentions that this correlation gives accurate predictions of flood points. In this equation, V_{load} is the vapour load factor and V_L is the volumetric liquid load, both in $m^3\ s^{-1}$, T_{FL} refers to the tray flow path length in m, A_{ac} represents the tray active area in m^2, and *CF* stands for the vapour capacity factor.

$$\%Flooding = \frac{35.32V_{load} + V_L T_{FL}}{10.76 \cdot A_{ac} \cdot CF} \tag{2.6}$$

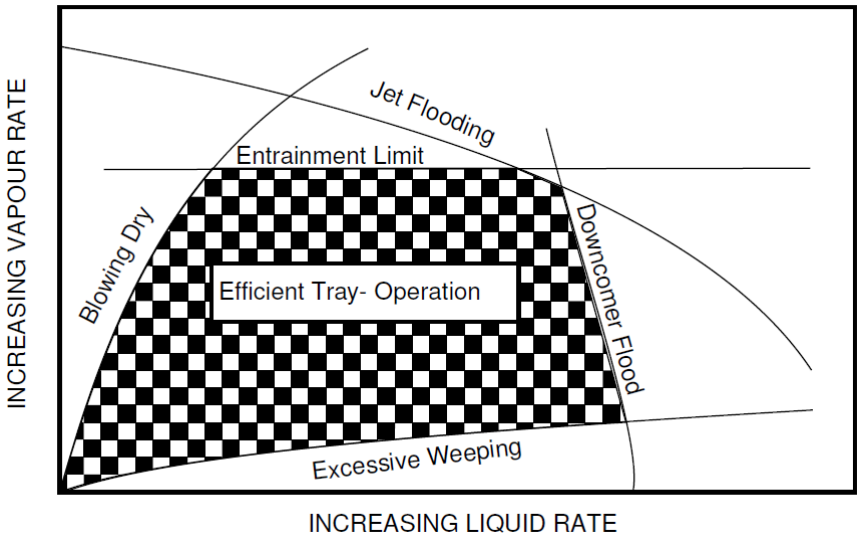

Figure 2.4 Tray operating region (adapted from Stichlmair, 1998, Ch. 8.2)

The vapour load factor is the volumetric vapour load V_G in $m^3\ s^{-1}$ corrected for vapour and liquid densities ρ_G and ρ_L, respectively, in kg m^{-3} (Branan, 2011):

$$V_{load} = V_G \sqrt{\frac{\rho_G}{\rho_L - \rho_G}} \tag{2.7}$$

The tray flow path length is a function of the tower diameter D_c in m, and the number of passes per tray, N_p (Branan, 2011):

$$T_{FL} = 30\frac{D_C}{N_p} \tag{2.8}$$

The vapour capacity factor *CF* is a function of the tray spacing T_S in m and the vapour density in kg m^{-3} (Branan, 2011):

$$CF = \left[0.58 - \frac{0.084}{T_S}\right] - \left[\frac{2.44 \cdot T_S \cdot \rho_G - 39.37 \cdot T_S}{1560}\right] \quad (2.9)$$

To account for the hydraulic constraints related to the liquid loads, this work assesses three hydraulic parameters: the liquid weir load, the downcomer exit velocity and the approach to downcomer flooding.

High liquid loads can prevent the vapour from disengaging completely from the liquid in the downcomer, entraining the vapour in the stage below. This phenomenon, known as downcomer flooding, occurs when the downcomer is too small to handle the liquid load, causing low downcomer residence time and/or downcomer 'back-up' (when the liquid backs up to the stage from the downcomer). To prevent tower malfunction, it is recommended that the approach to downcomer flooding does not exceed 80-85% of the design limit (Koch-Glitsch, 2013). At low liquid loads, liquid is almost completely vaporised, blowing dry the stage (Stichlmair, 1998, Ch. 8.2).

To predict the approach to downcomer flooding, the design equations presented by Branan (2011) for estimating the downcomer velocity are used, shown in Eqs. 2.10 to 2.13. In these equations, A_{DC} is the downcomer area in m^2 and v_{DCdes} is the downcomer design velocity in m s^{-1}. The smallest value obtained from Eqs. 2.11 to 2.13 should be used.

$$\%DCflooding = \frac{V_L}{A_{DC} \cdot N_p \cdot v_{DCdes}} \quad (2.10)$$

$$v_{DCdes} = 0.170 \quad (2.11)$$

$$v_{DCdes} = 0.03 \cdot \sqrt{\rho_L - \rho_G} \quad (2.12)$$

$$v_{DCdes} = 2.45 \cdot \sqrt{295 \cdot T_S \cdot (\rho_L - \rho_G)} \quad (2.13)$$

The expression used to estimate the liquid weir load L_w in $m^3\ m^{-1}\ h^{-1}$ is shown in Eq. 2.14 (Resetarits, 2010). In this equation, l_w is the weir length. The recommended design value is between 90 and 100 $m^3\ m^{-1}\ h^{-1}$; if exceeded, it is recommended to increase the number of passes per tray to enhance vapour-liquid contact, i.e. provide increased tray capacity (Koch-Glitsch, 2013).

$$L_W = \frac{V_L}{l_w \cdot N_p} \tag{2.14}$$

The downcomer exit velocity v_{DCexit} in m s^{-1} is estimated using Equation 2.15, where H_{cl} refers to the downcomer clearance in m (Koch-Glitsch, 2014b). The recommended design limit for v_{DCexit} is 0.46 m s^{-1}, otherwise the downcomer clearance should be adjusted (Koch-Glitsch, 2013).

$$v_{DCexit} = \frac{V_L}{l_w \cdot H_{cl} \cdot N_p} \tag{2.15}$$

Exceeding the limits of the approach to jet and downcomer flooding is not recommended (Stichlmair, 1998, Ch. 8.2). The correlations presented in this section are rather general; more accurate ones can be used if available.

Section 2.2.1.3 presents a comparison between the results obtained using these correlations and the ones obtained in Aspen HYSYS (Aspen Tech, 2012) and KG-Tower (Koch-Glitsch, 2014b).

2.2.1.3 Illustrative Example 2.1: Comparison between the hydraulic correlations for conventional trays found in the open literature and those in commercial design software.

The crude oil distillation unit (CDU) presented by Chen (2008) is used to compare the predictions obtained by applying the correlations listed in Section 2.2.1.2 and those obtained using commercial simulation and design software: Aspen HYSYS (Aspen Tech, 2012) and KG-Tower (Koch-Glitsch, 2014b).

The CDU processes 100,000 bbl d^{-1} (2562 kmol h^{-1}) of Tía Juana Light crude (Watkins, 1979) into five products: light naphtha (LN), heavy naphtha (HN), light distillate (LD), heavy distillate (HD) and residue (RES).

Figure 2.5 illustrates the distillation column configuration and stage distribution. It consists of three side-strippers, three pumparounds and a condenser. The main fractionator and the Btm SS use live steam as stripping agent, and the Top SS and Mid SS have reboilers. Table 2.2 lists the operating parameters of the distillation column and Table 2.3 presents the product flow rates.

Table 2.4 shows the distillation column stage numbering and diameters. Note that the stages in the side-strippers are numbered sequentially.

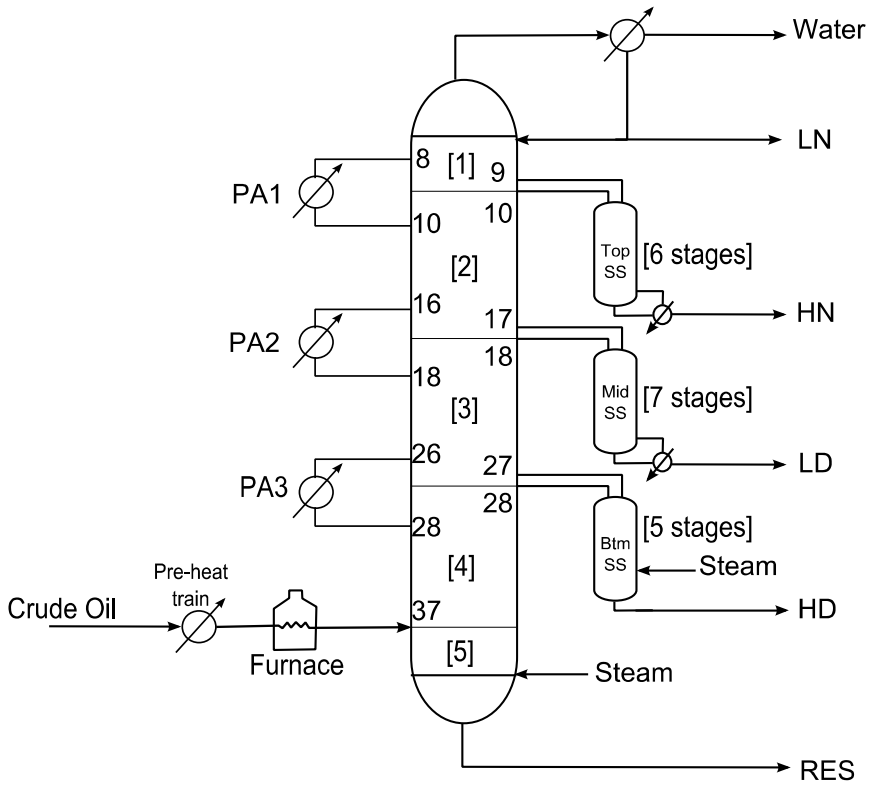

Figure 2.5 Column configuration and stage distribution (Chen, 2008, Ch. 6.1)

Table 2.2 Distillation column operating parameters (Chen, 2008, Ch. 6.1)

Parameter	Value
Feed pre-heat temperature, ℃	365
Operating pressure, bar	2.5
Main fractionation reflux ratio	4.17
Main steam flow rate, kmol h^{-1}	1200
Btm SS steam flow rate, kmol h^{-1}	250
Condenser duty, MW	47.87
Top SS reboiler duty, MW	6.63
Mid SS reboiler duty, MW	8.78
PA1 duty, MW	12.84
PA2 duty, MW	17.89
PA3 duty, MW	11.20
PA1 temperature drop, ℃	30
PA2 temperature drop, ℃	50
PA3 temperature drop, ℃	20

Table 2.3 Distillation column product flow rates (Chen, 2008, Ch. 6.1)

Product steam	Flow rate, kmol h^{-1}
Light naphtha, LN	678
Heavy naphtha, HN	496
Light distillate, LD	653
Heavy distillate, HD	149
Residue, RES	365

Table 2.4 Distillation column stage numbering and diameters (Chen, 2008, Ch. 6.1)

Column section	Stage numbering	Section diameter, m
Section 1	1-9	7.5
Section 2	10-17	7.5
Section 3	18-27	8.0
Section 4	28-36	8.0
Section 5	37-41	5.5
Top SS	42-47	3.5
Mid SS	48-54	3.5
Btm SS	55-59	3.5

The procedure to carry out this case study is the following:

1. The distillation column is simulated in Aspen HYSYS (Aspen Tech, 2012).
2. Using the simulation results, the approach to jet and downcomer flooding and liquid weir load are estimated using the rating mode of the tray sizing utility tool of Aspen HYSYS (Aspen Tech, 2012) using the diameters presented in Table 2.4 and assuming that the distillation column internals are valve trays with a tray spacing of 0.6 m and a downcomer clearance of 0.6 m. The approach to jet flooding is predicted using the four different correlations contained in the software: Glitsch, Koch, Nutter and Fair correlations. Table 2.5 lists the results calculated in Aspen HYSYS for the number of passes per trays and the percentage of active area.
3. The same results from the rigorous simulation (i.e. stage-wise vapour and liquid flow rates and transport properties) and the results from the tray sizing in Aspen HYSYS are extracted using a MATLAB—Aspen HYSYS interface and Eqs. 2.6 to 2.15 are used to predict the approach to jet and downcomer flooding, liquid weir load and downcomer exit velocity in MATLAB.
4. The same simulation and tray sizing results are input manually into KG-Tower (Koch-Glitsch, 2014b) to predict the approaches to jet and downcomer flooding, liquid weir load and downcomer exit velocity.
5. The results of the hydraulic analyses are plotted and compared.

Table 2.5 Tray sizing results using Aspen HYSYS (Aspen Tech, 2012)

Column section	Passes per tray	Percentage of active area, %
Section 1	4	88.5
Section 2	4	90
Section 3	4	92
Section 4	4	90
Section 5	2	75
Top SS	2	72
Mid SS	2	63
Btm SS	2	76

Results of illustrative example

Figure 2.6 illustrates the profiles obtained for the approach to jet flooding using different correlations. The predictions obtained using Eq. 2.6 (coded in MATLAB) are in good agreement with those of KG-Tower (Koch-Glitsch, 2014b) and Glitsch and Koch

correlations from Aspen HYSYS (Aspen Tech, 2012). Note that values obtained in stages 8, 9, 16, 17, 26 and 27 (i.e. the draw and return stages of the pumparounds) are approximately 10% and in the side-strippers (stages 40-59) around 20% higher using Glitsch and Koch correlations.

The Fair and Nutter correlations, contained in Aspen HYSYS (Aspen Tech, 2012), underestimate the flood points by approximately 30%, especially around the pumparounds. This is because Fair and Nutter correlations only account for the vapour loads to predict the approach to jet flooding. Therefore, these correlations are not suitable for distillation columns with high liquid loads (e.g. distillation column with pumparounds). Note that Eq. 2.6 does accounts for both the vapour and the liquid loads (Branan, 2011).

From this analysis, it can be concluded that the correlation used to predict the approach to jet flooding is suitable for this type of distillation system: i.e. a crude oil distillation column with side-strippers and pumparounds, as there is good agreement with the predictions obtained using design vendor software (i.e. KG-Tower).

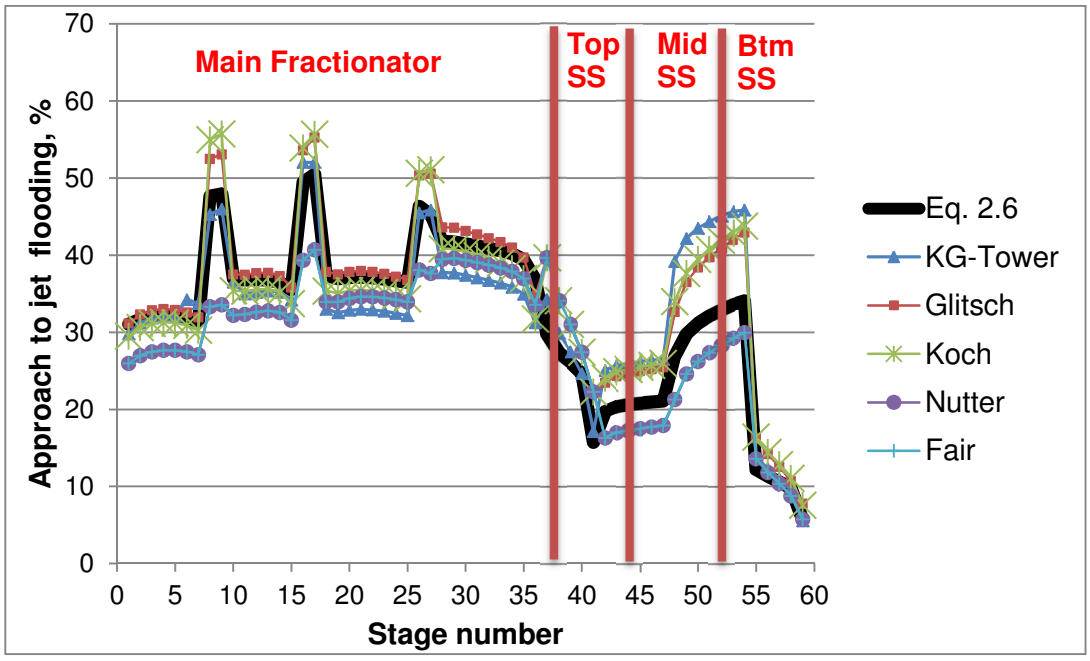

Figure 2.6 Approach to jet flooding profiles for valve trays

Figure 2.7 illustrates the predicted profiles for liquid weir load using Eq. 2.14, and Aspen HYSYS (Aspen Tech, 2012) and KG-Tower (Koch-Glitsch, 2014b). Note that Aspen HYSYS underestimates by around 30% the liquid weir loads predictions around the pumparounds (stages 8, 9, 16, 17, 26 and 27), while Eq. 2.14 and KG-Tower are in better agreement.

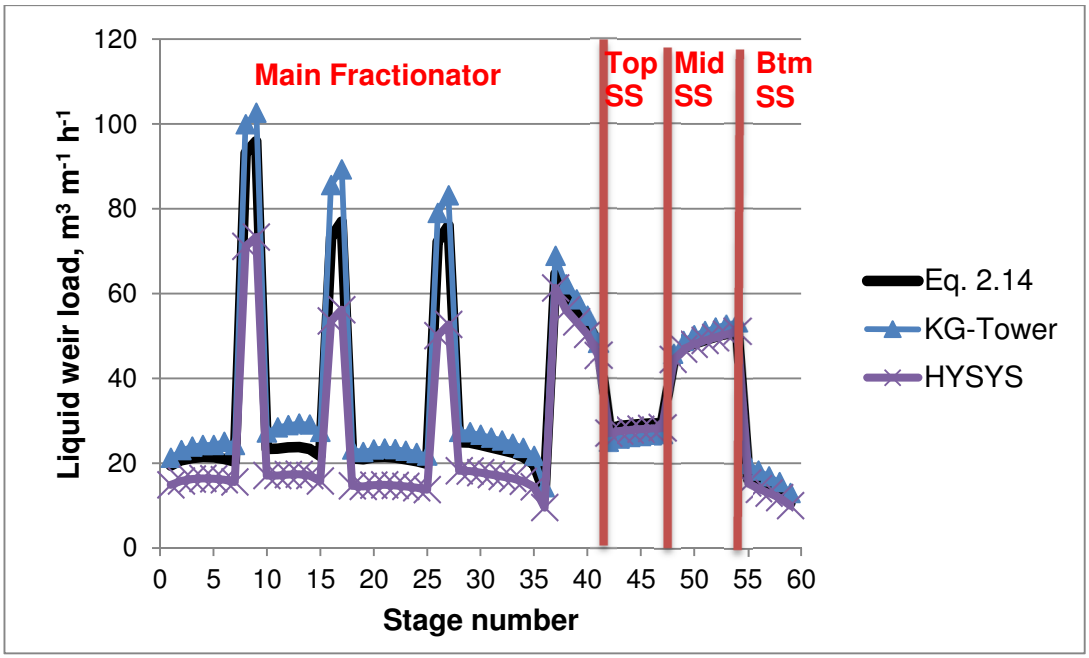

Figure 2.7 Liquid weir load profiles for valve trays

Figure 2.8 illustrates the downcomer exit velocity profiles obtained using Eq. 2.15 and KG-Tower (Koch-Glitsch, 2014b). This parameter is not estimated by Aspen HYSYS (Aspen Tech, 2012). Good agreement can be observed between both Eq. 2.15 and KG-Tower.

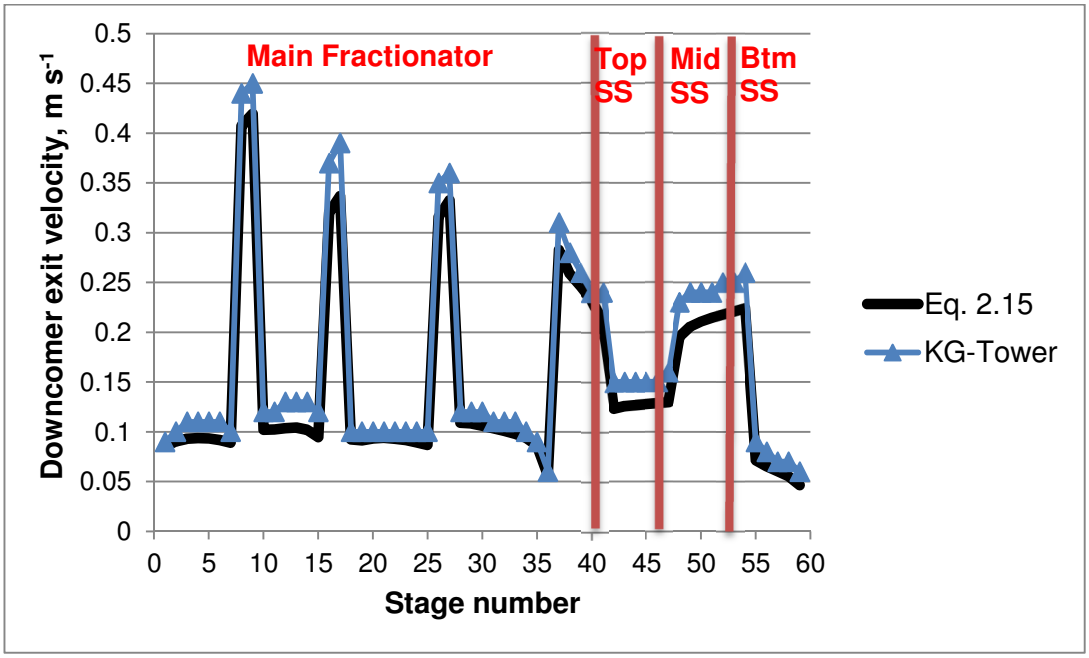

Figure 2.8 Downcomer exit velocity profiles for valve trays

Figure 2.9 illustrates the profiles for downcomer flooding. Note that the equations used in this work (Eqs. 2.10 to 2.13) are in better agreement with KG-Tower (Koch-Glitsch, 2014b) than with Aspen HYSYS (Aspen Tech, 2012).

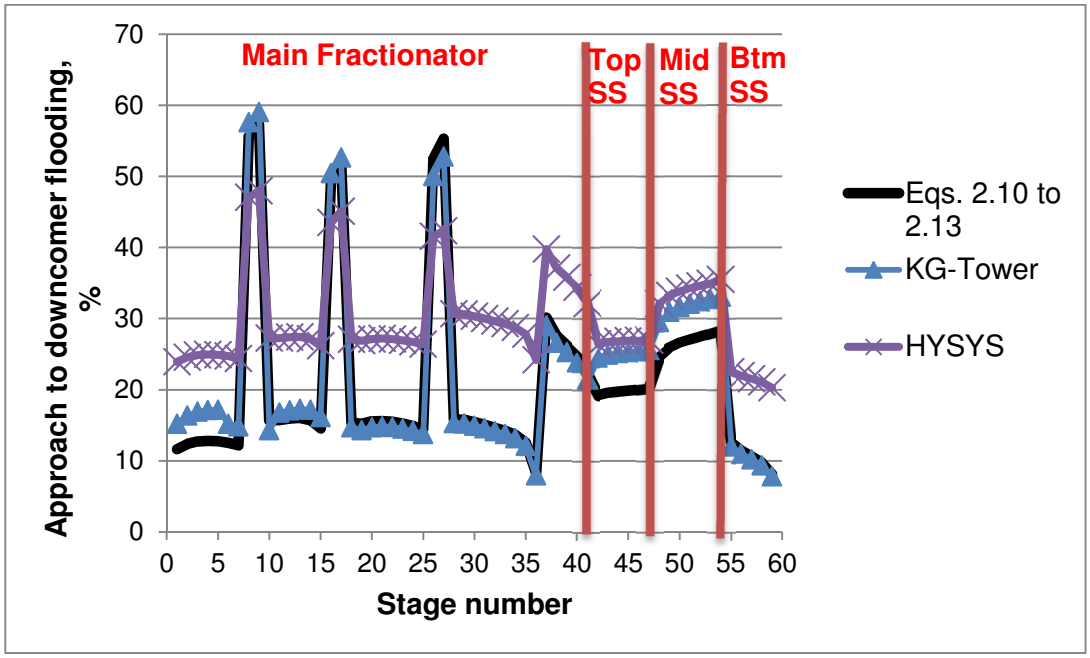

Figure 2.9 Approach to downcomer flooding profiles for valve trays

Summary and conclusions — illustrative example

In summary, the hydraulic correlations presented in Section 2.2.1.2 are in good agreement with the results obtained by KG-Tower (Koch-Glitsch, 2014b). Aspen HYSYS (Aspen Tech, 2012) does not predict values for the downcomer exit velocity. Sensitivity analysis shows that this parameter is affected by variations in pumparound flow rates. Note that the predictions obtained by Aspen HYSYS (Aspen Tech, 2012) for downcomer flooding differ from those in this work and of KG-Tower (Koch-Glitsch, 2014b). This is because, in this work and in KG-Tower (Koch-Glitsch, 2014b), the downcomer areas are specified to be equal, while Aspen HYSYS (Aspen Tech, 2012) uses default values that cannot be modified.

In conclusion, the correlations used in this work are in good agreement with the results obtained using commercial design software. However, significant differences around the pumparounds area and side strippers are observed with Aspen HYSYS (Aspen Tech, 2012). The agreement with KG-Tower (Koch-Glitsch, 2014b) is better, but the results have to be input manually, increasing the engineering effort.

For these reasons, it was decided to code the correlations of Eqs. 2.6 to 2.15 in MATLAB for Publications 1 to 4, in order to have more control over the plate design and to be able to reduce the engineering effort of the hydraulic analysis.

2.2.1.4 High-capacity trays — hydraulic analysis

Conventional trays can be modified in order to achieve more capacity and/or efficiency. These types of trays are commonly referred to as high-capacity trays (Penciak et al., 2006). The design of these trays aims to minimise the downcomer area in order to maximise the tray active area and to redirect liquid flows on tray to improve vapour-liquid contact and distribution of the liquid (Penciak et al., 2006).

Figure 2.10a illustrates high-capacity trays with sloped downcomers and smaller open areas (i.e. smaller than the ones used on conventional sieve and valve trays). Note that the sloped downcomers provide additional tray active area, thus increasing the area for vapour-liquid contact. Penciak et al. (2006) mention that small diameter open areas provide a higher jet flooding capacity and efficiency, compared with large size open areas.

Figure 2.10b illustrates high-capacity trays with truncated downcomers. Truncated downcomers provide even more active area than sloped downcomers, since the vapour-liquid contact also occurs in the disengagement area of the tray (Penciak et al., 2006). The vapour-liquid contact in the disengagement area is possible by installing patented designs of inlet weir, bubble promotors and hanging downcomers, as presented in the patents of Binkley et al. (1992), Yeoman et al. (1996), Yeoman et al. (1997) and Lee et al. (1999).

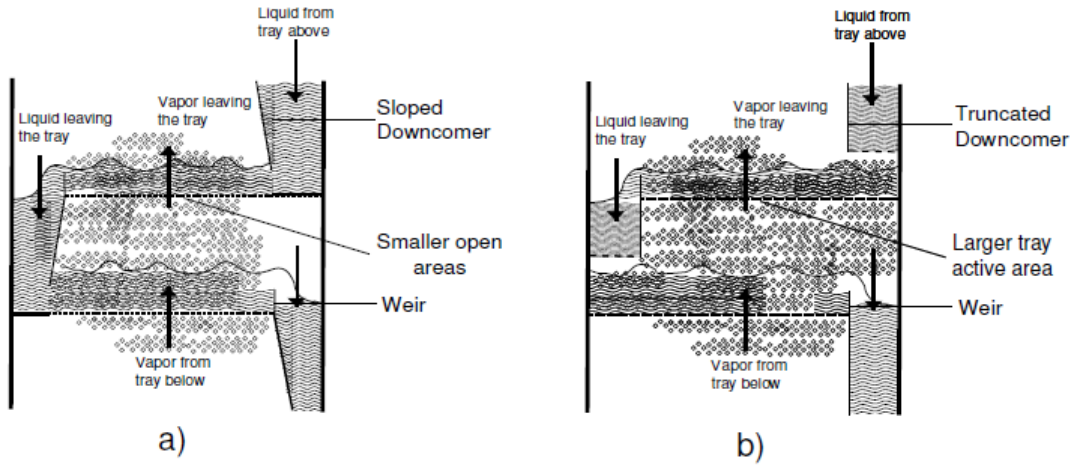

Figure 2.10 High-capacity trays **a)** with sloped downcomers and smaller open area, **b)** with hanging downcomers and larger tray deck area (adapted from Smith, 2005, Ch. 9)

Most high-capacity trays are patented designs and little information can be found about their geometry or hydraulic performance in the open literature. However, vendors provide information about their potential capacity enhancement compared to sieve and valve trays. Examples of this are SUPERFRAC trays (Koch-Glitsch, 2014a), which can accommodate 15 to 20% more flow that valve trays and come with different downcomer designs depending on the applications, and MVG high-capacity trays (Sulzer, 2014), which can provide an extra 20% of capacity compared to sieve and valve trays. High-capacity trays have been successfully used to retrofit distillation columns that are already operating at their maximum approach to jet flooding (Kister et al., 2002; Khalil et al., 2004).

2.2.1.5 Hydraulic analysis of high-capacity trays with sloped downcomers

In this work, only high-capacity trays with sloped downcomers are considered for retrofit since their hydraulic performance can be estimated using the same correlations as for sieve and valve trays if the additional area gained by sloping the downcomer is considered (Koch-Glitsch, 2014b). Figure 2.11 illustrates how active area is gained by the downcomer.

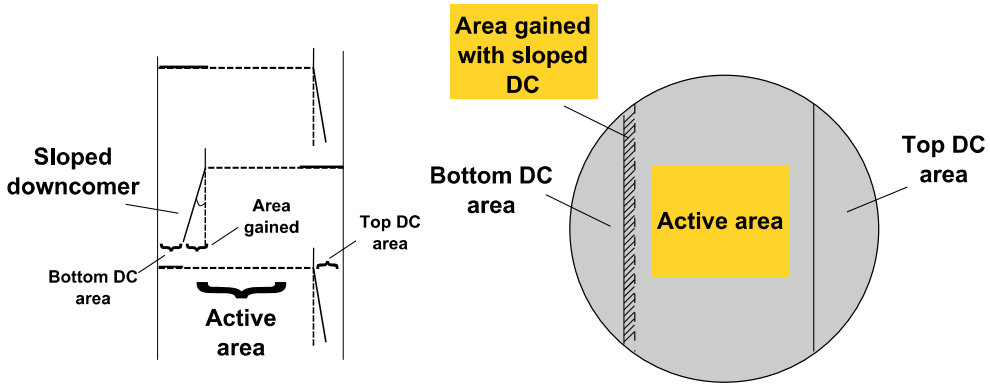

Figure 2.11 High-capacity trays with sloped downcomers (Enríquez-Gutiérrez et al., 2015)

To consider the increase in active area A_{acnew} in m^2, Eq. 2.16 can be used (Koch-Glitsch, 2014b). In this equation, A_T is the cross sectional area of the distillation column in m^2, A_{DCtop} refers to the top downcomer area in m^2 and A_{DCbtm} represents the bottom downcomer area in m^2.

$$A_{acnew} = A_T - A_{DCtop} + A_{DCbtm} \quad (2.16)$$

The active area gained at the bottom downcomer is estimated using Eq. 2.17, where θ is the downcomer slope angle relative to the vertical (Koch-Glitsch, 2014b).

$$A_{DCgained} = A_{DCtop} sin\theta \quad (2.17)$$

Eq. 2.16 is only valid for two-pass trays. For trays with four passes per tray, Eq. 2.18 can be used (Koch-Glitsch, 2014b).

$$A_{acnew} = A_T - A_{DCtop} + 2 \cdot A_{DCbtm} \quad (2.18)$$

2.2.1.6 Illustrative Example 2.2: Comparison between the hydraulic correlations for high-capacity trays with sloped downcomers found in the open literature and those in commercial design software.

In this example, the same crude oil distillation unit and procedure presented in Section 2.2.1.3 are used to compare the predictions obtained using the hydraulic correlations presented in Section 2.2.1.2 , corrected for high-capacity trays with sloped downcomers using the design equations, and the predictions of KG-Tower (Koch-Glitsch, 2014b).

In this example, the column internals are assumed to be valve trays with 15 degrees sloped downcomers; with the same number of passes per tray, active area and diameters as in Table 2.4.

Results

Figures 2.12, 2.13, 2.14 and 2.15 show the results of this analysis. Good agreement between the results predicted by the modified open literature hydraulic correlations and KG-Tower (Koch-Glitsch, 2014b) can be observed.

Summary and conclusions

Based on these results, it can be concluded that the correlations used in this work can predict similar values to the ones predicted by internals vendor software. Aspen HYSYS (Aspen Tech, 2012) is not used because it is not possible to control the tray geometry; thus, a fair comparison between methods could not be achieved.

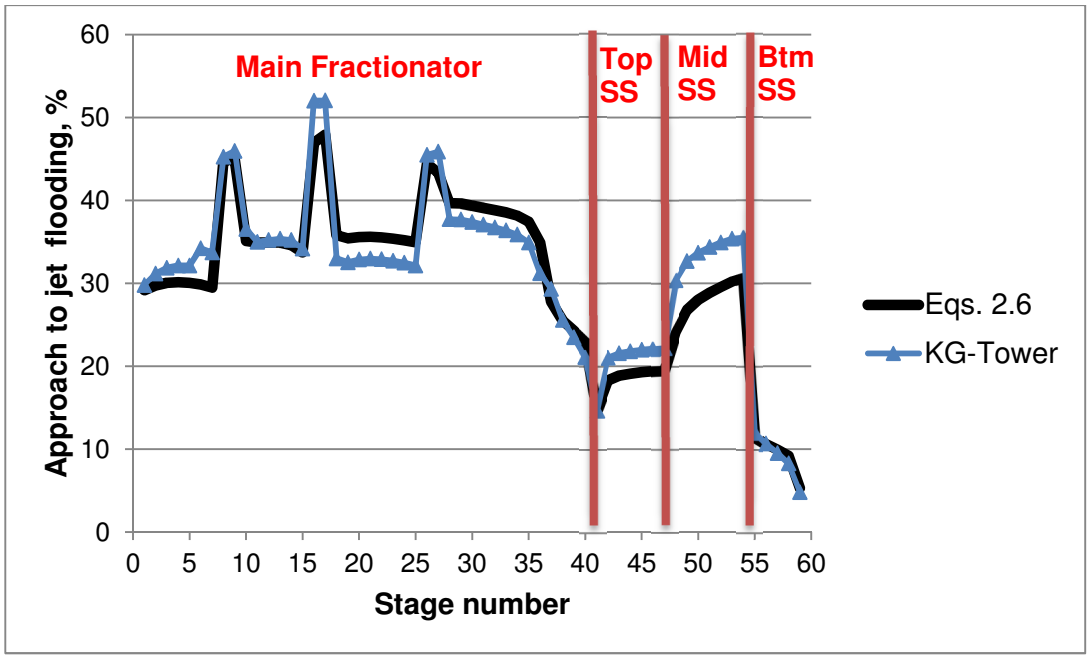

Figure 2.12 Approach to jet flooding profiles for high-capacity trays with sloped downcomers

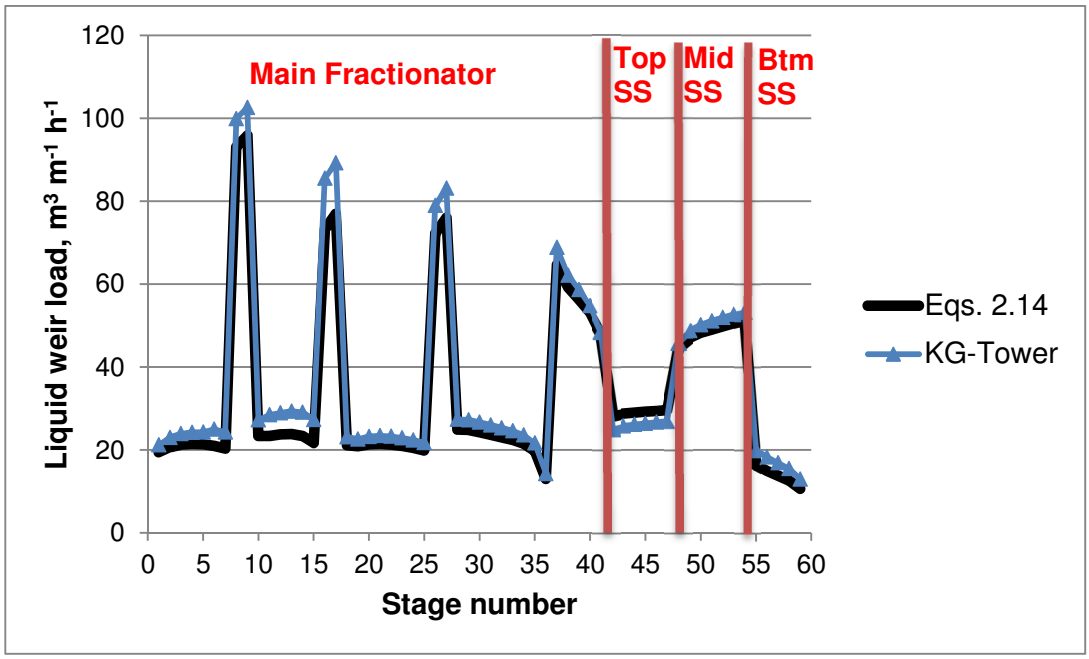

Figure 2.13 Liquid weir load profiles for high-capacity trays with sloped downcomers

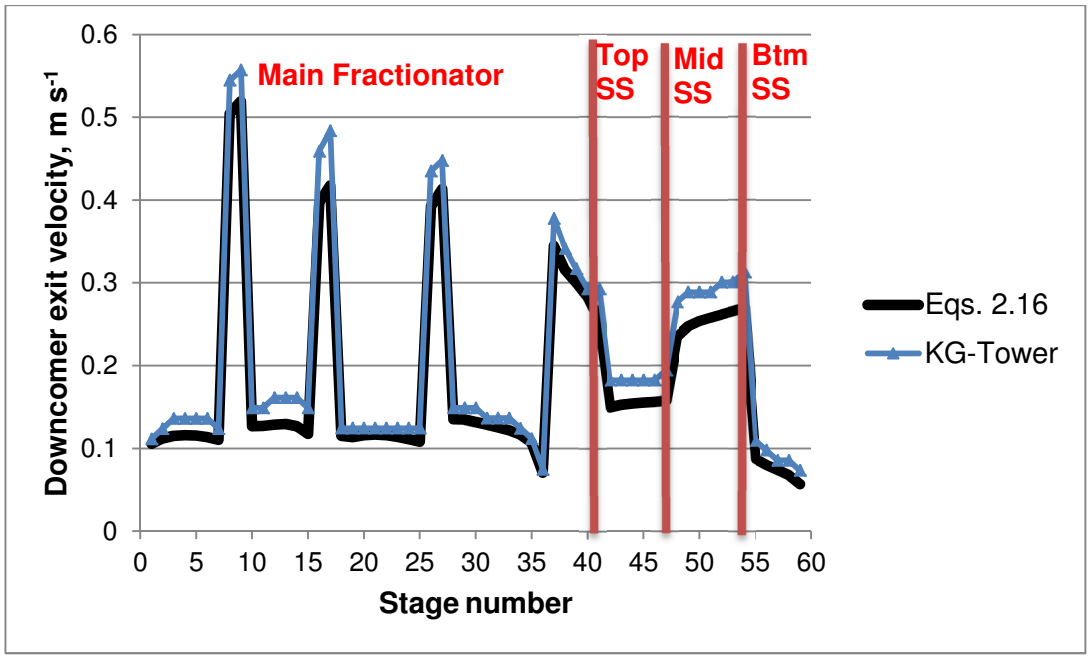

Figure 2.14 Downcomer exit velocity profiles for high-capacity trays with sloped downcomers

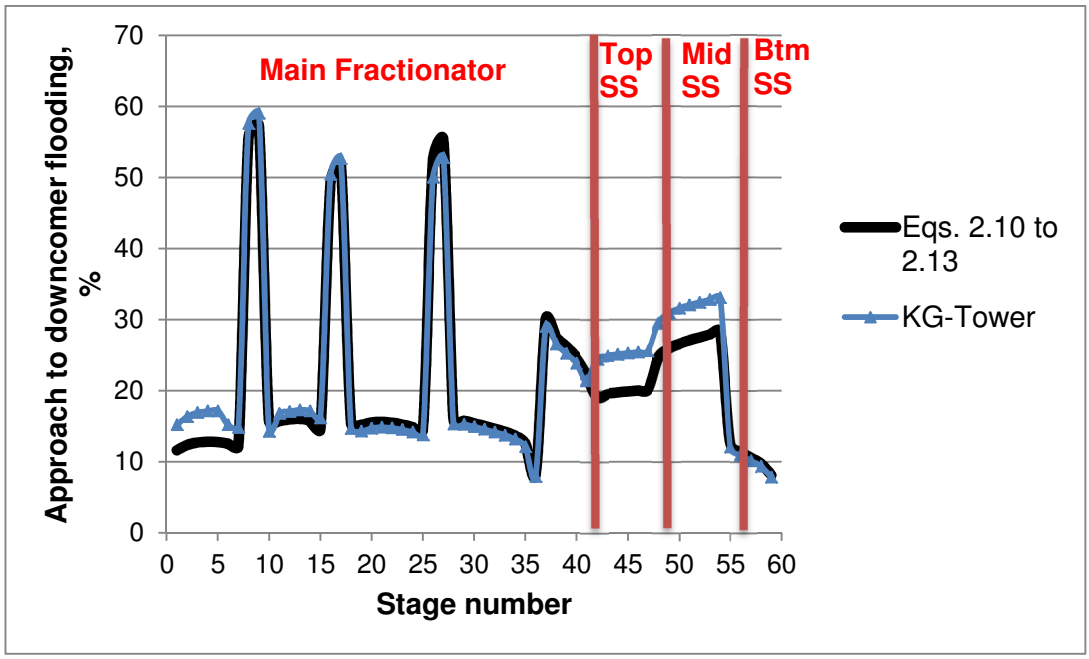

Figure 2.15 Approach to downcomer flooding profiles for high-capacity trays with sloped downcomers

2.2.2 Hydraulic performance of packings

Packed columns operate in countercurrent flow and use mass transfer devices (known as packings) with a high interfacial area to contact the gas and liquid flows (Stichlmair, 1998, Ch. 8.3). These mass transfer devices are known as packings and they can be divided into two categories: random packings and structured packings. Figure 2.16 illustrates a distillation column containing random and structured packings. Note that packed columns need liquid collectors and distributors to ensure even liquid distribution; otherwise the separation efficiency gets compromised (Stichlmair, 1998, Ch. 8.3).

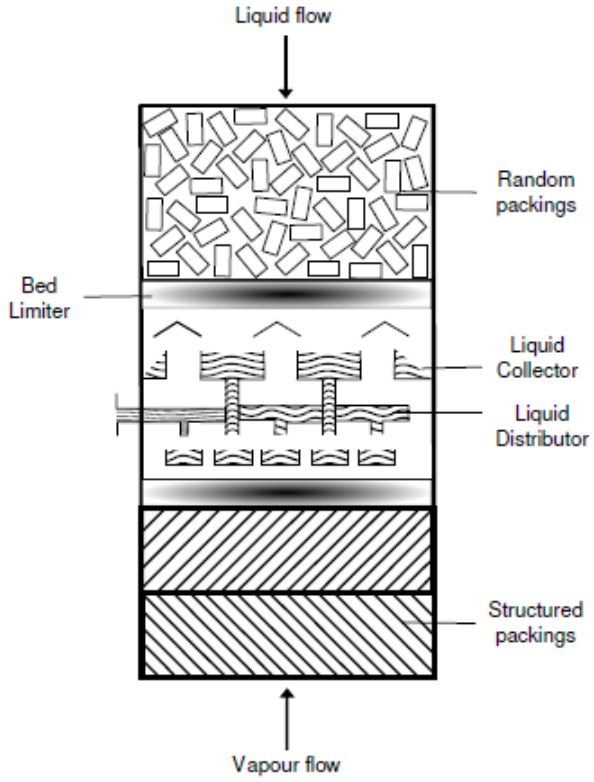

Figure 2.16 Distillation column containing packings (adapted from Smith, 2005, Ch. 9.2)

Random packings are preformed shapes which are dumped into distillation columns to produce a body with a high surface area (Smith, 2005, Ch. 9.2). Their efficiency and capacity depend on the shape, size and materials of the packing. For example, 10 mm ceramic Rasching rings have a specific area of 440 m^2 m^{-3} and 10 mm metal Rasching rings have a specific area of 500 m^2 m^{-3} (Stichlmair, 1998, Ch. 8.3).

Structured packings are metal or plastic sheets with corrugations and holes. Slabs of structured packings are stacked inside distillation columns, providing a high vapour-liquid contact area (Smith, 2005, Ch. 9.2). Their efficiency and capacity are dictated by their geometry (Stichlmair, 1998, Ch. 8.3). For example, Mellapak 125Y with an angle with horizontal of 45° has a 'packing factor' (an empirical factor depending of the packings size and shape) of 33 m^{-1}, while Mellapak 125X, with an angle of 60°, has a packing factor of 16 m^{-1} (Green and Perry, 2007).

Random packings have a certain degree of non-homogeneity, causing liquid maldistribution and mass transfer in-efficiency (Stichlmair, 1998, Ch. 8.3). In comparison, structured packings have a more homogeneous structure and offer a lower pressure drop than random packings (Stichlmair, 1998, Ch. 8.3). Structured packings can achieve higher separation efficiency and can increase the capacity of distillation columns (Shojaee et al., 2011). For these reasons, structured packing are more often used for retrofitting distillation columns than random packings.

Section 2.2.2.1 presents hydraulic correlations that can be used to predict the hydraulic performance of packed columns.

2.2.2.1 Hydraulic analysis of packings

Figure 2.17 illustrates the operational limits of packed columns. The flood point is defined as the vapour-phase pressure drop at which the liquid is no longer able to flow against the vapour, impeding the countercurrent flow (Stichlmair, 1998, Ch. 8.3). Packed columns are typically designed with an 80% approach to flooding (Stichlmair, 1998, Ch. 8.3). Packed columns require a minimum liquid load to operate; below this limit, the packing surface area is not completely wetted, reducing the mass transfer contact area and the separation efficiency. For organic mixtures, this limit takes a value of approximately 2 m^3 m^{-2} h^{-1} (Stichlmair, 1998, Ch. 8.3).

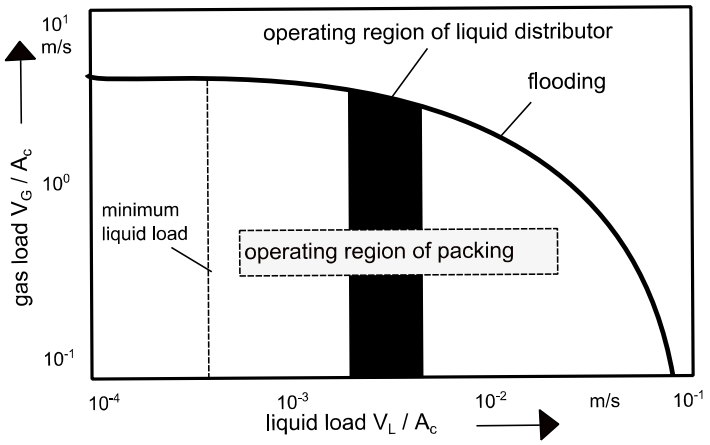

Figure 2.17 Operational limits for packed columns (adapted from Stichlmair, 1998, Ch. 8.3)

The approach to flooding for structured packings is defined as shown in Eq. 2.19, where C_{sb} is the operational capacity factor, also known as C-factor, and $C_{sb,flooding}$ is the C-factor at flooding conditions (Kister et al., 2007).

$$\%Flooding = \frac{C_{sb}}{C_{sb,flooding}} \times 100 \tag{2.19}$$

The C-factor at flooding conditions $C_{sb,flooding}$ for packed columns can be estimated using Eq. 2.20, where $CP_{flooding}$ is the capacity parameter at flooding conditions, F_p refers is the packing factor in m^{-1} and μ_L represents the liquid viscosity in kg m^{-1} s^{-1} (Kister et al., 2007).

$$C_{sb,flooding} = \frac{CP_{flooding}}{F_p^{0.5}\left(\mu_L/\rho_L\right)^{0.05}} \tag{2.20}$$

To estimate the capacity parameter at flooding conditions, Chapter 3 (i.e. Paper 1) presents a regressed model from the pressure drop correlation chart for structured and random packings of Kister and Gill (1992). Details are provided in Appendix A.

In this model, shown in Eq. 2.21, the capacity parameter at flooding conditions is a function of the flow parameter and two constants. The flow parameter F_{lv} is estimated using Eq. 2.22, where L and G are the liquid and vapour molar flow rates in kmol s^{-1}, respectively. The constants $A_{flooding}$ and $B_{flooding}$ are functions of the flooding pressure drop $\Delta P_{flooding}$ in Pa m^{-1}, which can be estimated using Eq. 2.23. Eqs. 2.24 and 2.25 apply to structured packings and Eqs. 2.26 and 2.27 to random packings.

$$CP_{flooding} = A_{flooding} ln(F_{lv}) + B_{flooding} \quad (2.21)$$

$$F_{lv} = \frac{L}{G}\left(\frac{\rho_G}{\rho_L}\right)^{0.5} \quad (2.22)$$

$$\Delta P_{flooding} = 40.91 F_p^{0.7} \quad (2.23)$$

$$A_{flooding} = -7.31x10^{-11}\Delta P_{flooding}^3 + 2.18x10^{-7}\Delta P_{flooding}^2 - 2.19x10^{-4}\Delta P_{flooding} - 0.0124 \quad (2.24)$$

$$B_{flooding} = 1.25x10^{-10}\Delta P_{flooding}^3 - 3.15x10^{-7}\Delta P_{flooding}^2 + 2.62x10^{-4}\Delta P_{flooding} + 0.0826 \quad (2.25)$$

$$A_{flooding} = 6.82x10^{-8}\Delta P_{flooding}^2 - 1.48x10^{-4}\Delta P_{flooding} - 0.0063 \quad (2.26)$$

$$B_{flooding} = 2.55x10^{-10}\Delta P_{flooding}^3 - 6.09x10^{-7}\Delta P_{flooding}^2 + 4.70x10^{-4}\Delta P_{flooding} + 0.0882 \quad (2.27)$$

For organic mixtures, the graphical correlation of the Kister and Gill (1992) chart is only valid for flow parameters between 0.03 to 0.3 (Kister et al., 2007).

When replacing trays with packings, practical considerations have to be accounted for. In trayed columns, the compositions change stage-by-stage, while in packed columns the composition changes continuously through the column. To approximate this change of composition to that of a theoretical stage, the concept of the height equivalent to a theoretical plate (HETP) can be used (Smith, 2005, Ch. 9.2).

Green and Perry (2007) present a rule of thumb to estimate the HETP of packings in m, shown in Eq. 2.28. In this equation, C_{xy} reflects the effect of the area of inclination and *a* is the packing surface area in $m^2\ m^{-3}$.

$$HETP = 100\left(\frac{C_{xy}}{a}\right) + 0.1 \quad (2.28)$$

This correlation only applies for organic and hydrocarbon mixtures with a surface tension σ smaller than 25 mN m^{-1} (Green and Perry, 2007). For Y-type, S-type of high-capacity structured packings, C_{xy} takes a value of 1. This correlation was developed using experimental data and assumes perfect liquid distribution. For this reason, the predictions obtained using this equation are slightly conservative (Green and Perry, 2007).

2.2.2.2 Illustrative Example 2.3: Comparison between the hydraulic correlations for structured packings found in the open literature and those in commercial design software.

This example uses the same crude oil distillation unit and procedure as Section 2.2.1.3 to compare the predictions between Eqs. 2.19 to 2.25 and KG-Tower (Koch-Glitsch, 2014b) for packed columns. Aspen HYSYS (Aspen Tech, 2012) is not considered in the analysis since it does not provide stage-by-stage flooding profiles for structured packings.

The distillation columns internals are assumed to be structured packings Intalox 2T, which characteristics are presented in Table 2.6. Intalox 2T is selected for this analysis since this type of packing is suitable for high-liquid rate applications (e.g. crude oil distillation columns with pumparounds) (Koch-Glitsch, 2016).

Table 2.6 Characteristics of structured packings Intalox 2T (Green and Perry, 2007; Koch-Glitsch, 2016)

Parameter	Value
Surface area, a, m^2 m^{-3}	215
Packing factor, F_p, m^{-1}	56
HETP, m*	0.38

* Vendor information (Koch-Glitsch, 2016)

Results of hydraulic analysis of structured packings

Figure 2.18 presents the results for the predictions of the approach to flooding. Good agreement can be observed between the correlations presented in Section 2.2.2.1 and KG-Tower (Koch-Glitsch, 2014b) for stages 1 to 36. A small discrepancy (of around 10%) is observed for stages 36 to 41; this is because the flow parameter F_{lv} in this section is smaller than 0.03. Thus, it is outside the range of applicability of the correlation.

The value of HETP obtained by applying Eq. 2.28 is 0.57 m, which is 0.19 m bigger than the value reported by the vendor presented in Table 2.6. However, the vendor mentions that this value is estimated based on atmospheric distillation systems with low relative volatility and good vapour-liquid distribution, and that vendor should be contacted for a better estimation (Koch-Glitsch, 2016).

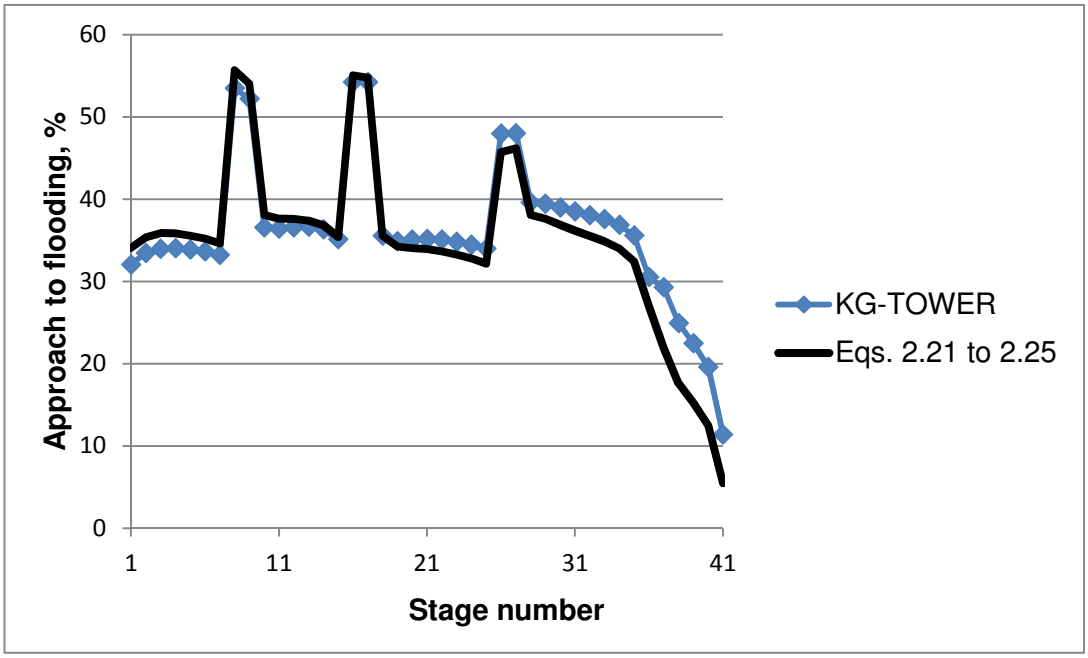

Figure 2.18 Approach to flooding profiles for strcutred pakckings Intalox 2T

Summary and conclusions — packed column hydraulics

The correlations used to predict the approach to flooding for one structured packing (i.e. Intalox 2T) is in good agreement with internals vendor software KG-Tower (Koch-Glitsch, 2014b).

2.2.3 Column hydraulic analysis in existing retrofit approaches

Liu and Jobson (2004) propose a performance hydraulic indicator, the fractional utilization of area (FUA), to assess the area required for vapour flow to avoid flooding. This parameter provides stage-wise information that allows the identification of column bottlenecks. To estimate the FUA, stage-by-stage information is needed. In this work (Liu and Jobson, 2004), the correlation of Kister and Haas (1990) for entrainment flooding is used to estimate the area required for vapour flow. This work does not consider the hydraulic of the downcomer.

Gadalla (2003) and Chen (2008) use results from shortcut models (Gadalla et al., 2003b; Chen, 2008) to estimate the required diameter of each section when modifying the distillation column operating conditions and/or topology in order to compare it with the existing diameter. In both works, the diameter is estimated using the correlation of Fair (1961) for jet flooding. Note in Section 2.2.1.3 , that the correlation of Fair (1961) underestimates the flood points at the draw and return stage of the pumparounds.

Thernesz et al. (2010) use software of internals vendors (i.e. SULCOL v1.0 and KG-Tower v2.0) to avoid unfeasible column designs and/or to evaluate/identify opportunities to replace column internals when increasing the capacity of crude oil distillation columns and/or changing the crude type. Results from rigorous simulations of the crude oil distillation columns are used as inputs of the vendor software. Four hydraulic parameters are assessed: approaches to jet and downcomer flooding, vapour velocity and liquid height in the downcomer. The drawback of this approach is that it requires significant engineering time and effort to evaluate multiple retrofit scenarios, as rigorous simulation and internals vendor software cannot work simultaneously. This approach is commonly followed in practice.

López C. et al. (2013) propose using second-order polynomial functions regressed from rigorous simulations to model crude oil distillation columns. These regressed models are input within an optimisation algorithm to optimise the column operating conditions. The results from the optimisation are re-simulated in PRO/II to validate the results and to check for jet flooding. The hydraulic correlations used are not reported. Downcomer flooding is not accounted for.

Ochoa-Estopier et al. (2015b) include the approach to jet flooding in the ANN models used to simulate the crude oil distillation columns in order to avoid unfeasible column designs. In this work (Ochoa-Estopier et al., 2015b), the ANN models are built regressing results from rigorous simulations in Aspen Tech (2012). Flooding is estimated using the tray sizing utility tool embedded in Aspen Tech (2012) using the default choices and parameters. The downcomer hydraulics is not considered.

Gadalla et al. (2015) follows the works of Gadalla (2003) and Chen (2008) by comparing the required column diameter against the existing one. Gadalla et al. (2015) use Fair's correlation (Fair, 1961) for jet flooding to estimate the required diameter using results from rigorous simulations. The hydraulics of the downcomer is not checked.

2.2.4 Hydraulics of distillation columns — summary and conclusions

In summary, the capacity of a distillation column is limited by the column hydraulics. The hydraulic performance depends on the type of internals used.

Tray hydraulic limits relate to vapour and liquid flows: high-vapour flows cause jet flooding, and high-liquid flows downcomer flooding. The hydraulic limit of packings is flooding. Thus, if a designer wished to increase the production capacity the column, the hydraulic performance of the distillation column has to be taken into account.

The review presented in Section 2.2.3 reveals that while existing retrofit approaches reported in the open literature for increasing processing capacity consider column hydraulics, most approaches only account for the effects of jet flooding, neglecting the downcomer hydraulics. The approach of Thernesz et al. (2010) considers replacing column internals with high-capacity trays and/or structured packings and checks for jet and downcomer flooding. However, the approach of Thernesz et al. (2010) requires significant engineering effort, as mentioned in Section 1.1 .

The predictions obtained using the hydraulic correlations presented in Sections 2.2.1.2 , 2.2.1.5 and KG-Tower (Koch-Glitsch, 2014b) are shown to be in good agreement. However, with the predictions of Aspen HYSYS (Aspen Tech, 2012) considerable discrepancies are observed. This is because it is not possible for users to specify fully the tray topology; thus, a fair comparison between the methods is not possible.

For these reasons, this work uses hydraulic correlations from the open literature and coded in MATLAB to check the hydraulic performance of distillation columns and to assess the potential benefit of replacing the existing internals with high-capacity trays or structured packings. Chapters 3 to 5 provide industrially relevant case studies that show how these correlations are applied.

2.3 Heat exchanger network design and retrofit

Heat exchanger networks (HENs) recover heat from process systems in order to reduce the consumption of hot and cold utilities and thus operational costs (Smith, 2005).

In heat-integrated distillation systems, the distillation column and the heat exchanger network (HEN) have strong interactions. Modifications to the distillation column operating parameters or structure can significantly affect the heat recovery and the required heat

transfer area (Gadalla et al., 2003a; Chen, 2008; Ochoa-Estopier et al., 2015b). In turn, the column and flow sheet modifications impact on the investment costs and thus affecting the profitability of the proposed modifications.

For this reason, existing retrofit methodologies for heat-integrated crude oil distillation systems usually include a method to assess the impacts on the HEN and/or to optimise the HEN for the modified distillation column operating conditions.

Methodologies to design HENs can be categorised into two groups: pinch analysis methods and optimisation methods (Smith et al., 2010a).

Sections 2.3.1 and 2.3.2 present a brief literature review of methods for designing heat exchanger networks that complements literature reviews presented in the publications of Chapters 3 to 5 , where design refers to grass-roots design, retrofit and operational optimisation.

2.3.1 Pinch analysis-based HEN design methods

Pinch analysis was developed by Linnhoff and Hindmarsh (1983) to estimate the minimum hot and cold utility demand based on a given *minimum temperature approach*. For HEN design, the minimum temperature approach is the minimum driving force required to exchange heat between the hot and cold streams so that the minimum heating and cooling utilities are used (Douglas, 1988). Pinch analysis is based on thermodynamic principles and heuristics and can be summarised as follows.

Using the ‘problem table’ algorithm (Linnhoff and Flower, 1978), composite curves (i.e. a graphical representation of the overall energy balances) are built from ‘stream data’ (i.e. inlet and outlet temperatures and heat capacities of the hot, cold and utility streams) in order to predict the minimum energy targets and utility requirements for a minimum temperature approach (Smith, 2005, Ch. 16)

From the composite curves, the heat recovery *pinch* can be identified. The pinch is defined as the temperature where the driving forces for the hot and cold streams are the lowest. Two heuristic rules apply at the pinch point: i) heat should not be transferred from above to below the pinch, and ii) no hot utilities should be used below the pinch and no cold utilities should be applied above the pinch. Based on this analysis, a ‘grid diagram’ of the HEN is obtained.

The pinch analysis method is very useful for HEN design, as it provides a good estimate of the trade-offs between the capital and operational costs of the HEN (Linnhoff and

Hindmarsh, 1983). However, it is not suitable for large scale problems, as it requires significant user interaction (Zhu and Asante, 1999). For this reason, optimisation methods based on pinch analysis (Zhu and Asante, 1999) and stochastic optimisation-based methods (Chen, 2008; Ochoa-Estopier et al., 2015a) have been developed.

2.3.2 HEN optimisation-based methods

Zhu and Asante (1999) propose a methodology based on the *network pinch* concept (Asante and Zhu, 1997). The *network pinch* represents a bottleneck to feasible heat recovery in HEN designs (Linnhoff and Hindmarsh, 1983). Beyond this point, topological changes (e.g. adding, deleting, resequencing and repiping the heat exchangers) are needed to increase the heat recovery of the network. Zhu and Asante (1999) divide the retrofit problem into three stages (i.e. diagnosis, evaluation and optimisation), and formulate the problem as a mixed integer linear problem (MILP). Their approach does not guarantee the optimum design with the minimum retrofit cost, since the objective function only considers the operational costs (Ochoa-Estopier et al., 2015a).

Gadalla (2003) proposes using network pinch analysis to create an Area-Energy curve to assess modifications to the HEN. Firstly, the HEN topology and area are input in SPRINT (Department of Process Integration, 2002). After optimising the operating conditions of the distillation column, the operating conditions and stream data are updated for the existing HEN. Secondly, the heat loads are optimised in SPRINT for no topology changes (i.e. the heat loads are re-distributed). With the results from the optimisation, a retrofit curve for zero modifications is generated; this curve represents the minimum heat exchanger area to achieve a feasible degree of heat recovery without changing the existing HEN structure. Thirdly, the pinching matches that cause network pinch are determined and a modification is proposed (i.e. relocating heat exchangers, adding new matches, splitting streams). The changes in area and energy are plotted in the curve and a network pinch analysis is applied for the modified HEN. This process is repeated for a number of modifications. The final curve is used for a cost-benefit analysis considering energy savings and capital expenditure. The drawbacks of this approach are that the cost for structural modification is neglected and that heat capacities are assumed constant (Chen, 2008).

Rodriguez (2005) presents a simulated annealing-based design methodology to mitigate HEN fouling. In this methodology, the HEN simulation model is formulated to predict fouling over a period of time. The HEN retrofit model is divided into two levels. In the first level, simulated annealing (SA) proposes HEN structural modifications (i.e. adding, removing, relocating heat exchangers and stream splitters); in the second level,

deterministic optimisation is used to balance the heat loads in order to meet the minimum temperature approach constraints and to satisfy the enthalpy balance. Although the scope of this work is mitigation of fouling, these simulation and retrofit models are later used by Chen (2008) to optimise the energy consumption and total annualised costs.

Based on the PhD Thesis of Chen (2008), Smith et al. (2010a) present an optimisation-based HEN retrofit approach for crude oil distillation systems based on the network pinch concept (Zhu and Asante, 1999). In the approach, the optimisation problem is divided into two levels. In the first level, a 'repair' algorithm, formulated as a nonlinear programming problem (NLP), finds the heat loads that regain the feasibility of the system (i.e. meets minimum temperature approach constraints and satisfies energy balances). In the second level, it uses simulated annealing (SA) to propose changes to the HEN structure (i.e. adding, deleting, repiping or resequencing heat exchangers). The work of Smith et al. (2010a) considers the temperature dependence of heat capacities, which is a more realistic approach for crude oil, since assuming constant heat capacities may overestimate the heat recovery of the system. In a case study presented by Chen (2008), in which a HEN is simulated with and without assuming constant heat capacities, it was found that when assuming constant heat capacities the calculated HEN temperatures are underestimated up to 27°C.

Ochoa-Estopier et al. (2015a) modifies the approach of Smith et al. (2010a) by describing the existing HEN topology using the principles of graph theory (de Oliveira Filho et al., 2007) instead of the network pinch concept. In this approach (Ochoa-Estopier et al., 2015a), the HEN topology is model using an incidence matrix that contains the matches between the process and utilities heat exchangers and the streams that form the HEN. The advantage of using this approach is that the HEN structure can be easily manipulated and modified. Similarly to the work of Smith et al. (2010a), the NLP 'repair' algorithm is used to optimise the heat loads and SA is used to proposed structural changes to the HEN. This approach is described and discussed in more detail in Chapter 4 .

2.3.3 Heat exchanger networks — summary and conclusions

Existing HEN retrofit approaches aim to maximise the heat recovery of the system. Two main approaches are followed: pinch analysis methods and optimisation-based methods. Pinch analysis methods are suitable for the design of small-scale problems, since they require significant user interaction due the usage of heuristic rules (Shenoy, 1995). Optimisation-based methods allow optimising both the heat exchanger heat loads and the

HEN structure. Simulated annealing (SA) has been used to propose structural changes to the HEN.

This work uses without significant modification the HEN retrofit approach of Ochoa-Estopier et al. (2015a) to simulate and to propose retrofit modification to the HEN.

2.4 Optimisation methods

Optimisation aims to find the value of the variables that lead to an optimal solution of an objective function (Cavazzuti, 2013). Thus, to set an optimisation problem, the following need to be specified (Cavazzuti, 2013):

1. The optimisation objective. Typically for the retrofit of heat-integrated distillation systems, this function can be an economic indicator (e.g. maximising the net profit, minimising operating costs) or an environmental indicator (e.g. reducing the CO_2 emissions for a given production yield).
2. The variables that influence the value of the objective. Having a large number of variables increases the complexity of an optimisation problem. For this reason, it is important to perform a sensitivity analysis of the variables to determine which ones should be included.
3. The system constraints (e.g. the distillation column hydraulics, product quality specifications)
4. A suitable optimisation algorithm. This depends on the nature of the problem.

Optimisation algorithms can be categorised into two groups: deterministic and stochastic methods. Sections 2.4.1 and 2.4.2 summarise the features of these algorithms and mention the optimisation methods used by some of the retrofit methodologies found in the open literature.

2.4.1 Deterministic methods

Deterministic methods are optimisation algorithms that rely heavily on linear algebra (Cavazzuti, 2013). These methods aim to find the gradients of the response variables. The advantages of using these methods for optimisation is that they required fewer iterations to find the optimal solution, compared to stochastic methods, and that the solutions are replicable. However, they are likely to find to local optimum for large non-linear optimisation problems since these algorithms look for stationary points (Cavazzuti, 2013).

Gadalla (2003) uses a successive quadratic programming (SQP) algorithm to find the optimal process conditions of heat-integrated crude oil distillation systems. SQP is a gradient-based method suitable for solving constrained optimisation problems in which both the objective function and constraints are smooth (Cavazzuti, 2013). In the work of Gadalla (2003), the optimisation objective can be one of the following: reducing the energy consumption, enhancing throughput, increasing profit and reducing CO_2 emissions. The optimisation variables are the distillation column operating conditions (i.e. furnace outlet temperature, stripping steam flow rates, pumparound duties and temperature drops). Practical constraints are considered, such as the hydraulic capacity limitations of the distillation column, the allowable pressure drop of crude oil in the pre-heat train, maximum duties of pumparounds, condenser and reboiler, component recoveries and product flow rates. Penalties are applied to the objective function if constraints are violated.

Chen (2008) mentions that the major drawback of this approach (Gadalla, 2003) is that it neglects the costs of structural modifications. Also, this method does not include structural design decisions (e.g. replacing column internals or adding preflash) within the optimisation. However, the work of Gadalla (2003) includes methodologies for considering these options.

López C. et al. (2013) aim to find the operating conditions and crude oil blending (optimisation variables) that maximise the profit (objective function) of an existing crude oil distillation system. López C. et al. (2013) formulate the problem as an non-linear programming (NLP) problem, and use CONOPT (a gradient-based method included in GAMS) to solve the optimisation problem. This approach does not include structural design decisions. The use of a gradient-based method to solve this problem is possible since second-order polynomial equations are used to simulate the system and constraints are linear (see Section 2.1.3). However, a good guess for the initial values is needed to avoid local solutions (Cavazzuti, 2013).

2.4.2 Stochastic methods

Stochastic optimisation methods include randomness in the search procedure (Cavazzuti, 2013). Examples of stochastic optimisation algorithms are simulated annealing (SA), particle swarm optimisation, evolutionary algorithms and genetic algorithms. In comparison with deterministic methods, stochastic methods are less mathematically complicated and have fewer chances of becoming trapped at local minima, but they need more computing time to converge to an optimal solution (Cavazzuti, 2013).

Stochastic optimisation methods are suitable for large problems that include continuous and discrete variable (also known as mixed integer non-linear programming, MINLP, problems) (Cavazzuti, 2013).

Chen (2008) proposes an optimisation-based retrofit approach for maximising the net profit of crude oil distillation systems. The problem is formulated as a MINLP problem, and is divided into two levels. In the first level, SA is used to propose random changes for the distillation column operating conditions (i.e. furnace outlet temperature, stripping steam flow rates, pumparound duties and temperature drops). In the second level, SA is also used to propose changes to the HEN structure (i.e. adding area, deleting, repiping and resequencing heat exchangers, and adding new heat exchangers) in order to minimise the fired heating consumption. Constraints related to the distillation column hydraulic capacity, product quality specifications, minimum temperature approach and HEN target temperatures are considered in this work (Chen, 2008).

Similarly to Chen (2008), Ochoa-Estopier et al. (2015b) use SA to optimise both the distillation column operating conditions and the HEN structure. The differences between these works are the methods used to simulate the system: Chen (2008) uses shortcut models (Suphanit, 1999) to simulate the distillation column and the network pinch concept (Asante and Zhu, 1997) to retrofit the HEN, while Ochoa-Estopier et al. (2015b) uses metamodels (Ochoa-Estopier and Jobson, 2015a) for the column and the principles of graph theory de Oliveira Filho et al. (2007) to model the HEN.

Chen et al. (2015) proposes a simultaneous process optimisation and heat integration based on rigorous simulation approach. In this approach, a derivative free optimiser (DFO) is used: the covariance matrix adaptation evolutionary strategy (Hansen, 2006). This optimisation algorithm is suitable for difficult nonlinear nonconvex problems in continuous domains (Chen et al., 2015). This work links the optimisation algorithm with rigorous simulation software and a heat integration module.

Neither of these approaches (Chen, 2008; Ochoa-Estopier et al., 2015b; Chen et al., 2015) include structural design decisions (e.g. replace column internals, add a preflash unit) within the optimisation.

2.4.3 Optimisation methods — summary and conclusions

Two types of optimisation methods have been used in existing retrofit methodologies for crude oil distillation systems: deterministic and stochastic methods.

Deterministic methods are computationally inexpensive, but are not suitable for large non-linear optimisation problems, such as the retrofit of heat-integrated crude oil distillation systems. However, they can be used if the problem is simplified as in the approaches of Gadalla (2003) and López C. et al. (2013), where simplified methods are used to simulate the distillation column. However, shortcut models for distillation columns (Gadalla et al., 2003b) are difficult to initialise and converge and do not provide stage-wise information to perform a hydraulic analysis of the distillation columns and metamodels require signification engineering time and effort to set up.

Stochastic methods take more time to find optimal solutions, but have more chances of finding the global solution due to the randomness of the methods. Chen (2008) and Ochoa-Estopier et al. (2015b) present methodologies in which SA has been successfully used to optimise the distillation column operating conditions and the HEN structure in order to increase the profitability of heat-integrated crude oil distillation columns. Chen et al. (2015) use a DFO, the covariance matrix adaptation evolutionary strategy (Hansen, 2006), to optimise the operating conditions and design parameters of existing processes while considering heat integration. This is possible by linking rigorous simulation software (e.g. Aspen Plus, Aspen Custom Modeller) with equation-based modelling environments (e.g. GAMS, MATLAB). Neither of these works (Chen, 2008; Ochoa-Estopier et al., 2015b; Chen et al., 2015) consider structural modifications to the distillation column (i.e. replacing column internals and/or adding a preflash unit). Only the works of Chen (2008) and Ochoa-Estopier et al. (2015b) apply a HEN retrofits model that do consider structural modifications to the HEN.

2.5 Literature review — summary and conclusions

When it is desired to increase the processing capacity of heat-integrated distillation systems, the following retrofit modifications are commonly considered for in both current practice and existing retrofit approaches from the open research literature:

- operational optimisation
- replacing the distillation column internals
- heat integration
- HEN retrofit
- adding separation equipment (i.e. a preflash unit and/or prefractionator)

Two types of retrofit approaches have been developed: sequential and simultaneous approaches (Chen et al., 2015).

Sequential approaches are commonly used in practice (Thernesz et al., 2010). In sequential approaches, each unit is analysed at the time (i.e. firstly, modifications to the distillation column are proposed and assessed; secondly, heat integration and/or HEN retrofit opportunities are explored) (Chen et al., 2015). The drawbacks of using sequential approaches for retrofitting heat-integrated distillation systems are:

- they may overestimate the utility costs, as heat integration is no considered during the optimisation (Chen et al., 2015)
- they required significant engineering time and effort, since commercial simulation and design software are commonly used to analyse the units and to assess the retrofit scenarios (Thernesz et al., 2010). Commercial simulation and design software cannot work simultaneously. This does not permit the implementation of optimisation environments
- they rely on experience and trial and error (Thernesz et al., 2010)

Simultaneous approaches aim to perform heat integration in conjunction with process flowsheet optimisation (Chen et al., 2015). Some of the existing simultaneous retrofit approaches for heat-integrated distillation systems found in the open research literature have also considered HEN retrofit (i.e. adding, deleting, repiping and resequencing heat exchangers and stream splitters) (Smith et al., 2010a; Ochoa-Estopier et al., 2015b).

Simulated annealing (Chen, 2008; Ochoa-Estopier et al., 2015b) and global search (Chen et al., 2015) optimisation algorithms have been used in sequential retrofit approaches to propose new operating conditions and design parameters and to evaluate the retrofit objective function. However, none of the existing simultaneous retrofit approaches for these types of systems include structural modifications to the distillation column and to the process flowsheet (i.e. replacing column internals and/or adding a preflash unit); even though these modifications are commonly applied in practice.

To simulate the distillation columns, three methods have been used for in existing sequential retrofit approaches: shortcut methods (Chen, 2008), rigorous simulation (Chen et al., 2015) and metamodels (Ochoa-Estopier et al., 2015b). To data been seen, only rigorous simulation have been implemented within optimisation environments that include structural design decisions (Caballero et al., 2005). However, this has not been applied in the context of retrofit of heat-integrated distillation systems.

To assess the hydraulic performance of distillation columns hydraulic correlations presented in the open literature and commercial software for internal design and hydraulic analysis have been used. Most of the existing retrofit approaches from the open research

literature have only considers the effects of jet flooding, neglecting the downcomer hydraulics. Commercial software for internals design (e.g. KG-Tower and SULCOL) require of user interaction to input the data needed to perform a hydraulic analysis (i.e. rigorous simulation results need to be exported or input manually), thus they cannot be implemented within optimisation environment.

The retrofit approaches for HEN that can include structural modifications (Smith et al., 2010a; Ochoa-Estopier et al., 2015a) have not been implemented in optimisation-based retrofit approaches that use rigorous simulation to model the distillation columns.

.

Chapter 3 Retrofit approach proposed to assess replacing column internals when increasing capacity

This chapter addresses the first specific objective of this work: i.e. to develop a methodology for assessing the hydraulic performance of distillation columns, to evaluate options to replace the column internals in constrained sections and to estimate the impacts on the HEN of increasing the throughput of heat-integrated distillation systems.

3.1 Introduction to Publication 1

Publication 1 presents a systematic methodology for assessing replacing the column internals with high-capacity trays with sloped downcomers or with structured packings when it is desired to increase the throughput of the same crude oil of a heat-integrated crude oil distillation system.

One of the novelties of this methodology is that it accounts for both the effects of jet and downcomer flooding for conventional trays and high-capacity trays with sloped downcomers. Retrofit approaches from the open research literature typically only account for jet flooding. In previous work (see Appendix A), it is shown that neglecting the downcomer hydraulics may lead to unfeasible column designs when increasing the processing capacity of heat-integrated crude oil distillation systems.

In practice, the hydraulic performance of a distillation column is typically assessed using internals vendor software (e.g. KG-Tower and SULCOL). However, to input the data required by the software (i.e. results from rigorous simulation or plant data) and to read the results, user interaction is required. Thus, analysing multiple retrofit scenarios requires significant engineering effort and time.

To overcome these limitations, this work links rigorous simulation software (i.e. Aspen HYSYS) with an equation-based modelling environment (i.e. MATLAB), in which hydraulic correlations from the open literature for conventional trays, high-capacity trays with sloped downcomers and structured packings are coded.

3.2 Publication 1

Enríquez-Gutiérrez, V. M., Jobson, M., Ochoa-Estopier, L. M., Smith, R., 2015, Retrofit of heat-integrated crude oil distillation columns, Chemical Engineering Research and Design, 99, 185-198, DOI: 10.1016/j.cherd.2015.02.008.

Contents lists available at ScienceDirect

Chemical Engineering Research and Design

journal homepage: www.elsevier.com/locate/cherd

Retrofit of heat-integrated crude oil distillation columns

V.M. Enríquez-Gutiérrez*, M. Jobson, L.M. Ochoa-Estopier, R. Smith

Centre for Process Integration, School of Chemical Engineering and Analytical Science, The University of Manchester, The Mill, Sackville Street, Manchester M139PL, United Kingdom

ARTICLE INFO

Article history:
Received 26 November 2014
Received in revised form 11 February 2015
Accepted 13 February 2015
Available online 20 February 2015

Keywords:
Crude oil distillation retrofit
Hydraulic analysis
Distillation internals

ABSTRACT

Engineering projects to increase the capacity of existing heat-integrated crude oil distillation columns are commonplace. Retrofit projects aim to exploit the processing capacity of existing units by changing operating parameters and/or modifying equipment. Operational modifications can be effective and usually incur little capital expenditure, but equipment changes may also be needed to achieve retrofit objectives. Existing retrofit methodologies for crude oil distillation systems mainly focus on increasing heat recovery, increasing crude oil throughput and/or increasing the yield of most valuable products by optimising column operating parameters. However, methodologies that also consider hardware modifications are lacking. The present work proposes a systematic retrofit methodology based on distillation column and heat exchanger network (HEN) simulation. Hydraulic correlations are used to consider replacing existing distillation column internals with high-capacity trays and/or structured packings. Industrially relevant case studies illustrate the benefits of the proposed methodology to analyse and assess hardware modifications for the retrofit of distillation systems when increasing capacity.

1. Introduction

Crude oil distillation is an important process in petroleum refining, where whole crude is separated into products each with a narrower boiling range. An associated heat exchanger network (HEN) recovers heat from the column to pre-heat the crude oil. Together the columns and HEN comprise the crude oil distillation system. Therefore, any operating or structural change to the distillation column will have an impact on the heat recovery of the system (Gadalla et al., 2003a), making the retrofit of crude oil distillation systems a complex problem with many degrees of freedom and constraints.

Retrofit projects aim to increase the profitability of a process by maximising the use of existing equipment when production objectives change (Liu and Jobson, 2004). Objectives of retrofit projects include increasing production capacity, reducing operating cost, adding new technologies, meeting new product specifications and reducing CO_2 emissions (Uerdingen et al., 2003).

This work focuses on enabling crude oil distillation systems to accommodate more throughput. Operational modifications are preferable because they usually require little or no capital investment. Nevertheless, capacity expansion cannot always be achieved by changing operating parameters, so structural or hardware changes may also be needed. The operating and physical constraints that limit the capacity of the system are called bottlenecks.

Retrofit methodologies can be classified as sequential and simultaneous approaches. Sequential approaches debottleneck each unit separately, first the distillation column and then the HEN or vice versa, until the retrofit objective is achieved. Simultaneous approaches aim to find the optimum

* Corresponding author. Tel.: +44 1613068750; fax: +44 1612367439.
E-mail addresses: victormanuel.enriquezgutierrez@manchester.ac.uk, iq.vic.enriquez@gmail.com (V.M. Enríquez-Gutiérrez).
http://dx.doi.org/10.1016/j.cherd.2015.02.008
0263-8762/

conditions to accommodate the new throughput while considering the heat recovery system and related trade-offs (Gadalla et al., 2013).

However, retrofit methodologies published in the open literature only account for jet flooding as a hydraulic constraint for distillation columns (related to internal vapour flows) to assess the feasibility of retrofit modifications, neglecting hydraulic constraints of the downcomer. Also, retrofit methodologies that consider replacing column internals are lacking.

This work proposes a systematic retrofit methodology for crude oil distillation systems for capacity expansion that considers structural modifications and system constraints. In the methodology, the crude oil distillation column is simulated using Aspen HYSYS and the heat exchanger network (HEN) is simulated using the model of Ochoa-Estopier et al. (2014). Hydraulic correlations are used to estimate jet and downcomer flooding, downcomer exit velocity and liquid load per weir length for conventional and high-capacity trays. Similarly, flooding and the height equivalent to a theoretical plate (HETP) for structured packings are predicted using suitable correlations. Economic correlations are applied to estimate retrofit costs.

This work applies the methodology to an industrially relevant case study, to illustrate the energy and economic trade-offs of retrofit modifications to increase the capacity of a crude oil distillation system.

2. Literature review

Gadalla et al. (2013) note that retrofit projects can be more cost effective than installing new designs when increasing the processing capacity of crude oil distillation systems. For this reason, retrofit methodologies that aim to increase the capacity of crude oil distillation systems are commonplace.

Gadalla et al. (2003a) propose an optimisation-based retrofit methodology that considers the interactions between the crude oil distillation column and HEN. Shortcut models for retrofit design (Gadalla et al., 2003b) are used to consider an existing crude oil distillation column, with a fixed number and distribution of stages. For the HEN, an 'area retrofit model' is proposed to relate the additional heat exchanger area required for retrofit to the energy consumption of the distillation column. Hydraulic constraints related to jet flooding in the distillation column are considered during the optimisation. However, downcomer flooding is not considered, neglecting the effect of liquid loads inside the distillation column. The specifications for the shortcut models used for retrofit are expressed in terms of recovery of key components, so are not straight forward to define. Constant thermal properties are assumed in the HEN retrofit model, which is known to introduce inaccuracies in the HEN modelling (Chen, 2008).

Chen (2008) overcomes some of these limitations by providing a method to estimate the key components of the product streams based on the required product specifications. The HEN retrofit model is also extended by considering temperature-dependent thermal properties and modelling of stream splitters and mixers, desalters and interconnections between HEN components (Smith et al., 2010). Jet flooding is the only hydraulic constraint considered. The downside of the shortcut methods for retrofit is that they are not computationally robust, so they require sensible initial guesses; nor do they provide the stage-by-stage information needed to perform hydraulic analysis.

Liu and Jobson (2004) propose a hydraulic performance indicator, the fractional utilization of area (FUA), to analyse the feasibility of retrofit modifications in distillation columns. Following from this work, Wei et al. (2012) propose a related hydraulic indicator, the 'maximum capacity expansion potential rate' (x_{max}), used together with the FUA to screen potential retrofit modifications in order to increase the processing capacity of distillation columns. Both hydraulic indicators are determined from results of rigorous simulations using commercial simulation software (e.g. Aspen HYSYS or Pro/II); both parameters are only related to jet flooding.

Thernesz et al. (2010) use commercial simulation software to analyse the effect of throughput increases on a crude oil distillation system. Pro/II is used to simulate the crude oil distillation unit. Internals vendor software, SULCOL and KG-TOWER, are used to perform hydraulic analysis of the existing column internals and to evaluate the option of replacing them with high-capacity or high-efficiency trays if the loads are exceeded. HEN design software, SUPERTARGET, is used to simulate and identify potentially useful retrofit options for the HEN. The advantages of this systematic approach is that rigorous simulation is used to simulate the distillation column, in which the models are computationally robust and provide stage-by-stage information; vendor information and suitable correlations are used to check the hydraulics of the distillation column; and the existing HEN structure and heat integration opportunities are considered. However, this approach requires significant engineering time to analyse multiple retrofit options (e.g. replacing existing trays with different high-capacity trays or structured packings), since the commercial software packages cannot work together.

Gadalla et al. (2013) propose an optimisation-based retrofit methodology in which rigorous simulation is used to model both the distillation column and HEN. To determine the energy targets, pinch analysis is used; the maximum required diameter is used as a hydraulic constraint. Adding a preflash, prefractionator or a new pump-around are considered as retrofit options in order to increase the capacity of the system and to enhance heat recovery. However, pinch analysis is not well suited to address HEN retrofit (Ochoa-Estopier et al., 2014). Also, the required diameter evaluation only considers jet flooding.

It can be concluded that when increasing the capacity of heat-integrated crude oil distillation columns, rigorous simulation is needed, since stage-by-stage information is required to assess the hydraulic performance of distillation columns. Published retrofit methodologies only consider jet flooding as the hydraulic constraint, neglecting the effect of the downcomer hydraulics in trays; none consider replacing existing column internals with high-capacity trays or structured packings as retrofit option, except for those which use internal vendor software. Internal vendor software packages have the advantage of using suitable correlations to assess the hydraulic performance of a wide range of internals. However, they cannot work together with commercial simulation software; therefore significant engineering effort is needed to assess several retrofit options. It can also be concluded that retrofit methodologies need to consider both parts of the overall system, i.e. the distillation column and HEN.

This work proposes a retrofit methodology for increasing the capacity of heat-integrated crude oil distillation columns. The methodology aims to overcome the limitations mentioned above, to find the maximum capacity of crude oil distillation systems and to evaluate the additional

heat exchanger area needed to accommodate the increased throughput. The methodology allows the engineer to analyse the effect of different column internals on the distillation column processing capacity, energy consumption and adequacy of the HEN.

3. Retrofit methodology

Fig. 1 presents the proposed retrofit methodology for the evaluation and assessment of hardware modifications to crude oil atmospheric distillation columns when increasing capacity. The impacts on the HEN are also considered in the methodology. Using a MATLAB interface, throughput and corresponding operating parameters (e.g. pump-around duties and steam flows) are increased pro-rata and input to Aspen HYSYS v7.3 (2012), where the distillation column is simulated. The results from the simulation are used as inputs to the hydraulic correlations for the columns to check for hydraulic bottlenecks, and to a HEN simulation model to estimate the required heat transfer area and fired heating demand. Both the hydraulic correlations and HEN simulation model are coded in MATLAB. The hydraulic performance is evaluated in terms of jet flooding, liquid weir loading, downcomer exit velocity and downcomer flooding for valve trays and high-capacity trays, or flooding and HETP for structured packings. This methodology allows, with relatively little engineering effort, the analysis of multiple retrofit scenarios, such as finding the maximum capacity of distillation columns without the need for retrofit modifications and replacing existing internals with high-capacity trays or structured packings if the column cannot accommodate more throughput.

Fig. 2 presents the key features of the atmospheric column and lists the information retrieved from HYSYS using the MATLAB code. For each stage in the column, the vapour and liquid phase flow rates and transport properties are needed for the hydraulic calculations. Inputs to the HEN simulation code are the product flowrates and temperatures, pump-around, condenser and reboiler duties and temperature drops.

Section 3.1 presents the hydraulic correlations used in this work to predict the hydraulics of distillation columns using different types of internals; the HEN simulation model is described in Section 3.2 and the economic model used to estimate the cost of retrofit is described in Section 3.3.

3.1. *Hydraulic analysis of distillation columns*

When increasing throughput for distillation columns, it is important to determine their maximum capacity in order to screen for bottlenecks (Wei et al., 2012). To determine column bottlenecks, gamma scanning of actual operation (Shahabinejad et al., 2014) or hydraulic correlations available in the open literature and simulation software (Wei et al., 2012) can be used.

This work uses hydraulic correlations to predict column bottlenecks. The hydraulic correlations that are presented in Sections 3.1.1 and 3.1.2 are also used in Aspen HYSYS v7.3 (2012) and KG-Tower v5.1 (2012). In practice, column pressure drop should be accounted for, as it affects the column internal flows and transport properties, thus affecting the column hydraulics. The case study used in this work assumes constant pressure in the distillation column. However, the same correlations can still be used in a column with a pressure drop, since the inputs for the hydraulic correlations are retrieved from results of converged simulations in which the column pressure drop is taken into account. Note that the methodology is not restricted to these correlations; it can also apply more accurate correlations if there are available.

Trays can operate efficiently between certain flows limits. At high vapour loads, liquid is carried over to the stage above; this phenomenon is known as jet flooding. Entrainment is when droplets of liquid are carried to the stage above (Stichlmair, 1998). To prevent both these phenomena, distillation columns are designed with an 'approach' to jet flooding. Weeping occurs at low vapour loads when the vapour is no longer able to prevent the liquid from leaking to the stage below (Stichlmair, 1998).

At high liquid loads, the vapour cannot disengage completely from the liquid causing vapour entrainment. This entrainment occurs when the downcomer is too small to handle the liquid load, resulting in a low downcomer residence time and/or downcomer back-up (liquid backs up to the stage from the downcomer), and it is known as downcomer flooding (Stichlmair, 1998). At low liquid loads, liquid may be almost completely vaporised, resulting in a 'dry' stage, on which counter-current vapour–liquid contact does not take place (Stichlmair, 1998). It is recommended that the downcomer flooding does not exceed 80 to 85% of the design limit (Koch-Glitsch, 2006) to prevent tower malfunction.

The literature review notes that published retrofit methodologies only consider jet flooding as a hydraulic constraint. In this work, the Glitsch correlation (Branan, 2011) is used to predict the approach to jet flooding for valve and high-capacity trays. To account for the hydraulics in the downcomer, three parameters are predicted: the liquid load per weir length and downcomer exit velocity, estimated using the same method as

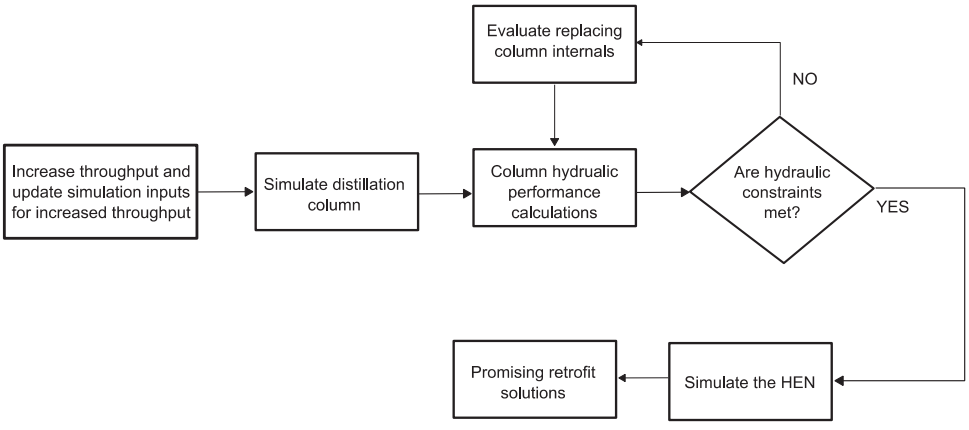

Fig. 1 – Proposed retrofit methodology.

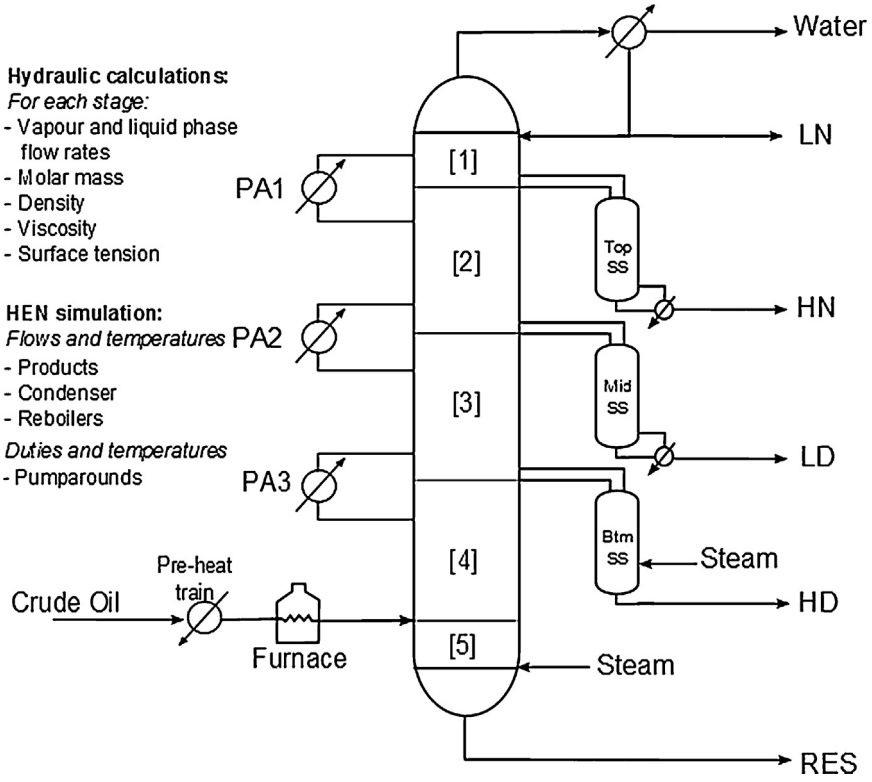

Fig. 2 – Distillation column information retrieved from HYSYS using MATLAB code.

in KG-Tower v5.1 (2012), and downcomer flooding, using the correlation presented by Branan (2011).

This work aims to assess proposed operational and design changes against these constraints so that only feasible solutions will be selected. That is, whichever constraint is violated first becomes the controlling constraint.

Packed columns operate in countercurrent flow and use mass transfer devices with a high interfacial area to contact vapour and liquid flows (Stichlmair, 1998). These mass transfer devices, known as packings, can be divided into two groups: random packings and structured packings, where structured packings are typically much more efficient in terms of height equivalent of a theoretical plate (HETP) (Kister, 1992). Replacing conventional trays with structured packings has been used to increase the capacity of distillation columns (Kencse et al., 2007); this work considers structured packings.

To predict flooding for structured packings, the regressed model from the pressure drop correlation chart of Kister and Gill (Kister et al., 2007) presented by Enríquez-Gutiérrez et al. (2014) is used as flooding calculation method. The correlation used in Aspen HYSYS v7.3 (2012) is said to be based on the same pressure drop chart; no details of the correlation are presented. To estimate the HETP, a rule of thumb presented by Green and Perry (2007) is used.

3.1.1. *Hydraulic correlations for trays*

In this work, the Glitsch correlation, also known as "Equation 13" (Branan, 2011), is used to predict the 'percent flooding' for conventional trays (Eq. (1)). Resetarits (2014) mentions that this correlation has been used for decades with reasonable success to estimate jet flood points. In this correlation, the percent flooding is a function of the vapour load factor, V_{load}, $m^3\,s^{-1}$; the liquid volumetric flowrate, V_L, in $m^3\,s^{-1}$; the tray flow path length, T_{FL}, in m; the tray active area, A_{ac}, in m^2; and the vapour capacity factor, CF:

$$\%\text{Flooding} = \frac{35.32V_{load} + V_L T_{FL}}{10.76 \times A_{ac} \times CF} \quad (1)$$

Distillation columns with large diameters are typically designed with an 80% approach to flooding (Branan, 2011), although some authors suggest that 85% can be considered for retrofit. This limit indicates an unacceptably high risk of jet flooding and tower malfunction (Koch-Glitsch, 2006).

The vapour load factor is the vapour rate corrected for vapour and liquid densities (Branan, 2011). It can be estimated using Eq. (2), in which V_G is the volumetric vapour load in $m^3\,s^{-1}$ and ρ_G and ρ_L are the vapour and liquid densities in $kg\,m^{-3}$, respectively (Branan, 2011):

$$V_{load} = V_G \times \sqrt{\frac{\rho_G}{\rho_L - \rho_G}} \quad (2)$$

The tray flow path length is function of the tower diameter in m, D_c, and the number of passes per tray, N_p (Branan, 2011):

$$T_{FL} = 30\frac{D_c}{N_p} \quad (3)$$

The vapour capacity factor CF is a function of the tray spacing in m, T_S, and the vapour density in $kg\,m^{-3}$ (Branan, 2011):

$$CF = \left[0.58 - \frac{0.084}{T_S}\right] - \left[\frac{2.44 \times T_S \times \rho_G - 39.37 \times T_S}{1560}\right] \quad (4)$$

Most retrofit methodologies neglect the effect of liquid loads on the distillation column hydraulic performance. As shown by Enríquez-Gutiérrez et al. (2014), liquid loads play an

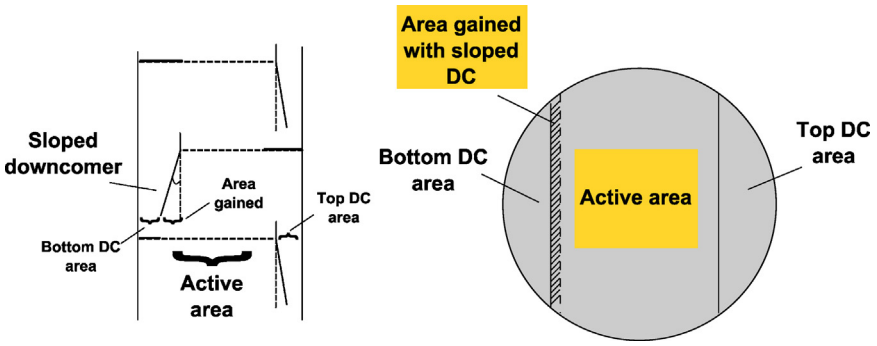

Fig. 3 – Increased active area when using sloped downcomers.

important role in the assessment of retrofit options for crude oil distillation systems. Enríquez-Gutiérrez et al. (2014) considered using the liquid load per weir length together with jet flooding to assess retrofit modifications. This work also considers the downcomer exit velocity and downcomer flooding. These parameters were observed to be sensitive to throughput increases by rating distillation columns using valve and high-capacity trays in KG-Tower v5.1 (2012) and Aspen HYSYS v7.3 (2012).

The liquid load per weir length, L_w, is function of the liquid volumetric flow rate in $m^3\,s^{-1}$, the weir length in m, l_w, and the number of passes per trays, as shown in Eq. (5). A value between 90 and 100 $m^3\,m^{-1}\,h^{-1}$ is used in practice as the design limit (Resetarits, 2010). If the design limit is exceeded, it is recommended to increase the number of passes to provide a better vapour–liquid contact, i.e. provide increased tray capacity (Koch-Glitsch, 2006).

$$L_W = \frac{V_L}{l_w \times N_p} \times 3600 \tag{5}$$

For the downcomer exit velocity, v_{DCexit}, a limit of 0.46 m s^{-1} is recommended (Koch-Glitsch, 2006); otherwise the downcomer clearance should be adjusted. This parameter can be predicted using Eq. (6), in which H_{cl} is the downcomer clearance in m (KG-Tower v5.1, 2012).

$$v_{DCexit} = \frac{V_L}{l_w \times H_{cl} \times N_p} \tag{6}$$

The phenomena that cause downcomer flooding are the tray pressure drop, the liquid height on the downcomer and the frictional losses in the downcomer. These phenomena in turn are caused by high velocities in the downcomer (Kister, 1992).

To predict flooding in the downcomer, Eq. (7) can be used (Branan, 2011), in which A_{DC} is the downcomer area in m^2 and v_{DCdes} is the design velocity that avoids flooding in the downcomer. The criteria used to determine the downcomer design velocity, also known as Glitsch correlations (Koch-Glitsch, 2013), are presented in Eqs. (8)–(10). The lowest value from Eqs. (8)–(10) is selected as the design velocity (Kister, 1992).

$$\%DCflooding = \frac{V_L}{A_{DC} \times N_p \times v_{DCdes}} \tag{7}$$

$$v_{DCdes} = 0.170 \tag{8}$$

$$v_{DCdes} = 0.03 \times \sqrt{\rho_L - \rho_G} \tag{9}$$

$$v_{DCdes} = 2.45 \times \sqrt{295 \times T_S \times (\rho_L - \rho_G)} \tag{10}$$

Conventional trays can be modified in order to achieve more capacity and/or efficiency. These types of trays are known as high-capacity trays. Most high-capacity trays are patented designs and little information can be found about their geometry in the open literature. However, for valve trays with sloped downcomers, the same correlations (Eqs. (1)–(10) can be used to predict their hydraulic behaviour if the active tray area is corrected by considering the area gained by sloping the downcomer as shown in Fig. 3 (KG-Tower v5.1, 2012).

The increased active area, when using a sloped downcomer, can be estimated (KG-Tower v5.1, 2012):

$$A_{acnew} = A_T - (A_{DCtop} - A_{DCbttm}) \tag{11}$$

where A_T is the cross sectional area of the distillation column in m^2 and A_{DCtop} and A_{DCbttm} are the top and bottom downcomer areas also in m^2, respectively. The bottom downcomer area can be estimated using Eq. (12), in which θ is the downcomer slope angle, relative to the vertical.

$$A_{DCbttm} = A_{DCtop} \sin\theta \tag{12}$$

Eq. (11) is only valid for trays with two passes. For trays with 4 passes per tray, the active area can be estimated with (KG-Tower v5.1, 2012):

$$A_{acnew} = A_T - (A_{DCtop} - 2 \times A_{DCbttm}) \tag{13}$$

3.1.2. *Hydraulic correlations for packings*

The hydraulic limit for structured packings is flooding. The flood point for structured packings is defined as the pressure drop at which the liquid is no longer able to flow against the vapour, impeding countercurrent flow (Stichlmair, 1998). Packed columns are typically designed with an 80% approach to flooding. In addition, packed columns require a minimum liquid load to operate; below this limit, the packing surface is not completely wetted, reducing the mass transfer contact area and separation efficiency. For organic mixtures, it is a rule of thumb that the liquid load should be at least 2 $m^3\,m^{-2}\,h^{-1}$ (Stichlmair, 1998).

The approach to flooding for structured packings is defined as (Kister et al., 2007):

$$\%Flooding = \left(C_{sb}/C_{sb,flooding}\right) \times 100\% \tag{14}$$

where C_{sb} is the operational capacity factor (also known as C-factor) and $C_{sb,flooding}$ is the C-factor at flooding conditions. The C-factor at flooding conditions for packed columns can

be estimated using Eq. (15), where $CP_{flooding}$ is the capacity parameter at flooding conditions, F_p is the packing factor, an empirical factor depending on the packing size and shape, in m^{-1} and μ_L is the liquid viscosity in $kg\,m^{-1}\,s^{-1}$ (Kister et al., 2007):

$$C_{sb,flooding} = \frac{CP_{flooding}}{F_p^{0.5}\left(\frac{\mu_L}{\rho_L}\right)^{0.05}} \quad (15)$$

Enríquez-Gutiérrez et al. (2014) proposed a regressed model from the pressure drop correlation chart for structured and random packings of Kister and Gill (1992), cited in Kister et al. (2007), to predict the capacity parameter at flooding conditions (Eq. (16)). In this model, the capacity parameter at flooding is a function of the flow parameter and two constants. The flow parameter F_{lv} is estimated using Eq. (17), where L and G are liquid and vapour molar flow rates, respectively, in $kmol\,s^{-1}$. The parameters $A_{flooding}$ and $B_{flooding}$ are functions of the flooding pressure drop $\Delta P_{flooding}$ in $Pa\,m^{-1}$ (Eq. (18)). Eqs. (19) and (20) provide these parameters.

$$CP_{flooding} = A_{flooding}\ln(F_{lv}) + B_{flooding} \quad (16)$$

$$F_{lv} = \frac{L}{G}\left(\frac{\rho_G}{\rho_L}\right)^{0.5} \quad (17)$$

$$\Delta P_{flooding} = 40.91 \times F_p^{0.7} \quad (18)$$

$$A_{flooding} = -7.31\times10^{-11}\Delta P_{flooding}^3 + 2.18\times10^{-7}\Delta P_{flooding}^2 - 2.19\times10^{-4}\Delta P_{flooding} - 0.0124 \quad (19)$$

$$B_{flooding} = 1.25\times10^{-10}\Delta P_{flooding}^3 - 3.15\times10^{-7}\Delta P_{flooding}^2 + 2.62\times10^{-4}\Delta P_{flooding} + 0.0826 \quad (20)$$

For organic mixtures this correlation is only valid for flow parameters between 0.03 to 0.3 (Kister et al., 2007). Kister et al. (2007) note that this correlation is sensitive to the packing factor; therefore it is important to obtain this parameter from a reliable source.

In distillation columns containing trays, the compositions change from stage to stage, while in packed columns the compositions change continuously through the column. To associate this change of compositions to that of a theoretical stage, the concept of height equivalent of a theoretical plate (HETP) is used. HETP is a measure of the separation efficiency of a packed column (Smith, 2005, Ch. 9.2). To estimate a value of HETP in m, Green and Perry (2007) presented the rule of thumb shown in Eq. (21), where C_{xy} reflects the effect of the area of inclination and a is the packing surface area in $m^2\,m^{-3}$.

$$HETP = 100\left(\frac{C_{xy}}{a}\right) + 0.10 \quad (21)$$

This correlation only applies for organic and hydrocarbon mixtures with a surface tension, σ, smaller than $25\,mN\,m^{-1}$ (Green and Perry, 2007). For Y-type, S-Type or high-capacity structured packings C_{xy} is equal to 1. This correlation was obtained using experimental data; however Green and Perry (2007) mention that since the data was measured assuming perfect liquid distribution, the results obtained are slightly conservative.

Packed columns need supplementary equipment to operate properly. For example, liquid distributors are installed to ensure even liquid distribution, as poor liquid distribution impacts on the separation efficiency. Liquid collectors need to be installed in distillation columns containing side streams and pump-arounds (Stichlmair, 1998, Ch. 8.3). Smith (2005) notes that liquid collectors and distributors require 0.5 to 1 m of column height per bed of packing. This work assumes a value of 0.5 m per liquid distributor.

3.2. *Heat exchanger network (HEN) simulation model*

As mentioned in the literature review, retrofit methodologies for crude oil distillation systems should consider both the distillation column and the HEN. This work uses the HEN simulation model proposed by Ochoa-Estopier et al. (2014). The simulation model applies the principles of graph theory, as proposed by de Oliveira Filho et al. (2007), and extended by Ochoa-Estopier et al. (2013) to consider temperature-dependent heat capacities.

This simulation model calculates the utility requirements of the network and the outlet temperatures of every heat exchange unit, splitter and mixer. Eq. (22) shows the feasibility solver used to ensure that the calculated temperatures do not violate stream energy balances or minimum temperature approach constraints. In Eq. (22), Q and *sf* are vectors that represent the heat exchanger loads and split fractions, respectively; TH and TC are the inlet and outlet temperatures of an exchanger i; N_{HX} and N_{ST} are the number of exchanger units and process streams, respectively; TT_{cal} and TT are the calculated and specified target temperature of a stream k; and ΔT_{min} is the minimum temperature approach. If any of these constraints is violated, i.e. the minimum temperature approach or the energy balance, the feasibility solver is called to determine new heat loads and split fractions that allow feasibility to be regained. The feasibility solver is based on that developed by Chen (2008). Though there is no unique solution (vectors Q and *sf*), the feasibility solver does not consider the optimality of the feasible solution.

$$\min_{Q,sf}||f(Q,sf)||_2^2 = \min_{Q,sf}\left[\sum_{i=1}^{N_{HX}}\min\left(TH_i^{out} - TC_i^{in} - \Delta T_{min}, TH_i^{in} - TC_i^{out} - \Delta T_{min}, 0\right)^2 + \left|\sum_{k=1}^{N_{ST}}(TT_{cal,k} - TT_k)^2\right|\right] \quad (22)$$

Ochoa-Estopier et al. (2014) uses the results generated by an artificial neural network (ANN) model of a crude oil distillation column as inputs for the HEN simulation model. This work instead generates the inputs from rigorous simulations of the distillation column using the MATLAB-HYSYS interface, allowing one to update the thermal heat capacities and outlet temperatures of the process streams for every retrofit modification.

Table 1 – Installation and removal factor for high-performance trays and structured packings.

	Installation factor	Removal factor (remove existing trays and replace with new hardware)
High-performance trays	1.4	0.1
Structured packings	0.8	0.1

The model of Ochoa-Estopier et al. (2014) employs the retrofit approach of Smith et al. (2010) to modify the duty of heat exchangers, add and/or delete heat exchangers, repipe and resequence heat exchangers, and add, delete or modify a bypass. In this work, the retrofit modifications allowed for the HEN are those found by the feasibility solver, i.e. vectors of heat loads and split fractions. Finding the optimum retrofit design for the HEN is out of the scope of this work. However, this methodology can be improved if an optimisation-based HEN retrofit methodology is included.

Another advantage of using this simulation model for the HEN is that heat exchangers are specified in terms of their heat capacities, allowing one to estimate the required heat exchanger additional area to accommodate the increased throughput.

3.3. *Retrofit cost estimation*

To estimate the cost of structural modifications to the distillation column when increasing capacity, simplified economic models found in the open literature are used to determine the retrofit cost of replacing existing internals to distillation columns and adding heat exchange area to the HEN. These economic models are described below. Where more accurate cost models are available, these can be applied instead.

3.3.1. *Retrofit cost of replacing distillation column internals*

Branan (2011) presents an analytical model for estimating the cost of replacing internals in a distillation column retrofit, citing Bravo (1997). In this model, the cost of replacing column internals is function of the hardware cost $\$Cost_{hardware}$ and installation and removal factors F_i and F_R, respectively.

The hardware cost of high performance trays, including liquid distributors, is given in Eq. (23), where D is the column diameter in m and N_t is the number of trays; the hardware cost of structured packing, including distributors, is given in Eq. (24) where S_H is the summation of bed heights in m and N_b is the number of beds. Installation and removal factors are presented in Table 1. These factors are only valid when replacing existing trays with new ones with the same tray spacing.

$$\$Cost_{HPT} = \left[11 \times D^2 \left(52N_t + 160\right)\right] \times F_i \times F_R \quad (23)$$

$$\$Cost_{SP} = 11 \times D^2 \left[260S_H + 160\left(2N_b - 1\right)\right] \times F_i \times F_R \quad (24)$$

The cost model was first presented by Bravo (1997), so costs should be updated; this work uses the annual Chemical Engineering Plant Cost Index (CEPCI) for 1997, 386.5 (Vatavuk, 2002) and the CEPCI for December 2013, 687.9 (Chemical Engineering, 2014).

3.3.2. *Retrofit cost of installing additional heat exchanger area*

Chen (2008) applies the cost model presented by Smith (2005) in which it is assumed that the capital cost of a heat exchanger can be predicted using a simple relationship between the surface area A_{HX} and three cost law constants a, b, and c, depending on the materials of construction, pressure rating and type of heat exchanger (Eq. (25)). Smith (2005) states that, even though this cost model is based on the assumption of the total heat exchanger area is divided equally between the heat exchangers, the model gives useful predictions of cost. Chen (2008) presents four cost models for: installing additional area to existing heat exchangers (Eq. (26)), installing new heat exchangers (Eq. (27)), heat exchanger repiping (Eq. (28)) and heat exchanger resequencing (Eq. (29)). The costs are given in US$ and A_{HX} in m^2.

$$\$Cost_{HX} = a + b \times \left(A_{HXreq}\right)^c \quad (25)$$

$$\$Cost_{HXarea} = 1530 \times \left(A_{HXreq}\right)^{0.63} \quad (26)$$

$$\$Cost_{HX} = 13,000 + 1530\left(A_{HXreq}\right)^{0.63} \quad (27)$$

$$\$Cost_{HXrepiping} = 60,000 \quad (28)$$

$$\$Cost_{HXresequencing} = 35,000 \quad (29)$$

The capital cost predicted by this model should be also updated, since it was presented by Smith (2005). The annual CEPCI for 2005, 468.2 and the CEPCI for heat exchangers and tanks of December 2013, 621.6, (Chemical Engineering, 2014) are used in this work.

3.4. *Methodology—Summary*

In summary, the proposed retrofit methodology for crude oil distillation systems for increased capacity comprises four parts. First, the distillation column is simulated using rigorous models in a commercial simulation package (HYSYS). Second, the hydraulic performance of different types of internals in the column is assessed using appropriate hydraulic correlations. Third, the existing HEN is simulated, considering the energy balance, the HEN structure and temperature-dependent heat capacities of streams. The heat loads and stream splits are adjusted to ensure that energy balances are maintained. Finally, the costs of modifications to the column and HEN are estimated using suitable cost correlations. The methodology is coded in MATLAB to allow modelling and analysis of the whole system with a view to increasing processing capacity.

In Section 4, the proposed retrofit methodology is applied to an existing heat-integrated crude oil distillation column to show the benefits of the methodology for analysis of the operating and hydraulic performance of an existing crude oil distillation system, assessment of the impacts on both distillation column and HEN when increasing throughput, and evaluation of the feasibility and viability of hardware modifications proposed as retrofit solutions.

4. Case studies

The atmospheric distillation unit used as the base case is based on the case presented by Watkins (1979). It processes 100,000 bbl d^{-1} (828 m^3 h^{-1}) of Venezuela Tía Juana Light crude oil. The unit consists of a main fractionator, three

Table 2 – Operating conditions of the crude oil distillation column (Chen, 2008, Ch. 6.1).

Parameter	Main fractionator	HD side-stripper	LD side-stripper	HN side-stripper
Feed pre-heat temperature (°C)	365	–	–	–
Operating pressure (bar)	2.5	2.5	2.5	2.5
Vaporisation mechanism	Steam	Steam	Reboiler	Reboiler
Reflux ratio	4.17	–	–	–
Steam flow (kmol h^{-1})	1200	250	–	–
Condenser duty (MW)	47.87	–	–	–
Reboiler duty (MW)	–	–	8.78	6.63

Table 3 – Product specifications (Chen, 2008, Ch. 6.1).

Products	T5 (°C, TBP)	T50 (°C, TBP)	T95 (°C, TBP)
RES	353	462	798
HD	285	339	372
LD	190	248	317
HN	117	156	196
LN	3	71	118

side-strippers and three pump-arounds. Five products are produced: Light Naphtha (LN), Heavy Naphtha (HN), Light Distillate (LD), Heavy Distillate (HD) and Residue (RES). The main fractionator and HD side-stripper use steam as the stripping agent. The distillation column operating conditions are presented in Table 2; product specifications are summarised in Table 3 and the column structure and stage distribution are illustrated in Fig. 4. For simplicity, it is assumed that there is no pressure drop in the column or heat exchangers; this assumption is not fundamental to the methodology.

The HEN structure is based on the heat exchanger network of Chen (2008), shown in Fig. 5; it consists of 22 heat exchangers, 5453 m^2 of heat transfer area, a fired heating demand of 62.1 MW and it is designed with ΔT_{min} equal to 25 °C. Process stream data and heat exchanger details are shown in Tables 4 and 5.

In the following sections, three case studies are presented. In Section 4.1, the base case, a hydraulic analysis of the base case is performed in order to determine how much throughput the distillation column can accommodate without needing retrofit solutions. In case study 1 (Section 4.2), the crude oil throughput and operating parameters are increased until the hydraulic limits are reached, identifying the column bottlenecks and the corresponding impacts on the HEN. In case study 2 (Section 4.3), hardware modifications are proposed in order to debottleneck the distillation column and the costs of replacing column internals and HEN modifications are estimated.

4.1. *Base case*

In the base case, the column internals are assumed to be valve trays with a tray spacing of 0.6 m, active area of 91% and a downcomer clearance of 0.05 m. As shown in Fig. 4, the main fractionator is divided into five sections and it has three side strippers. The trays in sections 1 to 4 have four passes per tray and Section 5 and the side-strippers have two passes per tray. Table 6 shows the tower diameters in each column section.

The base case is simulated in Aspen HYSYS v7.3 (2012) and, using the MATLAB interface, the results from the rigorous simulation are used to estimate the jet flooding, liquid load per weir length, downcomer exit velocity and downcomer flooding using the hydraulic correlations presented in Section 3.3.1.

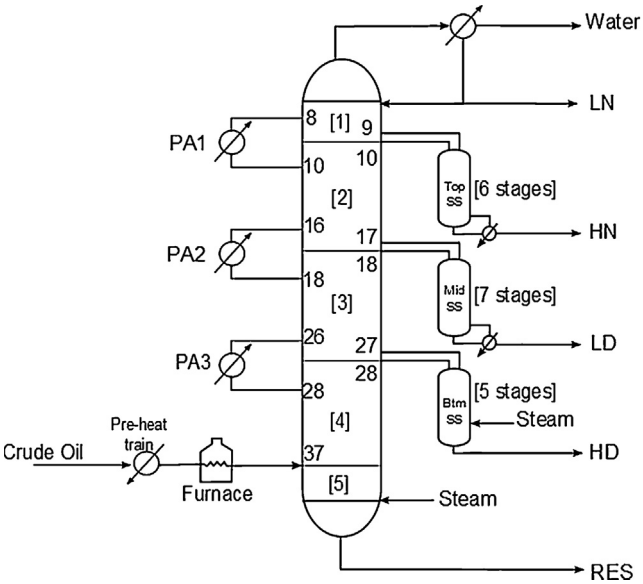

Fig. 4 – Stage distribution of the atmospheric distillation column (Chen, 2008, Ch. 6.1).

Table 4 – Process stream data (based on Chen, 2008).

Stream	Supply temperature (°C)	Target temperature (°C)	Enthalpy change (MW)
Crude oil	25.0	365.0	143.4
LD-reboiler	262.7	284.3	6.1
HN-reboiler	172.7	193.8	3.9
Cooling water (utility)	10.0	40.0	77.1
Pump-around 1 (PA1)	304.5	278.0	12.8
Pump-around 2 (PA2)	223.3	187.1	17.9
Pump-around 3 (PA3)	146.2	141.1	11.2
Condenser	97.2	76.0	46.7
RES	328.0	100.0	49.6
HD	262.1	50.0	5.4
LD	273.9	40.0	17.9
HN	179.3	40.0	6.5
LN	72.8	40.0	1.4
Fired heating (utility)	1500.0	800.0	62.1

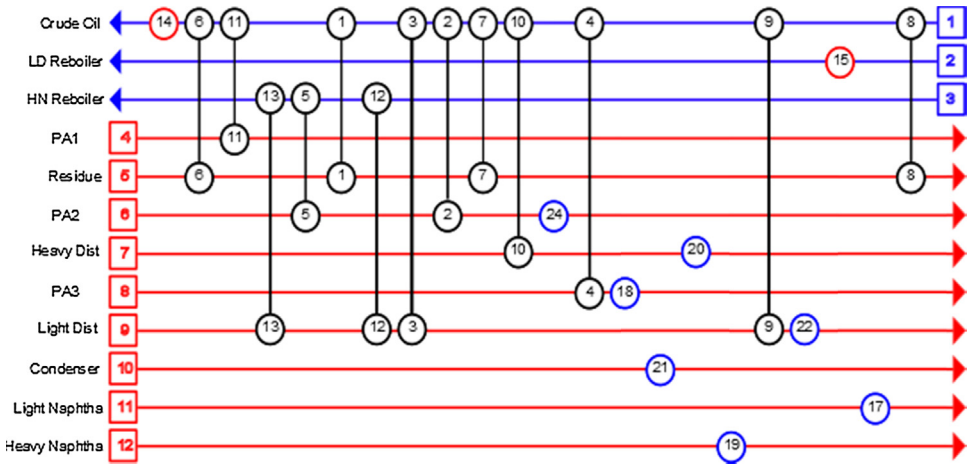

Fig. 5 – HEN structure (Chen, 2008, Ch. 6.1).

Table 5 – HEN details (based on Chen, 2008).

Heat exchanger number	Installed area (m^2)	Duty (MW)
h1	975	25.4
h2	332	11.5
h3	112	3.2
h4	196	5.7
h5	58	4.8
h6	105	3.3
h7	684	13.2
h8	312	10.8
h9	260	8.8
h10	46	2.1
h11	555	12.9
h12	22	1.1
h13	67	3.9
h14*	106	59.6
h15*	11	8.8
h17*	59	8.1
h18*	99	7.9
h19*	122	6.5
h20*	61	3.7
h21*	1036	52.9
h22*	179	6.5
h24*	56	10.5

* Utility heat exchanger.

Figs. 6–9 show the hydraulic results for the base case when using valve trays. As observed in the flooding profile presented in Fig. 6, the column seems to be operating below the hydraulic limit, which could lead to the conclusion that the column can accommodate more throughput without needing any modifications. From the liquid load per weir length profile (Fig. 7), it can be observed that the column is operating below this hydraulic limit. However, the downcomer exit velocity and

Table 6 – Distillation column section diameters.

	Stage number	Passes per tray	Section diameter (m^2)
Section 1	1–9	4	7.5
Section 2	10–17	4	7.5
Section 3	18–27	4	8
Section 4	28–36	4	8
Section 5	37–41	2	5.5
Top SS	42–47	2	3.5
Mid SS	48–54	2	3.5
Btm SS	55–59	2	3.5

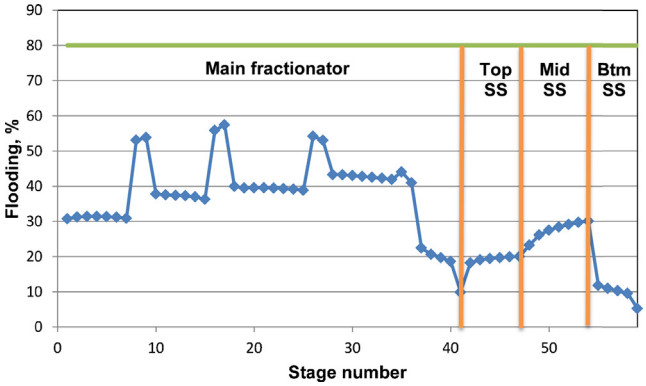

Fig. 6 – Percent flooding profile using standard valve trays (base case).

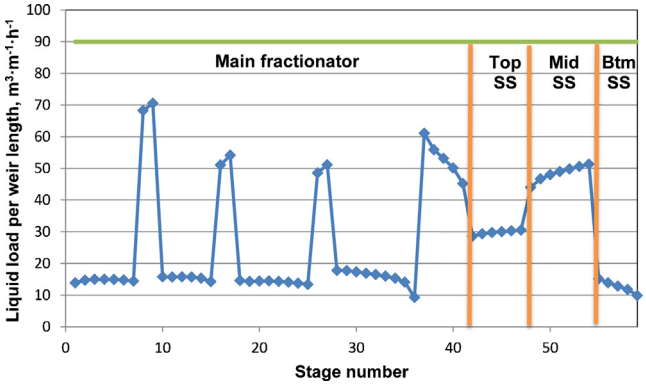

Fig. 7 – Liquid load per weir length profile using standard valve trays (base case).

flooding profiles (Figs. 8 and 9) show that both parameters are close to their hydraulic limits.

From the hydraulic analysis, it can be concluded that retrofit methodologies for crude oil distillation systems that only consider jet flooding as a hydraulic constraint may lead to unfeasible retrofit designs, as some important hydraulic parameters might already be operating close to their limits.

Nevertheless, the four hydraulic parameters indicate that the column can accommodate more throughput. The next step is to determine how much throughput can be accommodated without needing to modify the distillation column, and to identify which are the limiting hydraulic parameters that bottleneck the distillation column. This information will

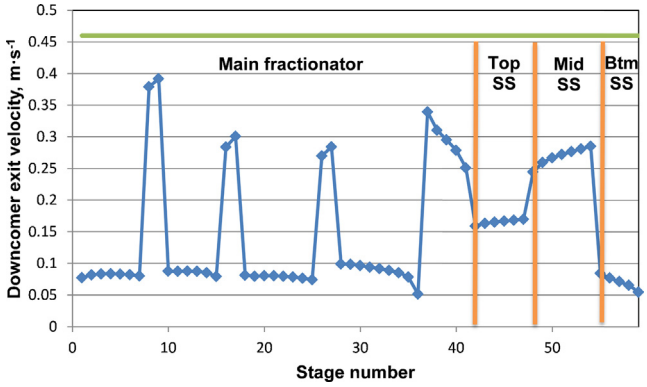

Fig. 8 – Downcomer exit velocity profile using standard valve trays (base case).

inform the proposed retrofit modifications for the distillation column.

In case studies 1 and 2 (Sections 4.2 and 4.3), the operating conditions of the column are maintained, i.e. there is no change in the compositions and temperature profiles; the product flow rates, stripping steam flowrate and pump-around duties are all left unchanged. Section 4.2 presents the case in which the throughput of this crude oil distillation system is increased.

4.2. *Case 1: Throughput increase of crude oil distillation system*

In this case study, the throughput (feed flowrate) of the base case is increased using the MATLAB-HYSYS interface by 5, 10, 15, 20, 25 and 30%. In each case the pump-arounds, reboilers and condenser duties and product and stripping steam flowrates are increased pro rata; the crude oil preheat temperature and pump-arounds temperature drop are the same as in the base case. For each iteration, a hydraulic analysis of the distillation column is carried out and the HEN is simulated with a minimum temperature approach of 25 °C. The aims of this case study are to determine how much additional throughput the distillation column can accommodate without requiring retrofit solutions, to identify the bottlenecks in the distillation column and to estimate how much additional heat transfer area is needed for the HEN.

From the hydraulic analysis, it can be observed that the crude oil distillation column is not limited by jet flooding when increasing throughput. Fig. 10 shows that the column can accommodate 30% more throughput without exceeding

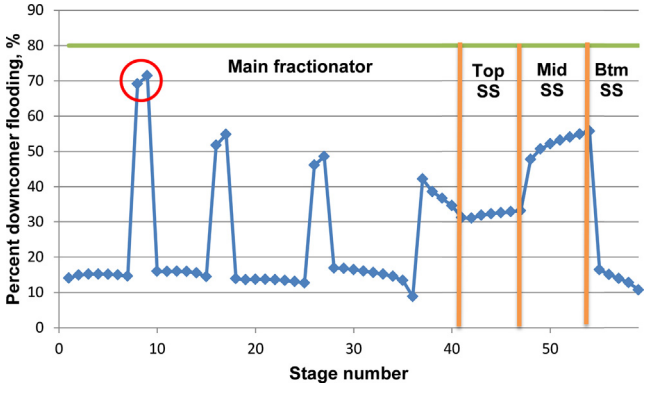

Fig. 9 – Downcomer flooding profile using standard valve trays (base case).

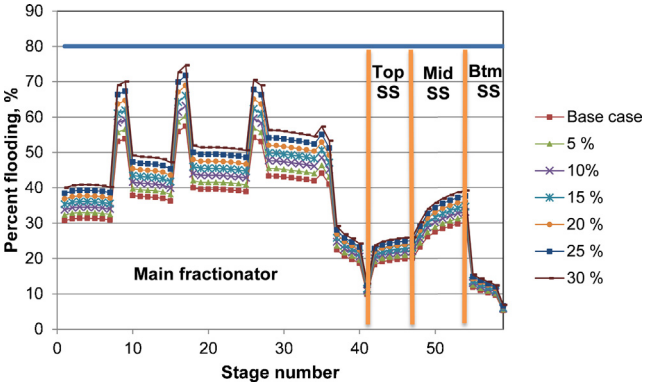

Fig. 10 – Percent flooding profile when increasing throughput.

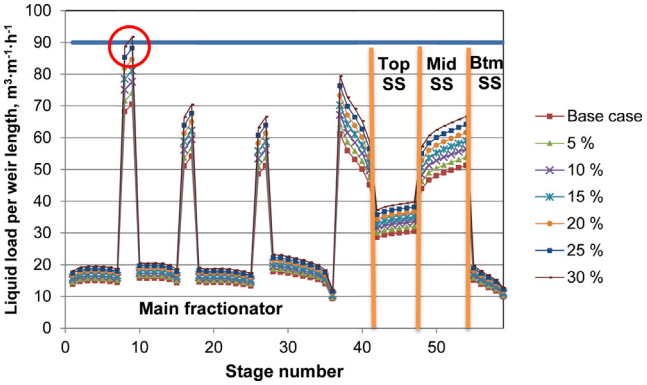

Fig. 11 – Liquid load per weir length profile when increasing throughput.

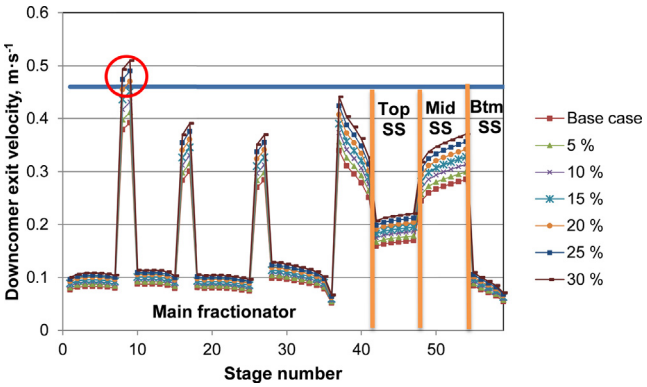

Fig. 12 – Downcomer exit velocity profile when increasing throughput.

the jet flooding limit. However, in Fig. 11 it can be observed that with 30% more throughput, the limit of liquid load per weir length is exceeded. Fig. 12 indicates that a 20% increase in throughput will exceed the limit for the downcomer exit velocity. Fig. 13 shows that the limit of downcomer flooding is exceeded if the throughput increases by 15%. It is also observed from Figs. 11–13 that Section 1 in the main fractionator is the distillation column bottleneck. Overall, it can be concluded that the column can accommodate 15% more throughput without column modifications.

Fig. 14 shows the HEN modelling results in terms of requirements for additional heat transfer area and fired heating demand. It can be observed that any increase in throughput requires HEN retrofit. For every throughput increase, the feasibility solver determines the new heat loads required by the heat exchangers to meet the target temperatures of the

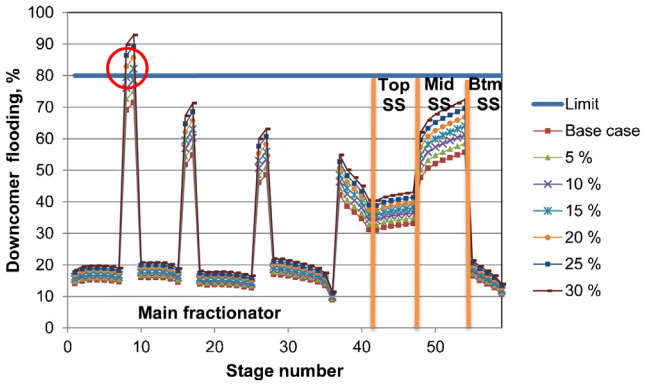

Fig. 13 – Downcomer flooding profile when increasing throughput.

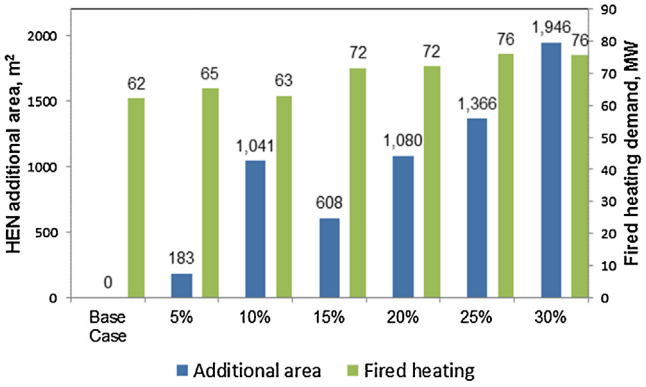

Fig. 14 – Impact on HEN when increasing throughput.

streams. With these new heat loads, the HEN model estimates the required additional area of the HEN. The results in Fig. 14 do not follow a monotonic trend, which is a consequence of the feasibility solver not seeking optimal solutions. An optimisation-based HEN retrofit methodology, e.g. the one proposed by Smith et al. (2010), is needed to identify the most economic HEN retrofit solutions. Considering HEN retrofit more systematically is a focus of future work.

Table 7 indicates which heat exchanger in the HEN requires the most additional heat exchange area, i.e. HEN bottlenecks. From Table 7, it can be observed that the heat exchangers that bottleneck the HEN are exchangers h1, h2 and h4. Of the utility exchangers, exchanger h21, the condenser, is the bottleneck. Such information could be useful for exploring HEN retrofit solutions, e.g. heat transfer enhancement of heat exchangers, splitting heat loads, etc.

Case study 1 demonstrates that the proposed retrofit methodology is useful to identify the bottlenecks of both the distillation column and HEN, and that a parametric analysis of crude oil distillation systems when increasing throughput provides valuable insights.

Table 7 – HEN bottleneck when increasing throughput.

Throughput increase (%)	Most constrained HE	Additional area required (m^2)
5	h1	64
10	h2	336
15	h1	124
20	h2	182
25	h4	376
30	h2	271

Table 8 – High-capacity valve trays parameters.

Type of trays	High-capacity tray
Tray spacing (m)	0.61
% Downcomer area	9, 10, 11, 12, 13
Downcomer clearance (m)	0.05, 0.055, 0.06
Number of flowpaths	4
Downcomer slope (°)	30

The parametric analysis reveals the maximum potential increase in throughput to the column that can be achieved without modifying the column itself. This increase, 15%, would need 6% more fired heating than the base case, but the existing HEN would need significantly more heat exchanger area (around 11%). The study has thus identified the potential of the column and highlighted the implications for HEN retrofit in a structured way.

The second case study considers hardware modifications as retrofit solutions for the distillation column. Again, finding the optimum HEN retrofit solution is not considered as it is out of scope of the present work.

4.3. *Case 2: Hardware modifications as retrofit solutions for crude oil distillation systems when increasing capacity*

The second case study aims to identify beneficial modifications to the crude oil distillation column for increased capacity. It is desired to increase the base case capacity by 30%. The base case cannot accommodate 30% more capacity: the distillation column constraints relate to the downcomer exit velocity and downcomer flooding in Section 1 of the main fractionator. This case explores replacing the existing internals in Section 1 of the main fractionator with high-capacity valve trays or structured packings.

4.3.1. *Replacing existing internals with high-capacity valve trays*

Table 8 provides the parameters of a range of high-capacity trays considered as the retrofit solutions—a high-capacity tray with a 30° sloped downcomer. Results of the hydraulic analysis of using high-capacity valve trays in Section 1 are shown in Figs. 15 and 16.

In Fig. 15, it can be observed that the liquid load per weir length is reduced as the downcomer area is increased. This

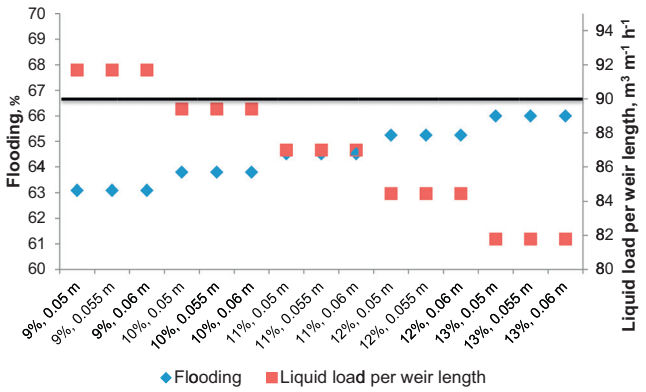

Fig. 15 – Maximum flooding and liquid load per weir length with high-capacity trays (% downcomer area, downcomer clearance) when increasing throughput by 30% (Section 1, main fractionator).

Table 9 – Structured packings considered as retrofit options (Green and Perry, 2007, Ch. 14).

Type of packing	Intalox 2T	Intalox 3T	Mellapak Plus 252Y	Mellapak Plus 452Y
Surface area ($m^2\ m^{-3}$)	215	170	250	350
Void fraction	0.99	0.99	0.98	0.98
Packing factor (m^{-1})	56	43	39	69
θ (°)	45	45	45	45
HETP (m)	0.57	0.69	0.50	0.39

is because, as the downcomer area increases, the weir length increases as well. It can also be observed from Fig. 15 that jet flooding does not constrain the column in any case. Note that jet flooding increases as the downcomer area increases (i.e. as the active area is reduced).

From Fig. 16, it can be concluded that only two sets of parameters for the high-capacity trays with a 30° sloped downcomer satisfy both hydraulic limits when increasing throughput by 30%: high-capacity trays with an 11% downcomer area and 0.06 m downcomer clearance, and 12% downcomer area and 0.06 m downcomer clearance. As expected, by increasing the downcomer area, the downcomer flooding is reduce; by increasing the downcomer clearance, the downcomer exit velocity is also reduced.

In summary, jet flooding increases when the tray active area is reduced. However, reducing the active area decreases the liquid load per weir length and the downcomer flooding. The solution for a high downcomer exit velocity is increasing the downcomer clearance. These results were expected, and shown that the proposed retrofit methodology is able to find feasible high-capacity valve trays to accommodate an increased throughput for distillation columns.

4.3.2. *Replacing existing internals with structured packings*

Table 9 presents the features of the four types of structured packing considered to replace the trays in Section 1 as retrofit solutions. It can be observed from Fig. 17 that the four proposed options satisfy the flooding constraint. However, as mentioned in Section 3.1.2, flooding is not the only parameter that needs to be considered. Using the HETP value of the packings, the required height to install the packings is estimated. In Table 10, the required height of the proposed structured packings, including the liquid distributors at the top of the column and the return stage of PA1 (stage 8), and the available height in the distillation column are presented. It can be observed that

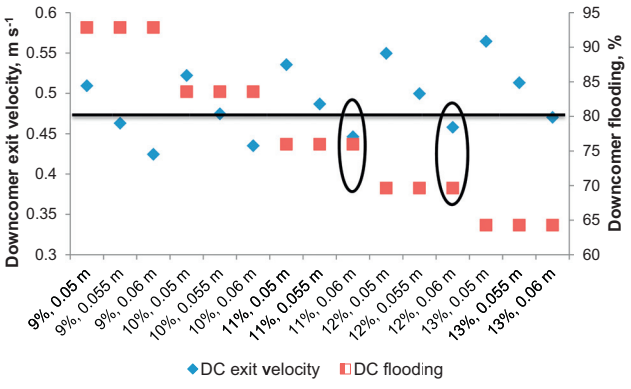

Fig. 16 – Maximum downcomer exit velocity and downcomer flooding with high-capacity trays (% downcomer area, downcomer clearance) when increasing throughput by 30% (Section 1, main fractionator).

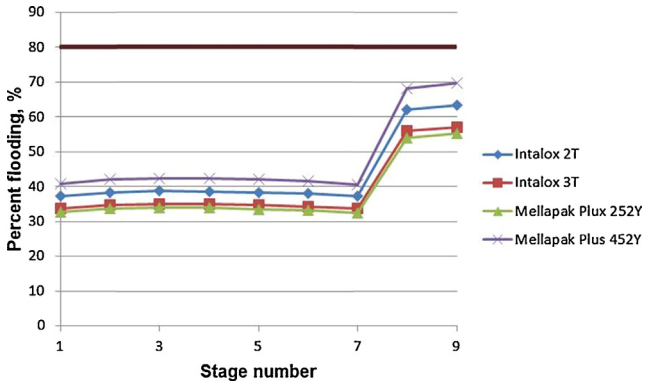

Fig. 17 – Percent flooding profile with structured packings when increasing throughput by 30% (Section 1, main fractionator).

only structured packings Mellapak Plus 452Y can be installed in the available space.

4.3.3. *Summary*

In total, nineteen hardware modifications are explored to increase the capacity of the base case by 30%. The engineering effort is relatively low, as the retrofit options are explored and assessed systematically, enabled by the MATLAB-HYSYS interface.

Only three of the proposed options satisfy both the hydraulic and physical constraints when increasing throughput by 30%: replacing existing internals in Section 1 by high capacity trays with a 30° sloped downcomer, 11 or 12% of downcomer area and 0.06 m of downcomer clearance, and Mellapak Plus 452Y structured packings.

Table 11 shows the cost estimation of the feasible retrofit options when increasing the base case capacity by 30%. The associated cost of installing additional HEN area is also considered (see Fig. 14). It can be observed that in all three retrofit scenarios the highest cost is that associated with the HEN. As mentioned before, an optimisation-based retrofit methodology can be included to reduce the HEN retrofit cost.

4.4. *Case study conclusions*

In this section, the proposed retrofit methodology was used to explore increasing the throughput of an existing heat-integrated crude oil distillation column. The column used as

Table 10 – Required height for replacing existing internals with structured packings.

	Height (m)
Available height	5.46
Intalox 2T	6.09
Intalox 3T	7.19
Mellapak Plus 252Y	5.50
Mellapak Plus 452Y	4.47

Table 11 – Retrofit cost estimation when increasing throughput by 30% and replacing existing internals in Section 1.

Retrofit cost	11%, 0.06 m*	12%, 0.06 m*	Mellapak Plus 452Y
Cost of replacing existing hardware	$96,823	$96,823	$116,520
Cost HEN additional area	$239,809	$239,809	$239,809
Total	$336,632	$336,632	$356,329

* % Downcomer area, downcomer clearance.

base case, consists of a main fractionator (steam stripped), three side strippers (one steam stripped, two reboiled), three pump-arounds and a condenser. The associated HEN is based on the one presented by Chen (2008), it consists of 22 heat exchangers with 5453 m^2 of heat transfer area and demands 62.1 MW of fired heating. For the base case (Section 4.1), the column internals were assumed to be valve trays.

In Section 4.1, a hydraulic analysis of the base case was performed. Jet flooding, liquid load per weir length, downcomer exit velocity and downcomer flooding profiles were predicted using the hydraulic correlations presented in Section 3.1. It was shown that the column was not constrained by any of these hydraulic parameters; thus the distillation column could accommodate more throughput without needing retrofit solutions to the column.

The next step was to find how much throughput could be accommodated without needing retrofit solutions to the distillation column. In case study 2 (Section 4.2), the proposed retrofit methodology was used to perform a parametric analysis of the heat-integrated crude oil distillation column for throughput increases of 5, 10, 15, 25 and 30%. The hydraulic analysis of the distillation column revealed that the column could accommodate 15% more throughput without needing retrofit solutions. From the hydraulic analysis, it was also learned that Section 1 of the main fractionator was the column bottleneck, and that the limiting hydraulic parameters were the downcomer exit velocity and downcomer flooding. Results from the HEN, showed that around 11% more heat exchanger area and 6% more fired heating were needed to accommodate 15% more throughput. It was noted that the HEN results did not follow a monotonic trend (see Fig. 14), as result of the feasibility solver not seeking an optimum solution for the heat loads and split fractions that regained the feasibility of the system. Therefore, it was concluded that the proposed methodology can be improved if an optimisation-based HEN retrofit methodology (e.g. the retrofit methodology proposed by Smith et al., 2010) is included.

In case study 3 (Section 4.3), it was desired to increase the throughput of the base case by 30%. As learned from case study 2, the column could not accommodate more than 15% without needing retrofit solutions. The column bottlenecks in Section 1 related to the downcomer exit velocity and downcomer flooding. High-capacity trays with 30° sloped downcomer and four structured packings were proposed to replace the existing internals in Section 1 of the main fractionator. First, feasible high-capacity trays were found using the proposed retrofit methodology. Then, the structured packings were checked in order to find which could be installed in the available space. Results showed that high-capacity trays with 11% and 12% downcomer area and 0.06 m of downcomer clearance could accommodate the increased throughput, and Mellapak Plus 452Y was the only structured packing that could fit in the available space. The economic analysis of the system revealed that the highest cost was that associated with HEN retrofit; it was concluded that an optimisation-based HEN retrofit methodology could be useful to improve these results and should be a focus of future work.

The case studies showed that the proposed methodology is useful to analyse the hydraulic performance of the base case, to analyse the impacts on both distillation column and HEN when increasing capacity and to identify system bottlenecks. It was also shown that the proposed retrofit methodology is useful to assess proposed equipment hardware modifications. However, it is always recommended to contact internals vendors in order to get more accurate estimations, given that the hydraulic and cost correlations used in this work are very general. Another limitation of the methodology is that practical considerations, such as downtime and lay-out of the plant are not considered.

5. Conclusions

The literature review argued that most retrofit methodologies only consider jet flooding as the hydraulic limit of distillation columns, and none systematically consider replacing existing internals with high-capacity trays or structured packings. It was noted that for crude oil distillation systems, both the distillation column and the HEN need to be considered, and that using commercial design software to simulate the distillation column and HEN and estimate the hydraulics of the distillation column requires significant engineering effort.

This work proposes a systematic retrofit methodology for the capacity enhancement of crude oil distillation systems focusing on retrofit of the column. Case studies show the importance of considering a wide range of hydraulic parameters in order to assess bottlenecks and proposed retrofit modifications: jet flooding, liquid load per weir length, downcomer exit velocity and downcomer flooding.

The proposed retrofit methodology can be improved if more accurate hydraulic and cost correlations are used and if other retrofit options, apart from equipment modifications, are considered (e.g. modifying operating conditions, adding separation equipment). A suitable optimisation-based HEN retrofit methodology is also needed to minimise HEN changes and thus HEN retrofit cost.

Acknowledgement

The authors gratefully acknowledge the Mexican National Council of Science and Technology (CONACyT) and the Roberto Rocca Education Program (RREP) for their financial support of PhD studies at the University of Manchester.

References

Aspen-HYSYS Software, 2012. Version 7.3. Aspen Tech Inc, USA.
Branan, C.R., 2011. Rules of Thumb for Chemical Engineers. Elsevier Science, Burlington, VT.
Bravo, J.L., 1997. Select structured packings or trays? Chem. Eng. Prog. 93 (7), 36–41.

Chen, L., 2008. Heat-integrated Crude Oil Distillation System Design. The University of Manchester, Manchester, UK (Ph.D. Thesis).
de Oliveira Filho, L.O., Queiroz, E.M., Costa, A.L.H., 2007. A matrix approach for steady-state simulation of heat exchanger networks. Appl. Therm. Eng. 27 (14–15), 2385–2393.
Enríquez-Gutiérrez, V.M., Jobson, M., Smith, R., 2014. A design methodology for retrofit of crude oil distillation systems. Comput. Aided Chem. Eng. 33, 1549–1554.
Gadalla, M., Jobson, M., Smith, R., 2003a. Optimization of existing heat-integrated refinery distillation systems. Chem. Eng. Res. Des. 81 (1), 147–152.
Gadalla, M., Jobson, M., Smith, R., 2003b. Shortcut models for retrofit design of distillation columns. Chem. Eng. Res. Des. 81 (8), 971–986.
Gadalla, M., Kamel, D., Ashour, F., din, H.N.E., 2013. A new optimisation based retrofit approach for revamping an Egyptian crude oil distillation unit. Energy Procedia 36 (0), 454–464.
Green, D.W., Perry, R.H., 2007. Perry's Chemical Engineers' Handbook. McGraw-Hill Professional, New York, NY.
Kencse, H., Manczinger, J., Szitkai, Z., Mizsey, P., 2007. Retrofit design of an energy integrated distillation system. Period. Polytech.: Chem. Eng. 51 (1), 11–16.
KG-Tower, 2012. KG-Tower Software, Version 5.1. Koch-Glitsch LP, USA.
Kister, H.Z., 1992. Distillation Design. McGraw-Hill, Boston, MA.
Kister, H.Z., Gill, D.R., 1992. Flooding and pressure drop prediction for structured packings. IChemE Symp. Ser. 128, A109–A123.
Kister, H.Z., Scherffius, J., Afshar, K., Abkar, E., 2007. Realistically predict capacity and pressure drop for packed columns. Chem. Eng. Prog. 103 (7), 28–38.
Koch-Glitsch, 2006. Introduction to KG-Tower: Tray& Packed Tower Sizing Software Program, Version 2.0 [Online]. Koch-Glitsch, L.P, Available ⟨http://www.nt.ntnu.no/users/skoge/prost/proceedings/distillation10/DA2010%20Sponsor%20Information/Koch%20Glitsch/KGTower/IntroKGTowerV2.0.pdf⟩ [Accessed October 2014].
Koch-Glitsch, 2013. Glitsch Ballast Tray Design Manual: Bulletin No. 4900 [Online]. Koch-Glitsch, L.P, Available ⟨http://www.koch-glitsch.com/Document%20Library/Bulletin-4900.pdf⟩ [Accessed October 2014].
Liu, Z.Y., Jobson, M., 2004. Retrofit design for increasing the processing capacity of distillation columns: 1. A hydraulic performance indicator. Chem. Eng. Res. Des. 82 (1), 3–9.
Ochoa-Estopier, L.M., Jobson, M., Chen, L., Rodríguez, C., Smith, R., 2014. Optimisation of heat-integrated crude oil distillation systems. Part II: Heat exchanger network retrofit model. Ind. Eng. Chem. Res. [Under review].
Ochoa-Estopier, L.M., Jobson, M., Smith, R., 2013. Retrofit of heat exchanger networks for optimising crude oil distillation operation. Chem. Eng. Trans. 35, 133–138.
Resetarits, M.R., 2010. Propelling distillation research. Chem. Eng. 117 (6), 26–27.
Resetarits, M.R., 2014. Chapter 2—distillation trays. In: Olujić, A.G. (Ed.), Distillation: Equipment and Processes. Academic Press, Boston, MA, pp. 35–84.
Shahabinejad, H., Feghhi, S.A.H., Khorsandi, M., 2014. Structural inspection and troubleshooting analysis of a lab-scale distillation column using gamma scanning technique in comparison with Monte Carlo simulations. Measurement 55 (0), 375–381.
Smith, R., 2005. Chemical Process Design and Integration. John Wiley & Sons, Ltd, Chichester, UK.
Smith, R., Jobson, M., Chen, L., 2010. Recent development in the retrofit of heat exchanger networks. Appl. Therm. Eng. 30 (16), 2281–2289.
Stichlmair, J., 1998. Distillation: Principles and Practice. Wiley-VCH, New York, NY.
Thernesz, A., Varga, Z., Rabi, I., Czaltig, Z., Lörincova, M., 2010. Applying process design software for capacity increase and revamp of distillation units. Clean Technol. Environ. Policy 12 (2), 97–103.
Uerdingen, E., Fischer, U., Hungerbühler, K., Gani, R., 2003. Screening for profitable retrofit options of chemical processes: a new method. AIChE J. 49 (9), 2400–2418.
Vatavuk, W.M., 2002. Updating the CE plant cost index. Chem. Eng. 109 (1), 62–70.
Watkins, R.N., 1979. Petroleum Refinery Distillation. Gulf Pub. Co., Book Division, Houston, TX.
Wei, Z.Q., Zhang, B.J., Wu, S.Y., Chen, Q.L., Hui, C.W., 2012. A hydraulics-based heuristic strategy for capacity expansion retrofit of distillation systems and an industrial application on a light-ends separation plant. Chem. Eng. Res. Des. 90 (10), 1527–1539.

Chapter 4 Retrofit approach proposed to optimise and to replace internals when increasing capacity

The case study results of Publication 1 note that since operational optimisation and HEN retrofit are not considered, significant heat transfer area and fired heating are needed to accommodate the increased capacity. These results indicate that the methodology presented in Chapter 3 needs to be improved to include operational optimisation and HEN retrofit, which is the focus of this chapter.

This chapter addresses the following specific objectives of this thesis:

- To propose a methodology to include rigorous simulation of distillation columns, hydraulic analysis of distillation columns and HEN retrofit within an optimisation environment, using suitable optimisation algorithms.
- To apply a HEN retrofit approach to ensure adequate heat transfer and to account for interactions between the distillation column and HEN.

4.1 Introduction to Publication 2

Publication 2 presents an optimisation-based retrofit approach for increasing the capacity of heat-integrated crude oil distillation systems, considering the following options:

- Operational optimisation
- Replacing the column internals
- Redistributing the heat loads of the HEN
- HEN retrofit (i.e. repiping, resequencing, adding new units, adding area)

The novelty of this approach is that it combines the methods used in current practice to simulate distillation columns and to assess their hydraulic performance (i.e. rigorous simulation software, open literature hydraulic correlations) with methods used by some

retrofit approaches from the open research literature to propose changes to the distillation column operating parameters and to the HEN structure. Also, a systematic methodology to assess the benefits of replacing column internals in the constrained sections of the column is presented. This approach allows exploring different retrofit scenarios with relatively little engineering effort.

4.2 Publication 2

Enríquez-Gutiérrez, V. M., Jobson, M., 2016, An optimisation-based retrofit approach for increasing the processing capacity of heat-integrated crude oil distillation systems, Industrial & Engineering Chemistry Research, under preparation.

An optimisation-based retrofit approach for increasing the processing capacity of heat-integrated crude oil distillation systems

Víctor M. Enríquez-Gutiérrez and Megan Jobson

Centre for Process Integration, School of Chemical Engineering and Analytical Science, The University of Manchester, Sackville Street, Manchester M13 9PL, United Kingdom

Keywords

Stochastic optimisation, replacing column internals, HEN retrofit

Highlights

- Hydraulic analysis of the distillation column.
- HEN retrofit options are identified.
- Constraints related to distillation column, HEN and products are considered.
- Two optimisation algorithms are applied and compared.

Abstract

Heat-integrated crude oil distillation systems are among the most energy intensive processes in the chemical industries. These systems comprise a distillation column that separates the crude oil into products for downstream processing, and a heat exchanger network (HEN) that recovers heat within the system. The distillation column and the HEN interact significantly. These interactions make the retrofit of crude oil distillation systems a complex problem with many degrees of freedom and constraints. Retrofit approaches aim to exploit these interactions in order to maximise the profitability of the system while minimising its energy consumption and CO_2 emissions. Existing retrofit approaches published in the open literature have succeeded in considering these interactions by applying operational optimisation to the distillation column together with HEN retrofit. However, retrofit approaches that also consider hardware modifications to the distillation column are lacking. This work proposes an optimisation-based retrofit approach for the capacity expansion of heat-integrated crude oil distillation systems that considers operational optimisation, hardware modifications to the distillation columns and HEN retrofit, in order to maximise the profitability of the process system.

The approach is based on previous work on retrofit of heat-integrated crude oil distillation systems, in which results from rigorous simulations of the distillation column are used to perform a detailed hydraulic analysis of the distillation column using different column internals, and as inputs of an optimisation-based HEN retrofit approach. Here, the system is optimised in two levels. In the first level, stochastic optimisation is used to optimise the column operating conditions; two optimisation algorithms are used by way of comparison: simulated annealing (SA) and global search (GS). In a second level, SA is used to retrofit the HEN. The benefits of the proposed retrofit approach are shown using an industrially relevant case study, in which it is desired to increase the processing capacity of an existing crude oil distillation system by 30%. In the case study, three retrofit scenarios are explored using the proposed retrofit approach: i) replacing columns internals in the constrained sections of the column and HEN retrofit; ii) operational optimisation of the column and HEN retrofit; iii) all three options together. Results show the benefits of using the proposed retrofit approach.

1. Introduction

The first separation unit in a petroleum refinery plant is the crude oil distillation column. In these units, the crude oil is separated into products for further downstream processing towards producing higher value products (i.e. gasoline, diesel, jet fuel). Before it enters the column, the crude oil is pre-heated to around 370°C by exchanging heat between the products and process streams in a complex heat exchanger network (HEN) and by a fired heating furnace [1]. Together, the crude oil distillation columns and its associated HEN, are known as heat-integrated crude oil distillation systems.

Heat-integrated crude oil distillation systems are energy intensive: it is estimated that the energy consumed in the furnace is equivalent to 1-2% of the total crude oil processed [2]. Furthermore, the system represents a valuable asset within the refinery. For these reasons, retrofit projects to increase the productivity and to reduce energy consumption of the existing system are commonplace.

Retrofit projects aim to increase the profitability of a plant by maximising the use of the existing equipment, installing new equipment or introducing new technology [3]. In crude oil distillation systems, the strong interaction between the distillation column and its associated HEN makes retrofit a complex problem with many degrees of freedom (operational, structural and flowsheet modifications to the distillation column and the

HEN) and constraints (distillation column hydraulic limits, product specifications, HEN installed area, ΔT_{min} constraints, etc.) [4].

The operation of a distillation column becomes infeasible if its hydraulic limits are exceeded (e.g. jet flooding, downcomer flooding, pressure drop, etc.) [5]. Therefore, the limit to the processing capacity of a crude oil distillation system is normally dictated by the distillation column hydraulics [4]. In practice, replacing the existing column internals can often overcome this issue [6]. Existing retrofit approaches found in the open literature have focused on optimising the column operating parameters and retrofitting the HEN in order to reduce the energy consumption, in which unfeasible column designs are avoided by applying hydraulic constraints to the optimisation problem [7]. Nevertheless, retrofit approaches that consider replacing column internals together with operational optimisation and HEN retrofit are lacking; therefore important interactions may be neglected in existing approaches.

This work is motivated by previous work on retrofit of heat-integrated crude oil distillation systems. Enríquez-Gutiérrez et al. [4] present a systematic retrofit methodology which aims to assess and evaluate hardware modifications (i.e. replacing existing column internals with high-capacity trays or structured packings) to increase processing capacity. The methodology of Enríquez-Gutiérrez et al. [4] can be summarised as follows. Firstly, the crude oil throughput and the column operating parameters (e.g. pumparound duties and steam flows) are increased pro rata using a MATLAB interface and are input to Aspen HYSYS. Secondly, using the results of the rigorous simulation, the hydraulic performance of the distillation column is assessed in terms of jet flooding, liquid load per weir length, downcomer exit velocity and downcomer flooding for conventional trays and high-capacity trays, and flooding for structured packings, using hydraulic correlations found in the open literature coded in MATLAB. Thirdly, with results from the same rigorous simulation, the fired heating demand and the required heat transfer area are estimated using a HEN simulation model. Finally, the retrofit cost is estimated using a simple economic model based on that proposed by Bravo [8] for replacing column internals and the cost model presented by Smith [1] to predict the capital cost of the HEN.

This sequential methodology [4] is shown to be useful to assess, with relatively low engineering effort, the impact on distillation column hydraulics, required heat transfer area and fired heating demand, and to evaluate feasible retrofit modifications to the distillation column when increasing the crude oil throughput. However, the case studies showed that the highest retrofit cost is due to the retrofit of the HEN. In part, this cost

stems from the use of a HEN simulation model that does not optimise the feasible solution, i.e. the HEN simulation model finds the heat loads and splits fractions that satisfy the energy balance and minimum temperature approach constraints, but does not optimises the HEN structure. In addition, the column operational parameters are fixed or increased pro rata; therefore, heat integration opportunities are not explored. Those shortcomings motivate the development of the optimisation-based approach presented in this work.

This work implements an optimisation framework in order to include operational optimisation of the column and HEN, while assessing replacing column internals and HEN retrofit, in order to increase the processing capacity of heat-integrated crude oil distillation columns. Maximising the production of higher-value products is out of the scope. To overcome the limitations of previous work with respect to HEN retrofit [4], the HEN retrofit approach of Ochoa-Estopier et al. [9] is included in the overall optimisation framework. The aim of this optimisation approach is to maximise the profitability of the system, evaluated in terms of the net profit. Constraints are accounted for by assigning penalties to the objective function when the hydraulic limits of the column are exceeded or when product specifications are not met.

The proposed retrofit approach is demonstrated on a case study in which the processing capacity of an existing crude oil distillation system is increased by 30%. It is known that this crude oil distillation system cannot accommodate 30% more throughput without needing retrofit modifications to the distillation column and the HEN [4]. Three retrofit scenarios are assessed using the proposed retrofit approach and are compared to case study results [4] in which only column internals are replaced but no HEN structural modifications are permitted.

To optimise the column operating parameters, two optimisation algorithms are used to assess their suitability: simulated annealing (SA) and global search (GS). The first is a stochastic optimisation algorithm, and the second applies both stochastic and deterministic optimisation [10, 11].

In the next section, a review of the retrofit approaches found in the open literature is presented. In Section 3, the proposed retrofit approach is introduced and explained in detail. Section 4 presents the case study and Section 5 provides conclusions on this work.

2. Literature review on retrofit of crude oil distillation systems

When increasing the processing capacity of an existing crude oil distillation system, retrofitting existing assets may be more cost-effective than installing new equipment [12].

Retrofit methodologies found in the open literature for crude oil distillation systems differ in the methods used to simulate the distillation unit at different operating conditions, to simulate the HEN topology, to retrofit the HEN and to assess the physical and operating constraints that limit the system, also known as bottlenecks (e.g. distillation column hydraulic limits, HEN constraints) [7, 13-16].

Zhang and Zhu [13] note that in crude oil distillation systems, changes to the process have an impact on the HEN retrofit. For example, changes to the distillation column operating conditions and/or configuration (e.g. changing a pumparound location, adding a preflash unit) impact on the stream supply and target temperatures and duties of the HEN; changes in product yields affect the product stream flow rates within the HEN. Optimisation-based retrofit methodologies aim to capture the interactions between the distillation column and the HEN.

2.1. Optimisation of operating parameters

Chen [14] proposes an optimisation framework for modelling, retrofit and operational optimisation of crude oil distillation systems. Chen [14] decomposes the problem into two levels. In a first level, simulated annealing (SA) is used to optimise the operational and structural variables of the distillation column and the HEN. Firstly, the SA algorithm changes the crude oil pre-heat temperature, stripping stream flow rates, pumparound flow rates and temperatures, pumparounds location, reflux ratio, key components, key component recoveries and column operating pressure. Then, using the shortcut models for retrofit extended from those of Suphanit [17], Gadalla et al. [18] and Rastogi [19], the distillation column is simulated considering the pumparound location as a design variable. These models require specification of key components and key component recoveries. In order to avoid unfeasible column designs, the required diameter is checked against the existing diameter. Hydraulic correlations only consider jet flooding, and neglect hydraulic limits of the downcomer. The shortcut models for retrofit do not provide the stage-by-stage information needed to perform a more detailed hydraulic analysis of the distillation column. In the second level of the

approach proposed by Chen [14], the HEN is retrofitted using an optimisation-based methodology, as discussed in Section 2.2.

López C. et al. [15] optimise the operating conditions of a crude oil distillation system in order to maximise the plant profit. In this work [15], the crude oil distillation columns are simulated using second order polynomial functions (also known as metamodels), regressed from the results of rigorous simulations. In this case, the crude oil flow rates, operating conditions, and the end boiling point of the products are the inputs, and the flow rates, temperatures and properties of the streams leaving the crude oil distillation columns are the outputs. PRO/II is used for process simulation, where the simulations are tuned using plant data. The advantage of using metamodels for large optimisation problems is that computational times can be reduced and are more robust [20]. On the other hand, distillation column hydraulics are not considered in the work of López C. et al. [15], which may lead to unfeasible solutions. For the HEN, a detailed HEN model is used. Maximum furnace duties and maximum hot and cold temperatures for the exchangers are used as constraints in the optimisation. Structural changes (e.g. adding new heat exchangers and/or adding area to existing heat exchangers) to the HEN are not considered.

Gadalla et al. [16] propose a systematic retrofit approach for the optimisation of existing crude oil distillation systems. In this approach, the crude oil distillation column and the pre-heat train are simulated in Aspen HYSYS v7.3. The use of rigorous simulation is well established as it can represent accurately the real operation of the plant and provides stage-by-stage information of the distillation column. The retrofit approach is used to optimise the pumparound duties and the HEN areas, where a preflash unit is installed in order to reduce the furnace duty. To avoid unfeasible solutions, the required diameter of the column is calculated using the correlation of Fair [21] and compared against the existing column diameter. However, this correlation can be considered as conservative for systems with high liquid rates (e.g. distillation columns with pumparounds) [1] and is only limited to jet flooding. The approach does not consider structural modifications, either for the distillation column (e.g. replacing existing column internals) or for the HEN.

Ochoa-Estopier et al. [7] develop an approach for the operational optimisation of heat-integrated crude oil distillation systems. The approach extends the work of Chen [14]: instead of using shortcut methods for column modelling, artificial neural networks (ANN) are employed to simulate the crude oil distillation unit [22]. The approach [7] separates the problem into two levels. In the first level, a SA algorithm randomly

changes the product flow rates, stripping steam flow rates, feed temperature, and pumparound duties and temperature drops, and the crude oil distillation system is then simulated. In the second level, the HEN is retrofitted using an optimisation-based retrofit methodology [9] based on the one by Chen [14], as described in Section 2.2. The best retrofit option can be assessed in terms of the net profit (product revenue less total annualised cost), total annualised cost or operating cost. Constraints considered relate to the distillation column (product quality specifications, column flooding), and to the HEN (minimum temperature approach, stream target temperatures). The approach considers the overall crude oil distillation system simultaneously (i.e. the distillation column and the HEN are considered simultaneously in the optimisation framework), and includes practical constraints related to the distillation column and the HEN, as mentioned above.

2.2. HEN retrofit in crude oil distillation systems

Zhu and Asante [23] present a HEN model based on the *network pinch* concept [24]. The network pinch can be explained as the maximum heat recovery that can be achieved in an existing HEN by increasing the area of the heat exchangers [23]. Beyond this point, topological changes are needed to increase the heat recovery of the network (e.g. adding, deleting, resequencing and repiping the heat exchangers). In the retrofit model, the problem is divided into three stages: diagnosis, evaluation and cost optimisation. The optimisation problem is formulated as a mixed integer linear problem (MILP). The approach does not guarantee the optimum design with the minimum retrofit cost, since the objective function considers only operational cost [9].

In the second level of the model proposed by Chen [14], the SA algorithm proposes changes to the HEN structure (i.e. adding, deleting, repiping or resequencing heat exchanges). The HEN is modified using an approach based on the network pinch concept [24], and described further by Smith et al. [25]. The work of Chen [14] also considers the temperature dependence of heat capacity, which provides a more realistic approach for crude oil distillation systems than previous work [24]. Considering heat capacities constant overestimates the heat recovery of the network, since possible pinch locations at the bubble and dew points are omitted; thus leading to unfeasible HEN designs [26]. A ‘repair’ algorithm is formulated as a nonlinear programming problem (NLP) that recalculates heat loads in order to regain the feasibility of the modified HEN by avoiding the violation of constraints related to the minimum temperature approach and energy balances.

The HEN simulation model proposed by Ochoa-Estopier et al. [9] applies principles of graph theory, as proposed by de Oliveira Filho et al. [27]. The HEN retrofit model [9] proposes the usual structural changes, as well as adding/deleting stream splits using simulating annealing (SA). The optimisation aims to find the best HEN design, according to the retrofit objective, e.g. minimum fired heating consumption, minimum required added area [9].

2.3. Literature review – summary

In summary, most retrofit approaches found in the open literature decompose the distillation system retrofit problem into different levels in order to ease the engineering effort and simplify the problem formulation. The aim of these approaches is to capture the interactions between the crude oil distillation column and the HEN in order to maximise the cost-effectiveness of system or to minimise the operating costs. Stochastic optimisation algorithms are used in some approaches to randomly change the column operating parameters [7, 14] and other approaches formulate the problem with a nonlinear programing (NLP) model and use deterministic optimisation algorithms [15].

To simulate the crude oil distillation column, previous approaches for retrofit have used simple linear models constructed from mass and energy balances [13], shortcut methods for retrofit based on the Fenske-Underwood-Gilliland (FUG) method [18], rigorous simulation using commercial software [4, 16] and metamodels regressed from results of rigorous simulations [7, 15]. For large optimisation problems, using simplified models of the distillation column reduces computational effort compared to rigorous simulation [15]; however, these models do not provide the stage-by-stage information needed to perform a detailed hydraulic analysis of the distillation column in order to avoid unfeasible designs. Only Enríquez-Gutiérrez et al. [4] consider the downcomer hydraulics for distillation columns using valve trays or high-capacity trays, or distillation columns with structured packings.

The approaches of Smith et al. [25] and Ochoa-Estopier et al. [9] consider changes to the HEN structure. These structural changes provide opportunities to exploit more heat integration opportunities rather than only considering adding heat exchange area. Also, these works [9, 25] consider temperature dependent heat capacities, providing a more realistic approach for crude oil, the properties of which vary significantly with temperature.

This work extends previous work on retrofit of crude oil distillation systems. Similarly to the works of Caballero et al. [28] and Enríquez-Gutiérrez et al. [4], this works simulates the distillation column by connecting Aspen HYSYS with MATLAB in order to include rigorous simulation within an optimisation environment. The approach of Enríquez-Gutiérrez et al. [4] is extended by including stochastic optimisation of the operating parameters of the distillation column. Also, the HEN retrofit methodology of Ochoa-Estopier et al. [9] is incorporated into the methodology without significantly modification. The crude oil distillation system is optimised in order to maximise the net profit, following the work of Ochoa-Estopier et al. [7]. In the next section, the proposed retrofit approach and the methods used are explained in detail.

3. Optimisation-based retrofit approach for increasing the processing capacity of heat-integrated crude oil distillation systems

Figure 1 illustrates the proposed optimisation-based retrofit approach for the capacity expansion of heat-integrated crude oil distillation systems. Figure 3 in Section 3.3 provides further detail.

The system is initialised using the current operating conditions of the distillation system (pumparound duties and temperatures drop, stripping steam flow rates and crude oil pre-heat temperature), the distillation column structure (number of stages, pumparounds and side-strippers locations, column diameters and type of internals), the HEN structure (heat exchangers matches, areas and heat loads) and product specifications (flow rates and product quality expressed in terms of true boiling point temperatures). Also, lower and upper bounds for the optimisation parameters are set (i.e. the column operating conditions) based on sensitivity studies and/or plant-specific constraints. Rigorous simulation of the distillation column using Aspen HYSYS v7.3 is assumed to provide a realistic representation of the system.

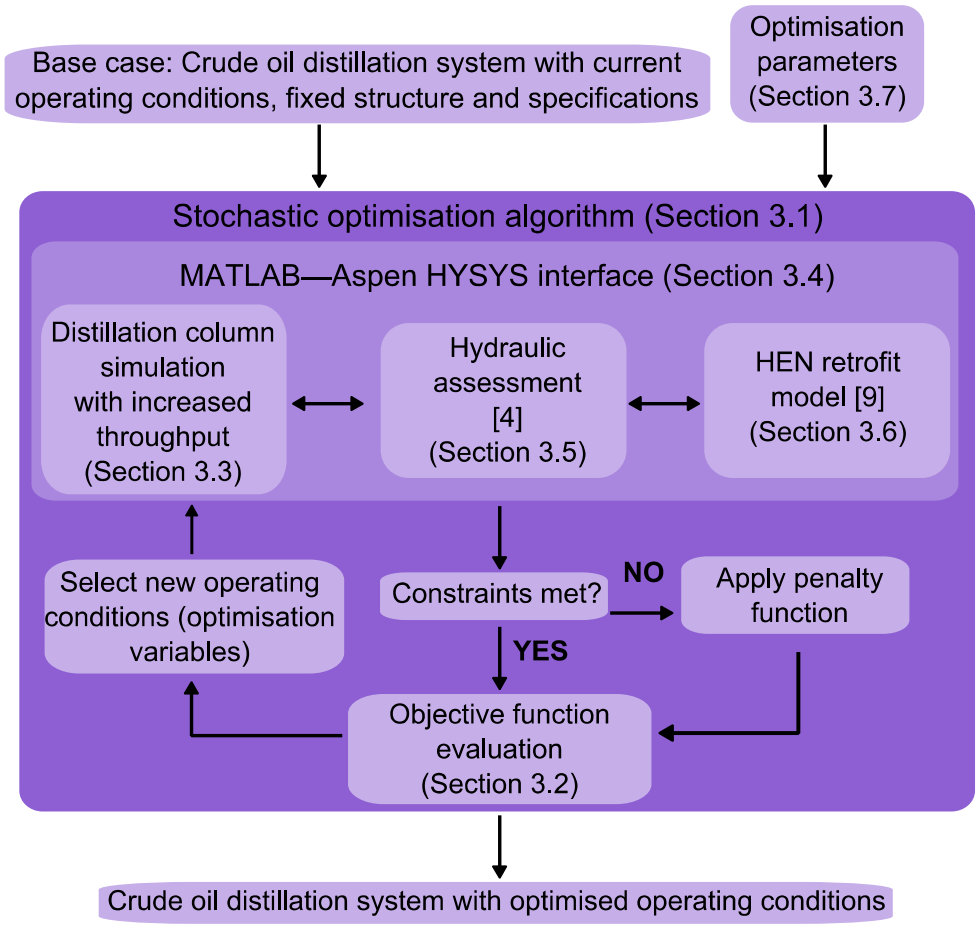

Figure 1 Optimisation-based retrofit approach for crude oil distillation systems

Using a stochastic optimisation algorithm, the distillation column operating conditions are randomly changed between the lower and upper bounds set by the designer. With these operating parameters, the distillation column is re-simulated in Aspen HYSYS v7.3 with an increased throughput. The product flow rates, and the reboilers and condenser duties are increased pro rata. Using the results from the simulation, a hydraulic analysis of the distillation column is performed, applying hydraulic correlations from the open literature [4] (see Section 3.5). A HEN retrofit solution is developed [9] (see Section 3.6). All these steps are performed using a MATLAB–Aspen HYSYS interface (see Section 3.3).

With the simulation results, the feasibility of the system is checked in terms of product specifications and hydraulic constraints of the distillation column (see Section 3.7), and the optimisation objective function is evaluated (see Section 3.2). If any constraint is not met, a penalty to the objective function is applied (See Section 3.7). This loop is repeated until the termination criteria of the optimisation algorithm is met, as illustrated in Figure 1.

The following sections explain the methods used in this optimisation approach for the capacity enhancement of heat-integrated crude oil distillation systems in more detail. Section 3.1 introduces the stochastic algorithms used to change the distillation column operating conditions.

3.1. Stochastic optimisation algorithms

The proposed retrofit approach aims to find the best set of operating conditions and to identify promising retrofit modifications when increasing the processing capacity of existing crude oil distillation systems without violating the system constraints. This problem involves continuous variables (operational modifications), discrete variables (structural modifications) and equality and inequality constraints; therefore, the retrofit of crude oil distillation systems can be formulated as a mixed-integer non-linear programming (MINLP) problem [29]. Such optimisation problems are typically solved using stochastic algorithms [30], such as genetic algorithms [31] or simulated annealing [7, 14].

In this retrofit approach, two stochastic optimisation algorithms are used to randomly change the system operating conditions: simulated annealing and global search, both available within the MATLAB 2014a optimisation toolbox. Also, the HEN retrofit approach [9] uses SA to perform structural changes to the HEN; this is further explained in Section 3.6.

Simulated annealing (SA) is a stochastic optimisation method that employs random numbers in the search of the optimal solution [32]. SA makes an analogy between the annealing process in metallurgy (a system with many degrees of freedom) and multivariate or combinatorial optimisation (optimisation problems with functions depending on many parameters) [32]. Cavazzuti [10] mention that stochastic optimisation algorithms, such as SA, have better chances in finding the global minimum in highly combinatorial problems (such as the HEN retrofit [9]) compared to deterministic gradient-based methods. However, deterministic methods are quicker and more exact than stochastic methods [10].

Chen [14] and Ochoa-Estopier et al. [7] use SA to optimise the column operational parameters and the HEN structure, while Zhang and Zhu [13] and López C. et al. [15] use deterministic optimisation for the HEN and the distillation column. Cavazzuti [10] recommends combining both stochastic and deterministic methods to find the global solution of large-scale optimisation problems, but only a few researchers have followed

this recommendation for HEN retrofit [25, 33]. Retrofit methodologies that combine both deterministic and stochastic methods to optimise the operating conditions of distillation columns have not been explored.

Global search (GS) is an optimisation algorithm included in the global optimisation toolbox of MATLAB 2014a which uses both stochastic and deterministic optimisation [34]. This algorithm is recommended for the solution of constrained mixed integer nonlinear programming (MINLP) problems [34]. The retrofit of heat-integrated crude oil distillation systems is a MINLP problem, as it includes both continuous and integer variables [14] An extensive search of literature did not provide evidence of previous use of this algorithm in the retrofit of crude oil distillation systems, but other global search algorithms have been used [26].

In this retrofit approach both optimisation algorithms, SA and GS, are used. The aim is to compare the results obtained by using only stochastic optimisation and a combination of stochastic and deterministic optimisation. For this reason, the same methods are used to simulate the distillation column, to predict the hydraulic performance of the distillation column and to simulate and retrofit the HEN in both cases. The same constraints and penalties to the objective function are also applied.

Section 3.2 presents the optimisation objective function used in this retrofit approach. An economic indicator is used as the objective function.

3.2. Objective function

Optimisation-based retrofit approaches typically use as the objective function an economic indicator [7], and/or an environmental indicators [35]. The aim of the proposed retrofit approach is finding the best retrofit design that allows the system to accommodate more throughput to enhance its profitability. Therefore, the economic indicator used in this work is the net profit (NP), which indicates the difference between benefit and cost of a project [36].

The net profit (NP) is defined as the sum of the revenue less the costs, as shown in Eq. 1 [36].

$$NP = \sum Revenue - \sum Costs \quad (1)$$

The revenue is estimated as shown in Eq. 2, where *C* and *F* refer to product value and flow rate, respectively; the subscript *prod,i* refers to the i^{th} product of the total number of products (N_{prod}) [7].

$$\sum Revenue = \sum_{i=1}^{N_{prod}} C_{prod,i} F_{prod,i} \quad (2)$$

The main costs associated with the crude oil distillation system are the crude oil cost, the operational costs (OC) and annual capital charges (ACC), as shown in Eq. 3 [7]. In this equation, the subscript *crude* refers to the crude oil feed.

$$\sum Costs = C_{crude} F_{crude} + OC + ACC \quad (3)$$

The operational costs considered are the cost of the utilities (i.e. fired heating and cooling water) and stripping steam, as shown in Eq. 4 [7]. In this equation, the subscript, *util,i* is the i^{th} utility of the total number of utilities (N_{util}), and *stm,j* refers to the j^{th} stripping steam stream of the total number of stripping steam feeds (N_{stm}).

$$OC = \sum_{i=1}^{N_{util}} C_{util,i} F_{util,i} + \sum_{j=1}^{N_{stm}} C_{stm,j} F_{stm,j} \quad (4)$$

Consistent units for the prices (e.g. \$ bbl^{-1}, \$ $kmol^{-1}$, \$ kg^{-1}), material flow rates (bbl s^{-1}, kmol s^{-1}, kg s^{-1}) and energy flow rates (W, MW, kJ s^{-1}) for *C* and *F*, are used in Eqs. 1, 2, 3 and 4.

The annualised capital charge (ACC) is the amount of money that needs to be repaid each year to cover the initial investment *P* in *n* years with an interest rate *i*.

As in the work of Enríquez-Gutiérrez et al. [4], the initial investment *P*, i.e. the retrofit cost, is evaluated using simple capital cost models found in the open literature for replacing the existing column internals with structured packings and for HEN modifications (i.e. adding area, resequencing and repiping existing heat exchangers and adding new heat exchangers).

To estimate the cost of replacing the column internals with structured packings, Bravo [8] correlates the cost in terms of the hardware cost $\$Cost_{hardware}$ in 1997 US\$ and installation and removal factors F_i and F_r, respectively, as shown in Eq. 5 [4]. In this

equation, D refers to the column diameter in m, S_H is the summation of bed heights in m and N_b is the number of beds. This cost model already takes into consideration the installation of liquid distributors [4, 37].

$$\$Cost_{SP} = 11 \cdot D^2[260S_H + 160(2N_b - 1)] \cdot F_i \cdot F_r \quad (5)$$

To account for the retrofit cost of the HEN, Sinnott and Towler [38] present a cost model to estimate the capital cost that correlates the required surface area A_{HXreq} and three cost law constants, a, b and c, that depend on the materials of construction, pressure rating and type of heat exchanger (Eq. 6). Smith [1] mentions that this models gives useful predictions.

$$\$Cost_{HX} = a + b\left(A_{HXreq}\right)^c \quad (6)$$

Based on this cost model, Chen [14] presents the following relationships to estimate the cost in 2005 US$ of adding new heat exchangers (Eq. 7), adding area to existing heat exchangers (Eq. 8), repiping existing heat exchangers (Eq. 9) and resequencing existing heat exchangers (Eq. 10):

$$\$Cost_{HXnew} = 13{,}000 + 1530\left(A_{HXreq}\right)^{0.63} \quad (7)$$

$$\$Cost_{HXarea} = 1530\left(A_{HXreq}\right)^{0.63} \quad (8)$$

$$\$Cost_{HXrepiping} = 60{,}000 \quad (9)$$

$$\$Cost_{HXresequencing} = 35{,}000 \quad (10)$$

In Section 3.7, the optimisation variables, retrofit modifications, constraints, penalties to the objective function considered in this work are presented. Since this approach aims to assess beneficial retrofit modifications when increasing the processing capacity of the existing crude oil distillation system, the optimisation variables considered are the column operating parameters: crude oil pre-heat temperature, pumparound flow rates and temperature drop and stripping steam flow rates. The retrofit modifications considered are replacing the existing distillation column internals and adding, deleting,

repiping and resequencing heat exchangers. Jet flooding, weir load, downcomer exit velocity and downcomer flooding are considered as constraints for distillation columns containing trays, and flooding is assumed to constrain packed columns. These hydraulic indicators are explained in more detail, together with the calculation methods used, in Section 3.5.

Section 3.3 presents the methodology used to simulate the distillation system. Using a MATLAB—Aspen HYSYS interface, the distillation column is simulated, the hydraulic performance of the distillation column is assessed and the HEN is retrofit solution is generated.

3.3. Simulation of distillation column

The literature review outlines four methods used in existing retrofit methodologies to simulate the atmospheric distillation column: simple linear models [13], shortcut models [14], rigorous simulation [4, 16] and metamodels [7, 15]. Of these four methods, only rigorous simulation has been applied to generate stage-by-stage information needed to perform a hydraulic analysis of the distillation column [4]. For this reason, the column retrofit methodology of Enríquez-Gutiérrez et al. [4] is incorporated into the optimisation-based retrofit approach proposed in this work.

The existing distillation column is set up in HYSYS: structure, inputs and specifications. Figure 2 illustrates the simulation flowsheet used to simulate the crude oil distillation column. Spreadsheets are used in HYSYS to record key inputs and results and read and write information sent to and from MATLAB. The spreadsheets include transport property data, steam flow rates, the furnace outlet temperature, product flow rates, pumparound duties and temperature drops, and reboiler duties.

The simulation uses “dummy” heat exchangers (highlighted in dashed lines in Figure 2 to calculate the thermal properties of the crude oil feed and products for specified temperature intervals; this information allows temperature-dependent heat capacities to be correlated. Section 3.6 explains the use of these correlations for HEN simulation and retrofit in more detail.

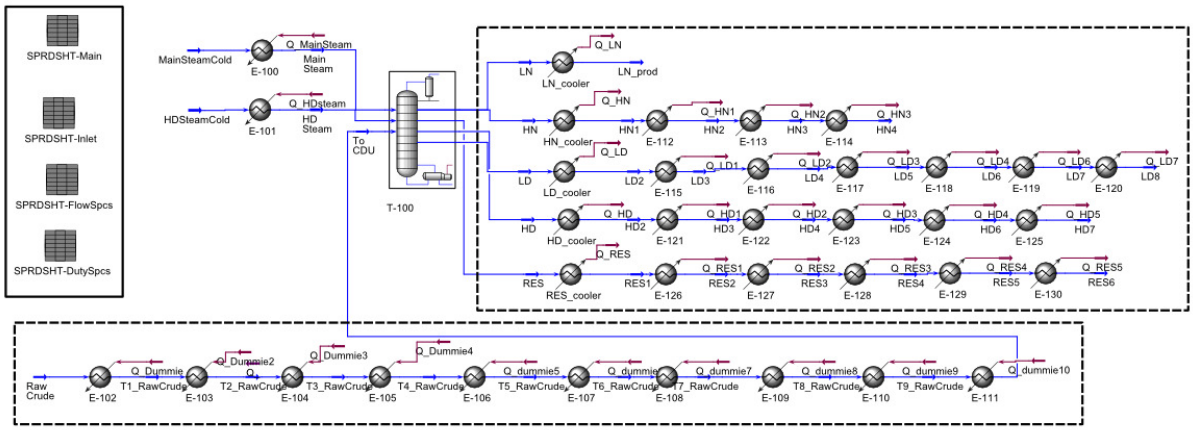

Figure 2 Simulation flowsheet in Aspen HYSYS v7.3

3.4. Optimisation of the distillation system

The flowchart in Figure 3 illustrates the proposed retrofit approach. The process begins with a random set of column operating parameters (i.e. crude oil pre-heat temperature, stripping steam flow rates, and pumparounds heat duties and temperature drops) chosen by the stochastic optimisation algorithm. The MATLAB–HYSYS interface then sends the column operational parameters to Aspen HYSYS, where the distillation column is simulated, and reads the simulation results if a converged solution is obtained.

The MATLAB–HYSYS interface checks whether the simulation has converged. If the simulation does not converge, the MATLAB–HYSYS interface resets the column operating parameters to the base case values, which are known to result in a converged simulation; the distillation column is re-simulated and a penalty is applied to the objective function. This step prevents Aspen HYSYS from opening pop-up windows that block communication between MATLAB and HYSYS and ending the optimisation stops without giving any output.

For converged solutions, stage-by-stage information is extracted by MATLAB to perform the hydraulic analysis of the distillation column for a given set of internals, i.e. liquid and vapour flow rates and transport properties of both phases: density, viscosity, surface tension and molar mass.

Information is also extracted from the column simulation to analyse and retrofit the HEN: crude oil feed and product flow rates, furnace outlet temperature, products outlet temperature and pumparound duties and temperature drops.

The converged solutions are also checked for feasibility, in terms of product quality. MATLAB extracts TBP information for all product streams and compares them to specifications. A penalty is applied if product quality specifications are not met.

Section 3.5 presents the hydraulic analysis of the distillation column and Section 3.6 outlines the HEN simulation and retrofit approach.

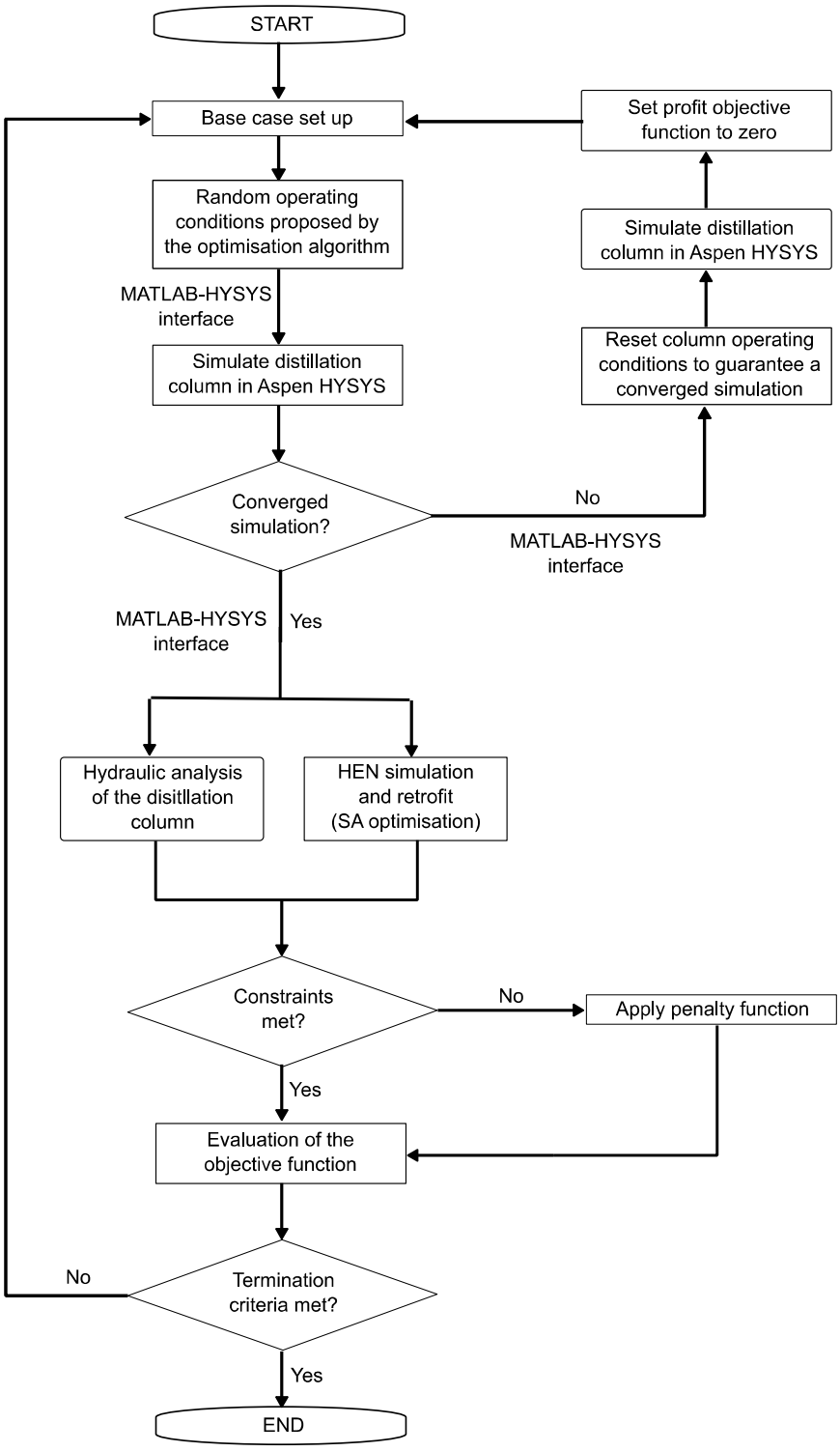

Figure 3 Flowchart of the proposed optimisation-based retrofit approach

3.5. Hydraulic analysis of distillation columns

This work uses hydraulic correlations available in the open literature to assess the hydraulic performance of an existing crude oil distillation column when increasing its processing capacity [4]. More accurate or specific correlations, if available, could be applied in a similar way.

The work follows the rating methodology of KG-Tower v5.1 [39], which cannot be automated to work simultaneously with MATLAB and Aspen HYSYS. For this reason in this approach, hydraulic correlations for conventional trays, high-capacity trays and structured packings are coded in MATLAB.

Jet flooding occurs due to high vapour rates, causing the liquid to be carried over to the stage above. When the first droplets of liquid start being carried to the stage above, the phenomenon is known as entrainment. Distillation columns are typically designed with an 80% approach to jet flooding to prevent from both of these phenomena [37]; this limit is applied. Jet flooding is predicted using the Glitsch correlation [40], also known as 'Equation 13' that gives reasonable estimations of flood points [41].

High liquid loads can cause downcomer flooding in trayed distillation columns: the vapour cannot disengage completely from the liquid, resulting in downcomer back-up (liquid is sent back to the stage above) [5]. As a result, distillation columns are typically designed with an 80% approach to downcomer flooding [42]; this work uses the same limit.

This work uses three hydraulic indicators to estimate the effects of the liquid loads in the downcomer: weir load, downcomer exit velocity and downcomer flooding [4]. The weir load and the downcomer exit velocity are estimated using the same correlations as KG-Tower software [39, 42]. In practice, the weir load is designed with a limit between 90 to 100 $m^3\ m^{-1}\ h^{-1}$ [43]. If this limit is exceeded, then the number of passes per tray have to be increased to provide better vapour-liquid contact [42]. The maximum recommended downcomer exit velocity is smaller than 0.46 $m\ s^{-1}$ [42]. If this limit is exceeded, the downcomer clearance has to be increased [42]. The approach to downcomer flooding is estimated using the Glitsch correlations for downcomer design velocity [40].

In packed columns, the pressure drop at which the liquid is no longer able to flow against the vapour is known as the flood point [5]. In practice, a value of 80% is used as the limit. The approach to flooding is estimated using a regressed model [44] from

the pressure drop correlation chart for structured and random packings of Kister and Gill [45]. This correlation is only valid for flow parameters of 0.03 to 0.3 for organic mixtures [46] and uses an empirical packing factor that depends on the packing size and shape [46].

The inputs to these correlations are results extracted from the rigorous simulations in Aspen HYSYS. The effects of pressure drop on the column hydraulics are accounted for by specifying the pressure drop in the simulation. If available, pressure drop correlations should also be included.

3.6. HEN retrofit approach

HEN retrofit methodologies in the open literature differ in the methods used to simulate the HEN and in the retrofit options and constraints considered. In every methodology, there is a trade-off between computational complexity and model accuracy [7].

This work uses the approach of Ochoa-Estopier et al. [9] to simulate and retrofit the HEN. The topology of the existing HEN is described using the principles of graph theory [27]; the HEN structure is represented using an 'incidence matrix' [9]. The incident matrix contains the matches between the process and utilities heat exchangers and the streams that form the HEN. Material and energy balances of each element of the matrix (i.e. heat exchangers, mixers and splitters) are formulated. The optimisation algorithm manipulates the structural and operational degrees of freedom of the HEN [9], in order to reduce the fired heating consumption.

The heat exchangers are specified in terms of heat loads. Eqs. 11 and 12 show the energy balances for the cold and hot sides of heat exchanger *k*, where $\overline{CP}$ is the average heat capacity flow rate, *T* is the temperature and *q* is the duty [9].

$$\overline{CP}_{k,c}\left(T_{k,c,out} - T_{k,c,in}\right) = q_k \tag{11}$$

$$\overline{CP}_{k,h}\left(T_{k,h,in} - T_{k,h,out}\right) = q_k \tag{12}$$

This work considers temperature-dependent heat capacities: the average heat capacity flow rate of each interval [$T_{k,h,in}$, $T_{k,h,out}$] can be represented as in Eq. 13, where *m* is the flow rate of the stream and $\overline{CP_k}$ is the average heat capacity for the temperature interval [9].

$$\overline{CP_k} = m_k CP_k \quad (13)$$

In this work, to obtain the heat capacity in a temperature interval, the *CP* model is generated using rigorous simulation: relationships between heat capacity and temperature are estimated using the 'dummy' heat exchangers installed in the simulation flowsheet, shown in Figure 2. These 'dummy' heat exchangers represent the temperature intervals at which the crude is pre-heated in the pre-heat train. Using the MATLAB–HYSYS interface, the heat capacities and temperatures of the inlet and outlet streams of the 'dummy' heat exchangers are extracted. The 'polyfit' function in MATLAB is used to regress third order equations for the crude oil and each of its products. In the same fashion, linear equations are generated for the streams passing through the pumparounds, the condenser and reboilers. The resulting CP correlations are applied within the methodology of Ochoa-Estopier et al. [9] to simulate and retrofit the HEN. The step is only performed once.

The procedure to simulate the HEN can be summarised as follows. Firstly, the HEN structure is represented using an incidence matrix and the material balances are solved, accounting for stream splits. Secondly, the energy balances are solved assuming values for the heat capacities. Thirdly, using the temperatures calculated with the energy balances, the heat capacities are re-calculated using the CP function regressed from the results of rigorous simulations until the heat capacities are within a given tolerance (10^{-6} kW K^{-1}). Finally, the heat transfer areas of the heat exchangers are calculated using the standard heat exchanger design equations for each heat exchanger.

The HEN retrofit methodology of Ochoa-Estopier et al. [9] aims to minimise the fired heating consumption of the HEN. The approach is based on the works of Rodriguez [33] and Chen [14], which divide the optimisation problem into two levels. Ochoa-Estopier et al. [9] extend these approaches by including constraints on heat transfer area and utility consumption.

In the first level, structural modifications to the HEN are proposed using simulated annealing. The following modifications are considered:

- adding, deleting, repiping and resequencing heat exchangers
- changing the heat loads of the heat exchangers
- adding/deleting stream splitters
- modifying the splitting ratios

Once the changes are proposed, the HEN is simulated using the procedure described above and the feasibility of the network is checked in terms of the minimum temperature approach of the network, stream enthalpy balances, installed heat transfer area, additional heat transfer areas, and utility consumption [9]. If any of these constraints is violated, the 'repair' algorithm optimises the heat loads and the split fractions in order to regain feasibility (see Eq. 16).

The above approach [9] is adopted in this work because it facilitates the finding of a cost-effective HEN design, which contributes to the aim of this work, which is maximising the net profit of heat-integrated crude oil distillation systems when increasing throughput.

3.7. Optimisation variables and constraints

The Introduction noted that retrofit approaches that consider operational optimisation of the distillation system together with structural modifications of the distillation column and the HEN are lacking. The proposed optimisation-based methodology considers the following:

- Optimisation of the column operating parameters:
    - furnace outlet temperature
    - stripping steam flow rates
    - pumparound duties
    - pumparound temperature drops
- Replacing existing distillation column internals in the whole column or in constrained sections
- Structural modifications to the HEN:
    - adding, deleting, resequencing and repiping heat exchangers
    - adding heat transfer area to existing heat exchangers
    - adding or deleting stream splitters

The optimisation is carried out using stochastic optimisation.

To determine the "best" location for replacing the existing column internals with structured packings, the system is optimised for different internals, e.g. the trays in a given section of the main fractionator are replaced with structured packing.

The modifications to the HEN are proposed by a SA algorithm embedded in the HEN retrofit methodology used [9], as explained in Section 3.6.

The following constraints for the distillation column and the HEN are considered to ensure practicable and sensible solutions:

- Product quality expressed in terms of true boiling point (TBP).
- Distillation column hydraulic limits:
    - jet flooding, weir load, downcomer exit velocity and downcomer flooding for trayed columns.
    - flooding for packed columns.
- Minimum temperature approach (ΔT_{min}), stream enthalpy balances, installed heat transfer area, additional heat transfer area, and utility consumption for the HEN.

Also, lower and upper bounds for the operating parameters are specified in the stochastic optimisation algorithm to reduce the search space.

The TBP of specified boiling fraction is a commonly applied indicator of product quality [5]. The TBP profile may be obtained experimentally using standardised tests, such as the ASTM D-285 [47]. Simulation packages such as Aspen HYSYS can predict the TBP of a stream, based on its composition expressed in terms of pseudo-components [48]. The TBP of product streams (for a given fraction vaporised) is obtained from rigorous simulation of the distillation column in Aspen HYSYS; this is further explained in Section 3.3.

The distillation column hydraulic parameters are calculated using hydraulic correlations found in the open literature [4]. These correlations are also used in commercial simulation software, such as Aspen HYSYS v7.3 [48] and KG-Tower v5.1 [39]. Section 3.5 explains further the calculation of hydraulic parameters. Considering these parameters as constraints during the optimisation helps avoiding unfeasible or impractical retrofit solutions.

A penalty is applied to objective function if any constraint is violated. As shown in Eqs. 14 and 15, where *y* refers to the T5% and T95% TBP temperatures of the N_{prod} distillation products and the hydraulic parameters, jet flooding, weir load, downcomer exit velocity and downcomer flooding for trays and flooding for packings, for the $N_{sections}$ of the crude oil distillation column. Superscripts *lb* and *ub* refer to the lower and upper bounds, respectively, and Y_i is a large negative number, known as the 'penalty factor' [7]. Note that lower bounds are not imposed for any of the hydraulic parameters.

$$Penalty_i = \gamma_i \left(y_i - y_i^{lb}\right)^2 \quad \text{if} \quad y_i < y_i^{lb} \quad i = 1,2,\dots,N_{prod} \tag{14}$$

$$Penalty_i = \gamma_i\left(y_i - y_i^{ub}\right)^2 \quad \text{if} \quad y_i > y_i^{ub} \quad i = 1,2,\dots,N_{prod} + N_{sections} \tag{15}$$

The penalty is subtracted from the objective function.

To account for the HEN constraints, the HEN retrofit approach uses a feasibility solver that ensures that the stream energy balances and ΔT_{min} constraint are not violated. The feasibility solver adjusts heat loads and stream split fractions to allow feasibility to be regained, as shown in Eq. 16 [49]:

$$\min_{Q,sf} \|f(Q,sf)\|_2^2 =$$

$$\min_{Q,sf}\left[\sum_{i=1}^{N_{HX}} \min\left(TH_i^{out} - TC_i^{in} - \Delta T_{min},\dots,TH_i^{in} - TC_i^{out} - \Delta T_{min},0\right)^2 + \sum_{k=1}^{N_{ST}}\left(TT_{cal,k} - TT_k\right)^2\right] \tag{16}$$

where *Q* and *sf* are the heat exchanger and split fractions vectors, respectively. *TH* and *TC* are the hot and cold inlet and outlet temperatures of exchanger *I*; TT_{cal} and TT_k are the calculated and the target temperature of a stream *k*; N_{HX} and N_{ST} are the number of heat exchanger and streams that form the HEN, and ΔT_{min} is the minimum temperature approach.

Since there is no unique solution for the vectors *Q* and *sf*, the solution found by the feasibility solver may not optimal [4]. This work uses a SA algorithm to modify the HEN configuration in order to find the optimum HEN retrofit design [9, 14].

3.8. Methodology – summary

The retrofit approach for the capacity enhancement of heat-integrated crude oil distillation systems proposed in this work is summarised as follows in Figure 3:

1. A stochastic optimisation algorithm changes the column operating conditions between lower and upper bounds set by the designer.

2. With these operating conditions, the distillation column is simulated using a MATLAB-Aspen HYSYS interface.
3. Using the results from the rigorous simulation, hydraulic analysis of the distillation column is performed.
4. The HEN is retrofitted using a stochastic optimisation approach [9]. The outputs for the HEN retrofit are the required heat transfer additional area, the number and type of modifications made, and the utility requirements.
5. The feasibility of the distillation column is checked against constraints: product specifications and hydraulic performance. If any of these constraints is violated, a penalty to the objective function is applied.
6. The system performance is evaluated in terms of net profit.
7. The process is repeated from Step 1 until the termination criteria of the optimisation algorithm are met.

The advantages of the proposed retrofit approach can be summarised as follows:

- Stochastic optimisation is used to find the best set of operating parameters that maximise the net profit of the system. Stochastic optimisation has more chances to find the global maxima for highly combinatorial problems such as the retrofit of crude oil distillation systems.
- The distillation column is simulated using rigorous models which provide with the stage-by-stage information needed to perform hydraulic analysis of the column. A stage-wise hydraulic analysis of the distillation column is performed, considering several hydraulic constraints. This prevents unfeasible column designs.
- The hydraulic correlations used are the ones used in commercial simulation software, such as Aspen Tech [48] and KG-Tower [39].
- A MATLAB–Aspen HYSYS interface is used to send and receive information to and from the simulation. This interface makes possible to capture the interactions between the distillation column and its corresponding HEN when optimising the operating conditions.
- In a first level, the HEN retrofit methodology [9] used identifies a feasible solution for the increased throughput; in a second level optimises the HEN structure in order to reduce the fired heating demand, thus reducing operating costs.

- Temperature-dependent heat capacities for the crude oil are considered in the HEN retrofit approach. This is a more realistic approach for crude oil, where thermal properties vary with temperature.

The proposed retrofit approach can be improved by using more accurate hydraulic and cost correlations are used if available.

Section 4 applies this approach to an industrially relevant case study.

4. Case study

The crude oil distillation case study presented in this section is the optimised design presented by Chen [14]. In the base case, the atmospheric crude oil distillation column processes 100,000 bbl d^{-1} (2562 kmol h^{-1}) of Venezuela Tía Juana Light crude oil into five products: light naphtha (LN), heavy naphtha (HN), light distillate (LD), heavy distillate (HD) and residue (RES); the heat recovery system pre-heats the crude oil using the product and process streams to 365℃. The crude oil assay based on the data provided by Watkins [50] is presented in Table 1.

Figure 4 illustrates the configuration of the crude oil distillation column comprising a main fractionator and three side-strippers. The main fractionator has 41 stages, uses live steam at 260℃ and 4.5 bar and has three pumparounds. The top side-stripper (Top SS), producing heavy naphtha (HN), has 6 stages and a reboiler. Light distillate (LD) is produced from the middle side-stripper (Mid SS), which consists of 7 stages and is also reboiled. The bottom side stripper (Btm SS) has 5 stages and uses stripping steam at 260℃ and 4.5 bar. Table 2 summarises the column operating conditions; Table 3 presents the product specifications and flow rates.

It is assumed that the column internals are valve trays with a tray spacing of 0.6 m, with 0.06 m of downcomer clearance, and an active area of 86% in Sections 1 to 4 of the main fractionator and of 91% in Section 5 of the main fractionator and the side-strippers. The standard approach for tray sizing is applied. Table 4 shows the distillation column diameters and the number of passes per tray in each section. For convenience, side stripper stages are numbered sequentially, as shown in Table 4.

Table 1 Crude oil assay [14, 50]

% Distilled (by volume)	TBP (℃)
0	-3.0
5	63.5
10	101.7
30	221.8
50	336.9
70	462.9
90	680.4
95	787.2
100	984

Density: 874.4 kg m^{-3}

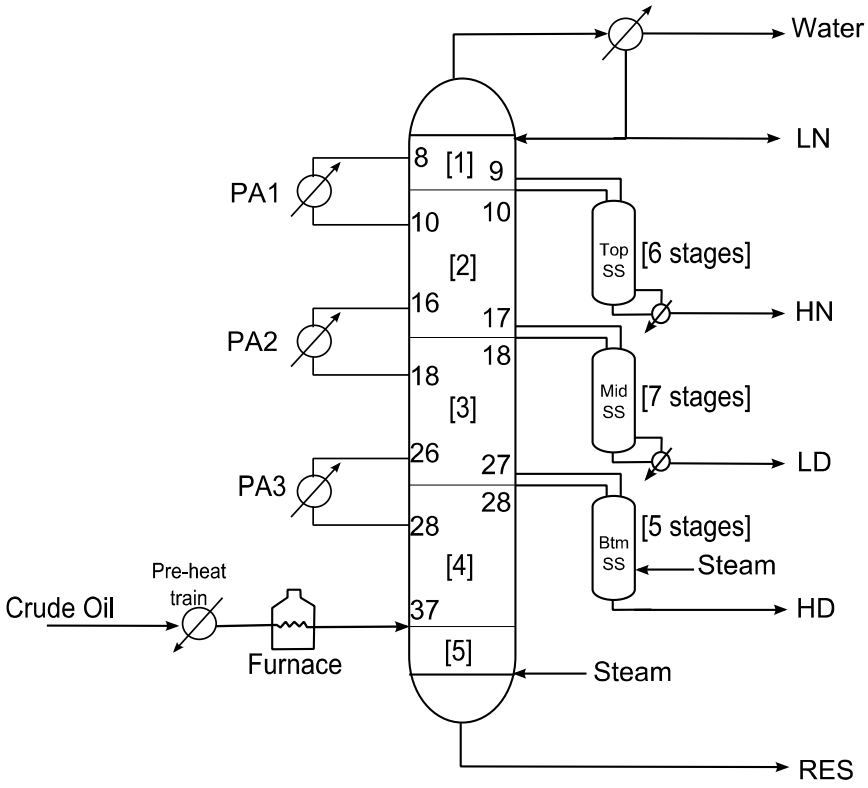

Figure 4 Stage distribution of the crude oil distillation column [4, 14]

Table 2 Crude oil distillation column operating conditions (100% throughput)

Parameter	Value
Feed pre-heat temperature (℃)	365
Column operating pressure (bar)	2.5
Main fractionator stripping steam flow rate (kmol h^{-1})	1200
Btm SS stripping steam flow rate (kmol h^{-1})	250
PA1 duty (MW)	12.8
PA1 ΔT (℃)	30
PA2 duty (MW)	17.9
PA2 ΔT (℃)	50
PA3 duty (MW)	11.2
PA3 ΔT (℃)	20
Condenser duty (MW)	47.87
Top SS reboiler duty (MW)	6.63
Mid SS reboiler duty (MW)	8.78

Table 3 Product specifications and flow rates [14]

Products	T5 (℃, TBP, in mole)	T95 (℃, TBP, in mole)	Flow rate (kmol h^{-1})
RES	353	804	315.7
HD	285	364	53.2
LD	190	310	120.5
HN	117	210	85.4
LN	3	122	85.2

Table 4 Crude oil distillation column section diameters

	Stage number	Passes per tray	Section diameter (m^2)	Approach to jet flooding (%)
Section 1	1-9	4	7.5	53
Section 2	10-17	4	7.5	53
Section 3	18-27	4	8.0	50
Section 4	28-36	4	8.0	44
Section 5	37-41	2	5.5	29
Top SS	42-47	2	3.5	22
Mid SS	48-54	2	3.5	30
Btm SS	55-59	2	3.5	13

Figure 5 illustrates the HEN structure presented by Enríquez-Gutiérrez et al. [4] and based on the optimised case presented by Chen [14]. It consists of 22 heat exchangers, has 5453 m^2 of heat transfer area, and a fired heating demand of 62.1 MW for a ΔT_{min} of 25℃. Tables 5 and 6 show the HEN stream information and HEN details, respectively.

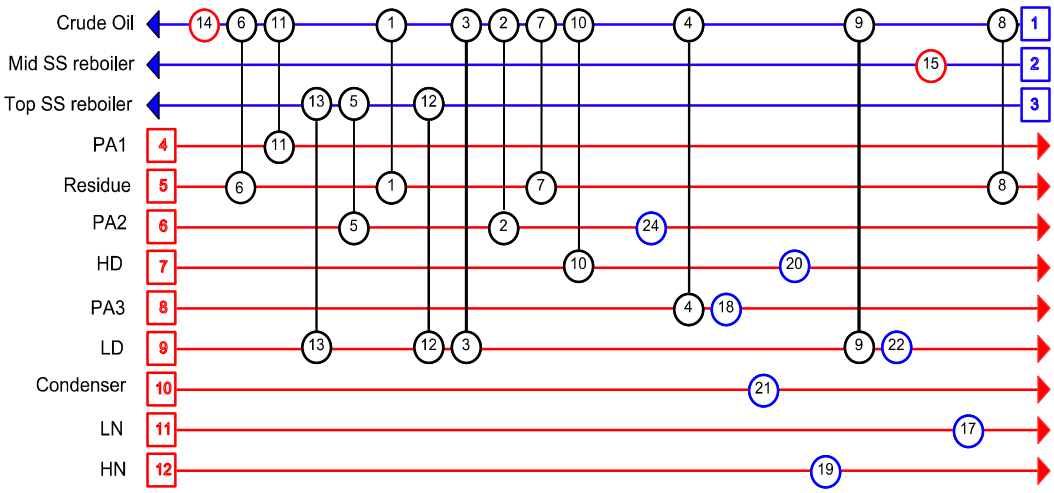

Figure 5 HEN structure [4, 14] (base case)

Table 5 HEN stream information [4, 14] (100 % throughput)

Stream	Supply temperature (℃)	Target temperature (℃)	Enthalpy change (MW)
Crude oil	25.0	365.0	143.4
Mid SS reboiler	262.7	284.3	6.1
Top SS reboiler	172.7	193.8	3.9
Pumparound 1 (PA1)	304.5	278.0	12.8
Pumparound 2 (PA2)	223.3	187.1	17.9
Pumparound 3 (PA2)	146.2	141.1	11.2
Condenser	97.2	76.0	46.7
RES	328.0	100.0	49.6
HD	262.1	50.0	5.4
LD	273.9	40.0	17.9
HN	179.3	40.0	6.5
LN	72.8	40.0	1.4
Fired heating (utility)	1500.0	800.0	62.1
Cooling water (utility)	10.0	40.0	77.1

Table 6 HEN details [4, 14] (base case)

Heat exchanger number	Installed area (m^2)	Duty (MW)
h1	975	25.4
h2	332	11.5
h3	112	3.2
h4	196	5.7
h5	58	4.8
h6	105	3.3
h7	684	13.2
h8	312	10.8
h9	260	8.8
h10	46	2.1
h11	555	12.9
h12	22	1.1
h13	67	3.9
h14*	106	59.6
h15*	11	8.8
h17*	59	8.1
h18*	99	7.9
h19*	122	6.5
h20*	61	3.7
h21*	1036	52.9
h22*	179	6.5
h24*	56	10.5

* Utility heat exchanger

In this case study, it is desired to increase the processing capacity of the crude oil distillation system by 30%, i.e. to 130, 000 bbl d^{-1} (3331 kmol h^{-1}) of the same crude oil. The system cannot accommodate this throughput without needing retrofit modifications to both the distillation column and the HEN [4].

To relieve the bottlenecks of the distillation column, previous work [4] proposes replacing the existing column internals in first section of the column (stages 1 to 9, see Figure 4) with structured packing Mellapak Plus 452 Y, a universal packing type sold by Sulzer that is reported to be useful for boosting capacity [51]. It is also mentioned that is suitable for a wide range of column liquid loads, from 0.2 to more than 200 $m^3\ m^{-2}\ h^{-1}$ [51]. The estimated cost of this is $97,000. In addition, 1,946 m^2 of additional heat transfer area is needed, costing $586,000. The system requires 76 MW of fired heating, 23% more than in the base case.

The concept of the height equivalent to a theoretical plate (HETP) is used to account for the performance of the packing. An empirical correlation is used to estimate the HETP [52]; this correlation assumes perfect liquid distribution, and its results are reported to be slightly conservative [52]. It is assumed that liquid collectors and distributors require 0.5 m of column height per bed of packing [1]. The height of the internals is 5.5 m; the HETP correlation predicts that 4.0 m of Mellapak Plus 452 Y will

provide the same separation performance. After accounting for liquid distribution, this type of structured packings can be installed in the available space [4].

Table 7 lists the retrofit scenarios considered for study. Case 1 increases the operating parameters pro rata, retrofits the HEN and replaces the column internals in Section 1. Case 2 optimises the operating parameters and retrofits the HEN. Case 3 replaces the column internals in Section 1 with structured packing Mellapak Plus 452 Y, optimises the operating parameters and retrofits the HEN.

Table 7 Retrofit scenarios considered

Retrofit scenario	HEN retrofit	Operational optimisation	Replace column internals in Section 1 **
Case 1*	X		X
Case 2	X	X	
Case 3	X	X	X

* Operating parameters are increased pro-rata
** With structured packings Mellapak Plus 452 Y

For the cases that do consider operational optimisation, i.e. Cases 2 and 3, the optimisation is carried out using two optimisation algorithms: SA and GS. Because of the large number of optimisation variables considered and the stochastic nature of both algorithms, the chance of finding the best solution gets reduce [10]. For this reason, each algorithm is run three times; the best solution is determined by comparing the results. This procedure aims to get confidence on the results and to observe trends. Also, it is intended to reveal if GS is a suitable optimisation algorithm for these types of systems, as it has not been used before for the retrofit of heat-integrated distillation systems.

The lower and upper bounds of the operating parameters are chosen based on sensitivity studies that revealed the ranges of column operating conditions leading to converged simulations. Table 8 presents these values. The stripping steam flow rates and pumparound heat flows are permitted to vary by ±30%, the crude oil pre-heat temperature between 350 and 370℃ and the pumparound temperature drops between 10 and 120℃.

The system constraints considered are:

- for trayed sections of the distillation column:
    - approach to jet flooding: 80%

- weir load, 90 m^3 m^{-1} h^{-1}
- downcomer exit velocity, 0.46 m s^{-1}
- approach to downcomer flooding, 80%

- for column sections containing structured packings:
  - approach to flooding: 80%
- product quality specifications, in terms of T5 and T95 TBP temperatures, as presented in Table 3. The tolerance for the T5 specifications is ±1; and for T95 specifications the tolerance is ±5 [22].

Table 8 Lower and upper bounds used for operational optimisation

Parameter	Lower bound	Upper bound
Main steam flow rate, kmol h^{-1}	1092	2028
Btm SS steam flow rate, kmol h^{-1}	227.5	422.5
Pre-heat temperature, ℃	350	370
PA1 heat flow, MW	10	19
PA2 heat flow, MW	16	31
PA3 heat flow, MW	11	22
PA1 ΔT, ℃	10	120
PA2 ΔT, ℃	10	120
PA3 ΔT, ℃	10	120

The objective of the optimisation is to increase the net profit, as evaluated using the correlations presented in Section 3.2. The cost components used in Eqs. 1, 2 and 3 are calculated as follows:

- *Variable costs:*

To estimate the transfer prices of intermediate products, the approach of Maples [53] is applied; in which the final prices are based on the price of crude oil, the crude oil products and the typical processing cost of each downstream process.

The prices of crude oil and its products are those reported by the US Energy Information Administration [54] for December 2014. Product yields and downstream operating costs are estimated based on Gary [47]. Table 9 lists the unit prices of crude oil and the distillation products used in this work.

The costs for the stripping steam and the hot and cold utilities are taken from Gary [47], updated for 2014 US$ using the inflation rate of each year [55] as shown in Table 10.

The values of F_i and F_r used in Eq. 5 are 0.8 and 0.1, respectively [4, 37]. Costs are updated using the CEPCI index; where the 1997 value is 386.5 [56] and the 2014 value is 576.1 [57].

The HEN capital cost is predicted by Eqs. 7 to 10, updated to 2014 using the CEPCI index; where the 2005 value is 468.2 [58].

Annualised capital cost is calculated assuming a 2-year project life with 5% interest rate.

Table 9 Crude oil, products and downstream operations prices

Item	End products	End product prices ($ bbl^{-1})	Downstream processes	Downstream operating costs ($ bbl^{-1})	Intermediate product prices ($ bbl^{-1})	($ kmol^{-1})
Light naphtha	Gasoline	$74.0			$74.0	$59.2
Heavy naphtha	Gasoline	$62.1	Hydrotreating	$6.0	$61.3	$80.0
	Propane	$9.7	Catalytic reforming	$4.6		
Light distillate	Jet fuel	$70.4	Hydrotreating	$6.0	$66.6	$107.9
	Propane	$2.2				
Heavy distillate	Diesel	$79.8	Hydrotreating	$6.0	$76.0	$193.8
	Propane	$2.2				
Residue	Light gas oil	$60.8	Vacuum distillation	$0.5	$66.5	$283.6
	Heavy gas oil	$4.2	Catalytic cracking	$2.5		
	Residue	$4.8	Hydrotreating	$0.3		
Crude oil feed		$46.0			$46.0	$74.6

Table 10 Prices of utilities [47]

Item	Value
Fired heating (1500-800℃), $/kWy	167
Cooling water (10-40℃), $/kWy	5.84
Stripping steam (260℃,4.5 bar), $/kmol	0.16

The termination criteria used for the optimisation algorithms are:

- For SA:
    - If the average change in the objective function value in 1500 iterations is less than $1x10^{-4}$.
    - If the number of iterations exceeds 3000 evaluations.
- For GS:

- It the average changes for the objective function value or for the optimisation variables are less than $1x10^{-4}$.

These values are chosen based on sensitivity analysis. In Section 4.1, results are presented and discussed.

4.1. Case study — Results

4.1.1. Case 1: Increasing operating parameters pro rata, HEN retrofit and replacing internals

Tables 11, 12 and 13 list the results for Case 1. Different from the case study presented in previous work [4], in which the operating parameters are also increased pro rata and the internals in Section 1 of the main fractionator are replaced with structured packing Mellapak Plus 452Y, Case 1 does consider HEN retrofit.

The benefits of considering HEN retrofit can be observed in Table 13. By applying HEN retrofit, the furnace inlet temperature is increased by 14℃, thus reducing the fired heating consumption by 5.5 MW. To achieve this energy recovery, the HEN requires 3331 m^2 of additional heat transfer area, 1385 m^2 more in comparison with the case that does not consider HEN retrofit [4]. However, the net profit of the system can be increased by around 2,000,000 \$ a^{-1}.

Table 11 Operating parameters results for Case 1

Parameter	Case 1
Main steam flow rate, kmol h^{-1}	1560
Btm SS steam flow rate, kmol h^{-1}	325
Furnace outlet temperature, ℃	365
PA1 heat flow, MW	14.7
PA2 heat flow, MW	23.4
PA3 heat flow, MW	16.3
PA1 ΔT, ℃	20
PA2 ΔT, ℃	50
PA3 ΔT, ℃	30

Table 12 Product flow rates results for Case 1

Product	Case 1
Light naphtha (kmol h^{-1})	899
Heavy naphtha (kmol h^{-1})	534
Light distillate (kmol h^{-1})	496
Heavy distillate (kmol h^{-1})	177
Residue (kmol h^{-1})	611

Table 13 HEN and economic results for Case 1

Parameter	**Enríquez-Gutiérrez et al. [4]**	**Case 1**
Additional HEN area, m^2	1946	3331
Furnace inlet temperature, ℃	260	274
Furnace outlet temperature, ℃	365	365
Fired heating demand, MW	76	70.5
Cost replacing column internals, $\$\cdot10^{-3}$	97	97
HEN retrofit cost, $\$\cdot10^{-3}$	586	761
Net profit, $\$\cdot10^{-3}\ a^{-1}$	966,663	968,746

Tables S1.1, S1.2 and S1.3 of the Supporting Information present the results for the HEN required heat transfer area, the product quality specifications and the column hydraulics for Case 1. No constraints are violated during this analysis.

4.1.2. Case 2: Operational optimisation and HEN retrofit

Figures 6 and 7 illustrate the operational optimisation results for this case and how they compare with the results from Case 1, in which the operating parameters are simply increased pro rata.

In both figures, the following trends can be observed: the main steam flow rate, the furnace outlet temperature and the pumparound heat flows tend to decrease; while the HD steam flow rate and the pumparound temperature drops tend to increase. It can also be observed that the most sensitive variables are the pumparound temperature drops, especially the one of PA3 (the hottest pumparound).

Tables 14 and 16 present the results for the product flow rates using SA and GS, respectively. Observe that increasing the HD steam increases the production of the heavy distillate; while decreasing the main steam decreases the residue production. In Tables 15 and 17 can be observed that there is also a relationship between these variables, the HD stripping steam and the main steam flow rates, and the heavy distillate and residue quality specifications, respectively.

As illustrated in Figures 6 and 7, the pumparound temperature drops exhibit drastic changes compared to the base case value. However, in Tables 15 and 17 can be observed that the product quality is unaffected by these changes. It can also be observed in Figures 6 and 7, that the pumparound heat flows tend to stay closer to the base case value. This reveals a relationship between the quality of light naphtha, heavy naphtha and light distillate with the pumparound heat flows; and indicates that

changing the pumparound temperature drops do not affect the quality of the products. This explains the trends observed in Figures 6 and 7 for these operating variables.

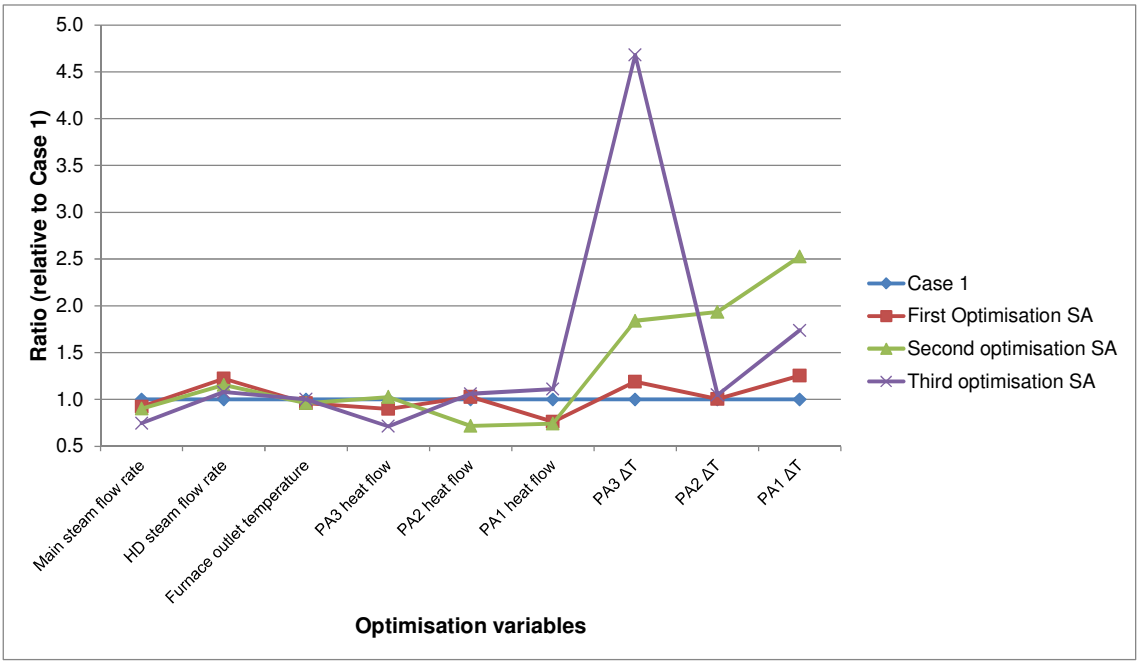

Figure 6 Optimisation results for Case 2 using SA

Table 14 Product flow rates for Case 2 using SA

Product	First optimisation		Second optimisation		Third optimisation	
	Value	Diff*	Value	Diff*	Value	Diff*
Light naphtha (kmol h^{-1})	893.6	-0.5%	899.2	0.1%	892.3	-0.6%
Heavy naphtha (kmol h^{-1})	551.9	3.3%	528.2	-1.1%	550.0	3.0%
Light distillate (kmol h^{-1})	484.6	-2.2%	493.5	-0.4%	485.4	-2.0%
Heavy distillate (kmol h^{-1})	195.5	10.7%	199.9	13.2%	184.8	4.7%
Residue (kmol h^{-1})	600.2	-1.7%	599.7	-1.8%	607.0	-0.6%

* Difference with respect to results from Case 1

Table 15 Product quality specifications for Case 2 using SA

Specification	Product	Base Case	First optimisation		Second optimisation		Third optimisation	
		Value	Value	Diff*	Value	Diff*	Value	Diff*
T5 (℃, volume)	LN	3	2	-1	2	-1	2	-1
	HN	117	117	0	117	0	117	0
	LD	190	190	0	190	0	190	0
	HD	285	285	0	285	0	285	0
	RES	353	353	0	353	0	353	0
T95 (℃, volume)	LN	122	121	-1	121	-1	118	-4
	HN	210	211	1	209	-1	210	0
	LD	310	310	0	306	-4	310	0
	HD	364	368	4	368	4	365	1
	RES	804	805	1	805	1	804	0

* Difference with respect to base case value

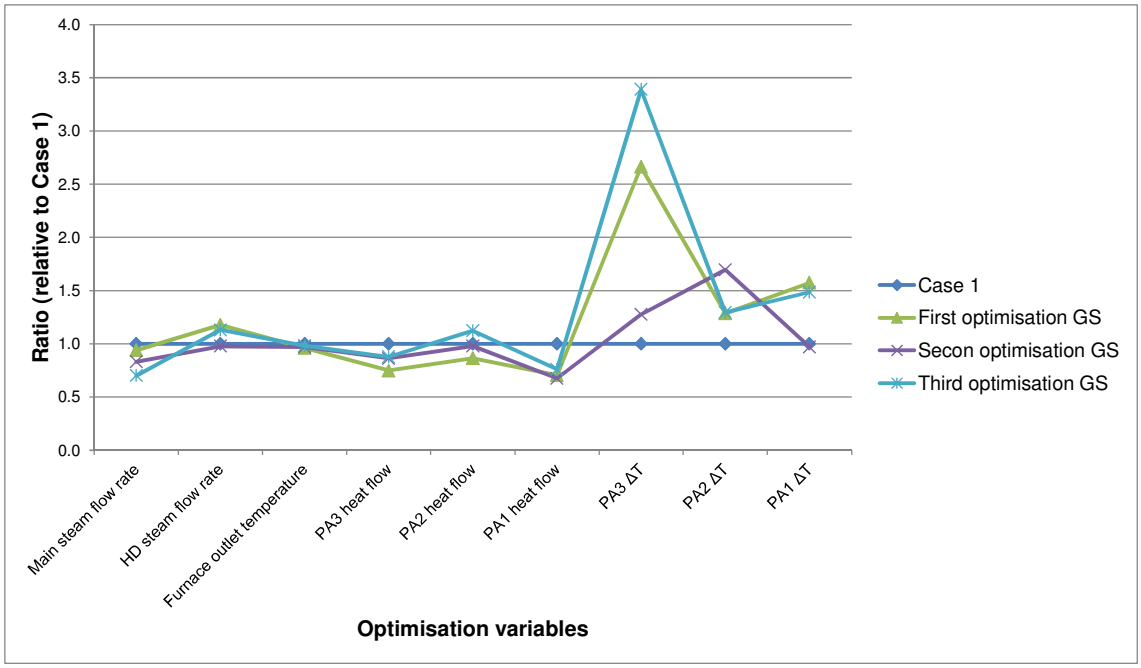

Figure 7 Optimisation results for Case 2 using GS

Table 16 Product flow rates for Case 2 using GS

Product	First optimisation		Second optimisation		Third optimisation	
	Value	Diff*	Value	Diff*	Value	Diff*
Light naphtha (kmol h^{-1})	896.2	-0.2%	897.8	0.0%	893.3	-0.5%
Heavy naphtha (kmol h^{-1})	535.6	0.3%	530.6	-0.7%	546.7	2.4%
Light distillate (kmol h^{-1})	490.8	-1.0%	502.3	1.4%	480.4	-3.0%
Heavy distillate (kmol h^{-1})	196.7	11.4%	191.2	8.3%	203.4	15.2%
Residue (kmol h^{-1})	601.1	-1.6%	600.2	-1.7%	599.1	-1.9%

* Difference with respect to results from Case 1

Table 17 Product quality specifications for Case 2 using GS

Specification	Product	Base case	First optimisation		Second optimisation		Third optimisation	
		Value	Value	Diff*	Value	Diff*	Value	Diff*
T5 (°C, volume)	LN	3	2	-1	2	-1	2	-1
	HN	117	117	0	117	0	117	0
	LD	190	190	0	190	0	190	0
	HD	285	285	0	285	0	285	0
	RES	353	353	0	353	0	353	0
T95 (°C, volume)	LN	122	119	-3	122	0	120	-2
	HN	210	210	0	209	-1	210	0
	LD	310	309	-1	310	0	309	-1
	HD	364	367	3	368	4	368	4
	RES	804	805	1	805	1	805	1

Tables 18 and 19 present the HEN retrofit and the economic results for Case 2 when using SA and GS, respectively.

Note that the third optimisation using SA has the highest furnace inlet temperature, and also has the highest PA3 temperature drop (i.e. the hottest pumparound, illustrated in Figure 6). A consistent trend is observed in the third optimisation using GS, which has the highest furnace inlet temperature and also the highest PA3 temperature drop (see Figure 7). This indicates a relationship between the furnace inlet temperature and the pumparound temperature drops.

Observe in Tables 18 and 19 that increasing the furnace inlet temperature also increases the requirements of heat transfer area.

The economic results reveal that the net profit of the system can be increased by around 973,500,000 \$ a^{-1}. Both, SA and GS, found similar values. However, note that not in every case the optimisers found the maximum value of net profit. This justifies the utilisation of two different optimisation algorithms to obtain robust results. These results also suggest that GS is suitable for optimising these types of systems.

The cases that found the maximum value of net profit are the first optimisation using SA and the third optimisation using GS.

The first optimisation using SA requires 252 m^2 more additional heat transfer area than the third optimisation using GS. However, the HEN retrofit cost is smaller in the first optimisation using SA. Both optimisations, found similar values for the furnace inlet

temperature: i.e. around 265℃. However, the furnace duty is smaller in the first optimisation using SA because the furnace outlet temperature is smaller.

Based on these results, it can be concluded that the best solution found is the one of the first optimisation using SA; since it has the biggest net profit and the smallest operational and investment costs.

Table 18 HEN and economic results for Case 2 using SA

Parameter	First optimisation	Second optimisation	Third optimisation
Additional HEN area, m^2	2421	1939	2938
Furnace inlet temperature, ℃	265	252	278
Furnace outlet temperature, ℃	351	351	365
Fired heating demand, MW	65.4	74.6	67.8
Cost replacing column internals, $\$\cdot 10^{-3}$	—	—	—
HEN retrofit cost, $\$\cdot 10^{-3}$	607	600	696
Net profit, $\$\cdot 10^{-3}\ a^{-1}$	973,447	972,123	971,031

Table 19 HEN and economic results for Case 2 using GS

Parameter	First optimisation	Second optimisation	Third optimisation
Additional HEN area, m^2	1519	1945	2169
Furnace inlet temperature, ℃	254	258	266
Furnace outlet temperature, ℃	351	354	359
Fired heating demand, MW	73.4	73.3	70.8
Cost replacing column internals, $\$\cdot 10^{-3}$	—	—	—
HEN retrofit cost, $\$\cdot 10^{-3}$	489	636	628
Net profit, $\$\cdot 10^{-3}\ a^{-1}$	971,670	971,150	973,409

Table 20 presents the optimisation times needed for each algorithm to find a solution, based on the stopping criteria mentioned in Section 4. Note that SA is less computationally expensive than GS. SA took around 8 hrs to find a solution, while GS around 18 hrs on a computer with an Intel Core processor of 3.3 GHz and 8 GB of installed RAM memory. However, both algorithms delivered the same quality of results.

Table 20 Optimisation times for Case 2

Optimisation algorithm	Optimisation time*, h		
	First optimisation	Second optimisation	Third optimisation
SA	8.2	8.2	5.8
GS	24.3	17.9	18

* On a computer with an Intel Core processor of 3.3 GHz and 8 GB of installed RAM memory

The values used to generate Figures 6 and 7 are reported in Tables S2.1 and S2.2 of the Supporting Information. The hydraulic results of Case 2 using SA and GS are reported in Tables S2.3 and S2.4. No hydraulics constraints are violated during the optimisations. The results for the HEN retrofit are reported in Tables S2.5 and S2.6. Section S4 of the Supporting Information provides an overview of the optimisations.

Case 3: Operational optimisation, HEN retrofit and replacing internals

Similar trends to those found in Case 2 (Section 4.1.2) can be also observed in this case. Figures 8 and 9 illustrate the results for the column operating parameters using SA and GS, respectively. The main steam, the pre-heat temperature and the pumparound heat flows tend to decrease; the HD steam and the pumparound temperature drops tend to increase.

Also the same influences between the operational parameters and the product flow rates and quality specifications can be observed in Tables 21, 22, 23 and 24.

Tables 25 and 26 present the HEN and economic results for this case when using SA and GS, respectively.

The best result found using SA (Table 25) is the one of the second optimisation. Note that this case is also the one with hottest furnace inlet temperature. The best result using GS (the second optimisation in Table 26) also has the hottest furnace inlet temperature. This confirms the importance of heat recovery for the global economic balance.

Also in this case both, SA and GS, found that the net profit of the system can be increased to around 973, 500,000 \$ a^{-1}.

The second optimisation using SA found the highest value, i.e. 973,659,000 \$ a^{-1}. Note in Table 21 that in this case the light naphtha flow rate (the most valuable product) is increased. Also, note that in the cases where replacing the column internals is not considered (i.e. in Case 2), the light naphtha production always decreases (see Tables 14 and 16).

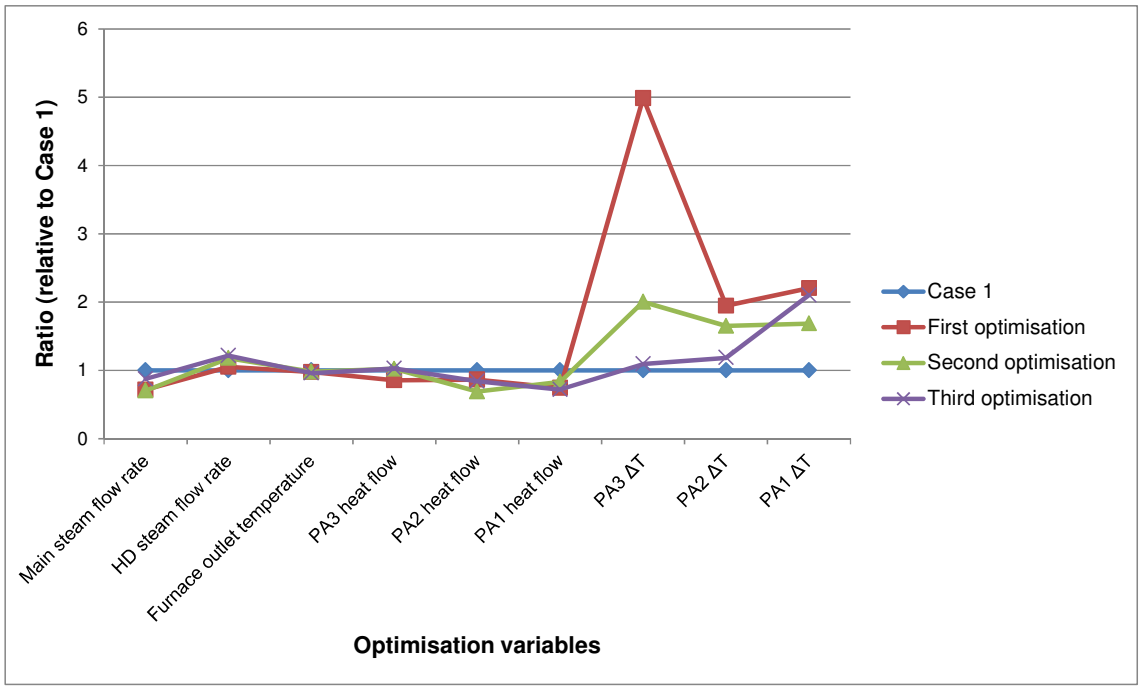

Figure 8 Optimisation results for Case 3 using SA

Table 21 Product flow rates distribution for Case 3 using SA

Product	First optimisation		Second optimisation		Third optimisation	
	Value	Diff*	Value	Diff*	Value	Diff*
Light naphtha (kmol h^{-1})	896.9	-0.1%	900.9	0.3%	898.1	0.0%
Heavy naphtha (kmol h^{-1})	530.3	-0.7%	526.4	-1.4%	536.1	0.4%
Light distillate (kmol h^{-1})	490.6	-1.0%	491.1	-0.9%	485.9	-1.9%
Heavy distillate (kmol h^{-1})	203.4	15.2%	203.6	15.3%	202.6	14.7%
Residue (kmol h^{-1})	598.8	-2.0%	598.9	-2.0%	599.4	-1.9%

* Difference with respect to results from Case 1

Table 22 Product quality specifications results for Case 3 using SA

Specification	**Product**	**Base Case**	**First optimisation**		**Second optimisation**		**Third optimisation**	
		Value	**Value**	**Diff***	**Value**	**Diff***	**Value**	**Diff***
T5, (℃, volume)	LN	3	2	-1	2	-1	2	-1
	HN	117	117	0	117	0	117	0
	LD	190	190	0	190	0	190	0
	HD	285	285	0	285	0	285	0
	RES	353	353	0	353	0	353	0
T95, (℃, volume)	LN	122	119	-3	121	-1	122	0
	HN	210	209	-1	209	-1	210	0
	LD	310	305	-5	309	-1	305	-5
	HD	364	369	5	369	5	368	4
	RES	804	805	1	805	1	805	1

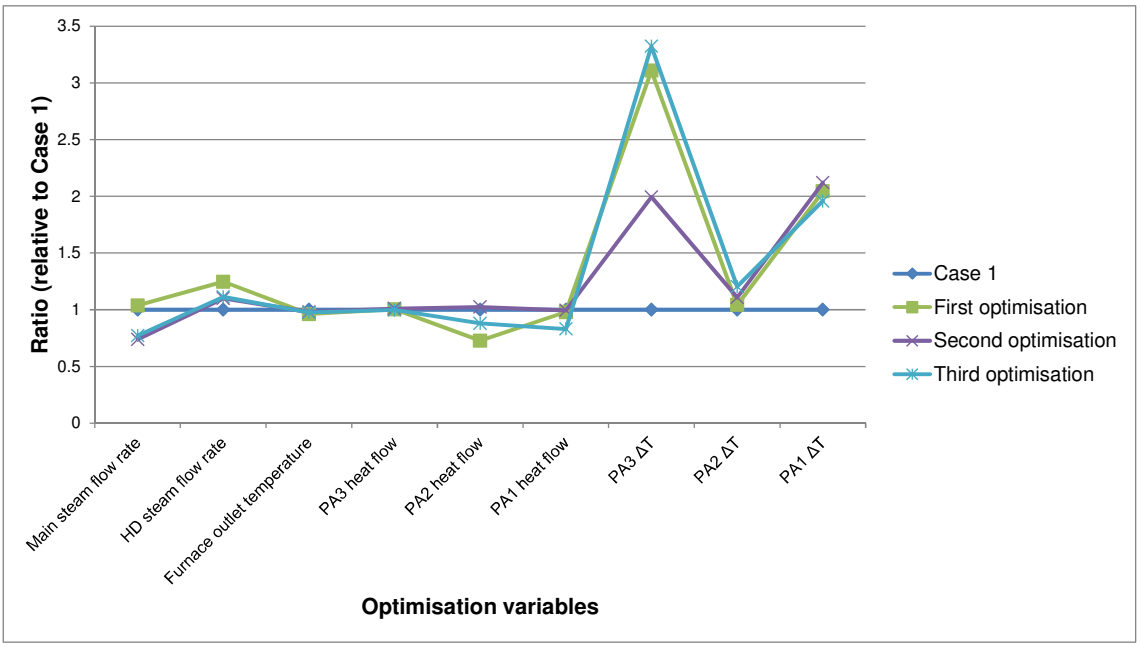

Figure 9 Optimisation results for Case 3 using GS

Table 23 Product flow rates distribution for Case 3 using GS

Product	First optimisation		Second optimisation		Third optimisation	
	Value	Diff*	Value	Diff*	Value	Diff*
Light naphtha (kmol h^{-1})	895.4	-0.3%	893.1	-0.6%	896.2	-0.2%
Heavy naphtha (kmol h^{-1})	539.8	1.1%	553.9	3.7%	537.6	0.6%
Light distillate (kmol h^{-1})	494.8	-0.1%	484.9	-2.1%	489.1	-1.3%
Heavy distillate (kmol h^{-1})	186.5	5.6%	194.4	10.1%	198.8	12.6%
Residue (kmol h^{-1})	604.1	-1.1%	600.2	-1.7%	600.1	-1.8%

* Difference with respect to results from Case 1

Table 24 Product quality specifications results for Case 2 using GS

Specification	**Product**	**Base Case**	**First optimisation**		**Second optimisation**		**Third optimisation**	
		Value	**Value**	**Diff***	**Value**	**Diff***	**Value**	**Diff***
T5 (℃, volume)	LN	3	2	-1	2	-1	2	-1
	HN	117	117	0	117	0	117	0
	LD	190	190	0	190	0	190	0
	HD	285	285	0	285	0	285	0
	RES	353	353	0	353	0	353	0
T95 (℃, volume)	LN	122	119	-3	122	0	120	-2
	HN	210	210	0	211	1	210	0
	LD	310	310	0	310	0	309	-1
	HD	364	365	1	368	4	368	4
	RES	804	804	0	805	1	805	1

Table 25 HEN and economic results for Case 3 using SA

Parameter	First optimisation	Second optimisation	Third optimisation
Additional HEN area, m^2	1599	2326	2162
Furnace inlet temperature, °C	254	260	255
Furnace outlet temperature, °C	357	358	351
Fired heating demand, MW	77.9	74.3	72.8
Cost replacing column internals, $\$\cdot 10^{-3}$	97	97	97
HEN retrofit cost, $\$\cdot 10^{-3}$	525	618	544
Net profit, $\$\cdot 10^{-3}\ a^{-1}$	971,799	973,659	973,117

Table 26 HEN and economic results for Case 3 using GS

Parameter	First optimisation	Second optimisation	Third optimisation
Additional HEN area, m^2	2414	2426	2044
Furnace inlet temperature, °C	260.5	270.8	262.2
Furnace outlet temperature, °C	350.9	357.8	356.2
Fired heating demand, MW	69.0	67.0	71.7
Cost replacing column internals, $\$\cdot 10^{-3}$	97	97	97
HEN retrofit cost, $\$\cdot 10^{-3}$	673	674	635
Net profit, $\$\cdot 10^{-3}\ a^{-1}$	970,986	973,497	972,905

In general, similar quality in the results are found when both using SA and GS. Table 27 shows the optimisation times for each case; note that SA needed less time to find an optimal solution. Section S4 of the Supporting information presents an overview of the optimisations.

Table 27 Optimisation times for Case 3

Optimisation algorithm	Optimisation time*, h		
	First optimisation	Second optimisation	Third optimisation
SA	5.8	8.2	7.0
GS	13.7	23.3	16.9

* On a computer with an Intel Core processor of 3.3 GHz and 8 GB of installed RAM memory

Tables S3.1 and S3.2 of the Supporting Information report the results used to generate Figures 8 and 9; Tables S3.3. and S3.4 presents the results for the hydraulic results of the CDU; no hydraulic constraints are violated during the optimisations. Tables S3.5 and S3.6 present the results for the heat transfer area needed per heat exchanger. Section S4 presents an overview of the optimisations.

4.2. Case study — summary and conclusions

Tables 28 and 29 summarise the best results for Cases 1, 2 and 3.

Case 1 shows that retrofitting the HEN can increase the net profit of the system, since operational cost can be reduced. However, more additional area is needed.

Case 2 reveals that combining operational optimisation and HEN retrofit reduces the fired heating demand and the required heat transfer area.

The cases that do consider operational optimisation, i.e. Cases 2 and 3, found that the net profit of the system can be increased to around 973,500,000 \$ a^{-1}; i.e. 4,754,000 \$ a^{-1} more than Case 1.

In both Cases 2 and 3, SA found a better solution than GS. However, the quality of the results obtained is very similar and the same trends can be observed. Also, using both optimisation algorithms helps to get robust results and to observe trends.

In Case 3, the case that considers all three retrofit options, the net profit of the system is increased the most. This is because by replacing the column internals in Section 1, the production of light naphtha (the more valuable product) increases by 0.3%, while in the best scenario of Case 2 the production of light naphtha decreases by 0.5%.

Table 28 Summary of best product flow rates distribution

Product	Case 1		Case 2		Case 3	
	Value	Diff*	Value	Diff*	Value	Diff*
Light naphtha (kmol h^{-1})	898.1	—	893.6	-0.5%	900.9	0.3%
Heavy naphtha (kmol h^{-1})	534.2	—	551.9	3.3%	526.4	-1.4%
Light distillate (kmol h^{-1})	495.5	—	484.6	-2.2%	491.1	-0.9%
Heavy distillate (kmol h^{-1})	176.6	—	195.5	10.7%	203.6	15.3%
Residue (kmol h^{-1})	610.9	—	600.2	-1.7%	598.9	-2.0%

Table 29 Summary of best HEN and economic results

Parameter	Case 1	Case 2	Case 3
Additional HEN area, m^2	3331	2421	2326
Furnace inlet temperature, °C	274	265	260
Furnace outlet temperature, °C	365	351	358
Fired heating demand, MW	70.5	65.4	74.3
Cost replacing column internals, $\$\cdot 10^{-3}$	97	—	97
HEN retrofit cost, $\$\cdot 10^{-3}$	761	607	618
Net profit, $\$\cdot 10^{-3}$ a^{-1}	968,746	973,447	973,659

Table 30 summarises the trends observed during the case study. Varying the stripping steam flow rates and the pumparound heat flows impact on the product flow rates, the quality of the products and the column hydraulics. Increasing the furnace outlet temperature increases the fired heating demand and affects the column hydraulics. Increasing the pumparound temperature drops helps to increase the furnace inlet temperature, thus reducing the fired heating demands. However more additional heat transfer area is needed. Combining operational optimisation with replacing column internals increases the flow rate of the most valuable products, this impact on the column hydraulics. Using optimisation to propose retrofit modifications for the HEN helps to reduce a furnace the fired heating duty for a given furnace outlet temperature.

Table 30 Impacts of retrofit modifications

Retrofit options	Product flow rate	Product quality specs	Furnace inlet temp.	HEN area	Fired heating demand	Column hydraulics
Main steam flow rate	X	X				X
Btm SS steam flow rate	X	X				X
Furnace outlet temperature					X	X
PA heat flows	X	X				X
PA temperature drops			X	X	X	X
Replacing column internals	X					X
HEN retrofit			X	X	X	

The results obtained in Case 3 reveal that the proposed retrofit approach is able to consider hardware modifications to the distillation column when increasing throughput and that replacing the column internals in the most constrained sections can improve the net profit of the system.

The case studies show the importance of performing hydraulic analysis of the distillation column: i.e. unfeasible column designs are avoided. It is also shown that formulating the objective function with penalties ensures that quality of the products is not violated.

In this particular case study, GS needed more time to find the solution, around 15 h, compared to the 6 h needed by SA (on a computer with an Intel Core processor of 3.3 GHz and 8 GB of installed RAM memory). However, the quality of the solutions is similar; suggesting that both optimisation algorithms are useful for the operational optimisation of heat-integrated crude oil distillation systems, and due the non-linear nature of the system, there is no benefit in using both deterministic and stochastic optimisation together over using stochastic optimisation only.

Note that the case study presented does not address the case of having multiple crude feeds and a vacuum distillation unit. However, these can be considered by this approach if the appropriate units are installed in the simulation. The methodology followed in this approach can be easily extended.

Although in these case studies the product quality is expressed in terms of the T5 and T95, the approach is not restricted to only consider these specifications. Other specifications may be considered if they can be predicted by the simulation package or suitable correlations are applied.

The method used to estimate the transfer prices of the products produced in the distillation column is simple; more realistic values can be obtained from plant data or more reliable sources. This cost correlations used in this work to estimate the net profit are also very simple, more accurate ones should be used if available.

5. Conclusions

The retrofit of heat-integrated crude oil distillation systems is a complex problem with many degrees of freedom and constraints due the strong interactions between the crude oil distillation column and its associated HEN. Existing retrofit methodologies from the open research literature aim the exploit these interactions in order to maximise the profitability of the system, to reduce the energy consumption or to increase its yield.

The optimisation-based retrofit approach for the capacity expansion of heat-integrated crude oil distillation systems proposed in this work uses stochastic optimisation to find the best set of column operating parameters that maximises the profitability of the system, while considering HEN retrofit and accounting for the system constraints.

Two optimisation algorithms are used: SA and GS. Based on the results from the case studies, it can be concluded that both optimisation algorithms are suitable for optimising the system, as with both algorithms similar values and trends are found.

This approach uses rigorous simulation to simulate the crude oil distillation column in Aspen HYSYS using a bespoke MATLAB—Aspen HYSYS interface. The interface reads information from HYSYS in order to evaluate profit, assess column hydraulics, check product specifications, and provide inputs for HEN retrofit. The benefit of linking MATLAB and Aspen HYSYS is that multiple retrofit scenarios can be explored and assessed with relatively little engineering effort. Rigorous simulation is widely used in practice, since it may represent acutely the real operation of the plan. However, it is

important that the information used to build the simulation come from real plat data, otherwise it may not be able to reflect the reality since idealise models are used.

Another benefit of using commercial simulation software to model the distillation column is that the stage-wise information needed for hydraulic analysis can be obtained. The estimation of the hydraulic parameters depends on the hydraulic correlation used. In this work, the hydraulic correlations used are rather general and can be found in the open literature; more accurate ones should be used if available.

The HEN retrofit approach used in this work [9] allows to modify the HEN structure as well as to optimise the heat loads and split fractions, reducing the additional area needed and the fired heating consumption.

The optimisation approach is able to find a solution between the numbers of trail points analysed, however it does not guarantee finding the global solution. For this reason, the strategy followed in this work of using both SA and GS (i.e. running each algorithm three times) helps to obtain robust results and to observe trends.

In conclusion, the proposed retrofit approach is useful to assess beneficial retrofit modifications when increasing the processing capacity of heat-integrated crude oil distillation systems. Practical constraints, such as the distillation column hydraulics and product quality, can be accounted for. This work does not consider other beneficial modifications commonly applied in practice, such as adding a preflash unit or replacing internals with high-capacity trays.

Associated content

Supporting Information:

- HEN required additional heat transfer area for Cases 1,2 and 3
- Product quality results for Cases 1,2 and 3
- Hydraulic results for Cases 1,2 and 3
- Operational optimisation results for Cases 2 and 3
- Overview of the optimisations for Cases 2 and 3

Corresponding Author

Víctor Manuel Enríquez-Gutiérrez
E-mail1: victormanuel.enriquezgutierrez@manchester.ac.uk
E-mail2: iq.vic.enriquez@gmail.com

Acknowledgment

The authors gratefully acknowledge the Mexican Council of Science and Technology (CONACyT) and the Roberto Rocca Education Program (RREP) for their financial support of PhD studies at the University of Manchester.

Abbreviations

GS	Global search
HEN	Heat exchanger network
MINLP	Mixed-integer non-linear programming
SA	Simulated annealing

References

1. Smith, R., *Chemical Process Design and Integration*. John Wiley & Sons, Ltd.: Chichester, UK, 2005.
2. Errico, M., Tola, G., and Mascia, M., Energy saving in a crude distillation unit by a preflash implementation. *Applied Thermal Engineering*, **2009**. *29*(8-9): p. 1642-1647.
3. Rapoport, H., Lavie, R., and Kehat, E., Retrofit design of new units into an existing plant: Case study: Adding new units to an aromatics plant. *Computers and Chemical Engineering*, **1994**. *18*(8): p. 743-753.
4. Enríquez-Gutiérrez, V.M., Jobson, M., Ochoa-Estopier, L.M., and Smith, R., Retrofit of heat-integrated crude oil distillation columns. *Chemical Engineering Research and Design*, **2015**. *99*: p. 185-198.DOI: 10.1016/j.cherd.2015.02.008.
5. Stichlmair, J., *Distillation: Principles and Practice*, ed. J.R. Fair. Wiley-VCH: New York, USA, 1998.
6. Kencse, H., Manczinger, J., Szitkai, Z., and Mizsey, P., Retrofit design of an energy integrated distillation system. *Periodica Polytechnica: Chemical Engineering*, **2007**. *51*(1): p. 11-16.
7. Ochoa-Estopier, L.M., Jobson, M., and Smith, R., Optimisation of heat-integrated crude oil distillation systems. Part III: Optimisation framework. *Industrial & Engineering Chemistry Research*, **2015**. *54*(18): p. 5018-5036.DOI: 10.1021/ie503805s.
8. Bravo, J.L., Select structured packings or trays? *Chemical Engineering Progress*, **1997**. *93*(7): p. 36-41.
9. Ochoa-Estopier, L.M., Jobson, M., Chen, L., Rodríguez, C., and Smith, R., Optimisation of heat-integrated crude oil distillation systems. Part II: Heat exchanger network retrofit model. *Industrial & Engineering Chemistry Research*, **2015**. *54*(18): p. 5001-5017.DOI: 10.1021/ie503804u.
10. Cavazzuti, M., *Optimization Methods From Theory to Design Scientific and Technological Aspects in Mechanics* Heidelberg: Berlin, 2013.

11. MATHWORKS. *How globalsearch and multistart work*. 2015 [access date October 2015]; Available from: http://uk.mathworks.com/help/gads/how-globalsearch-and-multistart-work.html.
12. Gadalla, M., Kamel, D., Ashour, F., and din, H.N.E., A new optimisation based retrofit approach for revamping an Egyptian crude oil distillation unit. *Energy Procedia*, **2013**. *36*(0): p. 454-464.DOI: 10.1016/j.egypro.2013.07.051.
13. Zhang, J. and Zhu, X.X., Simultaneous optimization approach for heat exchanger network retrofit with process changes. *Industrial & Engineering Chemistry Research*, **2000**. *39*(12): p. 4963-4973.DOI: 10.1021/ie990634i.
14. Chen, L., *Heat-integrated Crude Oil Distillation System Design*, PhD Thesis, The University of Manchester, Manchester, UK, 2008.
15. López C., D.C., Hoyos, L.J., Mahecha, C.A., Arellano-Garcia, H., and Wozny, G., Optimization model of crude oil distillation units for optimal crude oil blending and operating conditions. *Industrial & Engineering Chemistry Research*, **2013**. *52*(36): p. 12993-13005.DOI: 10.1021/ie4000344.
16. Gadalla, M.A., Abdelaziz, O.Y., Kamel, D.A., and Ashour, F.H., A rigorous simulation-based procedure for retrofitting an existing Egyptian refinery distillation unit. *Energy*, **2015**. *83*(0): p. 756-765.DOI: 10.1016/j.energy.2015.02.085.
17. Suphanit, B., *Design of Complex Distillation Systems*, PhD Thesis, UMIST Department of Process Integration, Manchester, UK, 1999.
18. Gadalla, M., Jobson, M., and Smith, R., Shortcut models for retrofit design of distillation columns. *Chemical Engineering Research and Design*, **2003**. *81*(8): p. 971-986.
19. Rastogi, V., *Heat-integrated Crude Oil Distillation System Design*, PhD, The University of Manchester, Manchester, UK, 2006.
20. Li, W., Hui, C.-W., Karimi, I.A., and Srinivasan, R., A novel CDU model for refinery planning. *Asia-Pacific Journal of Chemical Engineering*, **2007**. *2*(4): p. 282-293.DOI: 10.1002/apj.20.
21. Fair, J.R., How to predict sieve tray entrainment and flooding. *Petro. Chem. Eng.*, **1961**. *33*: p. 45.
22. Ochoa-Estopier, L.M. and Jobson, M., Optimisation of heat-integrated crude oil distillation systems. Part I: The distillation model. *Industrial & Engineering Chemistry Research*, **2015**. *54*(18): p. 4988-5000.DOI: 10.1021/ie503802j.
23. Zhu, X.X. and Asante, N.D.K., Diagnosis and optimization approach for heat exchanger network retrofit. *AIChE Journal*, **1999**. *45*(7): p. 1488-1503.DOI: 10.1002/aic.690450712.
24. Asante, N.D.K. and Zhu, X.X., An automated and interactive approach for heat exchanger network retrofit. *Chemical Engineering Research and Design*, **1997**. *75*(3): p. 349-360.DOI: 10.1205/026387697523660.
25. Smith, R., Jobson, M., and Chen, L., Recent development in the retrofit of heat exchanger networks. *Applied Thermal Engineering*, **2010**. *30*(16): p. 2281-2289.
26. Chen, Y., Eslick, J.C., Grossmann, I.E., and Miller, D.C., Simultaneous process optimization and heat integration based on rigorous process

simulations. *Computers & Chemical Engineering*, **2015**. *81*: p. 180-199.DOI: 10.1016/j.compchemeng.2015.04.033.
27. de Oliveira Filho, L.O., Queiroz, E.M., and Costa, A.L.H., A matrix approach for steady-state simulation of heat exchanger networks. *Applied Thermal Engineering*, **2007**. *27*(14-15): p. 2385-2393.
28. Caballero, J.A., Milán-Yañez, D., and Grossmann, I.E., Optimal synthesis of distillation columns: Integration of process simulators in a disjunctive programming environment. *Computer Aided Chemical Engineering*, **2005**. *20*: p. 715-720.DOI: 10.1016/S1570-7946(05)80241-X.
29. Grossmann, I.E., Review of nonlinear mixed-integer and disjunctive programming techniques. *Optimization and Engineering*, **2002**. *3*: p. 227-252.
30. Costa, L. and Oliveira, P., Evolutionary algorithms approach to the solution of mixed integer non-linear programming problems. *Computers & Chemical Engineering*, **2001**. *25*(2–3): p. 257-266.DOI: 10.1016/S0098-1354(00)00653-0.
31. Wang, K., Qian, Y., Yuan, Y., and Yao, P., Synthesis and optimization of heat integrated distillation systems using an improved genetic algorithm. *Computers and Chemical Engineering*, **1998**. *23*(1): p. 125-136.
32. Kirkpatrick, S., Gelatt, C.D., and Vecchi, M.P., Optimization by simulated annealing. *Science*, **1983**. *220*(4598): p. 671-680.
33. Rodriguez, C.A., *Fouling Mitigation Strategies for Heat Exchanger Networks*, PhD Thesis, The University of Manchester, Manchester, UK, 2005.
34. Ugray, Z., Lasdon, L., Plummer, J., Glover, F., Kelly, J., and Martí, R., Scatter search and local NLP solvers: a multistart framework for global optimization. *INFORMS Journal on Computing*, **2007**. *19*(3): p. 328-340.DOI: 10.1287/ijoc.1060.0175.
35. Gadalla, M.A., *Retrofit Design of Heat-integrated Crude Oil Distillation Systems*, PhD Thesis, The University of Manchester, Manchester, UK, 2003.
36. Towler, G. and Sinnott, R.K., *Chemical Engineering Design Principles, Practice and Economics of Plant and Process Design*. 2nd. ed. Butterworth-Heinemann: Boston, 2013.
37. Branan, C.R., *Rules of Thumb for Chemical Engineers*. 4th ed. Elsevier Science: Burlington, 2011.
38. Sinnott, R.K. and Towler, G.P., *Chemical Engineering Design*. 5th ed. Butterworth-Heinemann: Oxford, 2009.
39. KG-Tower, *KG-Tower*. 2012, Version 5.1, Koch-Glitsch LP: USA
40. Koch-Glitsch. *Glitsch Ballast Tray Design Manual: Bulletin No. 4900*. 2013 [access date October 2014]; 6th Edition:[Available from: http://www.koch-glitsch.com/Document%20Library/Bulletin-4900.pdf.
41. Resetarits, M.R., *Chapter 2 - Distillation Trays*, in *Olujić, A.G.*; Distillation: Equipment and Processes, Editor., Academic Press: Boston, USA, 2014.
42. Koch-Glitsch. *Introduction to KG-Tower: Tray& Packed Tower Sizing Software Program, Version 2.0*. 2006 [access date October 2014]; Available from: www.koch-glitsch.com.
43. Resetarits, M.R., Propelling distillation research. *Chemical Engineering*, **2010**. *117*(6): p. 26-27.

44. Enríquez-Gutiérrez, V.M., Jobson, M., and Smith, R., A design methodology for retrofit of crude oil distillation systems. *Computer Aided Chemical Engineering*, **2014**. *Volume 33*: p. 1549-1554.DOI: 10.1016/B978-0-444-63455-9.50093-3.
45. Kister, H.Z. and Gill, D.R., Flooding and pressure drop prediction for structured packings. *IChemE Symp. Ser*, **1992**. *128*: p. A109-A123.
46. Kister, H.Z., Scherffius, J., Afshar, K., and Abkar, E., Realistically predict capacity and pressure drop for packed columns. *Chemical Engineering Progress*, **2007**. *103*(7): p. 28-38.
47. Gary, J.H., *Petroleum Refining: Technology and Economics*. 5th ed. Taylor & Francis: Boca Raton, USA, 2007.
48. Aspen Tech, *Aspen HYSYS*. 2012, Version 7.3, Aspen Tech Inc: USA
49. Ochoa-Estopier, L.M., Jobson, M., and Smith, R., Retrofit of heat exchanger networks for optimising crude oil distillation operation. *Chemical Engineering Transactions*, **2013**. *35*: p. 133-138.DOI: 10.3303/CET1335022.
50. Watkins, R.N., *Petroleum Refinery Distillation*. Gulf Pub.Tab Co., Book Division: Houston, USA, 1979.
51. Sulzer. *Structured packings for distillation, absorption and reactive distillation*. 2015 [access November, 2015]; Available from: https://www.sulzer.com/es/-/media/Documents/ProductsAndServices/Separation_Technology/Distillation_Absorption/Brochures/Structured_Packings.pdf.
52. Green, D.W. and Perry, R.H., *Perry's Chemical Engineers' Handbook*. McGraw-Hill Professional: New York, USA, 2007.
53. Maples, R.E., *Petroleum Refinery Process Economics*. 2nd ed. PennWell Corp.: Tulsa, Okla., 2000.
54. US Energy Information Administration. *Petroleum Marketing Monthly*. 2015 [access date July 2015]; Available from: http://www.eia.gov/petroleum/marketing/monthly/pdf/pmmall.pdf.
55. US inflation calculator. *Current US inflation rates: 2005-2015*. 2015 [access date April 2015]; Available from: http://www.usinflationcalculator.com/inflation/current-inflation-rates/.
56. Vatavuk, W.M., Updating the *CE* plant cost index. *Chemical Engineering*, **2002**. *109*(1): p. 62-70.
57. Ondrey, G., Economic Indicators. *Chemical Engineering*, **2015**. *122*(5): p. 104.
58. Bailey, M.P., Economic Indicators. *Chemical Engineering*, **2013**. *120*(12): p. 71-72.

Chapter 5 Retrofit approach proposed to include structural design decisions

The case studies presented in Publication 2 (see Chapter 4) demonstrate that the approach proposed is appropriate to assess operational modifications to the distillation column, to explore HEN retrofit opportunities and to systematically assess replacing the column internals. It is also noted that replacing the column internals in the constrained sections of the column helps to improve the performance of the system. Additionally, it is shown that the methodology followed to optimise the system (i.e. running two different optimisation algorithms three times each), helps not only to find the 'best' retrofit design but also to observe trends. However, replacing column internals and adding a preflash unit are not considered within the optimisation. Thus, energy integration opportunities might be missed.

This chapter addresses three specific objectives of this thesis:

- Include a methodology within the optimisation environment to evaluate the option of replacing column internals.
- Include a methodology within the optimisation environment to evaluate the option of adding a preflash unit.
- Apply HEN retrofit to account for the interactions between the distillation column, HEN and a new preflash unit.

5.1 Introduction to Publications 3 and 4

These two publications present two aspects of the proposed retrofit approach – generation of retrofit solutions that involve replacing column internals and assessing the impact on the HEN and generation of retrofit solutions that also involve adding a preflash unit.

Publication 3 presents the approach followed to generate and evaluate the option of replacing the column internals within the optimisation. Publication 4 extends the approach

of Publication 3 by including the option of adding a preflash unit within the optimisation. To date, these options have not been included within optimisation environments in the context of retrofit of heat-integrated distillation systems.

5.2 Publication 3

Enríquez-Gutiérrez, V. M., Jobson, M., 2016, An optimisation-based retrofit approach for the assessment of structural and flowsheet modifications for heat-integrated crude oil distillation systems. Part 1.- Replacing column internals, Industrial & Engineering Chemistry Research, under preparation.

An optimisation-based retrofit approach for the assessment of structural and flowsheet modifications for heat-integrated crude oil distillation systems. Part 1. Replacing column internals

Víctor M. Enríquez-Gutiérrez and Megan Jobson

Centre for Process Integration, School of Chemical Engineering and Analytical Science, The University of Manchester, Sackville Street, Manchester M13 9PL, United Kingdom

Keywords

Column retrofit, crude oil distillation, operational optimisation, HEN retrofit.

Highlights

- Optimisation applies rigorous simulation model of the distillation column
- Structural design decisions are included within the optimisation environment.
- Internals may be replaced with high-capacity trays or with structured packings
- HEN retrofit is considered simultaneously.

Abstract

This work presents an optimisation-based retrofit approach for increasing the processing capacity of heat integrated crude oil distillation systems that considers operational, structural and flowsheet modifications. In this retrofit approach, structural design decisions (i.e. replacing column internals in the constrained sections and/or adding a preflash unit) are included within an optimisation environment. Part I of this two-part series presents the approach followed to evaluate replacing the column internals in the constrained sections together with operational optimisation and heat exchanger network (HEN) retrofit. Part II considers installing a preflash unit.

In the approach, the crude oil distillation unit (CDU) is rigorously simulated, the CDU hydraulics are assessed using hydraulic correlations, a HEN retrofit solution is generated using an optimisation-based approach, and the column and HEN operating parameters are optimised using stochastic optimisation.

An industrially relevant case study highlights the benefits of optimising operating conditions together with replacing internals and HEN retrofit when increasing the processing capacity of heat-integrated crude oil distillation systems.

1 Introduction

Heat-integrated crude oil distillation systems are usually the first process in a crude oil refinery [1]. Crude oil systems are energy intensive; it is estimated that their fuel consumption is equivalent to 1-2% of the crude oil processed [2].

Heat-integrated crude oil distillation systems comprise a crude oil distillation unit (CDU), in which the crude oil is separated into several products for downstream processing towards producing higher priced products, and a heat exchanger network (HEN), where the crude oil is preheated before it enters the column using the heat of product and process streams and a furnace [3]. The CDU and HEN interact strongly [3].

To stay competitive in the market, processes need constant improvement through retrofit [4]. Retrofit aims to exploit the existing assets in order to increase the profitability of the system; changes to the flowsheet structure (e.g. adding additional separation or heat exchange units) and/or equipment structure (e.g. replacing existing internals of the distillation column, adding heat transfer area to existing heat exchangers) may also be considered [5]. However, retrofit design is more complex than grassroots design since they should be able to assess the performance of the existing equipment far from the conditions at which it is designed [6].

Due to the strong interaction between the CDU and the HEN, the retrofit of heat-integrated crude oil distillation systems is a complex problem with many degrees of freedom and constraints [7].

Retrofit methodologies for crude oil distillation systems found in the open research literature aim to exploit the interactions between the CDU and the HEN to achieve different objectives. Examples of retrofit objectives are: increasing the system processing capacity [8], maximising the revenue of the most valuable products [9], changing feedstock [10], reducing energy consumption and CO_2 emissions [11], etc. This paper focusses on increasing processing capacity.

Liu and Jobson [12] mention that in order to increase the capacity of a distillation process, three main approaches can be followed:

i) modifying the operating conditions of the distillation system,
ii) replacing column internals and/or
iii) adding new equipment.

Typically, operational modifications are preferred since they incur little or no capital investment. However, increasing the processing capacity of crude oil distillation systems cannot always be achieved by only adjusting its operating conditions; thus, structural and flowsheet modifications may also be needed [8].

This work proposes an optimisation-based retrofit approach for increasing the processing capacity of heat-integrated crude oil distillation systems that considers operational, structural and flow sheet modifications. The approach presented in this work focuses on replacing the column internals in the constrained sections together with operational optimisation and HEN retrofit. Part II [18] of this series presents the approach to also consider installing preflash.

This approach extends previous work [8, 13] by including structural design decisions (i.e. replacing the column internals and/or adding a preflash unit) within an optimisation environment as a design sub-problem, similar to the design approach presented by Caballero et al. [14]. This approach has not been proposed previously for the retrofit of heat-integrated crude oil distillation systems. The advantage of using this approach is that economic and energy trade-offs can be captured, as the crude oil distillation system (i.e. the CDU and the HEN) and promising retrofit modifications are analysed simultaneously.

The advantages of the proposed approach are demonstrated with an industrially relevant case study which assesses the feasibility and viability of increasing the processing capacity of an existing crude oil distillation system.

2 Literature review

Caballero et al. [14] present an approach for the optimal synthesis of extractive distillation columns, in which structural design decisions are included within an optimisation environment. The approach [14] proposes using a superstructure-based optimisation algorithm to find the optimal column configuration (i.e. number of stages, feed location) and column operating conditions (i.e. reflux ratio, heat loads). The approach proposed [14] divides the problem into two: in the first sub-problem, the optimal number of trays is found, and in the second sub-problem, the optimal operating

conditions (i.e. entrainer to feed ratio, reflux ratio, molar composition in the product streams) are found using a non-linear programming solver external to the simulation software. This is accomplished by connecting a process simulator (Aspen HYSYS) with an external solver developed in MATLAB. The approach is demonstrated with an extractive distillation system of ethanol. Heat integration is not considered.

Previous work [8] presents a retrofit approach for increasing the processing capacity of heat-integrated crude oil distillations systems. In this approach, the CDU is simulated using rigorous simulation, the CDU hydraulics are assessed using open literature hydraulic correlations and the HEN is retrofitted using an approach that does not permit structural changes (i.e. adding, deleting, repiping and/or resequencing heat exchangers). The approach proved to be useful to assess the impacts of increasing the processing capacity and the operating conditions pro rata on the CDU hydraulics and HEN required additional area; also to explore different types of internals to replace the existing one in the constrained sections of the CDU. The drawbacks of the approach [8] are that operational optimisation is not considered, thus heat integration opportunities might be missing, and that the retrofitted designs needed a large amount of heat transfer area, since the optimum HEN structured is not sought.

In later work [13], the approach [8] is extended by including operational optimisation and an optimisation-based HEN retrofit approach [15]. Two optimisation algorithms are used as way of comparison, simulated annealing (SA) and global search (GS). The approach [13] is useful to assess beneficial retrofit designs (including those in which the column internals are replaced in the constrained sections) in order to maximise the profitability of the system (i.e. revenue minus costs). However, no structural design decisions are included (i.e. replacing column internals and/or adding a preflash unit). Therefore, important heat integration opportunities might be missed.

The work of Caballero et al. [14] and previous work [8, 13] motivate the development of the optimisation-based retrofit approach presented in this work.

Section 2.1 presents a literature review of distillation column hydraulics, and Section 2.2 discusses the existing retrofit approaches for crude oil distillation systems that have considered replacing column internals in order to increase the processing capacity of crude oil distillation systems. Section 2.3 summarises and concludes this section.

2.1 Distillation column hydraulics

Distillation columns can operate effectively between certain flow limits depending on the type of internals used [16]. Distillation columns internals can be classified into two categories: trays and packings [17].

In trayed columns, high vapour loads may cause jet flooding, a phenomenon in which liquid is carried over to the stage above, reducing the vapour-liquid contact. When droplets of liquid start being carried to the stage above the phenomenon is known as entrainment [16]. In practice, these two phenomena are prevented by designing the distillation column with an approach to jet flooding of 80 to 85% [18].

High liquid loads prevent the vapour from disengaging completely from the liquid, entraining the vapour flow to the stage below. This phenomenon occurs when the downcomer is too small to handle the liquid load, causing low downcomer residence time and/or downcomer back-up (liquid backs up to the stage from the downcomer; it is known as downcomer flooding). To prevent tower malfunction, it is recommended that the approach to downcomer flooding does not exceed 80 to 85% of the design limit [19].

In distillation columns containing structured packings, the flood point is defined as the vapour pressure drop at which the liquid is no longer able to flow against the vapour, impeding the countercurrent flow [16]. Packed columns are typically designed with an 80% approach to flooding [16].

The processing capacity of a distillation column is limited by the column hydraulics. Where the distillation column is the bottleneck of the distillation system, replacing the column internals with high-capacity trays [10, 20] and/or with structured packings may enable increased production.

Most of the existing retrofit approaches found in the open research literature apply operational optimisation and HEN retrofit in order to achieve more capacity and/or to reduce energy consumption [9, 21-23], and use the distillation column hydraulics as a constraint in order to avoid unfeasible column designs. Only a few retrofit approaches have contemplated replacing the column internals in a systematic way; this solution is usually considered together with operational optimisation and/or HEN retrofit [8, 10, 13, 24]. In the next section, these retrofit approaches are explained in more detail.

2.2 Retrofit approaches for crude oil distillation systems

Gadalla [24] proposes an optimisation-based retrofit approach for heat-integrated crude oil distillation systems. The retrofit objectives addressed in this approach are increasing throughput, reducing energy consumption, reducing CO_2 emissions and increasing profit. To achieve these retrofit objectives, operational optimisation and HEN retrofit are applied. The column retrofit problem is formulated as a non-linear programming problem (i.e. structural design options are not included in the optimisation). Gadalla [24] includes in the approach a methodology to replace the column internals with structured packings.

The methodology of Gadalla [24] can be summarised as follows. Firstly, a successive quadratic programming algorithm, a gradient-based method, proposes a new set of operating parameters for the CDU within certain upper and lower bounds. Secondly, the crude oil distillation column is decomposed into a thermodynamically equivalent sequence of columns [25] and is simulated using distillation column shortcut models [26], based on those of Suphanit [27]. Thirdly, the heat transfer area of the HEN required for a given energy demand at the optimised operating conditions is estimated using an Area-Energy curve generated from a network pinch analysis [28] of the HEN. Fourthly, the distillation column hydraulics are assessed by calculating the required diameter using Fair's correlation for jet flooding [29], and comparing it with the existing diameter. If the required diameter is bigger than the existing one, a suitable structured packing is then selected.

The criteria used to select a structured packing is the height equivalent to a theoretical plate (HETP). The HETP of different structured packings, is estimated using the rule of thumb presented by Kister [17]; the selected structured packing is the one that requires a packed bed smaller than the height of the trays to replace. Finally, flooding is checked using a regressed model from the pressure drop correlation of Kister and Gill [30] in order to avoid unfeasible designs. The cost of the replacing trays with structured packings is estimated using a cost correlation found in the open literature [31].

This systematic approach [24] is useful to assess retrofit modifications when increasing processing capacity. However, the correlation used to estimate the required diameter [29] only accounts for jet flooding, neglecting the downcomer hydraulic performance which may lead to unfeasible column designs. A regressed model is used to check for flooding in structured packings in order to be able to compute the correlation and to

reduce the engineering effort. However, the installation of liquid distributors is not accounted for.

Thernesz et al. [10] propose a systematic retrofit methodology for crude oil distillation systems for increasing throughput and/or changing the crude feedstock. The methodology [10] starts by collecting data of the process conditions (e.g. yield and product quality, temperatures, pressures, reflux ratios, flow rates and stripping stream flow rates) and constraints (e.g. maximum/minimum coil outlet temperature, maximum pressure, maximum pump capacity). With this information, the distillation units are modelled in Pro II v7.1. Once the simulation has been validated, the throughput is increased or the crude feedstock changed, and the column is re-simulated. The operating parameters are not modified. The results from the simulation are then exported to internals vendor software (SULCOL v1.0 and KG Tower v2.0) to assess the hydraulics of the CDUs. The following hydraulic parameters are analysed: jet flooding, downcomer flooding, vapour velocity and liquid height in the downcomer. If the limit of any of these parameters is violated, then the column internals can be replaced with high-capacity and/or high-efficiency trays.

The impacts of increasing throughput and/or changing crude feedstock on the HEN are assessed in SUPERTARGET, which applies the principles of pinch technology. Firstly, the grand composite curve is generated to establish the maximum heat recovery. Secondly, the heat exchangers that transfer heat across the pinch are identified. Thirdly, changes to the HEN are proposed (e.g. adding heat exchangers, resequencing heat exchangers) based on experience and observation. The resulting heat exchanger network is re-simulated in SUPERTARGET to estimate the energy savings. Finally, the operability and economic performance of the proposed modifications are assessed.

The approach of Thernesz et al. [10] uses a high level of detail to model both the distillation column and the HEN: commercial simulation software is used for this purpose. The hydraulic analysis of the distillation considers both jet and downcomer flooding, using vendor simulation design software. However, commercial simulation software and vendor software cannot be connected. Therefore, operational optimisation is not possible and heat integration opportunities are not systematically exploited within the retrofit design methodology. Also, this systematic methodology requires significant engineering effort since it requires the analysis of each unit individually.

2.3 Literature review — summary

In summary, only a few of the retrofit approaches found in the open research literature have considered replacing column internals with structured packings and/or high-capacity trays in order to increase capacity, even though these modifications are commonly implemented in practice.

The methodologies that do consider replacing internals follow a systematic approach. The approach proposed by Gadalla [24] has the advantage of using methods that can be easily implemented in a computational framework, reducing the engineering effort. However, the shortcut methods used to simulate the distillation column [26] are difficult to initialise and converge and do not provide the stage-wise information needed to perform a hydraulic analysis of the column. On the other hand, the methods used by Thernesz et al. [10] are more rigorous and can be relatively accurate; however they cannot be automated and therefore operational optimisation is not possible. Furthermore, heat integration opportunities may be neglected. A trade-off between accuracy and computational effort can be observed.

Section 3 presents the optimisation-based retrofit approach proposed in this work. This approach aims to overcome the shortcomings of the existing approaches by including structural design decisions within an optimisation environment and by connecting rigorous simulation software (i.e. Aspen HYSYS [32]) with MATLAB.

3 Retrofit approach for crude oil distillation systems — replacing column internals

The retrofit problem that this work aims to solve with the proposed retrofit approach can be stated as follows. It is desired to increase the processing capacity of an existing heat-integrated crude oil distillation system by a certain percentage. In order to achieve the objective, the following modifications are permitted: operational optimisation, replacing the column internals with high-capacity trays and or/ structured packings in one or more sections and HEN retrofit, subject to product quality specifications.

This work extends previous research on retrofit of crude oil distillation systems [8, 13] by including structural design decisions (i.e. replacing column internals) as a design sub-problem, similar to the approach proposed by Caballero et al. [14].

Figure 1 illustrates the proposed retrofit approach. Following previous work [8, 13], in this approach the operating parameters of the distillation column are optimised using stochastic optimisation; rigorous simulation is used to simulate the distillation columns; correlations from the open literature are used to assess the hydraulic performance of the distillation columns and the approach of Ochoa-Estopier et al. [15] is used to simulate and to retrofit the HEN.

However, instead of applying penalties to the objective function if any hydraulic constraint is violated, new column internals are selected and replaced in the constrained sections using a decision algorithm coded in MATLAB, as illustrated in Figure 1. Penalties are only applied when product quality specifications are not satisfied or column simulations do not converge.

The approach uses a MATLAB— Aspen HYSYS interface to transfer data between MATLAB and HYSYS. The advantages of using this interface are that simplified models are not needed to simulate the distillation column, since rigorous simulation can be implemented within an optimisation environment, and that stage-by-stage information can be extracted in order to perform a hydraulic analysis of the distillation column [13].

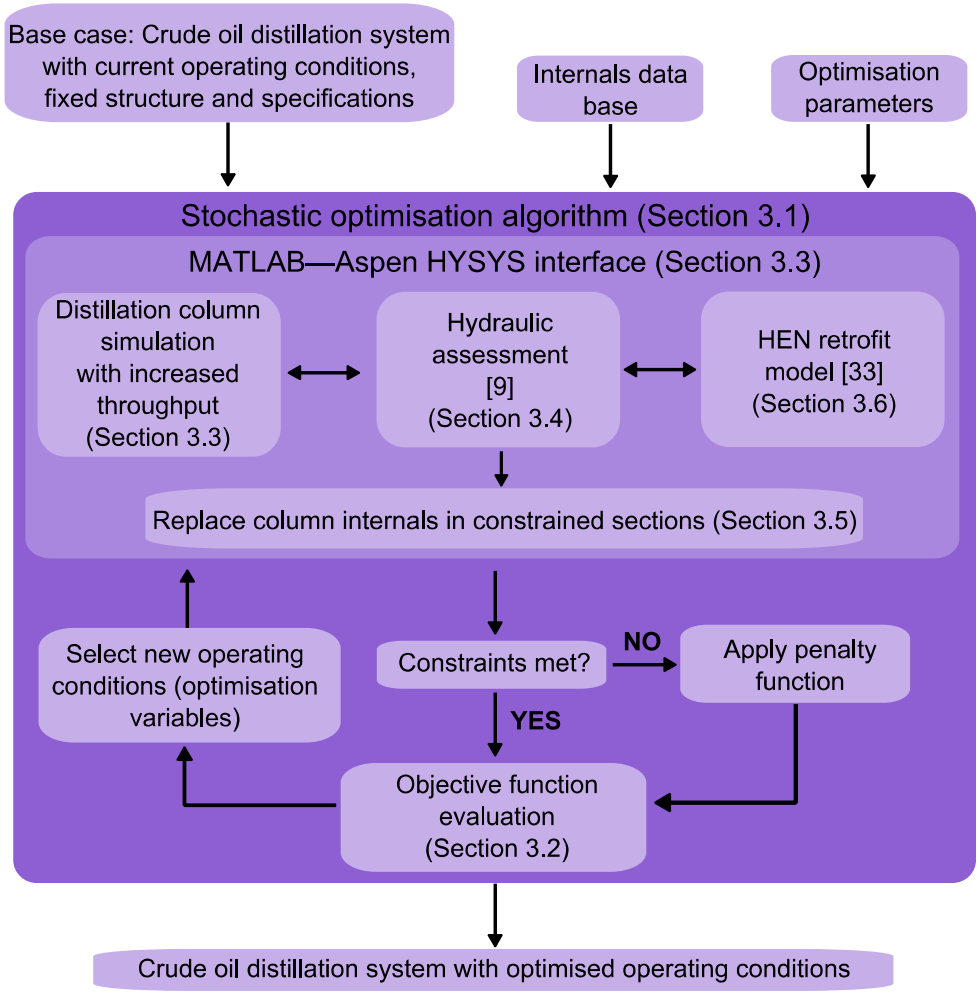

Figure 1 Proposed optimisation-based retrofit approach

The following information is needed to apply the proposed retrofit approach:

a. A rigorous simulation of the distillation column at the base case conditions.
b. The distillation column configuration, the HEN structure and the product quality specifications.
c. A data base containing the characteristics of the high-capacity trays and structured packings than can be used to replace the existing internals (i.e. percent of active area, downcomer clearance, number of flow paths per trays and angle of slope for high-capacity trays, and packing surface area, void fraction, packing factor and angle of inclination of the corrugated surface for structured packings).
d. Lower and upper bounds for the optimisation parameters (e.g. furnace outlet temperature, stripping steam flow rates, pumparound duties and temperature drops).

The proposed retrofit approach can be summarised as follows:

1. New operating conditions are proposed using a stochastic optimisation algorithm from the MATLAB optimisation toolbox. Section 3.1 presents the features of the optimisation algorithms used in this work (i.e. simulated annealing and global search).
2. With the MATLAB—Aspen HYSYS interface, a new set of operating parameters are input to Aspen HYSYS and the column is re-simulated.
3. If the simulation does not converge, the MATLAB—Aspen HYSYS interface chooses a set of operating parameters that is known to result in a converged simulation (e.g. the base case conditions), re-simulates the column and applies a penalty to the objective function. This step prevents the appearance of pop-up windows in Aspen HYSYS that block the communication between Aspen HYSYS and MATLAB, thus stopping the optimisation. Section 3.3 discusses the procedure followed to simulate the distillation column.
4. If the simulation does converge, stage-by-stage information for the vapour and liquid phases (i.e. molar flows, densities, viscosities, molar masses, surface tension) are read from Aspen HYSYS. With these data, a hydraulic analysis of the distillation column is performed. If any hydraulic constraint is violated, a decision algorithm proposes new internals for the constrained section. Section 3.4 describes the hydraulic correlations used in this work and Section 3.5 introduces the features of the structural design algorithm used to replace the column internals.
5. The following data are read from Aspen HYSYS to retrofit the HEN: crude oil and product flow rates, furnace outlet temperature, product outlet temperatures and crude oil and product heat capacities. These data are used as inputs for the optimisation-based retrofit approach of Ochoa-Estopier et al. [15] which estimates the additional heat transfer additional area and HEN modifications needed to minimise the fired heating duty. The approach of Ochoa-Estopier et al. [15] is applied in this work with relatively few modifications. Section 3.6 explains and discusses the HEN retrofit approach [15].
6. Product quality constraints are checked. If any specification is violated, a penalty to the objective function is applied. Section 3.2 introduces the penalty function.
7. The profitability of the system is estimated in terms of net profit, an economic indicator that reflects the cost-benefit trade-offs of a project [33]. Section 3.2 presents the costs correlations used in this work to estimate the net profit.
8. If the termination criteria are met, the optimisation stops and the outputs are analysed; otherwise the loop is repeated. Section 3.1 discusses the features of the optimisation algorithms used.

3.1 Stochastic optimisation algorithms

The retrofit of heat-integrated crude oil distillation systems can be classed as a mixed-integer non-linear programming (MINLP) problem [21], since it involves continuous variables (operational modifications), discrete variables (structural modifications) and equality and inequality constraints (column hydraulics, product specifications, minimum temperature approach, etc.). Such problems are typically solved using stochastic optimisation algorithms [6, 34], such as simulated annealing (SA) and global search (GS).

Simulated annealing (SA) emulates the annealing heat treatment process of steel (which is a system with many degrees of freedom that is typically solved using multivariate or combinatorial optimisation [35, 36]). The algorithm evaluates the objective function at random points within a given search space until the stopping criterion is met. In MATLAB, the search space is defined by giving lower and upper bounds for the optimisation variables. MATLAB uses five different stopping criteria: the maximum number of iterations, the maximum number of function evaluations, the average change in objective function value, the objective function limit and the time limit [37]. The advantage of using SA for highly combinatorial problems is that it is more likely to find the global minimum than deterministic algorithms due the random nature of the algorithm [36].

Global search (GS) is a heuristic algorithm designed to find the global optimum of MINLP problems [38]. The algorithm combines both stochastic and deterministic optimisation: scatter search [38] is used to generate multiple starting points and *fmicon*, a deterministic solver from the MATLAB optimisation toolbox, 'runs' for each point to generate different 'basins of attraction' (i.e. steepest descent paths that tend to the same minimum point [39]). Once the termination criterion is met, the algorithm generates a vector containing all the minima and finds the global minimum from these values. The termination criteria can be a maximum time, maximum number of trial points, the average change in objective function and the average change in the optimisation variables value [40].

Following previous work [8, 13], this approach also uses simulated annealing (SA) and global search (GS) to find a set of operating conditions that maximise the net profit of the system. The algorithms used are the ones from the MATLAB optimisation toolbox. Using both optimisation algorithms as way of comparison, proved to be beneficial to

gain confidence on the results [13]. SA is also used in the HEN retrofit approach [15] to modify the HEN structure (see Section 3.6).

Section 3.2 introduces the costs correlations used to calculate the optimisation objective function and discusses how penalties are applied for unsatisfactory designs.

3.2 Objective function

Following previous work [9, 13], this retrofit approach uses the net profit; the difference between the revenue and the cost of a project [33], as shown in Eq. 1.

$$NP = \sum Revenue - \sum Costs \tag{1}$$

The revenue is calculated by adding the value of each product, *C*, times its flow rate *F*, as shown in Eq. 2; where the subscript *i* refers to the i^{th} product of the total number of products (N_{prod}) [9].

$$\sum Revenue = \sum_{i=1}^{N_{prod}} C_i F_i \tag{2}$$

The costs associated with the crude oil distillation system are: the cost of crude oil feed, the operational costs (OC) and the annualised capital charges (ACC), as shown in Eq. 3 [9]; where the subscript *crude* refers to the crude oil.

$$\sum Costs = C_{crude} F_{crude} + OC + ACC \tag{3}$$

The operational costs associated with the crude oil distillation system are the cost of the utilities (i.e. fuel oil consumed in the furnace and cooling water) and stripping steam [9], as shown In Eq. 4. In this equation, the subscript *j* refers to the j^{th} utility of the total number of utilities (N_{util}), and *k* is the k^{th} stripping steam of the total number of stripping steam feeds (N_{stm}).

$$OC = \sum_{i=1}^{N_{util}} C_j F_j + \sum_{j=1}^{N_{stm}} C_k F_k \tag{4}$$

Consistent units should be used in Eqs. 1, 2, 3 and 4 (e.g. \$ $kmol^{-1}$, \$ kg^{-1} or \$ bbl^{-1} for prices; kmol s^{-1}, kg s^{-1} or bbl s^{-1} for material flowrates; kJ s^{-1}, W or MW for energy flow rates).

The annualised capital charge (ACC) accounts for the repayment of loans for covering the cost of new equipment or retrofit modifications.

The initial investment *P* accounts for the retrofit cost. In this approach, *P* is associated with:

- replacing column internals with high-capacity trays with sloped downcomer or with structured packings and,
- HEN modifications: adding area, resequencing and repiping existing heat exchangers and adding new heat exchangers.

These costs can be estimated using open literature cost correlations.

Bravo [41] presents correlations to estimate the cost of replacing trays with high-capacity trays (HCT) and structured packings (SP), shown in Eqs. 5 and 6. These equations correlate the hardware cost in 1997 US dollars and installation and removal factors, F_i and $F_{R,}$ respectively. In Eq. 5, *D* refers to the column diameter in m and N_t is the number of trays; this correlation is only valid when replacing trays with the same tray spacing [18]. In Eq. 6, S_H refers to the summation of the bed heights in m and N_b is the number of beds; the installation of liquid distributors is already accounted for in this model [18].

$$\$Cost_{HCT} = [11D^2(52N_t + 160)]F_iF_R \quad (5)$$

$$\$Cost_{SP} = 11D^2[260S_H + 160(2N_b - 1)]F_iF_R \quad (6)$$

To estimate the costs associated with HEN design, the cost model presented by Sinnott and Towler [42] is used. The cost model correlates the required surface area A_{HXreq} and three cost law constants, *a*, *b* and *c*, that depend on the materials of construction, pressure rating and type of heat exchanger, as shown in Eq. 7. It is mentioned that this model provides useful predictions [3].

$$\$Cost_{HX} = a + b\left(A_{HXreq}\right)^c \quad (7)$$

Based on the cost model presented in Eq. 7, Chen [21] presents four relationships to adding new heat exchangers (Eq. 8), adding area to existing heat exchangers (Eq. 9), repiping existing heat exchangers (Eq. 10) and resequencing existing heat exchangers (Eq. 11) in 2005 US dollars.

$$\$Cost_{HXnew} = 13{,}000 + 1530(A_{HXnew})^{0.63} \tag{8}$$

$$\$Cost_{HXarea} = 1530\left(A_{HXreq}\right)^{0.63} \tag{9}$$

$$\$Cost_{HXrepiping} = 60{,}000 \tag{10}$$

$$\$Cost_{HXresequencing} = 35{,}000 \tag{11}$$

This approach is not restricted to the used of the cost correlations presented in Eqs. 5 to 11. If a user has a set of correlations that are trusted and known to be satisfactory, those correlations can be used.

In this approach, a penalty to the objective function is applied when the product quality specifications are not met. The penalty helps to direct optimisation solutions away from those that do not meet specifications. The penalty is evaluated using Eqs. 12 and 13. In these equations, y_i refers to the quality specification (e.g. true boiling point temperature, ASTM D86 temperature) of the N_{prod}, the subscripts *lb* and *ub* refer to the upper and lower bounds, respectively, and γ_i is a large number known as the 'penalty factor' [9]. The penalty factor should be large enough to impact on the objective function.

$$Penalty_i = \gamma_i\left(y_i - y_i^{lb}\right)^2 \quad if \quad y_i < y_i^{lb} \quad i = 1,2,\dots,N_{prod} \tag{12}$$

$$Penalty_i = \gamma_i\left(y_i - y_i^{ub}\right)^2 \quad if \quad y_i > y_i^{ub} \quad i = 1,2,\dots,N_{prod} \tag{13}$$

The resulting value is then subtracted from the net profit, thus:

$$Objective\ Function = NP - Penalty \tag{14}$$

3.3 Simulation of the distillation column

Figure 2 illustrates the flowchart to simulate the distillation column using the MATLAB—Aspen HYSYS interface.

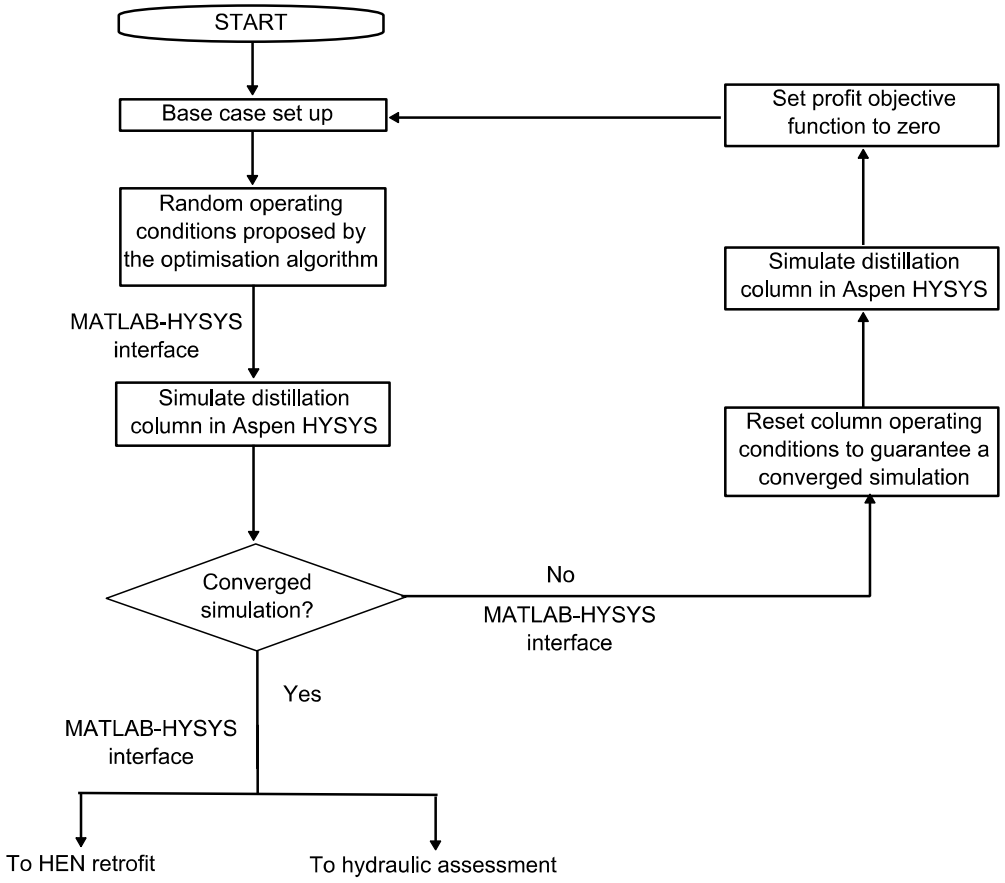

Figure 2 Flowchart to simulate the CDU [13]

The process begins by setting up the distillation column structure, inputs and specifications in Aspen HYSYS, as illustrated in Figure 3. Spreadsheets are used to record key inputs and to read and write information sent to and from MATLAB, such as the column operating parameters, vapour and liquid flow rates and transport property data (for the hydraulic assessment) and crude oil and product temperatures and flow rates (for HEN simulation and retrofit).

Also, “dummy” heat exchangers are installed to calculate the thermal properties of the crude oil feed and product streams for specified temperature intervals in order to

correlate the temperature dependence of stream heat capacities. Section 3.6 explains the function of these correlations.

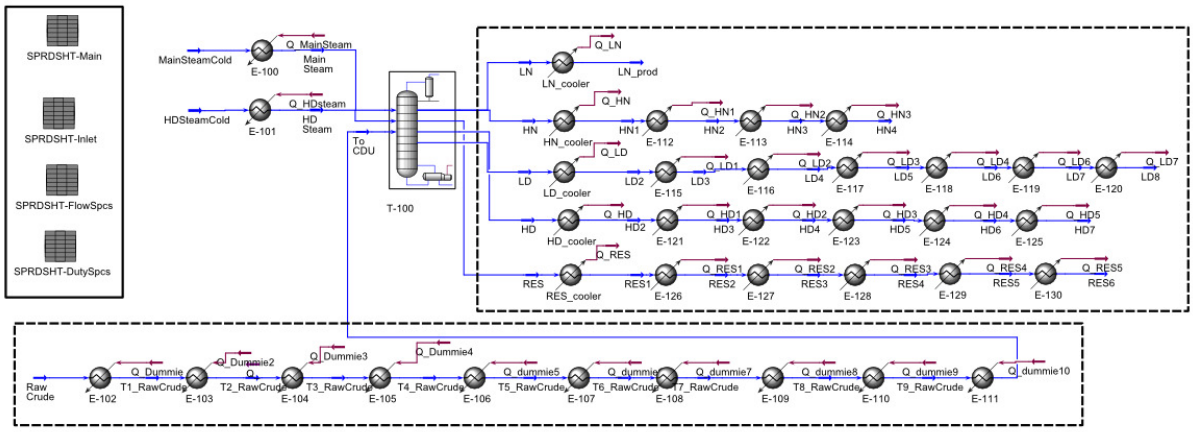

Figure 3 Simulation flowsheet in Aspen HYSYS v7.3

Next, a stochastic optimisation algorithm proposes a random set of column operating parameters (i.e. furnace outlet temperature, stripping steam flow rates and pumparound duties and temperature drops). These data are then sent to Aspen HYSYS and the distillation column is re-simulated.

If the simulation does not converge, the MATLAB—Aspen HYSYS re-simulates the distillation column using the base case conditions and applies a set the objective function to zero in order to discard this iteration. If the simulation converges, the data required to perform the hydraulic assessment of the distillation column and to retrofit the HEN are extracted.

3.4 Hydraulic assessment of crude oil distillation columns

Following previous work [8, 13], hydraulic correlations from the open literature are used to assess the hydraulic performance of the CDU when increasing its processing capacity and to assess options for replacing the column internals.

For distillation columns containing conventional trays and high-capacity trays with sloped downcomers, four parameters are assessed: approach to jet flooding, liquid weir load, downcomer exit velocity and approach to downcomer flooding.

To estimate the approach to jet flooding, the Glitsch correlation [19] is used. Resetarits [43] mentions that the flood points estimated by using this correlation are 'reasonable'; for this reason, it is widely used in practice by design engineers [43]. This work applies the limit used in practice, 80% [16, 18].

The liquid weir load is estimated following the design manual of KG-Tower [44, 45]. In practice, the design limit is between 90 and 100 $m^3\ m^{-1}\ h^{-1}$ [46], if exceeded, the number of passes in the trays is increased to provide better vapour-liquid contact [45]. The downcomer exit velocity is estimated with the design correlations used by KG-Tower [44, 45]. A value of 0.46 $m\ s^{-1}$ is recommended as design limit for the downcomer exit velocity; if this limit is exceeded the downcomer clearance has to be adjusted [45]. The Glitsch correlations for the downcomer design velocity are used to estimate the approach to downcomer flooding. Where, in practice, a value of 80% is used as the design limit [45].

To estimate the hydraulic performance of high-capacity trays with sloped downcomers, the same correlations for conventional trays can be used if the active area gained by sloping the downcomer is considered [8]. This work estimates the active area gained using the design correlations within KG-Tower [8].

For structured packings, the approach to flooding is estimated using a model [44, 47] regressed from the pressure drop correlation chart for structured packings of Kister and Gill [30]. The use of this correlation is restricted for organic mixtures with flow parameters (a relationship between the vapour and liquid flows and their densities) between 0.03 to 0.3 [48]. Also, since this correlation depends on the packing factor (an empirical parameter depending on the size and shape of the packing), it is important to obtain this parameter from a reliable source [8]. Packed columns are typically designed with an 80% approach to flooding; this limit is also applied in this work.

In order to replace trays with structured packings, practical considerations have to be accounted for [24].

In packed columns the compositions change continuously through the column, unlike in trayed columns, where the compositions change stage-wise [49]. To associate the concept of a theoretical plate with the change in compositions in packed columns, the concept of the height equivalent to a theoretical plate (HETP) is used [49]. The HETP can be estimated using the rule of thumb presented by Green and Perry [49]. Note that this is an empirical correlation that assumes perfect liquid distribution, and the results obtained may be slightly conservative [49]. Also, in this work it is considered that

packings need liquid distributors to ensure an even liquid distribution; otherwise the separation efficiency gets compromised. It is assumed that liquid collectors and distributors account for 0.5 m of column height per bed of packing [3].

The approach is not restricted to the use of these correlations; more accurate ones can be used if available. These hydraulic correlations for trays and packing are also used in Aspen Tech [32] and Koch-Glitsch [44], but in this approach the correlations are coded in MATLAB in order to allow automation of the process.

Section 3.5 explains and discusses the strategy followed to include replacing column internals together with operational optimisation.

3.5 Structural design algorithm: replacing column internals

Figure 4 provides a flowchart of the structural design algorithm used to replace the column internals. The process begins by extracting data from the simulation using the MATLAB—HYSYS interface. Then, a hydraulic analysis of the distillation column is performed using the correlations mentioned in Section 3.4. If any hydraulic parameter is violated, the algorithm for replacing column internals starts.

Firstly, the constrained sections of the distillation column are identified. Secondly, the limiting hydraulic parameters for each section are identified. If the limiting hydraulic parameter is jet flooding, then the algorithm proposes that the internals are replaced with high-capacity trays with sloped downcomers, as these can provide more active area than conventional trays. Replacing conventional trays with high-capacity trays may be cheaper than installing structured packings, since additional supports and liquid distributors are not needed [8]. However, by increasing the tray active area, the downcomer area is reduced [8, 44]. Thus, the CDU hydraulics needs to be re-assessed to ensure that no hydraulic limit is violated. If any constraint is violated, the process is repeated, and a different type of internals is proposed.

If the hydraulic constraint is related to the downcomer, the algorithm proposes that the internals are replaced with structured packings, given that high-capacity trays with sloped downcomers are not a suitable retrofit option when the downcomer is bottleneck of the column.

If all the internals available in the data base have been tested, then a penalty to the objective function is applied. Otherwise, the algorithm estimates the cost of replacing the column internals.

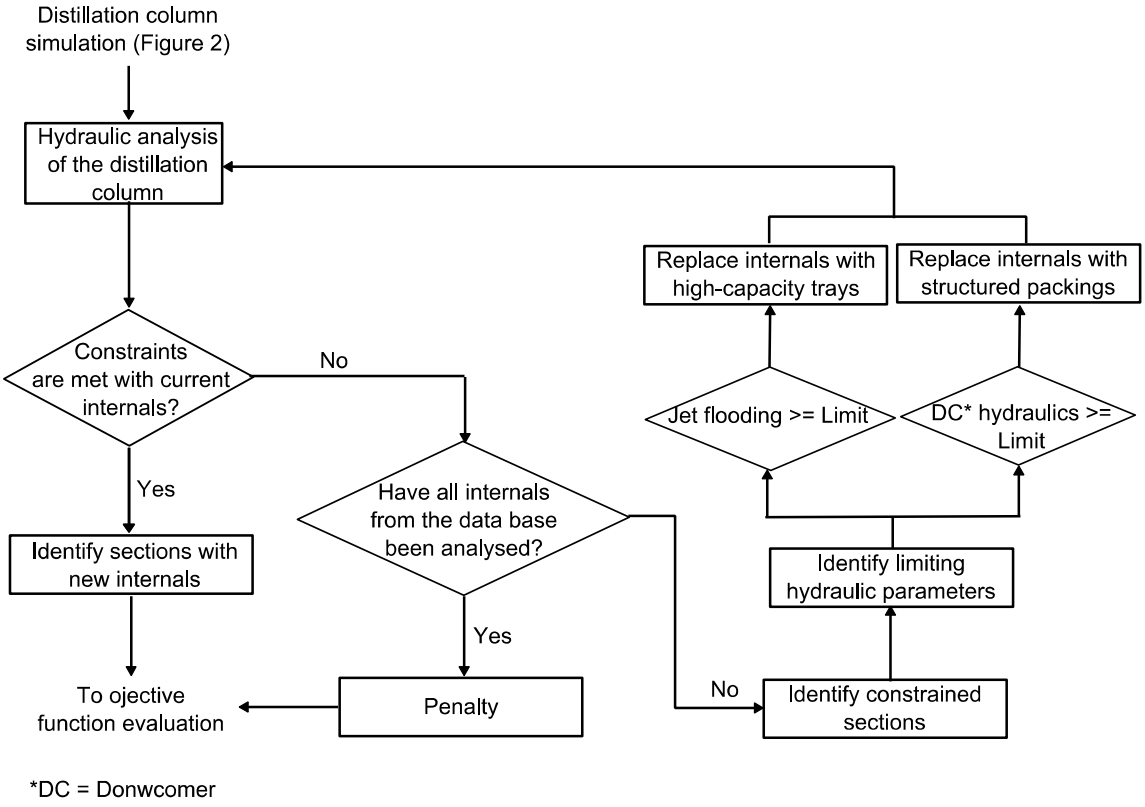

Figure 4 Flowchart of the structural design algorithm used to propose replacing column internals

3.6 HEN retrofit approach

The HEN retrofit approach used in this work with relatively few modifications, is that of Ochoa-Estopier et al. [15], which extends the optimisation-based retrofit methodology presented by Chen and co-authors [21, 50].

The HEN structure is represented using the principles of graph theory [51]: an incidence matrix represents with the 'matches' between streams and between the process and utility heat exchangers. For each element of the matrix, material and energy balances are formulated. This representation facilitates manipulation of the HEN structure by an optimisation algorithm [15].

The heat exchangers are modelled in terms of heat loads, as shown in Eqs. 15 and 16, which represent the energy balances of the cold and hot sides of a heat exchanger *k*, where *T* is the temperature and $\overline{CP}_{k,c}$ is the average heat capacity flow rate of the inlet and outlet streams.

$$\overline{CP}_{k,c}\left(T_{k,c,out} - T_{k,c,in}\right) = q_k \quad (15)$$

$$\overline{CP}_{k,h}\left(T_{k,h,in} - T_{k,h,out}\right) = q_k \quad (16)$$

3.6.1 Estimation of temperature dependent heat capacities

The dependence of the heat capacities on temperature is accounted for by estimating the average heat capacity *CP* for the temperature interval $[T_{in}, T_{out}]$,as shown in Eq. 17. Chen [21] reports, based on the results of a case study in which a crude oil preheat train is simulated with and without assuming constant heat capacities, that assuming constant heat capacities underestimates up to 27℃ the calculated HEN temperatures. These differences in temperatures may lead to different estimation of the HEN performance [21].

$$\overline{\overline{CP}_k} = m_k CP_k \quad (17)$$

As mentioned in Section 3.3, the average heat capacity is estimated using correlations generated prior to starting the optimisation: MATLAB is used to extract the *CP* at different temperature intervals for the crude oil freed and its products from the 'dummy' heat exchangers installed in the simulation flowsheet (see Figure 2) and to regress these data to third order polynomial equations (referred to as 'CP functions' in this work) using the 'polyfit' function in MATLAB, as shown in Eq. 18.

$$CP_k = A + BT + CT^2 + DT^3 \quad (18)$$

3.6.2 HEN simulation and retrofit

The procedure to simulate the HEN is the following [15]: i) the HEN structure is described with an incidence matrix and the material balances are solved; ii) heat capacities for the crude oil and its products are assumed and the energy balances are solved; iii) with the temperatures obtained by solving the energy balances, the heat capacities are re-calculated using the CP functions; iv) the assumed heat capacities are compared against the calculated ones. If the difference is bigger than 10^{-6} kW $°K^{-1}$, the loop is repeated using the heat capacities from the previous iteration. Then, the required heat transfer area is calculated using a design equation used in practice.

In order to reduce the furnace duty, the HEN structure is optimised following the approaches of Rodriguez [52] and Chen [21]. The optimisation approach [15] divides the problem into two levels.

In the first level, SA is used to propose the following retrofit modifications to the HEN:

- adding, deleting, repiping and resequencing heat exchangers
- changing the heat loads of the heat exchangers
- adding/deleting stream splitters
- modifying the splitting ratios

In the second level, the feasibility of the HEN is assessed in terms of the minimum temperature approach, stream enthalpy balances, installed heat transfer area, additional heat transfer area and utility consumption [15].

If any of these constraints is violated, the 'repair algorithm' [15] described in Eq. 19 is used to optimise the heat loads and split fractions in order to regain the feasibility of the network.

$$\min_{Q,sf} \|f(Q,sf)\|_2^2 = \min_{Q,sf}\left[\sum_{i=1}^{N_{HX}} \min\left(TH_i^{out} - TC_i^{in} - \Delta T_{min}, TH_i^{in} - TC_i^{out} - \Delta T_{min}, 0\right)^2 + \sum_{k=1}^{N_{ST}} \left(TT_{cal,k} - TT_k\right)^2\right] \quad (19)$$

where Q and sf are the heat loads and split fractions vectors, respectively; TC and TH refer to the cold and hot temperatures of a heat exchanger I; TT_{cal} and TT_k are the calculated and the target temperatures of stream k; N_{HX} and N_{ST} are the numbers of heat exchangers and streams that form the HEN, and ΔT_{min} is the minimum temperature approach.

3.7 Retrofit methodology — summary

Figure 5 provides a flowchart of the proposed retrofit approach, consisting of:

- An algorithm that enables communication between MATLAB and Aspen HYSYS, transfers data between MATLAB and Aspen HYSYS and connects Aspen HYSYS with an external optimiser.
- Correlations to evaluate the hydraulic performance of the CDU based on simulation results.
- A structural design algorithm that identifies the constrained sections of the CDU and selects suitable internals to replace the current ones.
- An optimisation-based HEN retrofit approach that simulates and retrofits the HEN and that determines the additional heat transfer area required and minimises the fired heating duty.
- Simple capital cost models to evaluate the viability of the proposed modifications in terms of the net profit.

All these methods are coded in MATAB and embedded within a stochastic optimisation algorithm from the MATLAB optimisation toolbox (i.e. simulated annealing or global search).

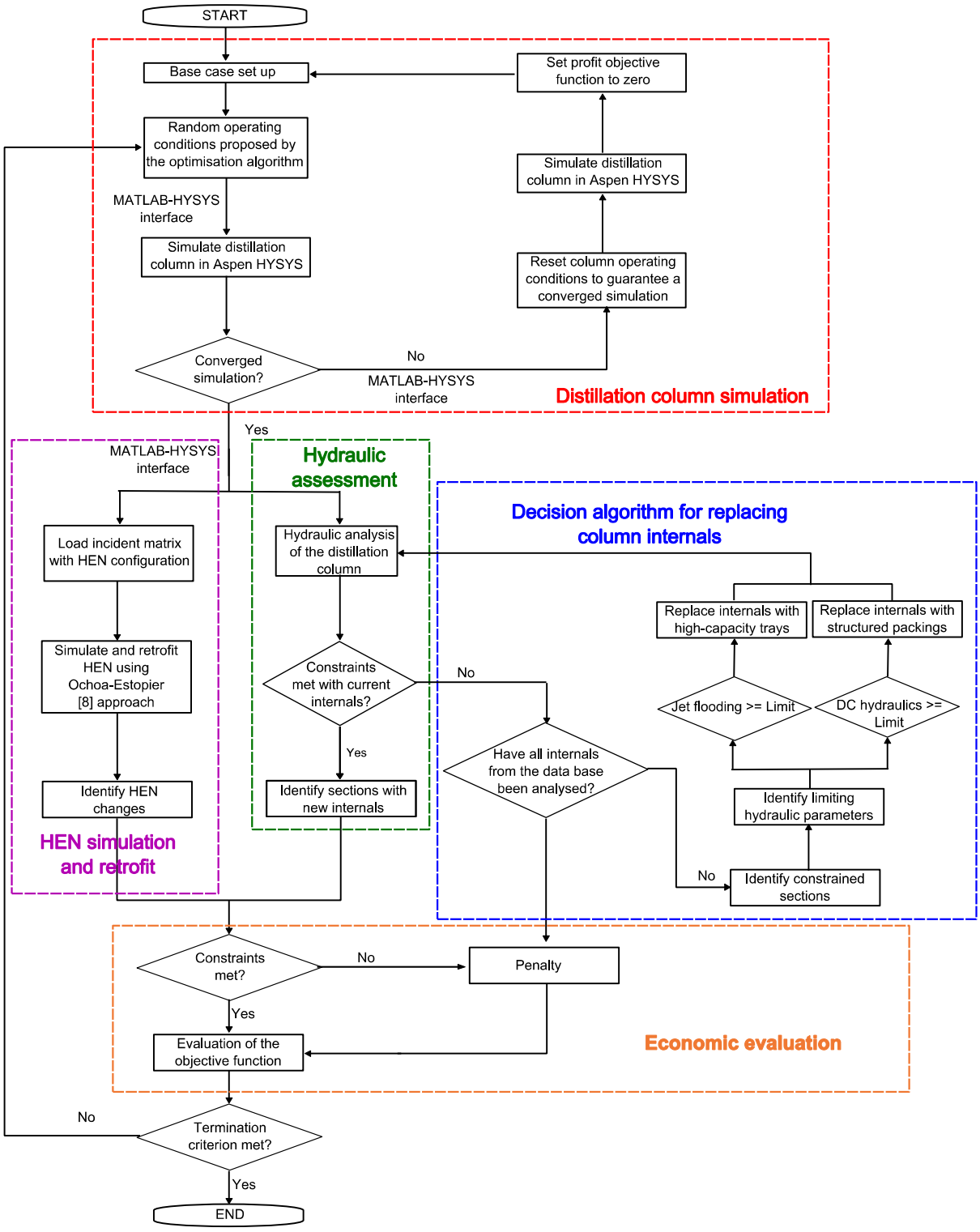

Figure 5 Flowchart of the proposed retrofit approach

4 Case study

This case study aims to demonstrate the effectiveness of the proposed retrofit approach to find the retrofit modifications needed to increase the processing capacity of a heat-integrated distillation system while maximising its net profit.

The crude oil distillation system used in this case study is the optimised design presented by Chen [21]. The system comprises an atmospheric distillation column that processes 100,000 bbl d^{-1} (2562 kmol h^{-1}) of Venezuela Tía Juana light crude oil into five products: light naphtha (LN), heavy naphtha (HN), light distillate (LD), heavy distillate (HD) and residue (RES), and a HEN that preheats the crude oil before it enters the column to 365℃ using the process and products streams and a furnace. Table 1 presents the crude oil essay [53].

Table 1 Crude oil assay [21, 53]

% Distilled (by volume)	TBP (℃)
0	-3.0
5	63.5
10	101.7
30	221.8
50	336.9
70	462.9
90	680.4
95	787.2
100	984

Density: 874.4 kg m^{-3}

Figure 6 illustrates the configuration and stage distribution of the crude oil distillation column. The column comprises a main fractionator with 41 stages that uses steam at 260℃ and 4.5 bar as stripping agent; three pumparounds are installed to recover heat and to enhance reflux. Light naphtha (LN) is produced at the top of the main fractionator and the residue (RES) at the bottom. Heavy naphtha (HN) is recovered in the top side-stripper (Top SS), which has 6 stages and a reboiler. Light Distillate (LD) is produced in the middle side stripper (Mid SS), which has 7 stages and is also reboiled. Heavy distillate (HD) is produced from the bottom side stripper (Btm SS), which has 5 stages and uses live steam at 260℃ and 4.5 bar as stripping agent. Table 2 summarises the distillation column operating conditions and Table 3 lists the product specifications and flow rates.

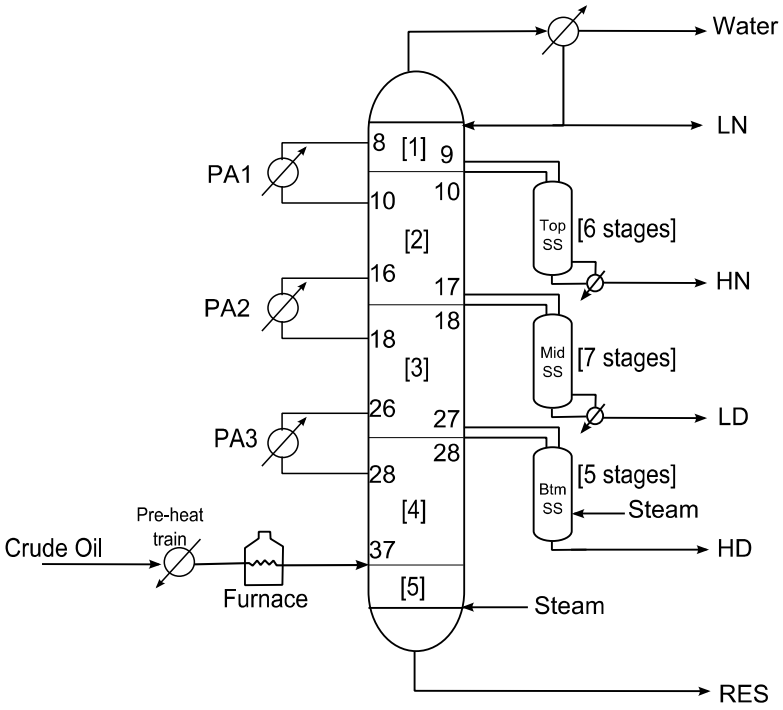

Figure 6 Stage distribution of the crude oil distillation column [8, 21]

Table 2 Crude oil distillation column operating conditions (100% throughput) [21]

Parameter	Value	Units
Feed pre-heat temperature	365	℃
Column operating pressure	2.5	bar
Main fractionator stripping steam flow rate	1200	kmol h^{-1}
Btm SS stripping steam flow rate	250	kmol h^{-1}
PA1 duty	11.2	MW
PA1 ΔT	20	℃
PA2 duty	17.9	MW
PA2 ΔT	50	℃
PA3 duty	12.9	MW
PA3 ΔT	30	℃
Condenser duty	47.87	MW
Top SS reboiler duty	6.63	MW
Mid SS reboiler duty	8.78	MW

Table 3 Product specifications and flow rates [21]

Products	T5 (℃, TBP)	T95 (℃, TBP)	Flow rate (kmol h^{-1})
RES	353	804	315.7
HD	285	364	53.2
LD	190	310	120.5
HN	117	210	85.4
LN	3	122	85.2

The crude oil distillation column section diameters and internals are designed in KG-Tower v5.2 [44]; the design limits used in practice for jet and downcomer flooding for conventional valve trays are also applied in this work (i.e. 80%) [19]. An overdesign factor of 10% is used for the final design, as commonly applied in practice [33]. Table 4 presents the stage numbering, the number of passes per trays and the distillation column diameters; Table 5 lists the characteristics of the column internals; and Table 6 shows the crude oil distillation column hydraulics for the base case. In Table 4 the side strippers are numbered sequentially for convenience.

Table 4 Tray sizing results: column sections and diameters

	Stage number*	Passes per tray*	Section diameter (m^2)
Section 1	1-9	4	7
Section 2	10-17	4	7
Section 3	18-27	4	7
Section 4	28-36	2	7
Section 5	37-41	2	4
Top SS	42-47	2	3
Mid SS	48-54	2	3
Btm SS	55-59	2	2

* Designer choices

Table 5 Tray sizing results: internals characteristics

	Tray active area, %	Tray spacing, m*	Downcomer clearance, m
Section 1	76	0.7	0.07
Section 2	80	0.7	0.07
Section 3	81	0.7	0.07
Section 4	93	0.6	0.07
Section 5	76	0.6	0.07
Top SS	76	0.6	0.07
Mid SS	73	0.6	0.07
Btm SS	74	0.6	0.07

* Designer choices

Table 6 Crude oil distillation column hydraulics (100% throughput)

	Approach to jet flooding (%)	Liquid weir load ($m^3\ m^{-1}\ h^{-1}$)	Downcomer exit velocity ($m\ s^{-1}$)	Approach to downcomer flooding (%)
Section 1	68	88	**0.45**	**67**
Section 2	66	71	0.38	62
Section 3	66	69	0.37	62
Section 4	58	53	0.31	59
Section 5	59	77	0.41	60
Top SS	53	42	0.27	44
Mid SS	63	64	0.35	61
Btm SS	44	29	0.21	42

Figure 7 illustrates the HEN structure based on the optimised case presented by Chen [21]. It consists of 22 heat exchangers with a total heat transfer are of 5453 m^2. The furnace (heat exchanger 14) has a duty of 62.1 MW for a minimum temperature approach of 25 ℃. Table 7 summarises the HEN stream information and Table 8 presents the HEN details.

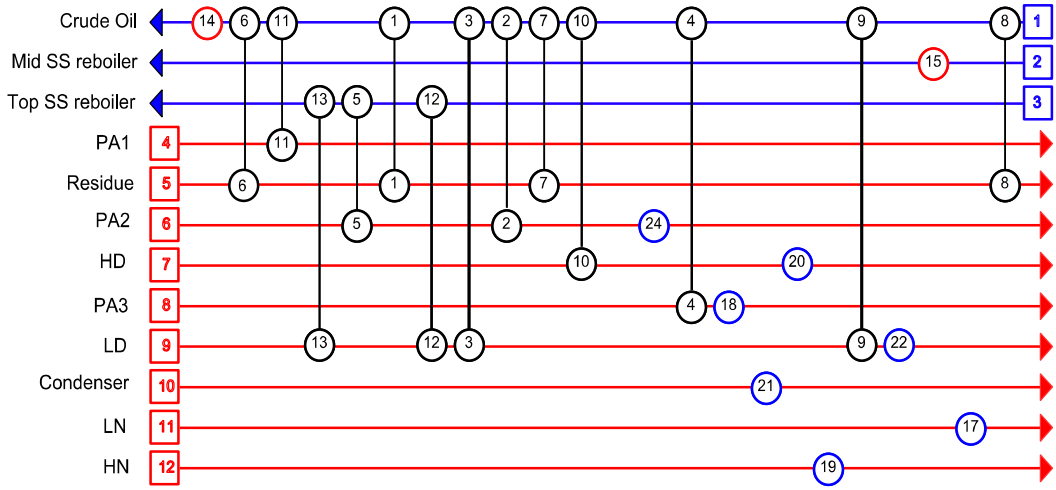

Figure 7 HEN structure [8, 21] (base case)

Table 7 HEN stream information [8, 21] (100% throughput)

Stream	Supply temperature (℃)	Target temperature (℃)	Enthalpy change (MW)
Crude oil	25.0	365.0	143.4
Mid SS reboiler	262.7	284.3	6.1
Top SS reboiler	172.7	193.8	3.9
Pumparound 1 (PA1)	304.5	278.0	12.8
Pumparound 2 (PA2)	223.3	187.1	17.9
Pumparound 3 (PA2)	146.2	141.1	11.2
Condenser	97.2	76.0	46.7
RES	328.0	100.0	49.6
HD	262.1	50.0	5.4
LD	273.9	40.0	17.9
HN	179.3	40.0	6.5
LN	72.8	40.0	1.4
Fired heating (utility)	1500.0	800.0	62.1
Cooling water (utility)	10.0	40.0	77.1

Table 8 HEN details [8, 21] (100% throughput)

Heat exchanger number	Installed area (m^2)	Duty (MW)
h1	975	25.4
h2	332	11.5
h3	112	3.2
h4	196	5.7
h5	58	4.8
h6	105	3.3
h7	684	13.2
h8	312	10.8
h9	260	8.8
h10	46	2.1
h11	555	12.9
h12	22	1.1
h13	67	3.9
h14*	106	59.6
h15*	11	8.8
h17*	59	8.1
h18*	99	7.9
h19*	122	6.5
h20*	61	3.7
h21*	1036	52.9
h22*	179	6.5
h24*	56	10.5

This case study aims to find the retrofit modifications needed for the crude oil distillation system, presented as the base case, to accommodate 30% (i.e. 3331 kmol h^{-1}) more throughput of the same crude oil in order to increase the net profit of the system. Table 9 shows the two retrofit scenarios considered.

Case 1 does not consider operational optimisation; i.e. the operating parameters are simply increased pro rata. If any hydraulic parameter is violated, the column internals are replaced with high-capacity trays with sloped downcomers or structured packings. The type of internals and the constrained sections of the column are identified using the structural design algorithm illustrated in Figure 4. Case 1 uses the HEN retrofit approach presented in Section 3.6 [15] to generate a HEN retrofit solution.

Case 2 simultaneously applies operational optimisation, replaces the column internals in the constrained section and applies the HEN retrofit approach presented in Section 3.

Table 9 Retrofit scenarios considered

Retrofit scenario	Operational optimisation	Replacing column internals	HEN retrofit
Case 1		X	X
Case 2	X	X	X

Case 2 uses two stochastic optimisation algorithms: SA and GS, both from the MATLAB optimisation toolbox. To gain confidence in the results, each algorithm is run three times and the best result is presented.

Table 10 shows the stopping criteria for both optimisation algorithms. For SA, the stopping criteria are the change in the objective function in 1500 iterations (i.e. the minimum value of the objective function does not change in a given number of iterations [37]) and the maximum number of iterations. For GS, the average change in objective function and in optimisation variables value. These values are chosen based on sensitivity analysis.

Table 10 Stopping criteria for the optimisation algorithms

Optimisation algorithm	Stopping criteria	Value
Simulated annealing	Average change in objective function (in 1500 iterations)	$1x10^{-4}$
	Maximum number of iterations	3000
Global search	Average change in objective function	$1x10^{-4}$
	Average change for optimisation variables	$1x10^{-4}$

Table 11 lists the upper and lower bounds of the optimisation variables. These bounds are chosen based on trends observed in previous work [13], which revealed the set of operating parameters that resulted in converged simulations and that meet the product quality specifications.

Table 11 Lower and upper bounds used of the operational variables

Parameter	Lower bound	Upper bound
Main steam flow rate, kmol h^{-1}	1092	1560
Btm SS steam flow rate, kmol h^{-1}	325	423
Furnace outlet temperature, ℃	350	365
PA1 heat flow, MW	12	18
PA2 heat flow, MW	16	23
PA3 heat flow, MW	11	16
PA1 ΔT, ℃	20	40
PA2 ΔT, ℃	40	100
PA3 ΔT, ℃	30	60

Table 12 presents the characteristics of the internals considered in the Cases 1 and 2 to replace the existing ones in the constrained sections: high-capacity trays with 25° sloped downcomers and Mellapak 452Y structured packing. The high-capacity trays have the same tray spacing and downcomer clearances as the current internals (Table 5), therefore Eq. 5 can be used to estimate their retrofit cost. The vendors report that the structured packing is a universal type of packing that can be useful for boosting

capacity and is suitable for a wide range of column liquid loads (from 0.2 to more than 200 $m^3\ m^{-2}\ h^{-1}$) [54].

Table 12 Characteristics of internals used for retrofit [49, 54]

Type of internal	Characteristics	Value
High-capacity tray with sloped downcomers	Active area, %	93
	Downcomer slope, degrees	25
Structured packing (Mellapak 452Y)	Packing surface area, $m^2\ m^{-3}$	350
	Void fraction	0.98
	Packing factor, m^{-1}	69
	Angle of inclination, degrees	45
	HETP, m*	0.3857

* Estimated using the rule of thumb presented by Green and Perry [49]

In both Cases 1 and 2, the system performance is evaluated in terms of the net profit, as described in Section 3.2. The cost components used in Eqs. 1, 2 and 3 are estimated as follows:

- *Revenue*

Following previous work [13], the value of the products is estimated using the procedure presented by Maples [55] for predicting the transfer prices of intermediate products. Firstly, the prices of crude oil and its end products are taken from the US Energy Information Administration [56] for December 2014. Secondly, the cost of each downstream operating unit is estimated based on the costs presented by Gary [1] in 2007 US$, updated to 2014 US$ using the inflation rate of each year [57]. Thirdly, the cost of processing the crude oil distillation products to produce final products is calculated. Table 13 lists the cost of the crude oil and the value of the products per barrel and per kmol.

Table 14 shows the US$ cost of the utilities (i.e. fired heating, cooling water and stripping steam), taken from Gary [1] and updated to 2014 using the inflation rate of each year [57].

The net profit of the base case is around 751,000,000 $ a^{-1}.

Table 13 Crude oil cost, product value and downstream operating costs [13]

Item	End products	End product prices ($ bbl^{-1})	Downstream processes	Downstream operating costs ($bbl^{-1})	Intermediate product prices ($ bbl^{-1})	($ kmol^{-1})
Light naphtha	Gasoline	$74.0			$74.0	$59.2
Heavy naphtha	Gasoline	$62.1	Hydrotreating	$6.0	$61.3	$80.0
	Propane	$9.7	Catalytic reforming	$4.6		
Light distillate	Jet fuel	$70.4	Hydrotreating	$6.0	$66.6	$107.9
	Propane	$2.2				
Heavy distillate	Diesel	$79.8	Hydrotreating	$6.0	$76.0	$193.8
	Propane	$2.2				
Residue	Light gas oil	$60.8	Vacuum distillation	$0.5	$66.5	$283.6
	Heavy gas oil	$4.2	Catalytic cracking	$2.5		
	Residue	$4.8	Hydrotreating	$0.3		
Crude oil feed		$46.0			$46.0	$74.6

Table 14 Cost of utilities [1]

Item	Value
Fired heating (1500-800℃), $/kWy	167
Cooling water (10-40℃), $/kWy	5.84
Stripping steam (260℃,4.5 bar), $/kmol	0.16

- *Annualised retrofit costs*

The values used for the installation and removal factors for Eqs. 5 and 6 are 1.4 and 0.1 and 0.8 and 0.1, respectively [18]. To update the costs of these equations, the CEPCI indexes for 1997 and 2014 (386.5 [58] and 576.1 [59], respectively) are used. To update the HEN capital cost predicted using Eqs. 8 to 11, the CEPCI index of 2005, 468.2 [60], is used. The capital cost is annualised assuming a 2-year project life with 5% interest rate, and an operating time of 8600 h per year.

- *System constraints*

Table 15 lists the system constraints. For conventional trays and high-capacity trays with sloped downcomers four hydraulic parameters are considered: approach to jet flooding, liquid weir load, downcomer exit velocity and approach to jet flooding; and approach to flooding for structured packings. The limits considered are to ones used in practice [43, 45, 46]. The product quality specifications, expressed in terms of true boiling point temperatures, are allowed to vary ±5 with respect to the values presented

in Table 3. Otherwise, a penalty is applied to the objective function. These constraints are applied for both Cases 1 and 2.

Table 15 System constraints

Item	Parameter	Value
Conventional trays and high-capacity trays with sloped downcomers	Approach to jet flooding, %	80
	Liquid weir load, $m^3\ m^{-1}\ h^{-1}$	90
	Downcomer exit velocity, $m\ s^{-1}$	0.46
	Approach to downcomer flooding, %	80
Structured packings	Approach to flooding	80
Product quality specifications: true boiling point temperature	T5, ℃	±5
	T95, ℃	±5

4.1 Case study — Results

This section presents the case study results. Section 4.2 summarises and concludes the case study.

4.1.1 Case 1 — results

Tables 16 and 17 list the results for the operating parameters and products flow rates for Case 1, respectively; in which the operating parameters and product yields are increased by 30% with respect to the base case; except for the pumparound temperature drops, which have the same values as the base case. Retrofit of column internals and HEN is addressed, but column operating conditions are simply change pro rata.

Table S1.1 of this paper's supporting information presents the quality specifications of the products for this case. Note that increasing the flow rates of crude oil, stripping steams, pumparounds and products pro rata does not affects the quality of the products.

Table 16 Operating parameters for Case 1

Parameter	Value
Main steam flow rate, kmol h^{-1}	1560.0
Btm SS steam flow rate, kmol h^{-1}	325.0
Furnace outlet temperature, ℃	365.0
PA1 heat flow, MW	14.7
PA2 heat flow, MW	23.4
PA3 heat flow, MW	16.3
PA1 ΔT, ℃	20.0
PA2 ΔT, ℃	50.0
PA3 ΔT, ℃	30.0

Table 17 Product flow rates for Case 1

Product	Value
Light naphtha (kmol h^{-1})	898.1
Heavy naphtha (kmol h^{-1})	534.2
Light distillate (kmol h^{-1})	495.5
Heavy distillate (kmol h^{-1})	176.6
Residue (kmol h^{-1})	610.9

Table 18 presents the distillation column internals needed to accommodate the increased throughput. The internals in Sections 1 and 5 are replaced with structured packings, while the internals in Section 3 are replaced with high-capacity trays. Table 19 shows that these modifications will incur a retrofit of $236,000.

In Table 6 that presents the base case hydraulic results, it can be observed that Sections 1, 2 and 3 operate close to the jet flooding limit. Thus, by increasing the throughput this limit is very likely to be exceeded. However, Section 1 also operates close the limits for the liquid weir load and downcomer exit velocity. For these reasons, it is proposed that Section 1 internals are replaced with structured packings and Sections 2 and 3 internals are replaced with high-capacity trays with sloped downcomers. Section 5 operates close to the limit for downcomer exit velocity; thus it is proposed that the internals in this section are replaced with structured packings.

Table S1.2 of the supporting information presents the hydraulic results with the new column internals. Note that no hydraulic constraint is violated.

Table 18 Distillation column internals for Case 1

Section	Internals
Section 1	Structured packings
Section 2	High-capacity trays
Section 3	High-capacity trays
Section 4	Existing valve trays
Section 5	Structured packings
Top SS	Existing valve trays
Mid SS	Existing valve trays
Btm SS	Existing valve trays

Table 19 presents the HEN retrofit and economic results for Case 1. To accommodate the increased throughput, the HEN requires 2689 m^2 of additional heat transfer area. By applying HEN retrofit, the furnace inlet temperature can be increased to around 271 ℃; resulting in a fired heat demand of 71 MW (i.e. 13% more compared to the base case).The total HEN retrofit cost is around $646,000.

With all these modifications, the net profit of the system can be increased up to around 968,000,000 $ a^{-1}, 23% more than in the base case.

Table 19 HEN retrofit and economic results for Case 1

Parameter	**30% increase pro rata**
Additional HEN area, m^2	2689
Furnace additional area, m^2	15
Furnace inlet temperature, ℃	271
Furnace outlet temperature, ℃	365
Fired heat demand, MW	71
Revenue, $\$\cdot10^{-3}\ a^{-1}$	1,001,000
Operating costs, $\$\cdot10^{-3}\ a^{-1}$	32,000
Cost to replacing column internals, $\$\cdot10^{-3}$	236
HEN retrofit cost, $\$\cdot10^{-3}$	646
Net profit, $\$\cdot10^{-3}\ a^{-1}$	968,248

Table S1.3 of the Supporting Information presents the required additional heat transfer area for each heat exchanger. In total, 16 heat exchangers require retrofit modifications. The furnace, i.e. heat exchanger 14, requires 15 m^2 of additional heat transfer area.

4.1.2 Case 2 — results

In Case 2, the optimisation algorithm selects column and HEN modifications as well as optimal operating conditions.

Figures 8 and 9 illustrate the optimisation results for Case 2 when using SA and GS, respectively. Similar and consistent results can be observed in both figures, suggesting that the chosen lower and upper bounds are appropriate and that both SA and GS are suitable for this type of analysis.

Similar trends to those found in previous work [13] are also observed. The main column stripping steam flow rate tends to the lower bound, while the Btm SS steam flow rate tends to the upper bound. The temperature drop of the hottest pumparound (PA3) tends to the upper bound. Previous work [13] demonstrated that increasing the temperature drop of the hottest pumparound increases the furnace inlet temperature. It can also be noted that the pumparound temperature drops of PA1 and PA3 stay close to the lower bound.

The values used to generate Figures 8 and 9 are presented in Tables S2.1 and S2.2 of the Supporting Information. Tables S2.3 and S2.4 of the Supporting Information present the product quality results. No constraints are violated during the optimisations, since penalties to the objective function are applied when the permissible ranges are exceeded. Tables S2.5 and S2.6 of the Supporting Information list the hydraulic results after the modifications when using SA and GS, respectively, showing that no constraints are violated. Tables S2.7 and S2.8 of the Supporting Information present the results for the required additional heat transfer area per heat exchanger. A brief discussion of the history of the optimisations is presented in Section S3 of the Supporting Information.

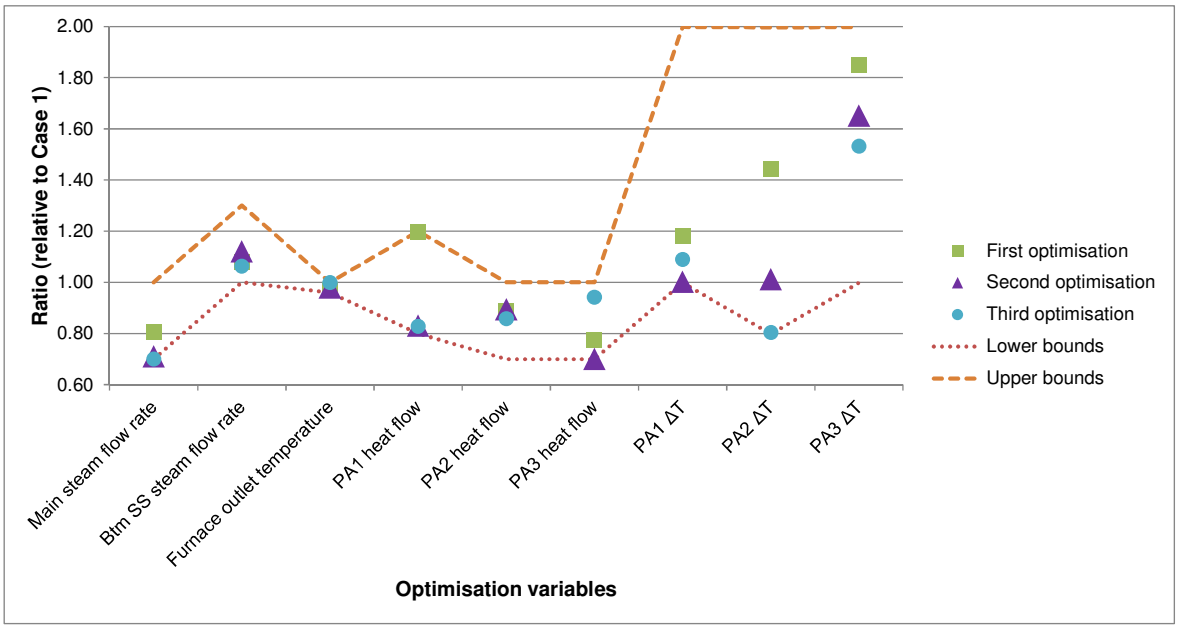

Figure 8 Optimisation results for Case 2 using SA

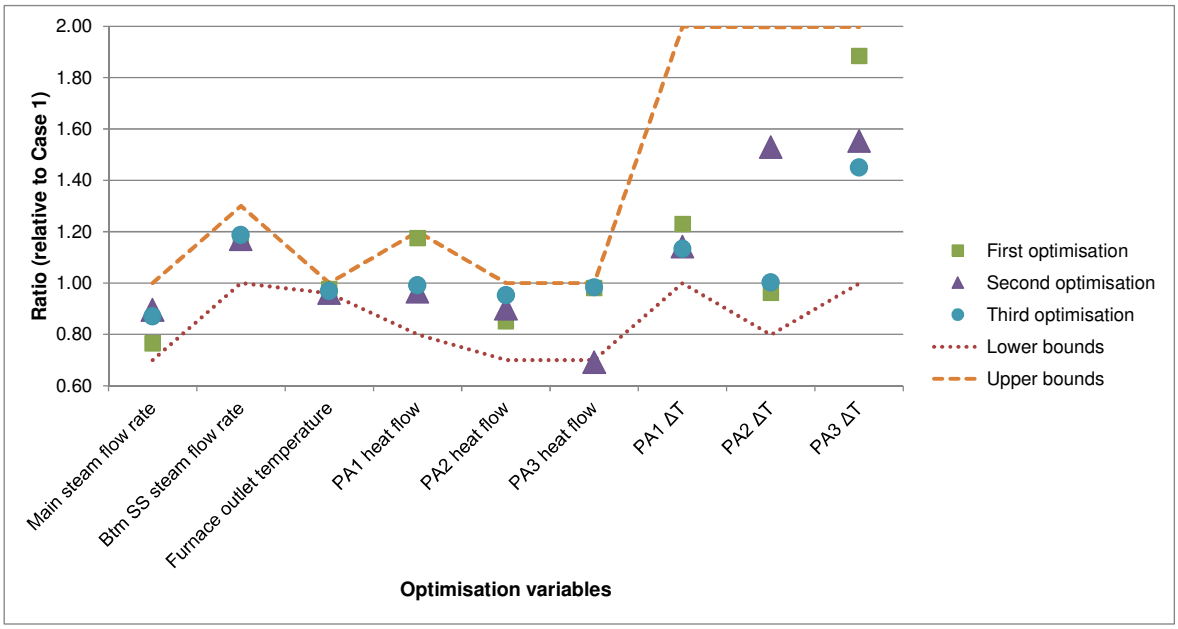

Figure 9 Optimisation results for Case 2 using GS

Tables 20 and 21 list the results for the product flow rates when using SA and GS, respectively, and show the results to be consistent. The majority of the product yields are unaffected; except for the heavy distillate yields, which production is increased between 6% and 16% in all cases. Previous work [13] shown that there is relationship

between the heavy distillate yield and the Btm SS steam flow rate; i.e. increasing the stripping steam flow rate increases the production of the product.

Table 20 Product flow rates for Case 2 using SA

Product	First optimisation		Second optimisation		Third optimisation	
	Value	Diff*	Value	Diff*	Value	Diff*
Light naphtha (kmol h^{-1})	897.3	-0.1%	900.3	0.2%	900.5	0.3%
Heavy naphtha (kmol h^{-1})	534.8	0.1%	534.2	0.0%	534.8	0.1%
Light distillate (kmol h^{-1})	493.4	-0.4%	484.0	-2.3%	488.4	-1.4%
Heavy distillate (kmol h^{-1})	198.4	12.3%	205.5	16.4%	191.6	8.5%
Residue (kmol h^{-1})	599.0	-1.9%	598.8	-2.0%	604.7	-1.0%

* Diff = difference relative to base case values (shown in **Error! Reference source not found.**)

Table 21 Product flow rates for Case 2 using GS

Product	First optimisation		Second optimisation		Third optimisation	
	Value	Diff*	Value	Diff*	Value	Diff*
Light naphtha (kmol h^{-1})	896.2	-0.2%	897.6	-0.1%	893.0	-0.6%
Heavy naphtha (kmol h^{-1})	543.4	1.7%	534.3	0.0%	552.5	3.4%
Light distillate (kmol h^{-1})	490.1	-1.1%	491.0	-0.9%	492.2	-0.7%
Heavy distillate (kmol h^{-1})	194.8	10.3%	199.4	12.9%	187.2	6.0%
Residue (kmol h^{-1})	600.2	-1.7%	599.6	-1.8%	601.4	-1.5%

* Diff = difference relative to base case values (shown in **Error! Reference source not found.**)

In all cases, the algorithm proposes that Section 1 internals are replaced with structured packings. Thus, the algorithm identifies that Section 1 is the hydraulic bottleneck.

Tables 22 and 23 present the HEN retrofit and economic results for Case 2 when using SA and GS, respectively. These results indicate that the net profit of the system can be increased to 973,500,000 \$ a^{-1} by applying the proposed modifications. In Case 2, the best result found is the one of the first optimisation using GS in where the net profit can be increased by up to around \$973,800,000 \$ a^{-1}.

The following can be commented of the best results (GS, first optimisation):

i. The production of heavy naphtha and heavy distillate are increased.
ii. It has one of the highest furnace inlet temperatures and one of the lowest differences between this temperature and the furnace outlet temperature.
iii. It has one of the highest HEN retrofit costs.

From these observations, it can be concluded that the revenue (i.e. the value of products less the cost of crude oil) has the largest contribution to the net profit. Fired heating has the next biggest effect on the net profit. This cost can be reduced by retrofitting the HEN, the cost of which has the third most significant effect on the net profit. Increasing the furnace inlet temperature can reduce the cost of fired heating at the expense of HEN retrofit.

SA optimisations took around 5 to 6 hours to find the best solution and GS took around 11 to 12 hours to find the best solution on a computer with an Intel Core processor of 3.30 GHZ and 8.00 GB of installed RAM memory. It can be observed that the solutions obtained by both optimisation algorithms are quite similar.

Table 22 HEN retrofit and economic results for Case 3 using SA

Parameter	First optimisation	Second optimisation	Third optimisation
Additional HEN area, m^2	2634	2253	3054
No. of HX* needing modifications	17	18	17
Furnace additional area, m^2	11	13	9
Furnace inlet temperature, ℃	261.8	265.5	276.6
Furnace outlet temperature, ℃	353.6	357.7	364.6
Fired heat demand, MW	70.1	70.7	67.9
Revenue, $\$\cdot10^{-3}\ a^{-1}$	1,005,000	1,006,000	1,004,000
Operating costs, $\$\cdot10^{-3}\ a^{-1}$	31,500	31,600	30,100
Cost to replacing column internals, $\$\cdot10^{-3}$	70	70	70
HEN retrofit cost, $\$\cdot10^{-3}$	647	610	730
Net profit, $\$\cdot10^{-3}\ a^{-1}$	973,375	973,550	973,360

*HX = heat exchangers

Table 23 HEN retrofit and economic results for Case 3 using GS

Parameter	First optimisation	Second optimisation	Third optimisation
Additional HEN area, m^2	3364	2339	2768
No. of HX* needing modifications	17	19	16
Furnace additional area, m^2	5	14	3
Furnace inlet temperature, ℃	271	256	269
Furnace outlet temperature, ℃	356.6	350.6	353.5
Fired heat demand, MW	66.0	71.8	65.2
Revenue, $\$\cdot10^{-3}\ a^{-1}$	1,004,000	1,005,000	1,001,000
Operating costs, $\$\cdot10^{-3}\ a^{-1}$	29,800	32,500	29,200
Cost to replacing column internals, $\$\cdot10^{-3}$	70	70	70
HEN retrofit cost, $\$\cdot10^{-3}$	748	622	661
Net profit, $\$\cdot10^{-3}\ a^{-1}$	973,860	972,778	972,929

*HX = heat exchangers

4.2 Case study — summary and conclusions

Table 24 presents a comparison between the results of Case 1 and the best result found in Case 2. By applying the proposed retrofit approach, the net profit of the system can be increased by around 973,860,000 \$ a^{-1}, i.e. around 1% more (5,000,000 \$ a^{-1}) compared to Case 1, and 23% more compared to the base case (i.e. close to 222,000,000 \$ a^{-1}).

Case 2 needs around 20% more additional heat transfer area compared to Case 1. However, Case 2 requires 8% less fired heating and 10 m^2 less of additional furnace area. Note that the furnace inlet temperature is around the same value (i.e. 271°C) in both cases. However, the furnace outlet temperature is lower in Case 2.

In Case 2, the case that applies operational optimisation, reduces by around 70% the cost of replacing the columns internals compared to Case 1. The structural design decision algorithm proposed in this work found in Case 2 that Section 1 of the main fractionator is the hydraulic bottleneck for the system, and that to accommodate 30% more throughput the internals of this section should be replaced with structured packings. It is observed that changing the flow rates affects duties; changing the operating conditions changes flows, duties and temperatures. Changing both, affects the hydraulic performance of the column.

Note that pro rata increase of operating conditions with feed flow rates can create several bottlenecks and does not recognise constraints/ impact on heat recovery system. On the other hand, optimising operating conditions together with internals and HEN retrofit means that interactions are accounted for and synergies can be exploited.

Note that the net profit of the system and the retrofitted designs are extremely high. This is because the transfer prices were estimated at a time where there was volatility in the oil market. However, this does not affect the results or compromises the effectiveness of the proposed approach. The results can be easily updated and reproduced if new values for the transfer prices are used.

Table 24 Comparison between Cases 1 and 2 results

Parameter	Case 1	Case 2
Additional HEN area, m^2	2689	3364
Furnace additional area, m^2	15	5
Furnace inlet temperature, °C	271	271
Furnace outlet temperature, °C	365	356.6
Fired heating demand, MW	71	66.0
Revenue, $\$\cdot10^{-3}\ a^{-1}$	1,001,000	1,004,000
Operating costs, $\$\cdot10^{-3}\ a^{-1}$	32,000	29,800
Cost replacing column internals, $\$\cdot10^{-3}$	236	70
HEN retrofit cost, $\$\cdot10^{-3}$	646	748
Net profit, $\$\cdot10^{-3}\ y^{-1}$	968,248	973,860

5 Summary and conclusions

This work proposes an optimisation-based retrofit approach for the capacity expansion of heat-integrated distillation systems. Even though retrofitting these types of systems in commonly performed in practice, to date, retrofit approaches that include all the degrees of freedom and constraints simultaneously are lacking.

The retrofit approach proposed is based on previous work [13], simulates the crude oil distillation column using rigorous simulation, reads and writes data to and from Aspen HYSYS with MATLAB using a customised interface, assesses the hydraulic performance of the distillation columns using suitable correlations and retrofits the HEN using an optimisation-based approach [15]. All these methods are embedded within a stochastic optimisation environment, which seeks the maximum net profit that the systems can achieve.

This work extends the previous approach [13] by including a structural design decision algorithm that identifies the constrained sections of the distillation column and the best type of internals to overcome bottlenecks. The case study presented shows that including these decisions within the optimisation environment benefit the heat recovery of the system.

This extended approach compares the use of two optimisation algorithms (i.e. simulated annealing and global search). This procedure helps to provide confidence in the results and to highlight trends.

The case study results reveal that when increasing the processing capacity of heat-integrated crude oil distillation systems, three parameters affect the net profit: the revenue desired from the most valuable products, the cost of fired heating and the HEN

retrofit cost. The case study results show that considering operational optimisation together with structural modifications helps to exploit the synergies of the system, reducing the operating and retrofit costs and thus increasing the net profit of the system.

The second part of this two-part series papers [61] extends this approach by including the structural design option of adding a preflash unit.

Associated content

Supporting Information:

- HEN required additional heat transfer area for Cases 1 and 2
- Product quality results for Cases 1 and 2
- Hydraulic results for Cases 1 and 2
- Operational optimisation results for Case 2
- Overview of the optimisations for Case 2

Corresponding Author

Víctor Manuel Enríquez-Gutiérrez
E-mail1: victormanuel.enriquezgutierrez@manchester.ac.uk
E-mail2: iq.vic.enriquez@gmail.com

Acknowledgment

The authors gratefully acknowledge the Mexican Council of Science and Technology (CONACyT) and the Roberto Rocca Education Program (RREP) for their financial support of PhD studies at the University of Manchester.

Abbreviations

CDU	Crude oil distillation unit
GS	Global search
HEN	Heat exchanger network
MINLP	Mixed-integer non-linear programming
SA	Simulated annealing

References

1. Gary, J.H., *Petroleum Refining: Technology and Economics*. 5th ed. Taylor & Francis: Boca Raton, USA, 2007.
2. Errico, M., Tola, G., and Mascia, M., Energy saving in a crude distillation unit by a preflash implementation. *Applied Thermal Engineering*, **2009**. *29*(8-9): p. 1642-1647.
3. Smith, R., *Chemical Process Design and Integration*. John Wiley & Sons, Ltd.: Chichester, UK, 2005.
4. Uerdingen, E., Fischer, U., Hungerbühler, K., and Gani, R., Screening for profitable retrofit options of chemical processes: A new method. *AIChE Journal*, **2003**. *49*(9): p. 2400-2418.
5. Rapoport, H., Lavie, R., and Kehat, E., Retrofit design of new units into an existing plant: Case study: Adding new units to an aromatics plant. *Computers and Chemical Engineering*, **1994**. *18*(8): p. 743-753.
6. Grossmann, I.E., Biegler, L.T., and Westerberg, A.W., *Retrofit design of processes*. Foundations of computer aided process operations (FOCAPO). Elsevier: Amsterdan, 1987.
7. Gadalla, M., Jobson, M., and Smith, R., Optimization of existing heat-integrated refinery distillation systems. *Chemical Engineering Research and Design*, **2003**. *81*(1): p. 147-152.
8. Enríquez-Gutiérrez, V.M., Jobson, M., Ochoa-Estopier, L.M., and Smith, R., Retrofit of heat-integrated crude oil distillation columns. *Chemical Engineering Research and Design*, **2015**. *99*: p. 185-198.DOI: 10.1016/j.cherd.2015.02.008.
9. Ochoa-Estopier, L.M., Jobson, M., and Smith, R., Optimisation of heat-integrated crude oil distillation systems. Part III: Optimisation framework. *Industrial & Engineering Chemistry Research*, **2015**. *54*(18): p. 5018-5036.DOI: 10.1021/ie503805s.
10. Thernesz, A., Varga, Z., Rabi, I., Czaltig, Z., and Lörincova, M., Applying process design software for capacity increase and revamp of distillation units. *Clean Technologies and Environmental Policy*, **2010**. *12*(2): p. 97-103.
11. Gadalla, M., Kamel, D., Ashour, F., and din, H.N.E., A new optimisation based retrofit approach for revamping an Egyptian crude oil distillation unit. *Energy Procedia*, **2013**. *36*(0): p. 454-464.DOI: 10.1016/j.egypro.2013.07.051.
12. Liu, Z.Y. and Jobson, M., Retrofit design for increasing the processing capacity of distillation columns: 1. A Hydraulic performance indicator. *Chemical Engineering Research and Design*, **2004**. *82*(1): p. 3-9.
13. Enríquez-Gutiérrez, V.M. and Jobson, M., An optimisation-based retrofit approach for increasing the processing capacity of heat-integrated crude oil distillation systems. *Chemical Engineering Research & Design*, **2016**. *submitted May 2016*.
14. Caballero, J.A., Milán-Yañez, D., and Grossmann, I.E., Optimal synthesis of distillation columns: Integration of process simulators in a disjunctive programming environment. *Computer Aided Chemical Engineering*, **2005**. *20*: p. 715-720.DOI: 10.1016/S1570-7946(05)80241-X.
15. Ochoa-Estopier, L.M., Jobson, M., Chen, L., Rodríguez, C., and Smith, R., Optimisation of heat-integrated crude oil distillation systems. Part II: Heat exchanger network retrofit model. *Industrial & Engineering Chemistry Research*, **2015**. *54*(18): p. 5001-5017.DOI: 10.1021/ie503804u.
16. Stichlmair, J., *Distillation: Principles and Practice*, ed. J.R. Fair. Wiley-VCH: New York, USA, 1998.
17. Kister, H.Z., *Distillation Design* McGraw-Hill: Boston, USA, 1992.

18. Branan, C.R., *Rules of Thumb for Chemical Engineers*. 4th ed. Elsevier Science: Burlington, 2011.
19. Koch-Glitsch. *Glitsch Ballast Tray Design Manual: Bulletin No. 4900*. 2013 [access date October 2014]; 6th Edition:[Available from: http://www.koch-glitsch.com/Document%20Library/Bulletin-4900.pdf.
20. Majumder, K., Mosca, G., and Mahon, K., High-capacity tray for debottlenecking a crude distillation unit. *Petroleum Technology Quarterly*, **2013**. *18*(1): p. 73-77.
21. Chen, L., *Heat-integrated Crude Oil Distillation System Design*, PhD Thesis, The University of Manchester, Manchester, UK, 2008.
22. López C., D.C., Hoyos, L.J., Mahecha, C.A., Arellano-Garcia, H., and Wozny, G., Optimization model of crude oil distillation units for optimal crude oil blending and operating conditions. *Industrial & Engineering Chemistry Research*, **2013**. *52*(36): p. 12993-13005.DOI: 10.1021/ie4000344.
23. Gadalla, M.A., Abdelaziz, O.Y., Kamel, D.A., and Ashour, F.H., A rigorous simulation-based procedure for retrofitting an existing Egyptian refinery distillation unit. *Energy*, **2015**. *83*(0): p. 756-765.DOI: 10.1016/j.energy.2015.02.085.
24. Gadalla, M.A., *Retrofit Design of Heat-integrated Crude Oil Distillation Systems*, PhD Thesis, The University of Manchester, Manchester, UK, 2003.
25. Carlberg, N.A. and Westerberg, A.W., Temperature-heat diagram for complex columns 2. Underwoord's method for side strippers and enrichers. *Ind. Eng. Chem. Res.*, **1989**. *28*: p. 1379.
26. Gadalla, M., Jobson, M., and Smith, R., Shortcut models for retrofit design of distillation columns. *Chemical Engineering Research and Design*, **2003**. *81*(8): p. 971-986.
27. Suphanit, B., *Design of Complex Distillation Systems*, PhD Thesis, UMIST Department of Process Integration, Manchester, UK, 1999.
28. Asante, N.D.K. and Zhu, X.X., An automated and interactive approach for heat exchanger network retrofit. *Chemical Engineering Research and Design*, **1997**. *75*(3): p. 349-360.DOI: 10.1205/026387697523660.
29. Fair, J.R., How to predict sieve tray entrainment and flooding. *Petro. Chem. Eng.*, **1961**. *33*: p. 45.
30. Kister, H.Z. and Gill, D.R., Flooding and pressure drop prediction for structured packings. *IChemE Symp. Ser*, **1992**. *128*: p. A109-A123.
31. Peters, M.S., Timmerhaus, K.D., and West, R.E., *Plant design and economics for chemical engineers*. 5th ed. ed. McGraw-Hill: Boston, 2004.
32. Aspen Tech, *Aspen HYSYS*. 2012, Version 7.3, Aspen Tech Inc: USA
33. Towler, G. and Sinnott, R.K., *Chemical Engineering Design Principles, Practice and Economics of Plant and Process Design*. 2nd. ed. Butterworth-Heinemann: Boston, 2013.
34. Costa, L. and Oliveira, P., Evolutionary algorithms approach to the solution of mixed integer non-linear programming problems. *Computers & Chemical Engineering*, **2001**. *25*(2–3): p. 257-266.DOI: 10.1016/S0098-1354(00)00653-0.
35. Kirkpatrick, S., Gelatt, C.D., and Vecchi, M.P., Optimization by simulated annealing. *Science*, **1983**. *220*(4598): p. 671-680.
36. Cavazzuti, M., *Optimization Methods From Theory to Design Scientific and Technological Aspects in Mechanics* Heidelberg: Berlin, 2013.
37. MATHWORKS. *Simulated annealing options*. 2015 [access date October 2015]; Available from: http://uk.mathworks.com/help/gads/examples/simulated-annealing-options.html#zmw57dd0e3957.
38. Ugray, Z., Lasdon, L., Plummer, J., Glover, F., Kelly, J., and Martí, R., Scatter search and local NLP solvers: a multistart framework for global optimization. *INFORMS Journal on Computing*, **2007**. *19*(3): p. 328-340.DOI: 10.1287/ijoc.1060.0175.

39. MATHWORKS. *Basins of attraction*. 2015 [access date October 2015]; Available from: http://uk.mathworks.com/help/gads/what-is-global-optimization.html#bsbalkx-1.
40. MATHWORKS. *How globalsearch and multistart work*. 2015 [access date October 2015]; Available from: http://uk.mathworks.com/help/gads/how-globalsearch-and-multistart-work.html.
41. Bravo, J.L., Select structured packings or trays? *Chemical Engineering Progress*, **1997**. *93*(7): p. 36-41.
42. Sinnott, R.K. and Towler, G.P., *Chemical Engineering Design*. 5th ed. Butterworth-Heinemann: Oxford, 2009.
43. Resetarits, M.R., *Chapter 2 - Distillation Trays*, in *Olujić, A.G.*; Distillation: Equipment and Processes, Editor., Academic Press: Boston, USA, 2014.
44. Koch-Glitsch, *KG-Tower*. 2014, version 5.2, Koch-Glitsch LP: USA
45. Koch-Glitsch. *Introduction to KG-Tower: Tray& Packed Tower Sizing Software Program, Version 2.0*. 2006 [access date October 2014]; Available from: www.koch-glitsch.com.
46. Resetarits, M.R., Propelling distillation research. *Chemical Engineering*, **2010**. *117*(6): p. 26-27.
47. Enríquez-Gutiérrez, V.M., Jobson, M., and Smith, R., A design methodology for retrofit of crude oil distillation systems. *Proceedings of the 24th European Symposium on Computer Aided Process Engineering-ESCAPE24*, **2014**. *Part A*: p. 1549-1554.DOI: 10.1016/B978-0-444-63455-9.50093-3.
48. Kister, H.Z., Scherffius, J., Afshar, K., and Abkar, E., Realistically predict capacity and pressure drop for packed columns. *Chemical Engineering Progress*, **2007**. *103*(7): p. 28-38.
49. Green, D.W. and Perry, R.H., *Perry's Chemical Engineers' Handbook*. McGraw-Hill Professional: New York, USA, 2007.
50. Smith, R., Jobson, M., and Chen, L., Recent development in the retrofit of heat exchanger networks. *Applied Thermal Engineering*, **2010**. *30*(16): p. 2281-2289.
51. de Oliveira Filho, L.O., Queiroz, E.M., and Costa, A.L.H., A matrix approach for steady-state simulation of heat exchanger networks. *Applied Thermal Engineering*, **2007**. *27*(14-15): p. 2385-2393.
52. Rodriguez, C.A., *Fouling Mitigation Strategies for Heat Exchanger Networks*, PhD Thesis, The University of Manchester, Manchester, UK, 2005.
53. Watkins, R.N., *Petroleum Refinery Distillation*. Gulf Pub. Co., Book Division: Houston, USA, 1979.
54. Sulzer. *Structured packings for distillation, absorption and reactive distillation*. 2015 [access November, 2015]; Available from: https://www.sulzer.com/es/-/media/Documents/ProductsAndServices/Separation_Technology/Distillation_Absorption/Brochures/Structured_Packings.pdf.
55. Maples, R.E., *Petroleum Refinery Process Economics*. 2nd ed. PennWell Corp.: Tulsa, Okla., 2000.
56. US Energy Information Administration. *Petroleum Marketing Monthly*. 2015 [access date July 2015]; Available from: http://www.eia.gov/petroleum/marketing/monthly/pdf/pmmall.pdf.
57. US inflation calculator. *Current US inflation rates: 2005-2015*. 2015 [access date April, 2015; Available from: http://www.usinflationcalculator.com/inflation/current-inflation-rates/.
58. Vatavuk, W.M., Updating the *CE* plant cost index. *Chemical Engineering*, **2002**. *109*(1): p. 62-70.
59. Ondrey, G., Economic Indicators. *Chemical Engineering*, **2015**. *122*(5): p. 104.
60. Bailey, M.P., Economic Indicators. *Chemical Engineering*, **2013**. *120*(12): p. 71-72.
61. Enríquez-Gutiérrez, V.M. and Jobson, M., An optimisation-based retrofit approach for the assessment of structural and flowsheet modifications for heat-

integrated crude oil distillation systems. Part 2.- Adding a preflash unit. *Chemical Engineering Research & Design*, **2016**. *submitted May 2016*.

5.3 Publication 4

Enríquez-Gutiérrez, V. M., Jobson, M., 2016, An optimisation-based retrofit approach for the assessment of structural and flowsheet modifications for heat-integrated crude oil distillation systems. Part 2.- Adding a preflash unit, Industrial & Engineering Chemistry Research, under preparation.

An optimisation-based retrofit approach for the assessment structural and flowsheet modifications for heat-integrated crude oil distillation systems. Part 2. Adding a preflash unit

Víctor M. Enríquez-Gutiérrez and Megan Jobson

Centre for Process Integration, School of Chemical Engineering and Analytical Science, The University of Manchester, Sackville Street, Manchester M13 9PL, United Kingdom

Keywords

Operational optimisation, HEN retrofit, stochastic optimisation

Highlights

- Rigorous simulation is used to simulate the distillation column and preflash unit
- Structural design decisions are included within an optimisation environment
- The impact of adding a preflash unit on column hydraulics and HEN retrofit is considered.
- Optimal HEN retrofit is addressed.

Abstract

This is the second of two papers that present a retrofit approach for increasing the processing capacity of heat integrated crude oil distillation systems, in which structural design decisions (i.e. replacing column internals and adding a preflash unit) are included within an optimisation environment. The approach is based on previous work on retrofit, where rigorous simulation is used to model the distillation column and to check product quality specifications, correlations are used to assess the hydraulic performance of the distillation column internals, an optimisation-based retrofit approach is used to simulate and retrofit the heat exchanger network (HEN) and stochastic optimisation is used to find the best set of operating parameters that maximise the profitability of the system.

This paper extends the work presented in Part 1 of the series by considering the installation of a preflash unit along with replacing column internals and HEN retrofit. In

practice, adding a preflash unit is considered when it is desired to increase the column capacity, debottlenecking the distillation columns and reduce the furnace duty.

An industrially relevant case study is presented to demonstrate the advantages of the proposed retrofit approach to explore and assess beneficial operational, structural and flowsheet modifications when increasing the processing capacity of heat-integrated crude oil distillation systems.

1. Introduction

Heat-integrated crude oil distillation systems comprise a crude oil distillation unit (CDU) in which the crude oil is fractionated and a heat exchanger network (HEN) that preheats the crude oil using product and process streams and a furnace.

Heat-integrated crude oil distillation systems are energy intensive. It is estimated that the equivalent to 1-2% of the crude oil processed [1] is used in the furnace to preheat the crude oil to around 370°C before it enters the distillation column.

Retrofit aims to exploit the interactions between the CDU and the HEN in order to increase the profitability of the system. Examples of retrofit projects to increase profitability are increasing throughput [2], reducing fired heating demand [1], increasing revenue from the most valuable products [3], and reducing CO_2 emissions [4].

Retrofit methodologies found in the open research literature consider installing a preflash unit to increase the distillation column capacity [5], to debottleneck the distillation column hydraulics [5] and to reduce the furnace duty [1, 5]. Structural design decisions associated with installing a preflash unit (i.e. the preflash location in the preheat train and/or the flashed vapour feed stage) are taken systematically [5] or based on experience [1]. Retrofit methodologies that include structural design decisions within an optimisation environment in order to exploit the interactions between the CDU and the HEN are lacking. Therefore, beneficial energy integration opportunities may be neglected and associated HEN retrofit costs may be unnecessarily high.

This retrofit approach and the one proposed in Part 1 [6] extend previous work [2, 7], which systematically assesses operational modifications (i.e. changing CDU operating conditions) and structural changes (i.e. replacing column internals, modifying the HEN structure) with relatively little engineering effort. However, analysing multiple retrofit scenarios (e.g. finding the best alternative for replacing the column internals or

installing a preflash unit) can be time consuming since each option needs to be analysed separately. Part I of this series [6] presents the approach followed for replacing column internals. This paper presents an approach to evaluate the options of adding a preflash unit.

The approach proposed in this two-part series overcomes this limitation by including structural design decisions within an optimisation environment, similarly to the design approach presented by Caballero et al. [8].

An industrially relevant case study shows the advantages of using the proposed retrofit approach to assess beneficial retrofit modifications that can increase the throughput and hence profitability of an existing heat-integrated crude oil distillation system.

2. Literature review

The literature review of existing retrofit approaches for crude oil distillation systems that have considered replacing column internals [6] is supplemented by a review of research literature on the retrofit approaches that have considered installing a preflash unit.

2.1. Retrofit approaches for crude oil distillation systems

Gadalla [5] proposes a retrofit approach for heat-integrated crude oil distillation systems that systematically optimises the CDU operating conditions and retrofits the HEN. This approach [5] includes a methodology to consider installing preflash in order to reduce the energy consumption, and to increase the crude oil throughput. Firstly, the CDU is decomposed into a thermodynamically equivalent sequence of columns [9] and is simulated using shortcut models [10, 11]. Secondly, a preflash unit is modelled at a given preflash temperature. Thirdly, the HEN retrofit options are represented using an Area-Energy curve constructed from network pinch analysis [12] to determine the required heat transfer area and the utility consumption. Fourthly, the operating variables of the distillation column (i.e. furnace outlet temperature, pumparound duties and temperature drops and steam flow rates) and the preflash temperature are optimised using a sequential quadratic programming algorithm. Only two locations are considered to feed the flashed vapour: i) mixed with the feed or, ii) mixed with the vapour of one of the side strippers. The best stage to feed the flashed vapour is

determined by repeating the methodology for every possible configuration, potentially incurring significant engineering time.

However, the shortcut models applied [11, 13] do not provide the stage-wise information needed to perform a hydraulic analysis of the CDU and they are difficult to initialise and converge.

Errico et al. [1] present a case study in which the installation of a preflash unit is considered in order to reduce the furnace duty. Rigorous simulation is used to simulate both the preflash unit and the CDU. Due to plant lay-out constraints, only one location is considered to install the preflash drum: after the pre-heat train at the furnace inlet temperature. The flashed vapour is fed together with the liquid feed in order to avoid the formation of black distillates below the feed due to quenching [1]. To compensate for the quench effect, the coil outlet temperature is increased by 5°C and the stripping steam is increased to the flooding limit to compensate for the lower carrier effect of the lighter components [1]. Product quality specifications are expressed in terms of ASTM D86 curves. Results from the case study presented showed that installing a preflash drum decreases the naphtha production, increases the production of kerosene and reduces the furnace duty by around 20%. Rigorous simulation was shown to provide an accurate representation of the system (if properly set up). In this work [1], heat integration opportunities are not explored.

Wang et al. [14] present a methodology to find the best predistillation scheme (i.e. adding a preflash unit or prefractionation column before the atmospheric distillation unit furnace) to process a heavy crude oil. The predistillation devices, the CDU and the furnace are simulated using rigorous simulation. Only two locations are considered to feed the flashed vapour: at the top of column and at the bottom of the column. To estimate the exergy losses and exergy efficiencies, conservation equations of mass, energy and entropy generation are used. The methodology [14] can be summarised as follows. Firstly, the CDU is simulated and the results are used to estimate the exergy losses, the exergy efficiencies and the fired heating duty. Secondly, a preflash unit or a prefractionation column is included in the simulation flowsheet and the CDU is re-simulated; the same performance indicators are estimated. In total, eight scenarios are analysed. The best option is taken to be the one that increases the exergy efficiency of the system, reduces the exergy losses and reduces the fired heating demand, compared to the base case. The CDU operating parameters are kept constant; i.e. there is not attempt to optimise the operating conditions. As a result interactions between columns and EN are not exploited or explored. Furthermore, the approach

does not account for the hydraulic performance of the column, so unfeasible column designs may be obtained. A further weakness of this work [14] is that significant engineering effort is required, as each scenario has be analysed separately.

Gadalla et al. [15] present a systematic simulation-based retrofit approach for crude oil distillation columns, where both the CDU and its associated pre-heat train are simulated in Aspen HYSYS. Results from the simulation (i.e. stream temperature, flows and duties for the preheat train heat exchangers) are extracted and used to generate composite curves in order to estimate the energy targets. Based on this analysis, the process conditions (i.e. furnace outlet temperature, reflux flow rate, pumparound duties and temperature drops, side-strippers flow rates) are optimised to meet the energy targets. Then structural modifications to the distillation column (i.e. new pumparounds, adding a preflash unit) and HEN (i.e. adding area, repiping and resequencing existing heat exchangers, adding new heat exchangers) are systematically proposed in order to reduce the energy demand. To avoid unfeasible column designs, the hydraulic performance of the distillation column is assessed in terms of by the diameter required to avoid jet flooding using Fair's correlation [16].

Gadalla et al. [15] presents a case study in which the installation of a preflash unit is considered before the furnace. The flashed vapour is fed at the column stage with the closest temperature to the preflash temperature. Installing a preflash unit is shown to reduce the fired heating duty by 32% and to enhance the capacity of the distillation column by 13%.

This approach [15] is able to assess the impacts of the retrofit modifications in both the CDU and the HEN. However, it requires significant engineering effort to analyse multiple retrofit scenarios since each modification has to be simulated and optimised individually. By including the hydraulic analysis of the distillation column, unfeasible designs are avoided. However, the correlation of Fair [16] only accounts for jet flooding thus the downcomer hydraulics is neglected. In previous work [17] this is shown to be an unrealistic approach for crude oil distillation units, since their hydraulic performance is also dictated by the hydraulics of the downcomer.

Retrofit approaches that do not consider installing a preflash unit are also available in the open research literature. Chen [13] presents a optimisation-based retrofit approach for heat-integrated distillation systems. In this approach, the crude oil distillation column is modelled using shortcut models extended from those of Suphanit [10], Gadalla [5] and Rastogi [18], structural modifications to the HEN (i.e. adding, deleting, repiping and resequencing heat exchangers) are proposed using an optimisation based retrofit

approach [13, 19] based on the network pinch concept [12], and the distillation column operating parameters are optimised using simulated annealing (SA). The drawback of this approach is that the shortcut models used are difficult to set up and converge.

López C. et al. [20] present an approach to optimise the operating conditions of crude oil distillation systems. In this approach, the distillation columns and the furnaces are modelled using second order polynomial functions (also known as metamodels) regressed from rigorous simulations. The metamodels are coded in GAMS, where CONOPT (a NLP solver) is used to solve the optimisation problem. The advantage of using this approach is that the optimisation of the system is computationally inexpensive. The drawback of this approach are that it does not address HEN retrofit, thus energy integration opportunities might be neglected, and that metamodels required significant engineering effort to set up.

Ochoa-Estopier et al. [3] extends the approach of Chen [13] by using metamodels, regressed from results of rigorous simulations using artificial neural networks [21], to model the distillation columns and by extending the HEN retrofit approach of Chen and co-workers [13, 19] by modelling the structure using the principles of graph theory [22], which facilitates the manipulation of the HEN structure [23]. SA in also used to optimise the distillation column operating parameters. The drawback of this approach is that building the metamodels requires significant engineering effort and time. However, it presents a useful guidance on how to simultaneously address operational optimisation and HEN retrofit.

Chen et al. [24] propose an approach for simultaneously address process optimisation and heat integration. In this approach, rigorous simulation software (e.g. Aspen Plus, Aspen HYSYS, gPROMS) is linked with a derivative free optimiser (i.e. the covariance matrix adaptation evolutionary strategy [25]) and a heat integration module [26, 27], coded in GAMS, to transfer data between each other. The drawback of this approach is that it does not consider HEN retrofit, thus beneficial heat integration opportunities might be missed.

2.2. Literature review – summary and conclusions

In summary, none of the published retrofit approaches for crude oil distillation systems that have consider installing a preflash unit include the associated structural design decisions within an optimisation environment. Thus, significant engineering effort is

needed to find the best configuration and they rely on trial-and-error to find the 'best' configuration.

To simulate the CDU and the preflash, two approaches are followed: applying shortcut models [11] and using rigorous simulation [1, 14, 15]. The first have been used in optimisation approaches that consider HEN retrofit. However, shortcut models [11] do not provide the stage-by-stage information needed to perform a hydraulic analysis of the CDU and they are difficult to initialise and converge. Rigorous simulation is widely used in practice and can provide a good representation of the system; but in some approaches each retrofit option (and sometimes the HEN) has to be analysed separately, increasing the engineering effort.

Most of the available retrofit only consider installing a preflash unit before the furnace rather than in other locations in the preheat train; therefore energy integration opportunities may be neglected. To feed the flashed vapour, two options are explored: at the liquid feed stage [1, 14] or at a the stage with similar temperature to the one of the flashed vapour [5, 15]. Therese decisions are either taken systematically (i.e. by analysing multiple options), by trial and error or based on experience. Thus, the benefits of installing a preflash unit, such as increasing the capacity of the distillation column, reducing the furnace duty and/or easing the retrofit of the HEN, might not be fully exploited.

Some of the simultaneous approaches found in the open research literature also propose using metamodels to model the distillation columns [3, 20]. However, metamodels require significant engineering effort to set up and to date there is no evidence of being capable of model structural modifications, such as replacing column internals and/or adding preflash.

The proposed retrofit approach overcomes these limitations by including rigorous simulation within an optimisation environment, together with a structural design algorithm that finds the best configuration for the preflash.

3. Retrofit approach for crude oil distillation systems — adding a preflash unit

Figure 1 provides an overview of the retrofit approach proposed in this work, where the structural design decisions associated with installing a preflash unit (i.e. the preflash location in the pre-heat train and the flashed vapour feed stage) are included within the

optimisation environment. This section presents the features of the proposed retrofit approach. Part 1 of this series [6] contains more details of the methods used.

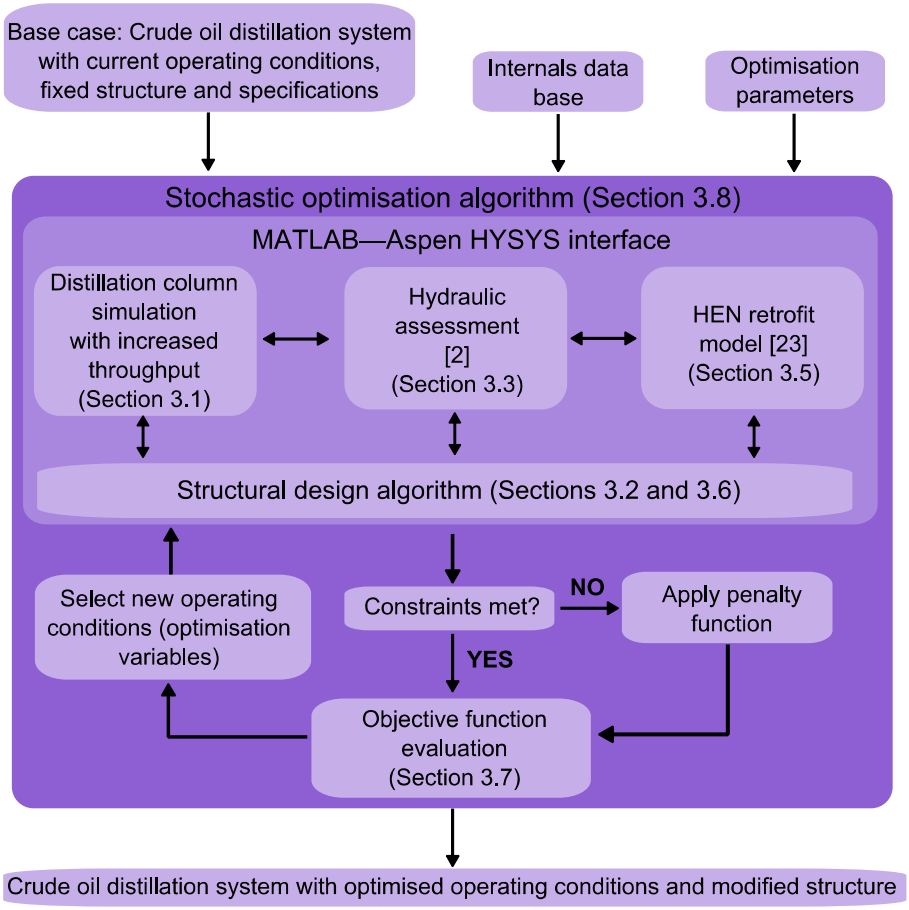

Figure 1 Proposed optimisation-based retrofit approach

3.1. Simulation of the distillation column

Figure 2 illustrates the Aspen HYSYS flowsheet used to simulate the distillation column and the upstream preflash unit. The crude oil is first pre-heated to the preflash temperature (an optimisation variable) using a heater and then is flashed. The flashed liquid is heated to the furnace outlet temperature (an optimisation variable) and is fed to the CDU. To represent the alternative of feeding the flashed vapour at different feed locations, vapour is fed to a splitter, where split fractions of 0 and 1 are allowed. Thus only one stream can be active at a time. The number of feed locations can be as many as the designer wants to explore. For example, in the flowsheet illustrated in Figure 2 three locations are explored: mixed with the returning vapour of the side-strippers, mixed with the liquid feed and mixed with the main column stripping steam.

In a case study presented by Chen [13], where a crude oil preheat train is simulated with and without assuming constant heat capacities, it is reported that assuming constant heat capacities lead to a less accurate estimation of the HEN performance. In the Part 1 of this series [6], it is mentioned that the HEN retrofit approach [23] used in this work does consider temperature-dependent heat capacities.

Figure 2 highlights in dashed lines the “dummy” heat exchangers installed to generate correlations between heat capacities and temperatures for the crude oil and its products, known in this work as CP functions. The use of these CP functions is explained in more detail in Section 3.5 and in Part 1 [6]. Spreadsheets are used to store relevant data for the optimisation and analysis of the crude oil distillation system.

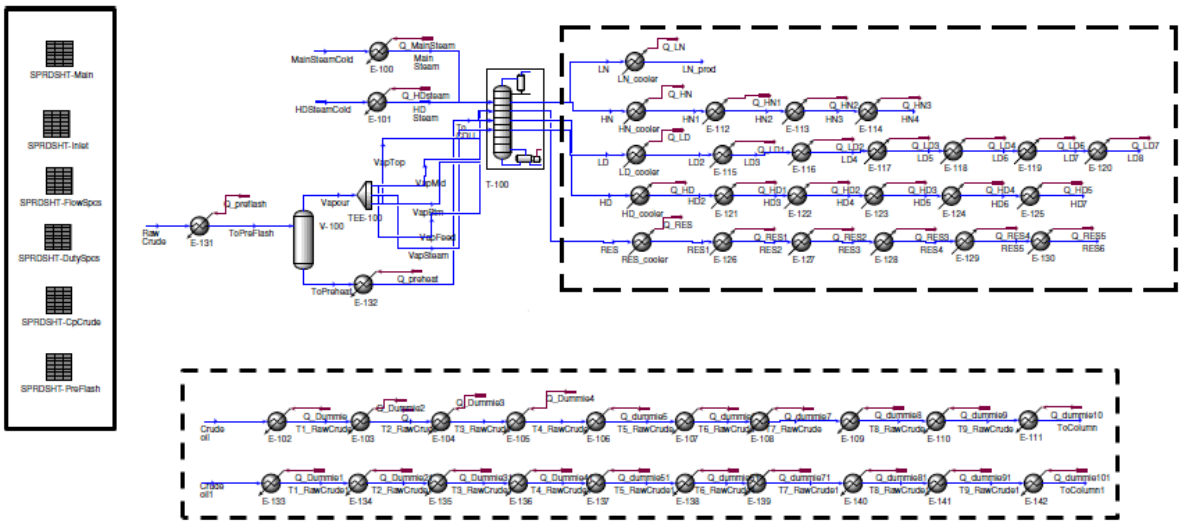

Figure 2 Simulation flowsheet in Aspen HYSYS v7.3

3.2. Structural design algorithm — selecting the flashed vapour location

As mentioned in section 2.2, most approaches of the open research literature have only considered two locations: mixed with the hot flashed liquid or at a column stage with a similar temperature to the one of the flashed vapour. In these approaches, the stripping steam flow rates, the pumparound flow rates or the furnace outlet temperature are manually adjusted until the convergence of the column is regained. The algorithm presented in this section, aims to select this location based on the operating variables selected by a stochastic optimisation algorithm, eliminating the need of trial and error calculations.

Figure 3 provides a flowchart showing how to simulate the CDU and to find the flashed vapour location. The process starts by setting up the base case (i.e. the CDU operating conditions, structure and constraints). Then, a stochastic optimisation algorithm proposes a set of column operating conditions (e.g. the furnace outlet temperature, stripping steam flow rates, pumparound flow rates and temperature drops) and preflash temperature. These inputs are sent to Aspen HYSYS using MATLAB and the column is re-simulated.

If the CDU does not converge, the algorithm actives one of the possible feed streams for the flashed, only one location can be active at the time. Secondly, the algorithm checks is the CDU has converged. If the simulation then converges, data are extracted from the simulation to perform a hydraulic analysis of the CDU in MATLAB and to identify suitable retrofit modifications and operational changes to the HEN. If the column does not converge, a new vapour feed location is explored. This process is repeated until all possible locations have been analysed. If convergence cannot be obtained for any of the proposed feed locations, the objective function is set to zero in order to discard the iteration.

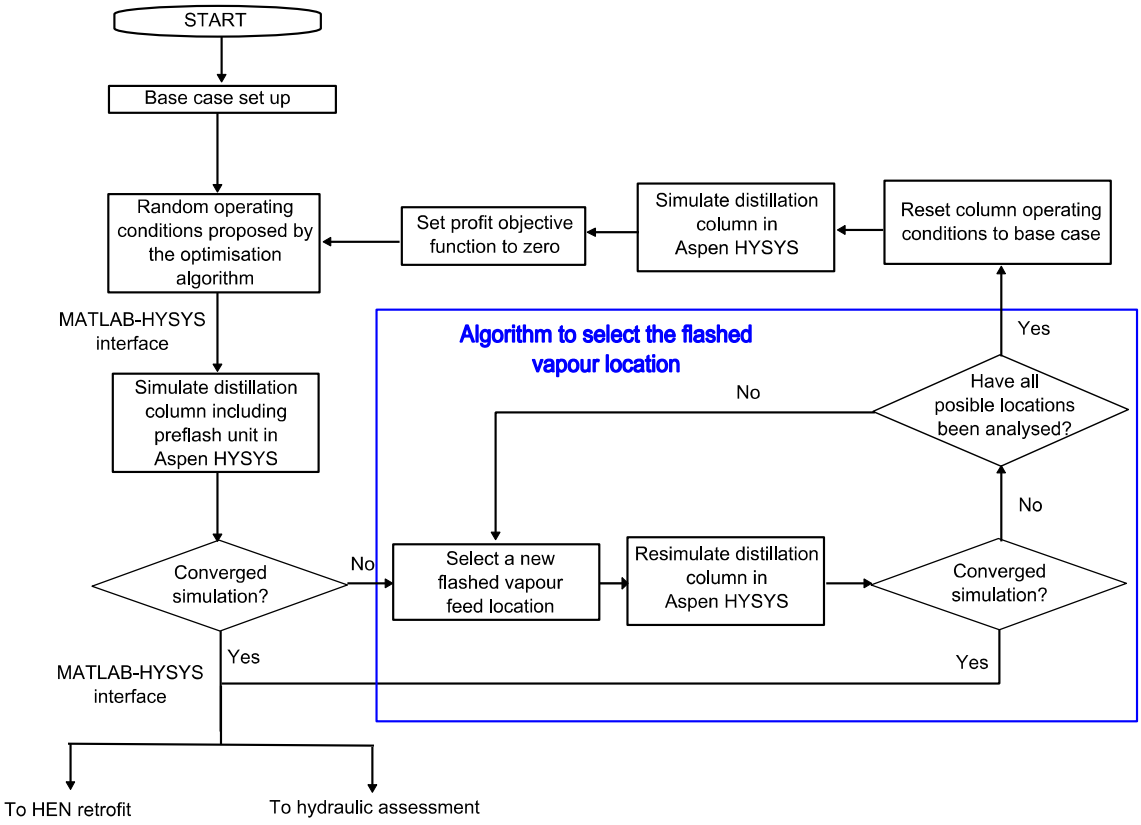

Figure 3 Flowchart of the procedure to simulate the CDU and to find the flashed vapour location

3.3. Distillation column hydraulic analysis

This approach uses the same correlations presented in Part 1 [6] to predict the hydraulic performance of the CDU when increasing its processing capacity.

Four parameters are estimated to assess the hydraulic performance of conventional trays and for high-capacity trays with sloped downcomers: approach to jet flooding, liquid weir load, downcomer exit velocity and downcomer flooding. Glitsch correlations for jet flooding and for downcomer design velocity are [28] are used to predict the approaches to jet and downcomer flooding, respectively, and KG-Tower [29, 30] design manual is used to estimate the liquid weir load and the downcomer exit velocity. KG-Tower [29, 30] design correlations are used to estimate the active area gained by using sloped downcomers. For structured packings, flooding is estimated using a regressed model [31] from the Kister and Gill pressure drop correlation chart for structured packings [32]. For all the hydraulic parameters considered, design limits used in practice are applied [28, 33].

3.4. Structural design decision algorithm — replacing column internals

Figure 4 presents the flowchart of the algorithm used to replace column internals [6]. Using the results from the simulation, a hydraulic analysis of the CDU is performed and is checked if any hydraulic limit is violated. If any hydraulic limit has been exceeded, the decision algorithm starts. Firstly, the constrained sections are identified. Secondly, the limiting hydraulic parameters are established. If the bottleneck relates to jet flooding, replacing the column internals with high-capacity trays is proposed; otherwise structured packings are proposed. The CDU hydraulics is re-assessed. If none of the internals in the data base satisfy the CDU hydraulics, a ‘penalty’ to the objective function is applied. Part 1 provides explains in detail how the penalties are applied.

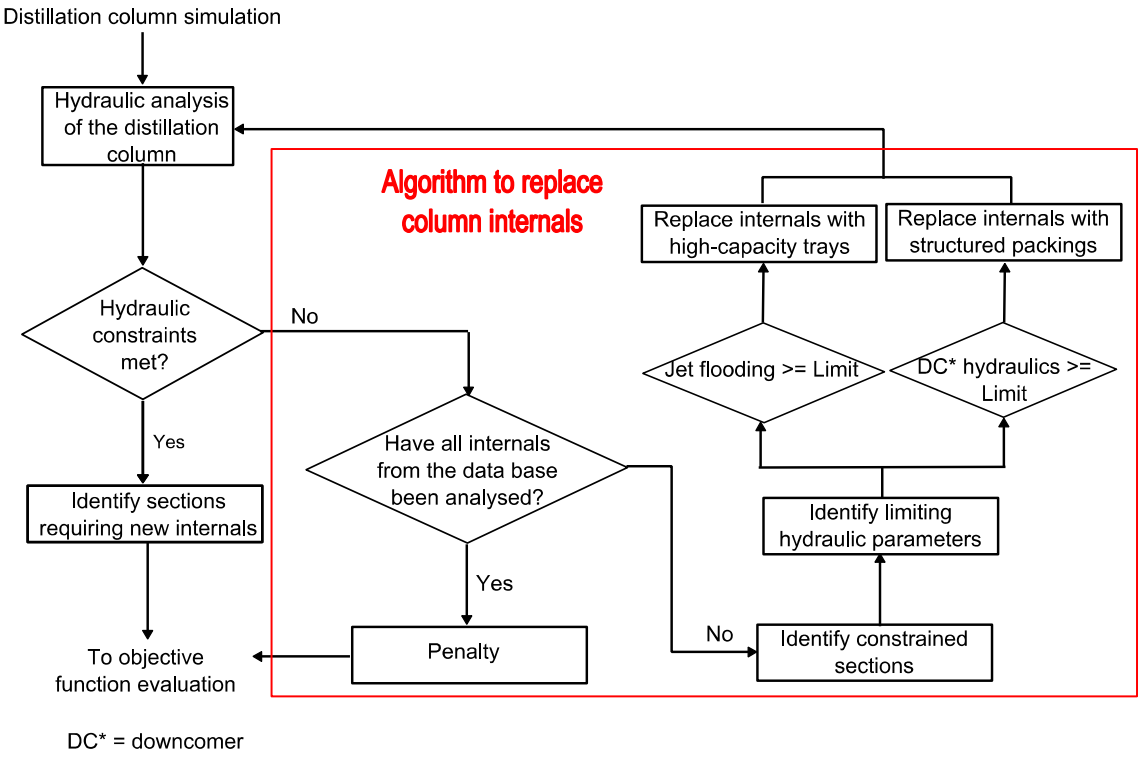

Figure 4 Flowchart of the structural design decision algorithm used to propose replacing column internals [6]

3.5. HEN retrofit approach

The HEN retrofit approach used in this work is that proposed by Ochoa-Estopier et al. [23]. In this work, this HEN retrofit approach is incorporated with relatively no modifications. More details and discussion about the retrofit approach used [23] can be found in Part 1 [6] of this series:

- The approach uses the principles of graph theory [22] to represent the HEN structure. Thus, the HEN structure can be easily manipulated [23].
- Temperature-dependent heat capacities are considered by including the CP functions mentioned in Section 3.1. As considering constant heat capacities may lead to the underestimation of the required heat transfer area [13], correlations are generated using rigorous simulations, whereas Ochoa-Estopier et al. [23] generated these correlations using metamodels regressed to rigorous simulations.
- A feasibility solver optimises heat loads and split fractions in order to meet the target temperatures and the ΔT_{min} constraints.

- The HEN retrofit methodology of Chen and co-workers [13, 19] uses SA to optimise the HEN structure by adding area, repiping and resequencing existing heat exchangers or by adding new exchangers in order to enhance the heat integration of the systems and thus to reduce fired heating demand.

3.6. Structural design algorithm — selecting preflash "location"

Figure 5 presents the flowchart of the algorithm proposed to simulate and retrofit the HEN accounting for preflash unit and modified column operating conditions. Using the results from the rigorous simulation, the HEN is simulated for the base case configuration, the crude oil temperatures are extracted and the closest temperature to the preflash temperature is identified. Then, the incidence matrix is modified to include the preflash unit (i.e. the crude oil stream is divided in two: before and after the preflash unit). Finally, the new HEN is simulated and retrofit modifications are proposed using the approach of Ochoa-Estopier et al. [23] HEN retrofit approach. The results are used to evaluate the objective function.

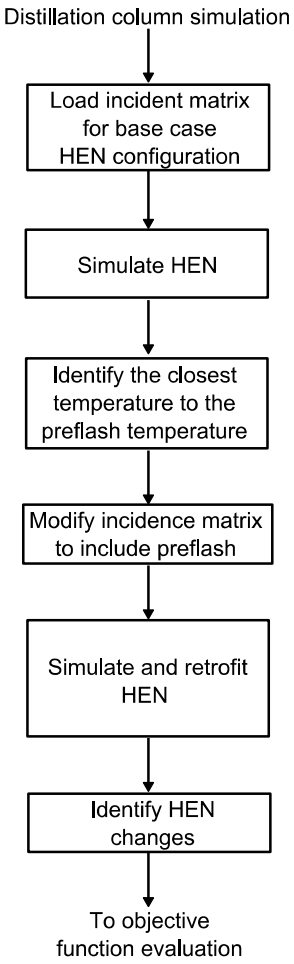

Figure 5 Flowchart of the algorithm used to retrofit the HEN including preflash

3.7. Objective function

The economic indicator used to assess the viability of a retrofit project in this work is the net profit, i.e. the difference between revenue and costs [34], as shown in Eq. 1.

$$NP = \sum Revenue - \sum Costs \quad (1)$$

The revenue is estimated from the transfer value of each product; the costs are calculated by adding the cost of crude oil, the operational costs and the annualised capital charges (ACC). Part 1 [6] explains in more detail how these values are estimated in this work.

The operational costs considered are the cost of the utilities (e.g. fired heating, cooling water) and stripping steam.

In this approach, three types of modifications are considered:

- replacing column internals with high-capacity trays and/or structured packings [6]
- HEN modifications: adding area, resequencing and repiping existing heat exchangers and adding new heat exchangers [6]
- adding a preflash unit

To estimate the cost of replacing column internals, the cost correlations presented by Bravo [35] are used. For the HEN, a in Part 1 [6], a cost model that correlates the required surface area of a heat exchanger and three constants depending of the materials of construction, pressure rating and type of exchanger [13] are used.

Eq. 2 presents the correlation used to estimate the cost of the preflash unit $\$Cost_{preflash}$ in 2003 US$ [5, 36], where D_{flash} and H_{flash} represent the diameter and the height of the flash drum in m, and F_m and F_p are correction factors for vessel materials and pressures, respectively.

$$\$Cost_{preflash} = 409 * \left(D_{flash}\right)^{1.066}\left(H_{flash}\right)^{0.802}\left(2.18 + F_m F_p\right) \quad (2)$$

Eqs. 3 and 4 are used to estimate the flash unit dimensions [5, 36], where V_L refers to the volumetric flow rate of liquid in $m^3 s^{-1}$, θ_R is the residence time in s and R_{flash} is the ratio of the height to the diameter.

$$D_{flash} = \left(\frac{4V_L\theta_R}{\pi R_{flash}}\right)^{1/3} \quad (3)$$

$$H_{flash} = R_{flash}D_{flash} \quad (4)$$

Penalties to the objective function are applied for unconverged simulations and/or for product quality out of specifications, as in Part 1 [6].

3.8. Stochastic optimisation algorithms

Similar to the approach presented in Part 1 [6], the CDU operating parameters are optimised using two stochastic optimisation algorithms: either simulated annealing (SA) or global search (GS). In this work, one additional optimisation variable is included: the preflash temperature. The two methods are compared and help to give confidence in the results.

More detail and discussion about the stochastic optimisation algorithms used are presented in Part 1 [6].

3.9. Proposed retrofit approach — summary

The retrofit approach proposed in this work extends previous work [6] by including structural design decisions for:

- selecting the flashed vapour location
- recommending replacing column internals with high-capacity trays with sloped downcomers or structured packings
- modifying the HEN structure to consider the a preflash unit

Figure 6 illustrates and summarises the proposed retrofit approach. The process begins by defining the base case (e.g. operating conditions, CDU and HEN structure, constraints, upper and lower bounds for the optimisation parameters) and setting up a base case simulation.

First, a stochastic optimisation algorithm proposes a new set of CDU operating conditions and preflash temperature. Initially, the flashed vapour is mixed with the liquid feed. Second, the CDU is simulated in Aspen HYSYS v7.3 including the preflash unit (as shown in Figure 2), MATLAB and Aspen HYSYS are linked in order to transfer data between software. Then, the MATLAB—Aspen HYSYS interface checks whether the simulation converges. It the simulation does not converge, and the decision algorithm discussed in Section 3.2 is used to change the flashed vapour location until the simulation converges.

Third, simulation results are extracted to assess the hydraulic performance of the CDU and to propose retrofit modifications to the HEN. If any hydraulic constraint is violated, the decision algorithm presented in Section 3.4 proposes new internals for the

constrained sections. If none of the internals proposed satisfies the hydraulic constraints, a penalty to the objective function is applied.

With the crude oil and product and process streams information extracted from the simulation, the HEN is simulated for the base case HEN structure, and the outlet temperatures of the heat exchangers that preheat the crude oil are extracted. Then, the algorithm introduced in Section 3.6 selects a temperature similar to the preflash temperature and 'divides' the crude oil stream into two (i.e. before and after the preflash unit). The HEN is re-simulated and structural modifications (i.e. adding, deleting, repiping and resequencing heat exchangers) are proposed and assessed.

Finally, the objective function is evaluated and penalties are applied if the required quality of the products is not satisfied.

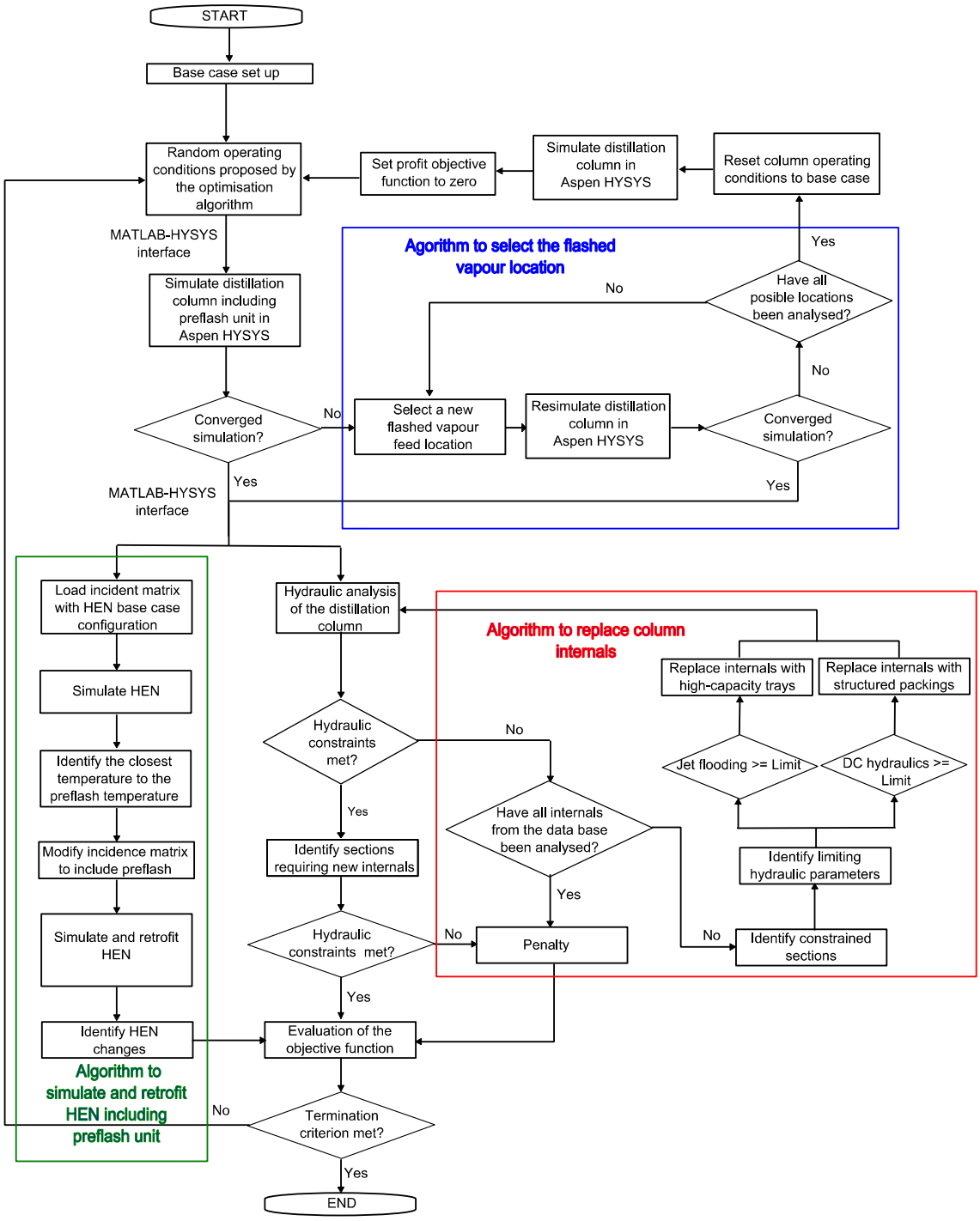

Figure 6 Flowchart of the proposed retrofit approach

4. Case study

The heat-integrated crude oil distillation system presented in Part 1 [6] provides the base case. The crude oil distillation system processes 100,000 bbl d^{-1} (2562 kmol h^{-1}) of Venezuela Tía Light Juana crude oil. The system comprises a crude oil distillation column that produces five products: light naphtha (LN), heavy naphtha (HN), light distillate (LD), heavy distillate (HD) and residue (RES), and a HEN and furnace to 365℃. Part 1 [6] provides details of the crude oil assay, the CDU stage distribution, operating conditions, product specifications and flow rates, section diameters and internals, and the HEN structure, stream data and other details.

The characteristics of the internals considered for retrofit (i.e. high-capacity trays with sloped downcomers and structured packings); the parameters used to evaluate the net profit (i.e. the prices of crude oil and its products, cost of fired heating, cooling water and stripping steam, and costs of replacing column internals and HEN modifications); and the stopping criteria for the optimisation algorithms can also be found in Part 1 [6].

This case study aims to identify retrofit modifications that can maximise the profitability of the system when increasing its processing capacity by 30%. The retrofit modifications considered are: i) operational optimisation; ii) replacing the column internals; iii) adding a preflash unit; iv) HEN retrofit. These options are explored simultaneously using the approach presented in Section 3.

Table 1 lists the optimisation variables and their lower and upper bounds. These bounds are chosen based on a previous optimisation runs reported in the Supporting Information.

Unlike in previous work [2, 6], the furnace outlet temperature is fixed. The optimisation runs found that decreasing the furnace outlet temperature when adding a preflash unit causes convergence problems and adversely affects product quality. Increasing the furnace outlet temperature always increased the furnace duty and required heat transfer area in the furnace.

Table 1 Lower and upper bounds used for operational optimisation

Parameter	Lower bound	Upper bound
Main steam flow rate, kmol h^{-1}	1678	1872
Btm SS steam flow rate, kmol h^{-1}	366	416
Furnace outlet temperature, ℃	365	365
PA1 heat flow, MW	11	19
PA2 heat flow, MW	18	20
PA3 heat flow, MW	11	14
PA1 ΔT, ℃	28	90
PA2 ΔT, ℃	75	100
PA3 ΔT, ℃	30	60
Preflash temperature	200	220

The values of both corrections factors in Eq. 2 to estimate the cost of installing a preflash unit, is of 1 [36], i.e. for a carbon steel vessel and an operating pressure below 345 kPa (50 psi). To update equipment costs, the CECPCI indexes of 2003 and 2014 (402 [37] and 576.1 [38], respectively) are used.

To estimate the dimensions of the flash unit (Eqs. 3 and 4) a residence time of 300 s and a ratio of height to the diameter of 5 are assumed, based on design practice [39].

4.1. Case study — results

Figures 7 and 8 show the optimisation results when using SA and GS, respectively, are similar and consistent giving confidence in the results; Tables 2 and 3 presents the product flow rates results after the optimisations; and Tables 4 and 5 summarise the HEN and economic results for the optimisations.

Tables S2.1 and S2.2 of the Supporting Information present the values use for constructing Figures 7 and 8. Tables S2.3 and S2.4 confirm that the product quality specifications are all met after the optimisations. Tables S2.5 and S2.6 present the column hydraulics results. No hydraulic constraint is violated in any case. Tables S2.7 and S2.8 present the results for the required additional heat transfer area needed per heat exchanger. Section S3 presents an overview of the optimisations.

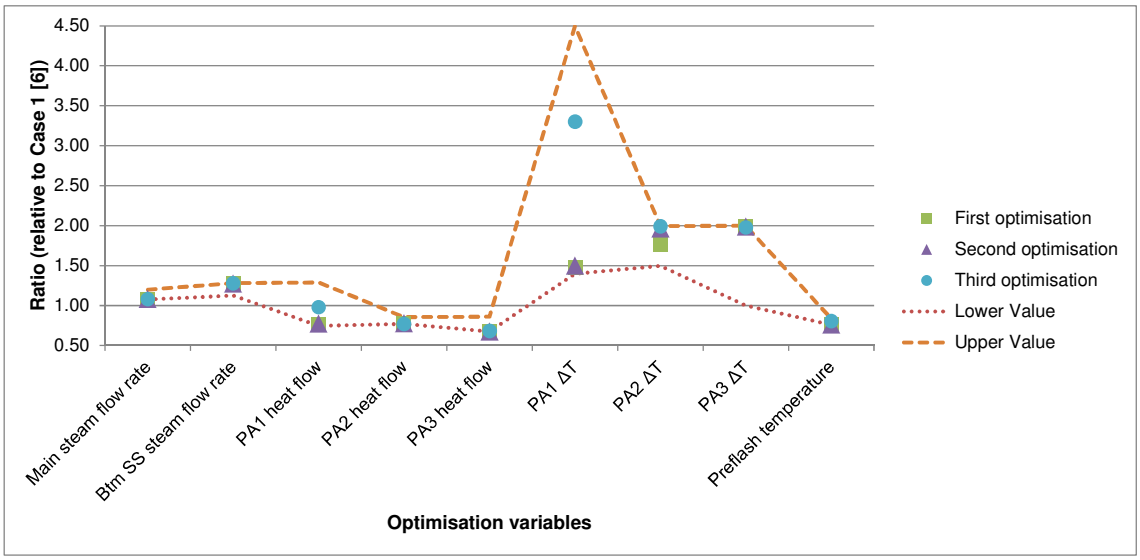

Figure 7 Results for optimisations using SA

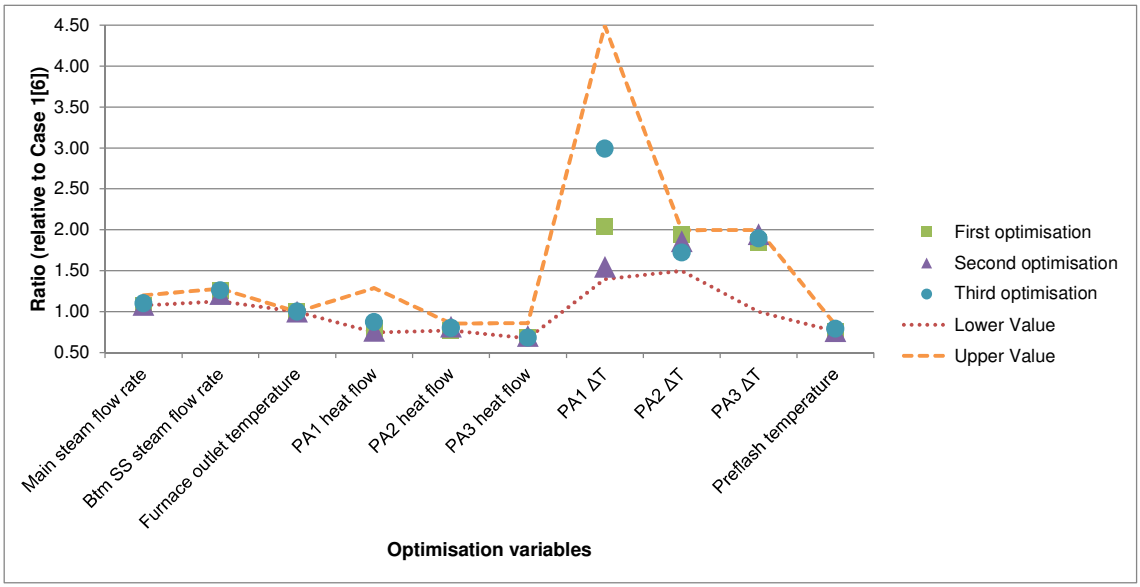

Figure 8 Results for optimisations using GS

Table 2 Product flow rates for optimisation using SA

Product	First optimisation		Second optimisation		Third optimisation	
	Value	Diff*	Value	Diff*	Value	Diff*
Light naphtha (kmol h^{-1})	898.1	0.0%	897.9	0.0%	895.5	-0.3%
Heavy naphtha (kmol h^{-1})	531.1	-0.6%	530.7	-0.6%	533.6	-0.1%
Light distillate (kmol h^{-1})	490.5	-1.0%	491.2	-0.9%	493.9	-0.3%
Heavy distillate (kmol h^{-1})	198.0	12.1%	197.7	12.0%	199.1	12.8%
Residue (kmol h^{-1})	601.6	-1.5%	601.5	-1.5%	599.0	-1.9%

*Diff = difference relative to increase by 30% pro rata [6]

Table 3 Product flow rates for optimisations using GS

Product	First optimisation		Second optimisation		Third optimisation	
	Value	Diff*	Value	Diff*	Value	Diff*
Light naphtha (kmol h^{-1})	897.3	-0.1%	897.1	-0.1%	895.5	-0.3%
Heavy naphtha (kmol h^{-1})	530.8	-0.6%	532.3	-0.4%	534.6	0.1%
Light distillate (kmol h^{-1})	492.4	-0.6%	493.7	-0.4%	492.8	-0.5%
Heavy distillate (kmol h^{-1})	196.8	11.4%	194.9	10.3%	196.8	11.4%
Residue (kmol h^{-1})	601.6	-1.5%	601.7	-1.5%	600.6	-1.7%

*Diff = difference relative to increase by 30% pro rata [6]

Table 4 HEN retrofit and economic results for optimisations using SA

Parameter	First optimisation	Second optimisation	Third optimisation
Additional HEN area, m^2	2355	2092	2357
No. of HX* needing modifications	13	16	14
Furnace additional area, m^2	0	0	0
Furnace inlet temperature, °C	264	260	265
Furnace outlet temperature, °C	365	365	365
Fired heating demand, MW	61	63	61
Revenue, $\$\cdot10^{-3}\ a^{-1}$	1,005,600	1,005,500	1,005,550
Operating costs, $\$\cdot10^{-3}\ a^{-1}$	28,200	29,100	27,700
Cost replacing column internals, $\$\cdot10^{-3}$	0	0	0
HEN retrofit cost, $\$\cdot10^{-3}$	554	507	567
Net profit, $\$\cdot10^{-3}\ a^{-1}$	977,136	976,175	977,112

*HX = heat exchangers

Table 5 HEN retrofit and economic results for optimisations using GS

Parameter	First optimisation	Second optimisation	Third optimisation
Additional HEN area, m^2	2659	2562	2597
No. of HX* needing modifications	14	13	14
Furnace additional area, m^2	0	0	0
Furnace inlet temperature, °C	260	260	263
Furnace outlet temperature, °C	365	365	365
Fired heating demand, MW	63	63	62
Revenue, $\$\cdot10^{-3}\ a^{-1}$	1,005,350	1,004,900	1,005,050
Operating costs, $\$\cdot10^{-3}\ a^{-1}$	29,150	29,130	28,200
Cost replacing column internals, $\$\cdot10^{-3}$	0	0	0
HEN retrofit cost, $\$\cdot10^{-3}$	558	563	579
Net profit, $\$\cdot10^{-3}\ a^{-1}$	976,867	976,434	976,172

*HX = heat exchangers

Based on three optimisation rungs by each method, the following trends can be observed in Figures 7 and 8:

a. The main steam flow rate, HD steam flow rates and pumparound temperature drops tend to increase.
b. The pumparound heat flows tend to decrease.
c. The preflash temperature is lower than the base case furnace inlet temperature.

Apart from the trend in stripping steam flow rates, the operating parameters followed similar trends to those observed in previous work [2, 6].

In Part 1 [6] when the same heat-integrated crude oil distillation system is retrofitted, without the option of adding a preflash unit, is it found that the main steam flow rate could be decreased. Conversely Figures 7 and 8 shown that adding a preflash unit tends to increase the main steam flow rate. This trend can be explained by analysing the results obtained by the decision algorithm presented in Section 3.2.

In all cases, the algorithm found that the flashed vapour should be fed at the liquid feed stage. For example, if 30% of the feed is flashed at 210°C, the vapour at 210°C and liquid at 365°C are mixed. After mixing, the temperature of the feed drops to around 347°C. Thus, to compensate this reduction of temperature and in order to meet the quality of the products, the main stripping steam flow rate must be increased. In practice, adding a preflash unit between heat exchangers in the preheat train might not be possible due to lay out constraints.

In previous work [2, 6], it is observed that there is a relationship between the main steam flow rate and the yield and quality of the residue stream. Therefore, the main steam flow rate can only change within a certain range. The stripping steam flow rate needs to be adjusted to compensate for the cold flashed vapour, but only a narrow range of preheat temperatures and stripping steam flow rates can satisfy all the constraints.

This finding justifies the importance of including structural design decisions within the optimisation, as the related trade-offs can be systematically explored.

Tables 2 and 3 presents the product flow rates results after the optimisations. The yields of light naphtha, heavy naphtha and light distillate slightly decrease (less than 1%) because of the decrease in pumparound heat flows. The heavy distillate yield increases by 12% due to the increase in Btm SS stripping steam flow rate; the residue production slightly decreases.

Tables 4 and 5 show that in all cases, no additional area is needed for the furnace and that there is no need to replace the column internals. This result is expected, as some of the benefits reported in the open research literature of installing a preflash unit are that it reduces the need of installing furnace area and that it helps to increase the column capacity.

The economic results reported in Tables 4 and 5, show that by adding preflash the net profit of the system can be increased to around 977,000,000 \$ a^{-1}. The best solution found is the one of the first optimisation using SA (Table 4), which reports that by installing the proposed modifications the net profit can be increased up to 977,136,000

$ a^{-1}. Note that the values obtained for the net profit are very high due to the values obtained for the revenue. This is because the values of the products and crude oil were taken at a time where there was volatility in the crude oil market. However, these results can be updated and reproduced.

Section 4.2 provides more analysis and discussions of these results, and compares this case study with the cases presented in Part 1 [6].

4.2. Case study — summary and conclusions

The case study results explored the option of installing a preflash unit to support increasing the processing capacity of a heat-integrated crude oil distillation system.

The results show that there is a limited range of values for the preflash temperature, the flashed vapour feed stage and the main stripping steam flow rate that satisfy all the constraints to be met.

Table 6 compares the best result obtained in this case study, with the results of the case study presented in Part I [6]. Case 1 refers to the case in which operational optimisation is not considered, Case 2 to the case in which the column is retrofitted using the approach proposed in Part I [6] and Case 3 is the best case found in this case study (i.e. the first optimisation using SA).

Table 6 Summary and comparison of best results

Parameter	Case 1 [6]	Case 2 [6]	Case 3
Additional HEN area, m^2	2689	3364	2355
No. of HX* needing modifications	16	17	13
Furnace additional area, m^2	15	5	0
Furnace inlet temperature, °C	271	271	264
Furnace outlet temperature, °C	365	356.6	365
Fired heating demand, MW	71	66.0	61
Revenue, $\$\cdot10^{-3}\ a^{-1}$	1,001,000	1,004,000	1,005,600
Operating costs, $\$\cdot10^{-3}\ a^{-1}$	32,000	29,800	28,200
Cost replacing column internals, $\$\cdot10^{-3}$	236	70	0
HEN retrofit cost, $\$\cdot10^{-3}$	646	748	554
Net profit, $\$\cdot10^{-3}\ a^{-1}$	968,248	973,860	977,136

*HX = heat exchangers

Installing a preflash unit can avoid the need to add heat transfer area of the furnace compared to the cases presented in Part 1 [6]. Similarly, the preflash unit can

debottleneck the distillation column, allowing increase in throughput without needing to replace column internals.

Note that these new results require less additional heat transfer area and none in the furnace, as well as a significant reduction in the furnace duty (around 10% compared to retrofitting the column). Additional, installing a preflash unit ease the HEN retrofit: i.e. less heat exchangers require additional area.

Furthermore, installing a preflash unit avoids the needs to replace column internals and the net profit of the systems can by increased up to 24% compared to Case 1 (i.e. around 226,000,000 \$ a^{-1}) and up to 1% compared to Case 2 (i.e. around 3,000,000 \$ a^{-1}).

A drawback of this approach is that is computationally intensive. The SA optimisations took 5 to 6 hours, and the GS optimisations took 15 and 22 hours using a desktop computer with an Intel Core processor of 3.30 GHZ and 8.00 GB of installed RAM memory.

5. Summary and conclusions

This paper extends previous work [6] that considers operational optimisation and replacing column internals by considering also the option of adding a preflash unit (i.e. selecting the preflash temperature and the flashed vapour feed location).

The main contribution of this work is the incorporation of structural design decisions within an optimisation environment for the retrofit of heat-integrated crude oil distillation systems, and in particular for the options of installing a preflash unit. There is no record in the open literature of retrofit being addressed with such a wide range of options in such a systematic and holistic manner.

The approach applies rigorous simulation to model the distillation column, were a MATLAB—Aspen HYSYS interface and an optimisation-based HEN retrofit approach [23] are used to generate HEN retrofit solutions to increase throughput. The method includes analysis of the hydraulic performance of the CDU and assesses replacing the CDU internals in the constrained sections. The optimisation framework, applying stochastic optimisation algorithms, is shown to be robust in its search for structural options and operating conditions.

Two stochastic optimisation algorithms are used in this work (simulated annealing and global search). Comparison of their results helps to create confidence in the results obtained. Each optimisation algorithm was run three times in order to observe trends and identify the most economic retrofit solution.

The benefits of the proposed retrofit approach are demonstrated with an industrially relevant case study. The optimisation results provide further insight into the known trade-offs between the distillation column hydraulics, product yields and quality specifications, HEN retrofit and net profit. The approach thus helps to exploit the interactions between the preflash unit, CDU and the HEN, and to assess beneficial retrofit modifications when increasing throughput.

Associated content

Supporting Information:

- Procedure to select upper and lower bounds
- HEN required additional heat transfer area for case study
- Product quality results for case study
- Hydraulic results for case study
- Operational optimisation results for case study
- Overview of the optimisations for case study

Corresponding Author

Víctor Manuel Enríquez-Gutiérrez

E-mail1: victormanuel.enriquezgutierrez@manchester.ac.uk
E-mail2: iq.vic.enriquez@gmail.com

Acknowledgment

The authors gratefully acknowledge the Mexican Council of Science and Technology (CONACyT) and the Roberto Rocca Education Program (RREP) for their financial support of PhD studies at the University of Manchester.

Abbreviations

CDU Crude oil distillation unit

GS	Global search
HEN	Heat exchanger network
MINLP	Mixed-integer non-linear programming
SA	Simulated annealing

References

1. Errico, M., Tola, G., and Mascia, M., Energy saving in a crude distillation unit by a preflash implementation. *Applied Thermal Engineering*, **2009**. *29*(8-9): p. 1642-1647.
2. Enríquez-Gutiérrez, V.M. and Jobson, M., An optimisation-based retrofit approach for increasing the processing capacity of heat-integrated crude oil distillation systems. *Chemical Engineering Research & Design*, **2016**. *submitted May 2016*.
3. Ochoa-Estopier, L.M., Jobson, M., and Smith, R., Optimisation of heat-integrated crude oil distillation systems. Part III: Optimisation framework. *Industrial & Engineering Chemistry Research*, **2015**. *54*(18): p. 5018-5036.DOI: 10.1021/ie503805s.
4. Gadalla, M., Kamel, D., Ashour, F., and din, H.N.E., A new optimisation based retrofit approach for revamping an Egyptian crude oil distillation unit. *Energy Procedia*, **2013**. *36*(0): p. 454-464.DOI: 10.1016/j.egypro.2013.07.051.
5. Gadalla, M.A., *Retrofit Design of Heat-integrated Crude Oil Distillation Systems*, PhD Thesis, The University of Manchester, Manchester, UK, 2003.
6. Enríquez-Gutiérrez, V.M. and Jobson, M., An optimisation-based retrofit approach for the assessment of structural and flowsheet modifications for heat-integrated crude oil distillation systems. Part 1.- Replacing column internals. *Chemical Engineering Research & Design*, **2016**. *submitted May 2016*.
7. Enríquez-Gutiérrez, V.M., Jobson, M., Ochoa-Estopier, L.M., and Smith, R., Retrofit of heat-integrated crude oil distillation columns. *Chemical Engineering Research and Design*, **2015**. *99*: p. 185-198.DOI: 10.1016/j.cherd.2015.02.008.
8. Caballero, J.A., Milán-Yañez, D., and Grossmann, I.E., Optimal synthesis of distillation columns: Integration of process simulators in a disjunctive programming environment. *Computer Aided Chemical Engineering*, **2005**. *20*: p. 715-720.DOI: 10.1016/S1570-7946(05)80241-X.
9. Carlberg, N.A. and Westerberg, A.W., Temperature-heat diagram for complex columns 2. Underwoord's method for side strippers and enrichers. *Ind. Eng. Chem. Res.*, **1989**. *28*: p. 1379.
10. Suphanit, B., *Design of Complex Distillation Systems*, PhD Thesis, UMIST Department of Process Integration, Manchester, UK, 1999.
11. Gadalla, M., Jobson, M., and Smith, R., Shortcut models for retrofit design of distillation columns. *Chemical Engineering Research and Design*, **2003**. *81*(8): p. 971-986.
12. Asante, N.D.K. and Zhu, X.X., An automated and interactive approach for heat exchanger network retrofit. *Chemical Engineering Research and Design*, **1997**. *75*(3): p. 349-360.DOI: 10.1205/026387697523660.
13. Chen, L., *Heat-integrated Crude Oil Distillation System Design*, PhD Thesis, The University of Manchester, Manchester, UK, 2008.

14. Wang, Y., Hou, Y., Gao, H., Sun, J., and Xu, S., Selecting the optimum predistillation scheme for heavy crude oils. *Industrial and Engineering Chemistry Research*, **2011**. *50*(18): p. 10549-10556.
15. Gadalla, M.A., Abdelaziz, O.Y., Kamel, D.A., and Ashour, F.H., A rigorous simulation-based procedure for retrofitting an existing Egyptian refinery distillation unit. *Energy*, **2015**. *83*(0): p. 756-765.DOI: 10.1016/j.energy.2015.02.085.
16. Fair, J.R., How to predict sieve tray entrainment and flooding. *Petro. Chem. Eng.*, **1961**. *33*: p. 45.
17. Enríquez-Gutiérrez, V.M., Jobson, M., and Smith, R., A design methodology for retrofit of crude oil distillation systems. *Computer Aided Chemical Engineering*, **2014**. *Volume 33*: p. 1549-1554.DOI: 10.1016/B978-0-444-63455-9.50093-3.
18. Rastogi, V., *Heat-integrated Crude Oil Distillation System Design*, PhD, The University of Manchester, Manchester, UK, 2006.
19. Smith, R., Jobson, M., and Chen, L., Recent development in the retrofit of heat exchanger networks. *Applied Thermal Engineering*, **2010**. *30*(16): p. 2281-2289.
20. López C., D.C., Hoyos, L.J., Mahecha, C.A., Arellano-Garcia, H., and Wozny, G., Optimization model of crude oil distillation units for optimal crude oil blending and operating conditions. *Industrial & Engineering Chemistry Research*, **2013**. *52*(36): p. 12993-13005.DOI: 10.1021/ie4000344.
21. Ochoa-Estopier, L.M. and Jobson, M., Optimization of heat-integrated crude oil distillation systems. Part I: The distillation model. *Industrial & Engineering Chemistry Research*, **2015**. *54*(18): p. 4988-5000.DOI: 10.1021/ie503802j.
22. de Oliveira Filho, L.O., Queiroz, E.M., and Costa, A.L.H., A matrix approach for steady-state simulation of heat exchanger networks. *Applied Thermal Engineering*, **2007**. *27*(14-15): p. 2385-2393.
23. Ochoa-Estopier, L.M., Jobson, M., Chen, L., Rodríguez, C., and Smith, R., Optimisation of heat-integrated crude oil distillation systems. Part II: Heat exchanger network retrofit model. *Industrial & Engineering Chemistry Research*, **2015**. *54*(18): p. 5001-5017.DOI: 10.1021/ie503804u.
24. Chen, Y., Eslick, J.C., Grossmann, I.E., and Miller, D.C., Simultaneous process optimization and heat integration based on rigorous process simulations. *Computers & Chemical Engineering*, **2015**. *81*: p. 180-199.DOI: 10.1016/j.compchemeng.2015.04.033.
25. Hansen, N., *The CMA Evolution Strategy: A Comparing Review*, in *Towards a New Evolutionary Computation: Advances in the Estimation of Distribution Algorithms*. Springer: Berlin, Heidelberg, 2006 p. 75-102.
26. Papoulias, S.A. and Grossmann, I.E., A structural optimization approach in process synthesis—II. *Computers & Chemical Engineering*, **1983**. *7*(6): p. 707-721.DOI: 10.1016/0098-1354(83)85023-6.
27. Jeżowski, J.M., Shethna, H.K., and Castillo, F.J.L., Area Target for Heat Exchanger Networks Using Linear Programming. *Industrial & Engineering Chemistry Research*, **2003**. *42*(8): p. 1723-1730.DOI: 10.1021/ie020643i.
28. Koch-Glitsch. *Glitsch Ballast Tray Design Manual: Bulletin No. 4900*. 2013 [access date October 2014]; 6th Edition:[Available from: http://www.koch-glitsch.com/Document%20Library/Bulletin-4900.pdf.
29. Koch-Glitsch, *KG-Tower*. 2014, version 5.2, Koch-Glitsch LP: USA
30. Koch-Glitsch. *Introduction to KG-Tower: Tray& Packed Tower Sizing Software Program, Version 2.0*. 2006 [access date October 2014]; Available from: www.koch-glitsch.com.
31. Enríquez-Gutiérrez, V.M., Jobson, M., and Smith, R., A design methodology for retrofit of crude oil distillation systems. *Proceedings of the 24th European Symposium on Computer Aided Process Engineering-ESCAPE24*, **2014**. *Part A*: p. 1549-1554.DOI: 10.1016/B978-0-444-63455-9.50093-3.

32. Kister, H.Z. and Gill, D.R., Flooding and pressure drop prediction for structured packings. *IChemE Symp. Ser*, **1992**. *128*: p. A109-A123.
33. Branan, C.R., *Rules of Thumb for Chemical Engineers*. 4th ed. Elsevier Science: Burlington, 2011.
34. Towler, G. and Sinnott, R.K., *Chemical Engineering Design Principles, Practice and Economics of Plant and Process Design*. 2nd. ed. Butterworth-Heinemann: Boston, 2013.
35. Bravo, J.L., Select structured packings or trays? *Chemical Engineering Progress*, **1997**. *93*(7): p. 36-41.
36. Douglas, J.M., *Conceptual Design of Chemical Processes* International ed. McGraw-Hill: New York, 1988.
37. Lozowski, D., Economic Indicators. *Chemical Engineering*, **2010**. *117*(13): p. 59-60.
38. Ondrey, G., Economic Indicators. *Chemical Engineering*, **2015**. *122*(5): p. 104.
39. Golden, S.W., Prevent preflash drum foaming. *Hydrocarbon processing*, **1997**: p. 141-153.

Chapter 6 Conclusions and future work

6.1 Conclusions — proposed retrofit approach

In practice, retrofit is commonly applied to process plants when process objectives change. For example, when it is desired to increase the profitability of a process by increasing its processing capacity, to reduce the CO_2 emissions, to increase the quality of the products or to maximise the yield of the most valuable products. To achieve these objectives, operational, structural and/or flowsheet modifications can be considered.

Heat-integrated crude oil distillation systems comprise a distillation column, in which the crude oil is separated into products for downstream processing, and a HEN that preheats the crude oil using products and process streams and a furnace. Retrofit projects to increase the profitability of crude oil distillation systems are relatively common.

The retrofit of these heat-integrated distillation systems is a complex problem with many degrees of freedom and constraints due the strong interactions between the distillation column and its associated HEN. An extensive literature review of the open research literature revealed that retrofit approaches for these types of systems are lacking.

In this thesis, three approaches are presented to assess beneficial retrofit modifications when increasing the processing capacity of heat-integrated distillation systems.

The approach proposed in Publication 1 takes advantage of the ability of some commercial rigorous simulation software (e.g. Aspen HYSYSY) to be linked with equation-based modelling environments (e.g. MATLAB). In this approach, the distillation column is simulated in Aspen HYSYS, and MATLAB is used to transfer data between software. Also in MATLAB, open literature hydraulic correlations for conventional trays, high-capacity trays and structured packings and a HEN simulation model are coded. This approach permits to systematically assess the impacts of increasing throughput on the distillation

column hydraulic performance, the heat transfer area and the fired heating consumption, and to explore the suitability of different column internals to debottleneck the distillation column. A novelty of this approach is that four hydraulic parameters are assessed for conventional and high-capacity trays: jet flooding, liquid weir load, downcomer exit velocity and downcomer flooding. Retrofit approaches from the open research literature only account for jet flooding, possible leading to ineffective retrofit solutions for the distillation column when increasing throughput (see Appendix A). In practice, these parameters are usually accounted for using internal vendor software, such as KG-Tower and SULCOL (Thernesz et al., 2010). However, internals vendor software require user interaction to input data from rigorous simulations and to read the results, thus significant engineering time and effort are needed to analyse several retrofit scenarios. This approach overcomes these limitations.

The approach presented in Publication 2 aims to simultaneously explore and assess operational changes to the distillation column and structural modifications to the HEN (i.e. adding, deleting, repiping and resequencing heat exchangers) in order to increase the profitability of heat-integrated distillation systems when increasing capacity. This is accomplished by including rigorous simulation in Aspen HYSYS, open literature hydraulic correlations for conventional trays, high-capacity trays and structured packings and an optimisation-based HEN retrofit approach (Ochoa-Estopier et al., 2015a) within an optimisation framework. In Publication 2, the suitability of two stochastic optimisation algorithms is explored: simulated annealing (SA) and global search (GS), both from the MATLAB optimisation toolbox. To date, there is no evidence in the open research literature of this GS algorithm being used in any other retrofit approach, but other global search algorithms have been used (Chen et al., 2015). Due the random nature of both algorithms, the approach proposes running each algorithm three times in order to select the ‘best’ retrofit design. This methodology proved to be useful to obtain robust results and to observe trends of the distillation column operating parameters. Current practice can benefit from this approach by using it to select a feasible and viable retrofit design that improves the profitability of a heat-integrated distillation system.

Publication 3 presents an optimisation-based retrofit approach that extends previous work by including the option of replacing the column internals within the optimisation environment. This is possible by incorporating in the approach a structural design algorithm that assesses the suitability of different column internals to debottleneck the distillation column. To date, this option has not being included in any retrofit approach from the open research literature. This could benefit current practice by reducing the engineering time and effort of exploring suitable column internals to debottleneck the

column, and to exploit more effectively the synergies between the internal flows of the distillation column and the heat recovery system of heat-integrated crude oil distillation systems.

Publication 4 presents an optimisation-based retrofit approach that allows exploring the benefits of adding a preflash unit when increasing the capacity of heat-integrated distillation systems. In this approach, the structural design options associated with adding a preflash unit (i.e. the location of the preflash unit in the preheat train and the flashed vapour feed) are selected within the optimisation framework by a structural design algorithm coded in MATLAB. This has not been implemented before in any retrofit approach from the open research literature. This approach allows to explore more effectively the trade-offs between the operating parameters of the distillation column, the distillation column hydraulics, the preflash temperature and the HEN. In practice and in some approaches from the open research literature, these design options are commonly selected systematically (Gadalla et al., 2015) or by trial-and-error (Wang et al., 2011). Thus, the benefits of adding a preflash unit might not be fully exploited.

The approaches presented in Publications 1 to 4 are not limited to the use of the hydraulic and cost correlations presented. More accurate or specific ones can be used instead if available. Furthermore, the approach is not limited to using the same rigorous simulation software (i.e. Aspen HYSYS) or equation-based modelling environment (i.e. MATLAB). Most rigorous simulation software (e.g. Aspen Plus, Aspen Custom Modeller, Pro II, gPROMS) are capable of being connected with one or more modelling and optimisation environments (e.g. GAMS, Visual Basic).

One drawback of the approaches that include operational optimisation is that they are computationally expensive. The optimisations with SA needed 5 to 6 hours and with GS 15 to 16 hours on a computer with an Intel Core processor of 3.3 GHz and 8 GB of installed RAM memory. In the case studies, it is shown that to get confident results each algorithm should be run at least 3 times. Thus, at least 102 hours (i.e. over 4 days) are needed to get robust results. Plus, time and knowledge in programming are needed to connect rigorous simulation software with the equation-based modelling environment. However, once the system is set up, very little engineering effort is needed to simultaneously explore multiple retrofit modifications: e.g. changing the operating parameters of the distillation column, replacing the column internals in the constrained sections, adding a preflash unit and exploring structural changes to the HEN.

6.2 Conclusions — case studies

Chapter 3 presents a case study to illustrate the benefits of the methodology proposed to assess the impacts of increasing the crude oil throughput on the distillation column hydraulics, the HEN required heat transfer area and fired heating duty. This case study does not contemplate changing operating parameters of the distillation column (i.e. crude oil preheat temperature, stripping steam flow rates, and pumparound duties and temperature drops); these are simply increased pro rata with the crude oil feed. HEN retrofit (i.e. adding, deleting, repiping and resequencing heat exchangers) is also not considered.

Results from the case study reveal that the methodology is capable of assessing the suitability of different column internals for debottlenecking constrained sections. It is also shown that connecting rigorous simulation software with equation-based modelling software helps to reduce the engineering time and effort when exploring multiple retrofit scenarios.

Chapter 4 presents an industrially relevant case study to show the benefits of the proposed optimisation-based retrofit approach to increase the profitability of heat-integrated distillation systems when increasing their processing capacity. Constraints related to the distillation column hydraulic performance and to the quality of the products (in terms of the true boiling point temperature of the distillation products) are imposed during the optimisation. The suitability of replacing the internals to debottleneck the distillation column is systematically assessed: i.e. the system is optimised for a case where the column internals are the same as the base case and for a case where the internals in the most constrained section are replaced with structured packings.

Results from the case study show that the approach can capture the synergies between the distillation column and HEN, since changes to the operating conditions of the distillation column and to the HEN structure are explored and assessed simultaneously. It is also shown that the approach is useful to assess the effects of replacing the internals in the constrained sections of the distillation column on the distillation column hydraulics and its associated heat recovery system.

Chapter 5 presents two case studies that illustrate the benefits of including the options of replacing the column internals and adding a preflash unit within the optimisation framework.

The case study results of Publication 3 show that the benefits of exploring the suitability of different column internals within the optimisation are that the hydraulic bottlenecks of the distillation column can be identified and that the energy integration of the system can be more effectively exploited. The results of Publication 4 demonstrate that adding a preflash unit helps to increase the capacity of the distillation column, to ease the retrofit of the HEN and to reduce the fired heating duty. Including the structural design options associated with adding a preflash unit within the optimisation environment avoids the used of trial-and-error calculations and reduces the engineering effort.

6.3 Future work

The following future work can be proposed based on a critical analysis of the benefits, assumptions and limitations of the work presented in this thesis:

1. The proposed retrofit approach should be studied further to explore its suitability for assessing other retrofit objectives to increase profitability, such as changing the crude oil feedstock or the crude oil blend, which is an option commonly explored in practice (Thernesz et al., 2010; López C. et al., 2013).
2. The approach could be extended to consider prefractionation (using a distillation column), rather than only preflash units. This option has been proved to reduce energy consumption and to increase capacity (Wang et al., 2011).
3. The approach could be extended to assess beneficial retrofit modifications for increasing the capacity of other types of distillation columns with complex heat recovery systems, such a low-temperature separation systems (e.g. the ethylene separation process).
4. The HEN retrofit approach could be extended to consider pressure drop and heat transfer enhancement. Considering pressure drop may give a better estimation of the real heat recovery of the system; heat transfer enhancement may help to reduce the costs of adding heat transfer area (Akpomiemie and Smith, 2016).

References

Akpomiemie, M. O., Smith, R., 2016, Retrofit of heat exchanger networks with heat transfer enhancement based on an area ratio approach, Applied Energy, 165, 22-35, DOI: 10.1016/j.apenergy.2015.11.056.

Asante, N. D. K., Zhu, X. X., 1997, An automated and interactive approach for heat exchanger network retrofit, Chemical Engineering Research and Design, 75, 3, 349-360, DOI: 10.1205/026387697523660.

Aspen Tech, 2012, Aspen HYSYS, Version 7.3, Aspen Tech Inc, USA.

Binkley, M. J., Thorngren, J. T., Lewis, R. P., Grigson, W. W. 1992. *Contact tray assembly and method*. US Patent 5147584 A.

Branan, C. R., 2011, *Rules of Thumb for Chemical Engineers*, Elsevier Science, Burlington.

Caballero, J. A., Milán-Yañez, D., Grossmann, I. E., 2005, Optimal synthesis of distillation columns: Integration of process simulators in a disjunctive programming environment, Computer Aided Chemical Engineering, 20, 715-720, DOI: 10.1016/S1570-7946(05)80241-X.

Carlberg, N. A., Westerberg, A. W., 1989, Temperature-heat diagrams for complex columns. 2. Underwood's method for side strippers and enrichers, Industrial & Engineering Chemistry Research, 28, 9, 1379-1386, DOI: 10.1021/ie00093a017.

Cavazzuti, M., 2013, *Optimization Methods From Theory to Design Scientific and Technological Aspects in Mechanics* Heidelberg, Berlin.

Chen, L., 2008, *Heat-integrated Crude Oil Distillation System Design*, PhD Thesis, The University of Manchester, Manchester, UK.

Chen, Y., Eslick, J. C., Grossmann, I. E., Miller, D. C., 2015, Simultaneous process optimization and heat integration based on rigorous process simulations, Computers & Chemical Engineering, 81, 180-199, DOI: 10.1016/j.compchemeng.2015.04.033.

de Oliveira Filho, L. O., Queiroz, E. M., Costa, A. L. H., 2007, A matrix approach for steady-state simulation of heat exchanger networks, Applied Thermal Engineering, 27, 14-15, 2385-2393.

Department of Process Integration, 2002, SPRINT, Version 1.6, The University of Manchester, Manchester, UK.

Douglas, J. M., 1988, *Conceptual Design of Chemical Processes* McGraw-Hill, New York.

Enríquez-Gutiérrez, V. M., Jobson, M., 2016a, An optimisation-based retrofit approach for increasing the processing capacity of heat-integrated crude oil distillation systems, Chemical Engineering Research & Design, submitted May 2016.

Enríquez-Gutiérrez, V. M., Jobson, M., 2016b, An optimisation-based retrofit approach for the assessment of structural and flowsheet modifications for heat-integrated crude oil distillation systems. Part 1.- Replacing column internals, Chemical Engineering Research & Design, submitted May 2016.

Enríquez-Gutiérrez, V. M., Jobson, M., 2016c, An optimisation-based retrofit approach for the assessment of structural and flowsheet modifications for heat-integrated crude oil distillation systems. Part 2.- Adding a preflash unit, Chemical Engineering Research & Design, submitted May 2016.

Enríquez-Gutiérrez, V. M., Jobson, M., Ochoa-Estopier, L. M., Smith, R., 2015, Retrofit of heat-integrated crude oil distillation columns, Chemical Engineering Research and Design, 99, 185-198, DOI: 10.1016/j.cherd.2015.02.008.

Enríquez-Gutiérrez, V. M., Jobson, M., Smith, R., 2014, A design methodology for retrofit of crude oil distillation systems, Proceedings of the 24th European Symposium on

Computer Aided Process Engineering-ESCAPE24, Part A, 1549-1554, DOI: 10.1016/B978-0-444-63455-9.50093-3.
Errico, M., Tola, G., Mascia, M., 2009, Energy saving in a crude distillation unit by a preflash implementation, Applied Thermal Engineering, 29, 8-9, 1642-1647.
Fair, J. R., 1961, How to predict sieve tray entrainment and flooding, Petro. Chem. Eng., 33, 45.
Fenske, M. R., 1932, Ind. Eng. Chem., 24, 482-485.
Gadalla, M., Jobson, M., Smith, R., 2003a, Optimization of existing heat-integrated refinery distillation systems, Chemical Engineering Research and Design, 81, 1, 147-152.
Gadalla, M., Jobson, M., Smith, R., 2003b, Shortcut models for retrofit design of distillation columns, Chemical Engineering Research and Design, 81, 8, 971-986.
Gadalla, M., Kamel, D., Ashour, F., din, H. N. E., 2013, A new optimisation based retrofit approach for revamping an Egyptian crude oil distillation unit, Energy Procedia, 36, 0, 454-464, DOI: 10.1016/j.egypro.2013.07.051.
Gadalla, M. A., 2003, *Retrofit Design of Heat-integrated Crude Oil Distillation Systems*, PhD Thesis, The University of Manchester, Manchester, UK.
Gadalla, M. A., Abdelaziz, O. Y., Kamel, D. A., Ashour, F. H., 2015, A rigorous simulation-based procedure for retrofitting an existing Egyptian refinery distillation unit, Energy, 83, 0, 756-765, DOI: 10.1016/j.energy.2015.02.085.
Gary, J. H., 2007, *Petroleum Refining: Technology and Economics*, Taylor & Francis, Boca Raton, USA.
Gilliland, E., 1940, Multi-component rectification. Estimation of the number of theoretical plates a a function of the reflux ratio., Ind. Eng. Chem. Res., 32, 1220.
Green, D. W., Perry, R. H., 2007, *Perry's Chemical Engineers' Handbook*, McGraw-Hill Professional, New York, USA.
Hansen, N., 2006, The CMA Evolution Strategy: A Comparing Review, *Towards a New Evolutionary Computation: Advances in the Estimation of Distribution Algorithms*, Springer, Berlin, Heidelberg, 75-102.
Invensys Process Systems, 2005, PRO/II, Version7.1, Invensys process systems, Plano.
Jeżowski, J. M., Shethna, H. K., Castillo, F. J. L., 2003, Area Target for Heat Exchanger Networks Using Linear Programming, Industrial & Engineering Chemistry Research, 42, 8, 1723-1730, DOI: 10.1021/ie020643i.
KBC Energy Services, 2005, SUPERTARGET, Version 6.0, KBC Energy Services, Chesire, UK.
Khalil, A. M., Goswamy, V., Busaleh, H. A., Al-Khaldi, H. A., Hood, T., 2004, High-capacity trays hike demeth capacity, efficiency at two Middle East gas plants, Oil and Gas Journal, 102, 46, 50-55.
Kister, H. Z., 1992, *Distillation Design* McGraw-Hill, Boston, USA.
Kister, H. Z., Gill, D. R., 1992, Flooding and pressure drop prediction for structured packings, IChemE Symp. Ser, 128, A109-A123.
Kister, H. Z., Haas, J. R., 1990, Predict entrainment flooding on sieve and valve trays, Chemical Engineering Progress, 86, 9, 63-69.
Kister, H. Z., Hanson, D. W., Morrison, T., 2002, California refiner identifies crude tower instability using root cause analysis, Oil and Gas Journal, 100, 7, 42-48.
Kister, H. Z., Scherffius, J., Afshar, K., Abkar, E., 2007, Realistically predict capacity and pressure drop for packed columns, Chemical Engineering Progress, 103, 7, 28-38.
Koch-Glitsch, 2005, KG-Tower, Version 2.0, Koch-Glitsch LP, Wichita, USA.
Koch-Glitsch, 2013, Glitsch Ballast Tray Design Manual: Bulletin No. 4900 [Online]: Koch-Glitsch, L.P., Available: http://www.koch-glitsch.com/Document%20Library/Bulletin-4900.pdf [Accessed October 2014].
Koch-Glitsch, 2014a, High performance trays [Online], Available: http://www.koch-glitsch.com/masstransfer/pages/high_performance_trays.aspx [Accessed February 2014].

Koch-Glitsch, 2014b, KG-Tower, version 5.2, Koch-Glitsch LP, USA.
Koch-Glitsch, 2016, Structured packing [Online], Available: http://www.koch-glitsch.com/Document%20Library/KGSP.pdf [Accessed January 2016].
Lee, A. T., Wu, K., Burton, L., Fan, L. 1999. *Downcomer for chemical process tower*. US Patent 6003847 A.
Liebmann, K., Dhole, V. R., Jobson, M., 1998, Integrated design of a conventional crude oil distillation tower using pinch analysis, Chemical Engineering Research and Design, 76, 3, 335-347, DOI: 10.1205/026387698524767.
Linnhoff, B., Flower, J. R., 1978, Synthesis of heat exchanger networks: I. Systematic generation of energy optimal networks, AIChE Journal, 24, 4, 633-642, DOI: 10.1002/aic.690240411.
Linnhoff, B., Hindmarsh, E., 1983, The pinch design method of heat exchanger networks, Chem Eng Sci, 38, 745-763.
Liu, Z. Y., Jobson, M., 2004, Retrofit design for increasing the processing capacity of distillation columns: 1. A Hydraulic performance indicator, Chemical Engineering Research and Design, 82, 1, 3-9.
López C., D. C., Hoyos, L. J., Mahecha, C. A., Arellano-Garcia, H., Wozny, G., 2013, Optimization model of crude oil distillation units for optimal crude oil blending and operating conditions, Industrial & Engineering Chemistry Research, 52, 36, 12993-13005, DOI: 10.1021/ie4000344.
Miller, D. C., Ng, B., Eslick, J. C., Tong, C., Chen, Y., 2014, Computational tools for accelerating carbon capture process development, Proceedings of the 8th international conference on foundations of computer-aided process design - FOCAD 2014, 2014.
Ochoa-Estopier, L. M., 2014, *Optimisation of Existing Heat-integrated Crude Oil Distillation Systems*, PhD Thesis, The University of Manchester, Manchester, UK.
Ochoa-Estopier, L. M., Jobson, M., 2015a, Optimisation of heat-integrated crude oil distillation systems. Part I: The distillation model, Industrial & Engineering Chemistry Research, 54, 18, 4988-5000, DOI: 10.1021/ie503802j.
Ochoa-Estopier, L. M., Jobson, M., 2015b, Optimization of heat-integrated crude oil distillation systems. Part I: The distillation model, Industrial & Engineering Chemistry Research, 54, 18, 4988-5000, DOI: 10.1021/ie503802j.
Ochoa-Estopier, L. M., Jobson, M., Chen, L., Rodríguez, C., Smith, R., 2015a, Optimisation of heat-integrated crude oil distillation systems. Part II: Heat exchanger network retrofit model, Industrial & Engineering Chemistry Research, 54, 18, 5001-5017, DOI: 10.1021/ie503804u.
Ochoa-Estopier, L. M., Jobson, M., Smith, R., 2014, The use of reduced models for design and optimisation of heat-integrated crude oil distillation systems, Energy, 75, 5-13, DOI: 10.1016/j.energy.2014.06.043.
Ochoa-Estopier, L. M., Jobson, M., Smith, R., 2015b, Optimisation of heat-integrated crude oil distillation systems. Part III: Optimisation framework, Industrial & Engineering Chemistry Research, 54, 18, 5018-5036, DOI: 10.1021/ie503805s.
Papoulias, S. A., Grossmann, I. E., 1983, A structural optimization approach in process synthesis—II, Computers & Chemical Engineering, 7, 6, 707-721, DOI: 10.1016/0098-1354(83)85023-6.
Penciak, J., Nieuwoudt, I., Spencer, G., 2006, High-performance trays: getting the best capcity and efficiency, Distillation and Absorption Symposium Series, 152, 311-316.
Rapoport, H., Lavie, R., Kehat, E., 1994, Retrofit design of new units into an existing plant: Case study: Adding new units to an aromatics plant, Computers and Chemical Engineering, 18, 8, 743-753.
Rastogi, V., 2006, *Heat-integrated Crude Oil Distillation System Design*, PhD, The University of Manchester, Manchester, UK.
Resetarits, M. R., 2010, Propelling distillation research, Chemical Engineering, 117, 6, 26-27.

Resetarits, M. R., 2014, Chapter 2 - Distillation Trays, *In:* Distillation: Equipment and Processes, ed. *Olujić, A.G.*, Academic Press, Boston, USA.
Rodriguez, C. A., 2005, *Fouling Mitigation Strategies for Heat Exchanger Networks*, PhD Thesis, The University of Manchester, Manchester, UK.
Sathyanarayanamurthy, H., Chinnam, R. B., 2009, Metamodels for variable importance decomposition with applications to probabilistic engineering design, Computers & Industrial Engineering, 57, 3, 996-1007, DOI: 10.1016/j.cie.2009.04.003.
Shenoy, U. V., 1995, *Heat Exchanger Network Synthesis*, Gulf Publishing Company, Houston, Texas.
Shojaee, S., Hosseini, S. H., Rafati, A., Ahmadi, G., 2011, Prediction of the effective area in structured packings by computational fluid dynamics, Industrial and Engineering Chemistry Research, 50, 18, 10833-10842.
Smith, R., 2005, *Chemical Process Design and Integration*, John Wiley & Sons, Ltd., Chichester, UK.
Smith, R., Jobson, M., Chen, L., 2010a, Recent development in the retrofit of heat exchanger networks, Applied Thermal Engineering, 30, 16, 2281-2289.
Smith, R., Jobson, M., Chen, L., Farrokhpanah, S., 2010b, Heat integrated distillation systems design, Chemical Engineering Transactions, 21, 19-24, DOI: 10.3303/CET1021004.
Stichlmair, J., 1998, *Distillation: Principles and Practice*, Wiley-VCH, New York, USA.
Sulzer, 2014, High performance trays [Online], Available: http://www.sulzer.com/en/Products-and-Services/Separation-Technology/High-Performance-Trays [Accessed February 2014].
Sulzer Chemtech, 2005, SULCOL, Version 1.0, Sulzer Chemtech, Winterhur.
Suphanit, B., 1999, *Design of Complex Distillation Systems*, PhD Thesis, UMIST Department of Process Integration, Manchester, UK.
Szklo, A., Schaeffer, R., 2007, Fuel specification, energy consumption and CO2 emission in oil refineries, Energy, 32, 7, 1075-1092, DOI: 10.1016/j.energy.2006.08.008.
Thernesz, A., Varga, Z., Rabi, I., Czaltig, Z., Lörincova, M., 2010, Applying process design software for capacity increase and revamp of distillation units, Clean Technologies and Environmental Policy, 12, 2, 97-103.
Treese, S. A., Pujadó, P. R., Jones, D. S. J., 2015, *Handbook of Petroleum Processing*, Springer Energy ebooks 2015, DOI: 10.1007/978-3-319-14529-7.
Uerdingen, E., Fischer, U., Hungerbühler, K., Gani, R., 2003, Screening for profitable retrofit options of chemical processes: A new method, AIChE Journal, 49, 9, 2400-2418.
Underwood, V., 1948, Fractional distillation of multi-component mixtures., Chemical Engineering Progress, 44, 603.
Wang, Y., Hou, Y., Gao, H., Sun, J., Xu, S., 2011, Selecting the optimum predistillation scheme for heavy crude oils, Industrial and Engineering Chemistry Research, 50, 18, 10549-10556.
Watkins, R. N., 1979, *Petroleum Refinery Distillation*, Gulf Pub. Co., Book Division, Houston, USA.
Yeoman, N., Griffith, V. E., Hsieh, C.-L. 1997. *Vapor-liquid contact tray and downcomer assembly and method employing same*. US Patent 5632935 A.
Yeoman, N., Griffith, V. E., Hsieh, C. 1996. *Vapor-liquid contact tray and downcomer assembly and method employing same*. US Patent 5480595 A.
Zhu, X. X., Asante, N. D. K., 1999, Diagnosis and optimization approach for heat exchanger network retrofit, AIChE Journal, 45, 7, 1488-1503, DOI: 10.1002/aic.690450712.
Zobel, C. W., Keeling, K. B., 2008, Neural network-based simulation metamodels for predicting probability distributions, Computers & Industrial Engineering, 54, 4, 879-888, DOI: 10.1016/j.cie.2007.08.012.

Appendix A Conference paper presented in ESCAPE 2014

Enríquez-Gutiérrez, V. M., Jobson, M., Smith, R., 2014, A design methodology for retrofi of crude oil distillation systems, Proceedings of the 24th European Symposium on Computer Aided Process Engineering-ESCAPE24, Part A, 1549-1554.

Jiří Jaromír Klemeš, Petar Sabev Varbanov and Peng Yen Liew (Editors)
Proceedings of the 24th European Symposium on Computer Aided Process Engineering – ESCAPE 24
June 15-18, 2014, Budapest, Hungary.

A Design Methodology for Retrofit of Crude Oil Distillation Systems

Víctor M. Enríquez-Gutiérrez*, Megan Jobson, Robin Smith

Centre for Process Integration, School of Chemical Engineering and Analytical Science, The University of Manchester, Manchester, UK
victormanuel.enriquezgutierrez@postgrad.manchester.ac.uk

Abstract

Retrofit of crude oil distillation systems is a non-trivial problem with many degrees of freedom and constraints. This work proposes a systematic retrofit methodology for increasing the throughput to crude oil distillation systems, embedded in a computational tool with mass and energy balance results from rigorous simulations, hydraulic correlations for valve trays and structured packings and a retrofit model for heat exchanger networks. The feasibility of retrofit options is assessed against constraints related to product specifications, jet flooding and liquid load per weir length in the main fractionator and side strippers and the required area for heat exchangers in the heat exchanger network (HEN). The methodology is applied to an existing crude oil distillation system; the results show the impact of increasing throughput on column hydraulics and heat transfer area requirements. Retrofit solutions are proposed for relieving hydraulic bottlenecks and minimizing impact on the HEN by varying column operating conditions.

Keywords: Crude oil distillation retrofit, HEN retrofit, hydraulic design

1. Introduction

The crude oil distillation system consists of an atmospheric distillation unit, in which crude oil is separated into more valuable products, and a heat exchanger network (HEN) which pre-heats the crude oil before it enters the column. The atmospheric distillation unit and the HEN interact with each other, making the retrofit of crude oil distillation systems a complex problem requiring analysis of column hydraulics and HEN performance.

Retrofit aims to increase the profitability of the process by maximizing the use of existing equipment. Examples of retrofit objectives are increasing the throughput, changing the feedstock, increasing the production or the quality of the products and reducing the energy demand or atmospheric emissions. (Liu and Jobson, 2004).

Gadalla et al. (2003a) developed a retrofit methodology for atmospheric crude oil distillation columns and associated HENs. The distillation columns are evaluated using shortcut models for retrofit design (Gadalla et al., 2003b) and retrofit models were used for the HEN. However, the shortcut distillation models cannot identify bottlenecks within the main column and side strippers. Although the diameter required to avoid entrainment flooding is used as hydraulic indicator, the effect of pressure drop and liquid loads inside the column are neglected. In the HEN retrofit model constant stream properties were assumed. Smith et al. (2010) extended and modified the HEN retrofit methodology by considering temperature dependent thermal properties.

Liu and Jobson (2004) developed a hydraulic indicator, the "fractional utilization of area" (FUA), defined as the ratio between the area required for vapour flow in the column and the available area. A useful graphical tool was developed to identify capacity bottlenecks for distillation columns and screen retrofit solutions. This parameter was applied to evaluate alternative solutions with respect to capacity enhancement. Wei et al. (2012) proposed the utilization of FUA together with a new hydraulic indicator, the maximum capacity expansion (x_{max}), to screen hydraulic bottlenecks when increasing capacity. Determining the FUA and x_{max} requires rigorous distillation simulation results. The key shortcoming of these methods is that they only account for jet flooding.

Thernesz et al. (2010) used process design software to evaluate retrofit modifications in crude oil distillation systems. PRO II v7.1 (2005) was used to simulate the distillation column, SULCOL v1.0 (2005) and KG-TOWER v2.02 (2005) evaluated the hydraulic design and SUPERTARGET v6.0 (2005) analyzed the performance of the HEN. However, the software was applied sequentially for each proposed modification, requiring significant engineering resources to screen the many design options.

Kamel et al. (2013) developed a retrofit methodology for crude oil distillation systems in which rigorous simulation and optimisation procedures are used to optimise the process conditions and to explore structural modifications to the flowsheet in order to increase the capacity and the energy efficiency of the system. However, this methodology does not account the effects of the capacity enhancement to the column hydraulics.

Therefore, the retrofit of heat- integrated crude oil systems needs to consider both the distillation columns and the HEN and their capacity constraints. Furthermore, the impact of changing distillation operating conditions or equipment on the HEN should be assessed. This work develops a systematic retrofit methodology, considering the interactions between operating parameters, the hydraulic performance of the distillation column and the heat transfer performance of the HEN for crude oil distillation systems. This work focuses on increasing throughput, where capacity limits (jet flooding and downcomer flooding) in the column and heat transfer area constraints in the HEN are avoided.

2. Retrofit methodology

Figure 1 represents the proposed methodology which employs converged simulations of the atmospheric distillation column (using Aspen HYSYS v7.3, 2012) and Matlab code which can exchange inputs and outputs with the simulator.

The column is simulated at the desired increased throughput. Then the simulation results (stage-by-stage flow rates and physical properties) are read by Matlab and used as inputs for column hydraulic calculations. Next, the stream data (temperatures, flow rates and enthalpy changes) are used as inputs to the HEN retrofit model, which is also embedded in Matlab. Feasibility is checked in terms of product specifications, hydraulic constraints and heat exchange area requirements in the HEN. The simulation inputs are then modified to address infeasibilities and this sequence of calculations is repeated.

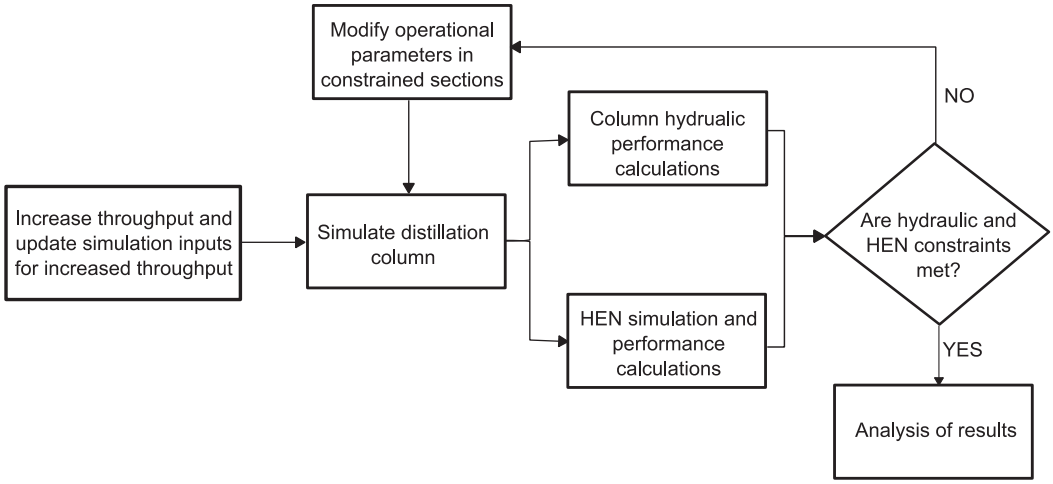

Figure 1. Proposed retrofit methodology for crude oil distillation systems

2.1. Hydraulic methodology

Distillation columns containing trays can operate efficiently only within certain limits. The upper limit of the vapour flow rate is related to jet flooding, which occurs when the vapour rate is high enough to carry over liquid to the stage above. The upper limit of the liquid flow rate is related to downcomer flooding: in this case, the liquid flow rate in the downcomer is too high to allow the vapour in the downcomer to disengage, leading to entrained vapour being carried to the tray below (Stichlmair, 1998, Chap. 8.2).

The percent of flooding is defined in Eq. (1) as the ratio of the C-factor at the operating conditions of interest to that under flooding conditions (Kister et al., 2007). A maximum value of 80 % is assumed in line with design practice. To predict jet flooding, the correlation of Kister and Haas (1990) is used to predict the flooding C- factor $C_{sb(flooding)}$. Downcomer flooding is evaluated in terms of liquid load per weir length L_w using Eq. (2) (Stichlmair, 1998, Chap. 8.2) where V_L is the volumetric flow rate of the liquid in m^3 h^{-1}, l_w is the weir length in m and N_p is the number of passes per tray. A limit of 110 m^3 m^{-1} h^{-1} is assumed, as this value is typically applied in practice (Resetarits, 2010).

$$\%Flooding = \left(C_{sb} / C_{sb(flooding)}\right) \cdot 100\% \tag{1}$$

$$L_w = \frac{V_L}{l_w N_p} \tag{2}$$

For distillation columns containing structured and random packings, the flood point is defined by the pressure drop at which the liquid is no longer able to flow (Stichlmair, 1998, Chap. 8.3). In this work, to estimate the capacity parameter at flooding conditions $CP_{flooding}$ a correlation is proposed, regressed from the pressure drop correlation chart for structured and random packings of Kister and Gill (cited by Kister et al., 2007). The regressed model is given in Eq. (3), where A and B are functions of the pressure drop, estimated using Eqs. (4) and (5) for structured packings and Eqs. (6) and (7) for random packings. The definitions of the capacity parameter $CP_{flooding}$ and flow parameter F_{lv} are presented in Kister et al. (2007). Eq. (1) is also applied in order to predict the percent of flooding. The pressure drop is predicted using the correlation of Rocha et al. (1993).

$$CP_{flooding} = A\ln(F_{lv}) + B \tag{3}$$

$$A = -7.31x10^{-11}\Delta P^3 + 2.18x10^{-7}\Delta P^2 - 2.19x10^{-4}\Delta P - 0.0124 \tag{4}$$

$$B = 1.28x10^{-10}\Delta P^3 - 3.15x10^{-7}\Delta P^2 + 2.62x10^{-4}\Delta P + 0.0826 \tag{5}$$

$$A = 6.82x10^{-8}\Delta P^2 - 1.48x10^{-4}\Delta P - 0.0063 \tag{6}$$

$$B = 2.55x10^{-10}\Delta P^3 - 6.09x10^{-7}\Delta P^2 + 4.70x10^{-4}\Delta P + 0.0882 \tag{7}$$

Eq. (3) is only valid between flow parameters from 0.03 to 0.3. The pressure drop is given in Pa m^{-1}.

2.2. HEN retrofit methodology

This work simulates the HEN using the model of Ochoa-Estopier et al. (2013) which extends the approach of de Oliveira Filho et al. (2007) by specifying each heat exchanger in terms of heat load and considering heat capacities as temperature-dependent and uses the approach of Smith et al. (2010) is applied to identify and evaluate HEN retrofit options.

3. Case Study

The distillation system used to illustrate the proposed methodology comprises an atmospheric distillation column and its corresponding HEN (Figure 2). The atmospheric distillation unit consists of a main fractionator, three side-strippers (SS), three pump-arounds (PA) and one condenser. The column processes 100,000 bbl d^{-1} (0.23 m^3 s^{-1}) of Venezuela Tía Juana Light crude (Watkins, 1979) into five products: residue (RES), light naphtha (LN), heavy naphtha (HN), heavy distillate (HD) and light distillate (LD). The operating conditions, stage distribution and product specifications of the atmospheric distillation unit are those presented by Chen (2008, Chap. 6.1). The HEN has 22 heat exchangers with a total heat transfer area of 5325 m^2; the demand for fired heating is 55.4 MW. Heat exchanger details and process and stream data are given by Chen (2008, Appendix C). Column internals are assumed to be standard valve trays for all sections except for Section 3 which is assumed to use Flexipac 3.5Y structured packing. The retrofit methodology was applied stepwise for throughput increases of 5% until the flooding or liquid load limits were reached. Pump-around flow rates in constrained sections were varied and the impact of these modifications on the HEN were analysed. Throughout the study, product specifications, expressed in terms of TBP5 and TBP95, were maintained.

4. Results

Figure 3 presents hydraulic profiles for the atmospheric distillation column for the base case and for throughput increases of 5 % to 25 %.

It is observed that a 25 % increase creates two hydraulic bottlenecks: jet flooding in Section 2 (82 % of flooding) and downcomer flooding in Section 1 (liquid load per weir length is 110.5 m^3 m^{-1} h^{-1}). The HEN was simulated and optimised; results show that

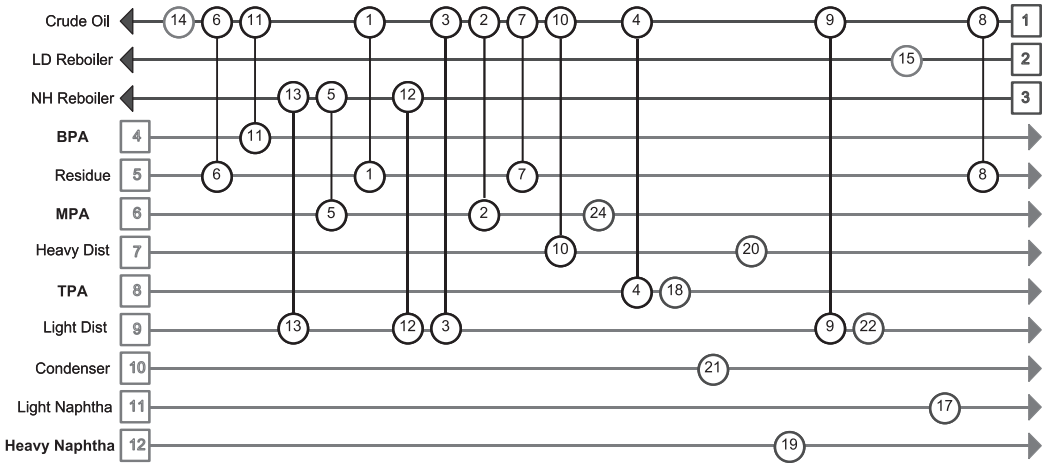

Figure 2. Case study: Existing heat exchanger network (Chen, 2008).

fifteen heat exchangers will require additional area (2012 m^2 in total). After HEN optimisation, the demand for fired heating increases by 32 % to 73.5 MW.

To debottleneck the column for a throughput increase of 25 %, two scenarios were considered, namely changing the flow rates of pump-arounds MPA and BPA. It is found that a 10 % reduction in the flow rate of MPA reduces flooding in Section 2 to 79.7 %, but the modification had no significant effect on Section 1. However, reducing the flow rate of TPA by 10 % relieves both bottlenecks (79.6 % flooding in Section 2 and a liquid load per weir length of 102.2 m^{-1} h^{-1} in Section 1). At this new operating condition, 13 heat exchangers require additional area (2678 m^2 in total) and the demand for fire heating increases slightly, to 74.8 MW. It is observed that the modified pump-around flow rate have little effect on the hydraulic performance of the side strippers.

5. Conclusions

The case studied illustrates the benefit of the proposed methodology to screen and evaluate retrofit options to increase the throughput of crude oil distillation systems.

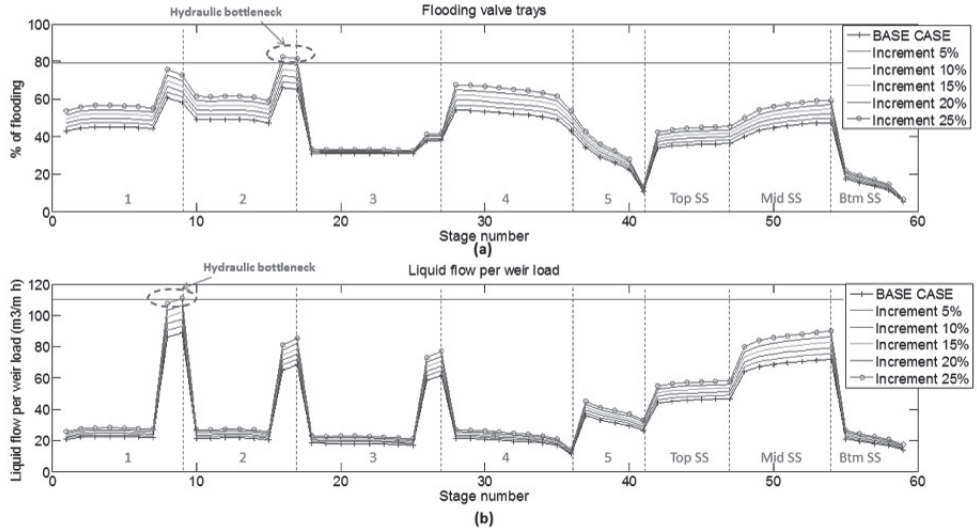

Figure 3. Hydraulic profiles: (a) Flooding profile in main column and side strippers; (b) Liquid loading profile in main column and side strippers.

The methodology can be applied to distillation columns containing trays and/or structured packings, and accounts for the impact of operational changes on the HEN. In this case study, the distillation column could accommodate throughput increases less than 25 % without encountering hydraulic bottlenecks. However, the HEN would require some retrofitting.

It was observed that reducing the pump-around flow rate in constrained sections can reduce flooding and the liquid load per weir length, but reduce heat recovery; as a result, the HEN require more additional area. The methodology also assessed impact of the operational changes on the hydraulic performance in other parts of the column too. Cost- benefit analysis would be needed to further evaluate the retrofit solutions.

References

L. Chen, 2008, Heat-integrated crude oil distillation system design, PhD. Thesis, The University of Manchester, Manchester, UK.

L. O. de Oliveira Filho, E. M. Queiroz, A. L. H. Costa, 2007, A matrix approach for steady-state simulation of heat exchanger networks, Applied Thermal Engineering, 27, 14-15, 2385-2393.

D. Kamel, M. Gadalla, F. Ashour, 2013, New retrofit approach for optimisation and modification for a crude oil distillation system, Chemical Engineering Transactions, 35, 1363-1368

M. Gadalla, M. Jobson, R. Smith, 2003a, Optimization of existing heat-integrated refinery distillation systems, Chemical Engineering Research and Design, 81, 1, 147-152.

M. Gadalla, M. Jobson, R. Smith, 2003b, Shortcut models for retrofit design of distillation columns, Chemical Engineering Research and Design, 81, 8, 971-986.

H.Z. Kister, J. R. Haas, 1990, Predict entrainment flooding on sieve and valve trays, Chemical Engineering Progress, 86, 9, 63-69.

H. Z. Kister, J. Scherffius, K. Afshar, E. Abkar, 2007, Realistically predict capacity and pressure drop for packed columns, Chemical Engineering Progress, 103, 7, 28-38.

Z. Liu, M. Jobson, 2004, Retrofit design for increasing the processing capacity of distillation columns: 1. A hydraulic performance indicator, Chemical Engineering Research and Design, 82, 1, 3-9.

L. M. Ochoa-Estopier, M. Jobson, R. Smith, 2013, Retrofit of heat exchanger networks for optimising crude oil distillation operation, Chemical Engineering Transactions, 35, 133-138.

M. Resetarits, 2010, Propelling distillation research, Chemical Engineering, 117, 6, 26-27.

J.A. Rocha, J.L. Bravo, J. R. Fair, 1993, Distillation columns containing structured packings: A comprenhensive model for their performance. 1. Hydraulic models, Industrial and Engineering Chemistry Research, 32, 4, 641-651.

R. Smith, M. Jobson, L. Chen, 2010, Recent development in the retrofit of heat exchanger networks, Applied Thermal Engineering, 30, 16, 2281-2289.

J. Stichlmair, 1998, Distillation: Principles and practice, Wiley-VCH, New York, USA.

A. Thernesz, Z. Varga, I. Rabi, Z. Czaltig, M. Lörincova, 2010, Applying process design software for capacity increase and revamp of distillation units, Clean Technologies and Environmental Policy, 12, 2, 97-103.

R.N. Watkins, 1979, Petroleum Refinery Distillation, Gulf Pub. Co., Houston, USA.

Z. Q. Wei, B. J. Zhang, S. Y. Wu, Q. L. Chen, C. W. Hui, 2012, A hydraulics-based heuristic strategy for capacity expansion retrofit of distillation systems and an industrial application on a light-ends separation plant, Chemical Engineering Research and Design, 90, 1527-153.

Appendix B Supporting Information for Publications 2, 3 and 4

B.1 Supporting Information for Publication 2

Enríquez-Gutiérrez, V. M., Jobson, M., 2016, An optimisation-based retrofit approach for increasing the processing capacity of heat-integrated crude oil distillation systems, Industrial & Engineering Chemistry Research, under preparation.

Supporting information

This document presents supporting information for the paper entitled: *An optimisation-based retrofit approach for increasing the processing capacity of heat-integrated crude oil distillation systems* [1].

S1. Supporting information and tables for Case 1

1.1. Required additional heat transfer area for Case 1

Table S1.1 HEN required additional heat transfer area for Case 1 — 30% increase pro rata

Heat exchanger number	Additional area required m^2
	Case 1
h1	82
h2	774
h3	127
h4	844
h5	152
h6	126
h7	265
h8	173
h9	0
h10	0
h11	273
h12	44
h13	0
h14*	14
h15*	2
h17*	16
h18*	0
h19*	39
h20*	40
h21*	306
h22*	53
h24*	0
Total additional area, m^2	3331
No. of heat exchangers needing modifications	17

* Utility exchangers

1.2. Product quality results for Case 1

Table S1.2 Product quality results for Case 1— 30% increase pro rata

Specification	Product	Base Case	Case 1	
		Value	Value	Diff*
T5 (℃, volume)	LN	3	2	-1
	HN	117	117	0
	LD	190	190	0
	HD	285	285	0
	RES	353	353	0
T95 (℃, volume)	LN	122	122	0
	HN	210	209	1
	LD	310	310	0
	HD	364	363	1
	RES	804	803	1

* Diff = difference with respect to base case value

1.3. Distillation column hydraulic results for Case 1

Table S1.3 Hydraulic results for Case 1 — 30% increase pro rata

	Section	Case 1
Jet flooding, %	**Section 1**	79.8
	Section 2	79.9
	Section 3	74.3
	Section 4	73.4
	Section 5	74.4
	Top SS	42.9
	Mid SS	61.2
	Btm SS	55.7
Weir load, $m^3\ m^{-1}\ h^{-1}$	**Section 1**	—
	Section 2	85.7
	Section 3	87.1
	Section 4	66.2
	Section 5	97.8
	Top SS	42.9
	Mid SS	63.8
	Btm SS	35.8
Downcomer exit velocity, $m\ s^{-1}$	**Section 1**	—
	Section 2	0.4
	Section 3	0.4
	Section 4	0.4
	Section 5	0.4
	Top SS	0.3
	Mid SS	0.4
	Btm SS	0.2
Downcomer flooding, %	**Section 1**	—
	Section 2	74.1
	Section 3	78.2
	Section 4	73.9
	Section 5	75.8
	Top SS	44.3
	Mid SS	61.0
	Btm SS	53.0

— = parameter non applicable for the packed sections of the column

Limit for approach to jet flooding (conventional trays and high-capacity trays) = 80%
Limit for liquid weir load = 90 $m^3\ m^{-1}\ h^{-1}$
Limit for downcomer exit velocity = 0.46 $m\ s^{-1}$
Limit for approach to downcomer flooding = 80%
Limit for approach flooding (structured packings) = 80%

S2. Supporting information and tables for Case 2

1.1. Operational optimisation results for Case 2

Table S2.1 Optimisation results for Case 2 using SA

Parameter	First optimisation	Second optimisation	Third optimisation
Main steam flow rate, kmol h^{-1}	1440.2	1407.8	1163.7
Btm SS steam flow rate, kmol h^{-1}	397.4	375.7	350.7
Furnace outlet temperature, ℃	350.3	350.5	365.6
PA1 heat flow, MW	13.2	15.1	10.5
PA2 heat flow, MW	24.0	16.8	24.8
PA3 heat flow, MW	12.4	12.1	18.1
PA1 ΔT, ℃	23.8	36.8	93.7
PA2 ΔT, ℃	50.4	96.9	52.5
PA3 ΔT, ℃	37.7	75.9	52.2

Table S2.2 Optimisation results for Case 2 using GS

Parameter	First optimisation	Second optimisation	Third optimisation
Main steam flow rate, kmol h^{-1}	1466.7	1296.6	1095.1
Btm SS steam flow rate, kmol h^{-1}	382.4	317.5	367.5
Furnace outlet temperature, ℃	350.6	353.7	358.4
PA1 heat flow, MW	11.0	12.7	12.9
PA2 heat flow, MW	20.2	22.9	26.3
PA3 heat flow, MW	11.5	11.0	12.4
PA1 ΔT, ℃	53.3	25.6	67.9
PA2 ΔT, ℃	64.4	85.0	64.9
PA3 ΔT, ℃	47.3	29.1	44.6

1.2. Distillation column hydraulic results for Case 2

Table S2.3 Hydraulic results for Case 2 using SA

	Section	First optimisation	Second optimisation	Third optimisation
Jet flooding, %	**Section 1**	54.7	59.3	48.3
	Section 2	63.6	62.4	62.8
	Section 3	56.8	55.1	59.0
	Section 4	48.1	48.0	52.9
	Section 5	42.8	42.6	45.8
	Top SS	28.1	27.1	28.1
	Mid SS	36.9	37.7	37.0
	Btm SS	18.7	18.5	18.0
Weir load, m^3 m^{-1} h^{-1}	**Section 1**	91.5	83.0	44.6
	Section 2	84.5	57.1	85.2
	Section 3	56.9	42.7	64.4
	Section 4	19.6	19.7	26.4
	Section 5	84.9	84.6	88.0
	Top SS	49.0	47.0	48.8
	Mid SS	70.5	71.8	70.6
	Btm SS	29.0	29.6	28.4
Downcomer exit velocity, m s^{-1}	**Section 1**	0.4	0.4	0.2
	Section 2	0.4	0.3	0.4
	Section 3	0.3	0.2	0.3
	Section 4	0.1	0.1	0.1
	Section 5	0.4	0.4	0.4
	Top SS	0.2	0.2	0.2
	Mid SS	0.3	0.3	0.3
	Btm SS	0.1	0.1	0.1
Downcomer flooding, %	**Section 1**	47.6	43.2	23.2
	Section 2	44.0	29.7	44.3
	Section 3	27.7	20.8	31.4
	Section 4	9.6	9.6	12.9
	Section 5	50.4	50.2	52.2
	Top SS	45.7	43.8	45.6
	Mid SS	65.8	67.0	65.9
	Btm SS	27.1	27.6	26.5

Limit for approach to jet flooding (conventional trays and high-capacity trays) = 80%
Limit for liquid weir load = 90 m^3 m^{-1} h^{-1}
Limit for downcomer exit velocity = 0.46 m s^{-1}
Limit for approach to downcomer flooding = 80%
Limit for approach flooding (structured packings) = 80%

Table S2.4 Hydraulic results for Case 2 using GS

	Section	First optimisation	Second optimisation	Third optimisation
Jet flooding, %	**Section 1**	55.6	56.6	48.3
	Section 2	64.2	62.9	63.0
	Section 3	56.8	57.4	56.8
	Section 4	48.7	48.3	48.3
	Section 5	43.3	42.6	42.1
	Top SS	27.4	27.1	27.9
	Mid SS	37.5	38.3	36.7
	Btm SS	18.5	16.7	19.0
Weir load, m^3 m^{-1} h^{-1}	**Section 1**	59.0	88.5	53.0
	Section 2	71.2	67.9	80.3
	Section 3	50.2	61.7	55.0
	Section 4	20.2	20.4	21.6
	Section 5	85.3	84.8	84.2
	Top SS	47.6	47.2	48.5
	Mid SS	71.4	73.0	69.9
	Btm SS	29.2	28.0	30.7
Downcomer exit velocity, m s^{-1}	**Section 1**	0.3	0.4	0.2
	Section 2	0.3	0.3	0.4
	Section 3	0.2	0.3	0.3
	Section 4	0.1	0.1	0.1
	Section 5	0.4	0.4	0.4
	Top SS	0.2	0.2	0.2
	Mid SS	0.3	0.3	0.3
	Btm SS	0.1	0.1	0.1
Downcomer flooding, %	**Section 1**	30.7	46.1	27.6
	Section 2	37.0	35.3	41.8
	Section 3	24.5	30.1	26.8
	Section 4	9.8	10.0	10.5
	Section 5	50.6	50.3	50.0
	Top SS	44.4	44.0	45.3
	Mid SS	66.6	68.1	65.3
	Btm SS	27.2	26.1	28.6

Limit for approach to jet flooding (conventional trays and high-capacity trays) = 80%
Limit for liquid weir load = 90 m^3 m^{-1} h^{-1}
Limit for downcomer exit velocity = 0.46 m s^{-1}
Limit for approach to downcomer flooding = 80%
Limit for approach flooding (structured packings) = 80%

1.3. Required additional heat transfer are for Case 2

Table S2.5 HEN required additional heat transfer area for Case 2 using SA

Heat exchanger number	Additional area required m^2		
	Fist optimisation	**Second optimisation**	**Third optimisation**
h1	74	0	0
h2	1121	23	1021
h3	120	138	128
h4	156	925	16
h5	86	106	212
h6	34	602	402
h7	414	0	427
h8	25	177	41
h9	0	0	59
h10	0	93	22
h11	188	-40	469
h12	0	19	0
h13	25	0	0
h14*	3	19	9
h15*	2	2	2
h17*	16	17	16
h18*	0	0	30
h19*	44	37	44
h20*	46	36	35
h21*	225	304	178
h22*	16	58	1
h24*	0	23	0
Total additional area, m^2	2592	2540	3110
No. of heat exchanger needing modifications	17	16	18

* Utility exchangers

Table S2.6 HEN required additional heat transfer area for Case 2 using GS

Heat exchanger number	**Additional area required m^2**		
	Fist optimisation	**Second optimisation**	**Third optimisation**
h1	0	0	147
h2	545	221	829
h3	168	141	91
h4	0	845	241
h5	232	137	103
h6	336	498	71
h7	0	40	311
h8	98	207	91
h9	0	0	0
h10	44	85	129
h11	0	0	124
h12	0	0	0
h13	0	0	0
h14*	17	17	14
h15*	2	2	2
h17*	16	16	16
h18*	2	61	0
h19*	39	0	43
h20*	36	36	30
h21*	371	222	112
h22*	20	45	49
h24*	0	42	0
Total additional area, m^2	1519	1945	2168
No. of heat exchangers needing modifications	14	16	17

* Utility exchangers

S3. Supporting information and tables for Case 3

1.1. Operational optimisation results for Case 3

Table S3.1 Optimisation results for Case 3 using SA

Parameter	First optimisation	Second optimisation	Third optimisation
Main steam flow rate, kmol h^{-1}	1120.9	1097.7	1365.7
Btm SS steam flow rate, kmol h^{-1}	342.2	383.1	395.7
Furnace outlet temperature, ℃	357.3	358.2	351.2
PA1 heat flow, MW	12.6	15.1	15.1
PA2 heat flow, MW	20.2	16.2	19.7
PA3 heat flow, MW	12.1	13.5	11.7
PA1 ΔT, ℃	99.8	40.1	21.9
PA2 ΔT, ℃	97.6	82.7	59.4
PA3 ΔT, ℃	66.3	50.6	63.2

Table S3.2 Optimisation results for Case 3 using GS

Parameter	First optimisation	Second optimisation	Third optimisation
Main steam flow rate, kmol h^{-1}	1616.8	1149.4	1203.8
Btm SS steam flow rate, kmol h^{-1}	405.1	357.4	361.9
Furnace outlet temperature, ℃	350.9	357.8	356.2
PA1 heat flow, MW	14.8	14.9	14.7
PA2 heat flow, MW	17.0	23.9	20.6
PA3 heat flow, MW	15.9	16.2	13.5
PA1 ΔT, ℃	62.2	39.9	66.5
PA2 ΔT, ℃	52.1	55.5	60.3
PA3 ΔT, ℃	61.4	63.7	58.8

1.2. Distillation column hydraulic results for Case 3

Table S3.3 Hydraulic results for Case 3 using SA

	Section	First optimisation	Second optimisation	Third optimisation
Jet flooding, %	**Section 1**	42.3	43.0	39.7
	Section 2	58.7	66.7	68.2
	Section 3	62.1	62.6	63.8
	Section 4	55.5	56.2	55.7
	Section 5	48.1	48.2	47.9
	Top SS	45.4	45.5	45.5
	Mid SS	27.0	26.9	27.2
	Btm SS	35.7	35.7	35.1
Weir load, $m^3\ m^{-1}\ h^{-1}$	**Section 1**	—	—	—
	Section 2	62.3	60.4	72.6
	Section 3	46.5	54.0	45.3
	Section 4	21.2	21.4	19.8
	Section 5	84.1	84.1	84.5
	Top SS	47.2	46.9	47.6
	Mid SS	71.4	71.5	70.7
	Btm SS	30.4	30.8	30.2
Downcomer exit velocity, $m\ s^{-1}$	**Section 1**	—	—	—
	Section 2	0.3	0.3	0.3
	Section 3	0.2	0.2	0.2
	Section 4	0.1	0.1	0.1
	Section 5	0.4	0.4	0.4
	Top SS	0.2	0.2	0.2
	Mid SS	0.3	0.3	0.3
	Btm SS	0.1	0.1	0.1
Downcomer flooding, %	**Section 1**	—	—	—
	Section 2	32.4	31.4	37.8
	Section 3	22.7	26.3	22.1
	Section 4	10.4	10.4	9.7
	Section 5	49.9	50.0	50.2
	Top SS	44.0	43.7	44.5
	Mid SS	66.6	66.7	66.0
	Btm SS	28.3	28.7	28.2

— = parameter non applicable for the packed sections of the column

Limit for approach to jet flooding (conventional trays and high-capacity trays) = 80%
Limit for liquid weir load = 90 $m^3\ m^{-1}\ h^{-1}$
Limit for downcomer exit velocity = 0.46 $m\ s^{-1}$
Limit for approach to downcomer flooding = 80%
Limit for approach flooding (structured packings) = 80%

Table S3.4 Hydraulic results for Case 3 using GS

	Section	First optimisation	Second optimisation	Third optimisation
Jet flooding, %	**Section 1**	40.8	32.7	38.7
	Section 2	60.2	54.2	58.3
	Section 3	62.5	60.1	62.6
	Section 4	56.7	55.0	55.8
	Section 5	50.3	48.6	48.5
	Top SS	48.2	46.1	46.0
	Mid SS	29.5	28.0	27.3
	Btm SS	35.3	34.5	35.3
Weir load, $m^3\ m^{-1}\ h^{-1}$	**Section 1**	—	—	—
	Section 2	68.8	78.8	73.3
	Section 3	52.0	52.3	50.2
	Section 4	21.2	21.5	21.2
	Section 5	86.8	84.7	84.7
	Top SS	48.0	49.1	47.8
	Mid SS	72.0	70.5	71.2
	Btm SS	27.8	29.2	29.8
Downcomer exit velocity, $m\ s^{-1}$	**Section 1**	—	—	—
	Section 2	0.3	0.4	0.3
	Section 3	0.2	0.2	0.2
	Section 4	0.1	0.1	0.1
	Section 5	0.4	0.4	0.4
	Top SS	0.2	0.2	0.2
	Mid SS	0.3	0.3	0.3
	Btm SS	0.1	0.1	0.1
Downcomer flooding, %	**Section 1**	—	—	—
	Section 2	35.8	41.0	38.1
	Section 3	25.4	25.5	24.5
	Section 4	10.3	10.5	10.4
	Section 5	51.5	50.3	50.3
	Top SS	44.8	45.8	44.6
	Mid SS	67.1	65.8	66.4
	Btm SS	26.0	27.2	27.8

— = parameter non applicable for the packed sections of the column

Limit for approach to jet flooding (conventional trays and high-capacity trays) = 80%
Limit for liquid weir load = 90 $m^3\ m^{-1}\ h^{-1}$
Limit for downcomer exit velocity = 0.46 $m\ s^{-1}$
Limit for approach to downcomer flooding = 80%
Limit for approach flooding (structured packings) = 80%

1.3. Required additional heat transfer area for Case 3

Table S3.5 HEN required additional heat transfer area for Case 3 using SA

Heat exchanger number	Additional area required m^2		
	Fist optimisation	**Second optimisation**	**Third optimisation**
h1	130	204	0
h2	231	51	704
h3	133	138	49
h4	77	864	0
h5	73	117	29
h6	242	104	345
h7	159	120	376
h8	57	126	0
h9	31	0	79
h10	48	94	103
h11	0	104	0
h12	0	0	56
h13	0	0	0
h14*	25	19	16
h15*	2	2	2
h17*	16	17	16
h18*	54	0	70
h19*	38	36	39
h20*	43	46	27
h21*	223	240	253
h22*	3	42	0
h24*	14	2	0
Total additional area, m^2	1599	2326	2162
No. of heat exchangers needing modifications	19	18	15

* Utility exchangers

Table S3.6 HEN required additional heat transfer area for Case 3 using GS

Heat exchanger number	Additional area required m^2		
	Fist optimisation	**Second optimisation**	**Third optimisation**
h1	0	0	13
h2	437	899	597
h3	135	139	156
h4	637	94	332
h5	127	223	217
h6	620	775	305
h7	358	368	72
h8	0	23	219
h9	0	0	0
h10	-36	78	40
h11	154	219	110
h12	0	0	0
h13	0	0	-67
h14*	9	7	15
h15*	2	2	2
h17*	16	16	16
h18*	0	0	0
h19*	41	45	40
h20*	52	28	40
h21*	350	62	186
h22*	68	54	54
h24*	0	0	0
Total additional area, m^2	2414	2426	2044
No. of heat exchangers needing modifications	14	16	17

* Utility exchangers

S4. Overview of the optimisations

Figures S4.1 to S4.12 illustrate the progress of the optimisations for Cases 2 and 3 in the paper [1]. Note that in all figures the values for the best function value and current function value are negative numbers. This is because the optimisation algorithms used, simulated annealing (SA) and global search (GS) both from the MATLAB optimisation toolbox, are designed to find the minimum of the objective function and the aim of this work [1] is to maximise the net profit of a crude oil distillation system by doing retrofit. Therefore, the objective function is formulated using the negative value. Also, in order to avoid large numbers, the net profit is multiplied by 10^{-9} \$ a^{-1}.

1.1. Optimisation using SA

Figures S4.1 to S4.6 illustrate the progress of the optimisations for the cases that were simulated using SA. In every figure, the continuous line represents the best function value found on each iteration and the dots represent the actual value found.

Tables S4.1 and S4.2 summarise the most important features of the optimisations. As mentioned in the paper [1], two stopping criteria are used for SA:

- if the average change in the objective function value in 1500 iterations is less than $1x10^{-4}$.
- if the number of iterations exceeds 3000 evaluations.

Note that in most cases, the number of iterations is smaller than 3000. This confirms that the approach provides robustness.

The number of unconverged simulations is relatively low (between 2 and 8%) since the lower and upper bounds chosen were obtained performing a sensitivity analysis that revealed the bounds that guaranteed converged simulations.

However, the percentage of iterations that resulted in unfeasible designs is relatively high (around 30%). Thus, it is concluded that with large scale problems such as the retrofit of crude oil distillation systems, the criteria to choose the lower and upper for the optimisation variables should also consider the quality of the products or any other relevant constraints.

Table S4.1 Overview of the optimisations using SA for Case 2

Parameter	First optimisation	Second optimisation	Third optimisation
No. of iterations	3000	2140	1706
Unconverged simulations, %	8	6	2
Unfeasible designs, %	30	21	20

Table S4.2 Overview of the optimisations using SA for Case 3

Parameter	First optimisation	Second optimisation	Third optimisation
No. of iterations	2164	2673	3000
Unconverged simulations, %	2	2	3
Unfeasible designs, %	26	32	29

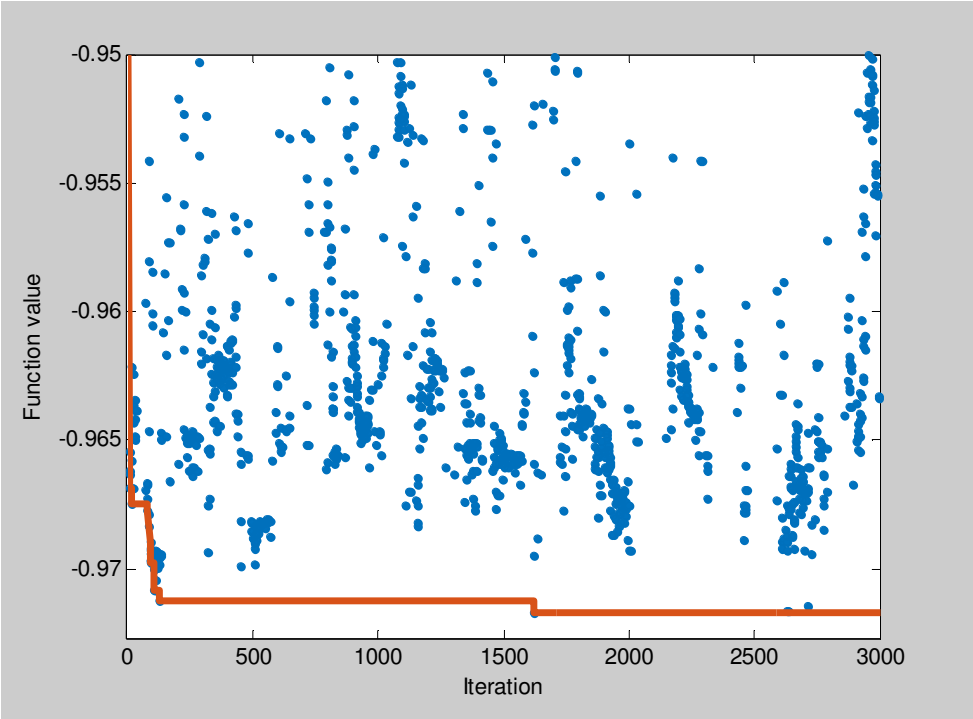

Figure S4.1 Progress of first optimisation using SA for Case 2

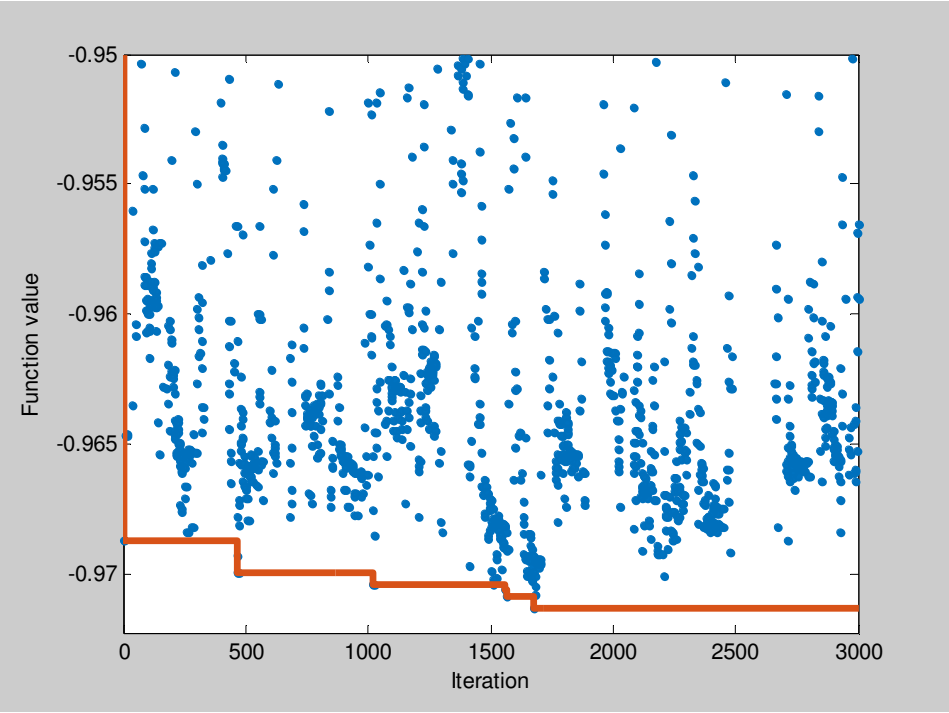

Figure S4.2 Progress of second optimisation using SA for Case 2

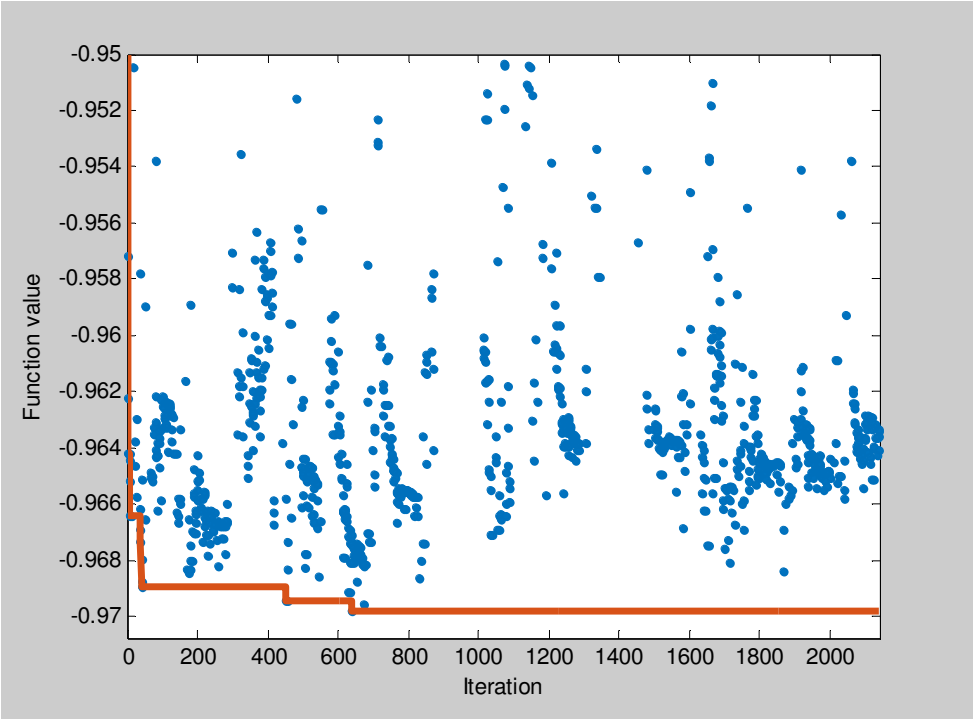

Figure S4.3 Progress of third optimisation using SA for Case 2

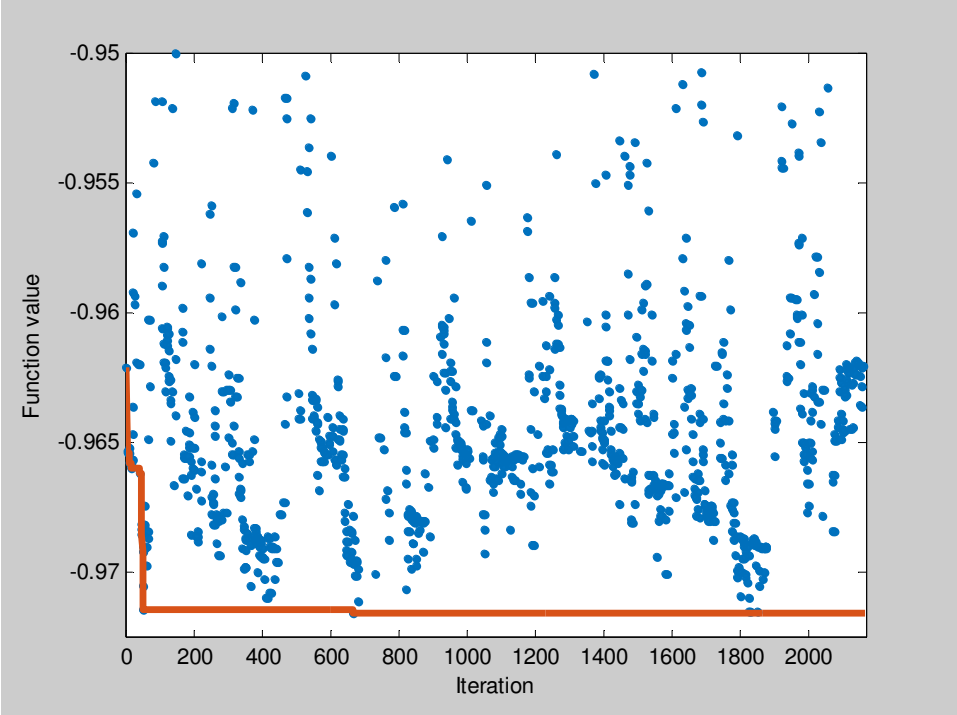

Figure S4.4 Progress of first optimisation using SA for Case 3

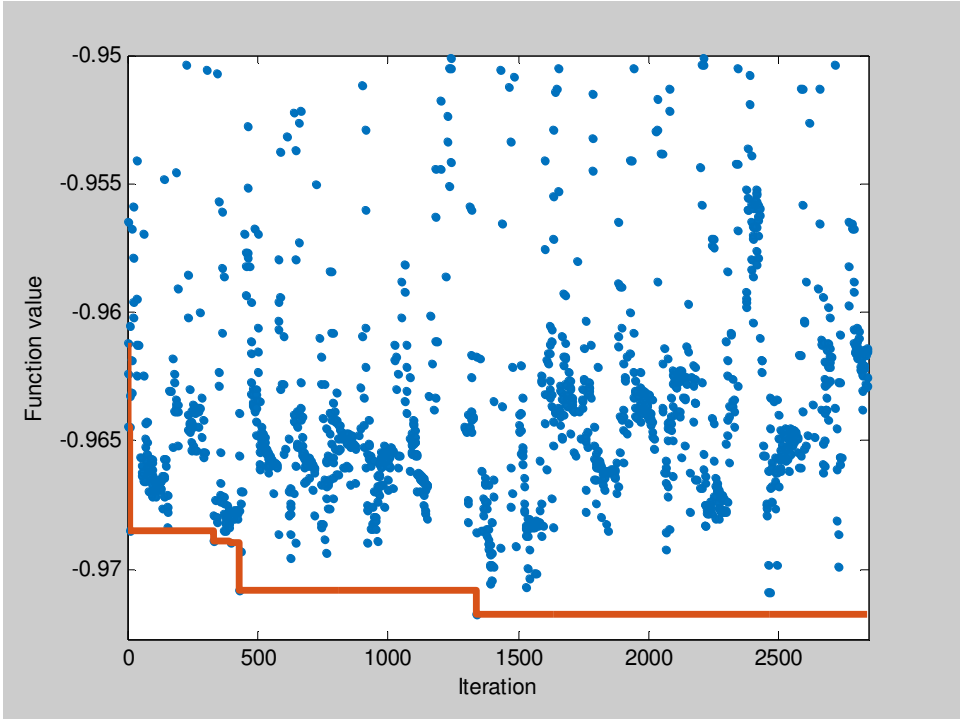

Figure S4.5 Progress of second optimisation using SA for Case 3

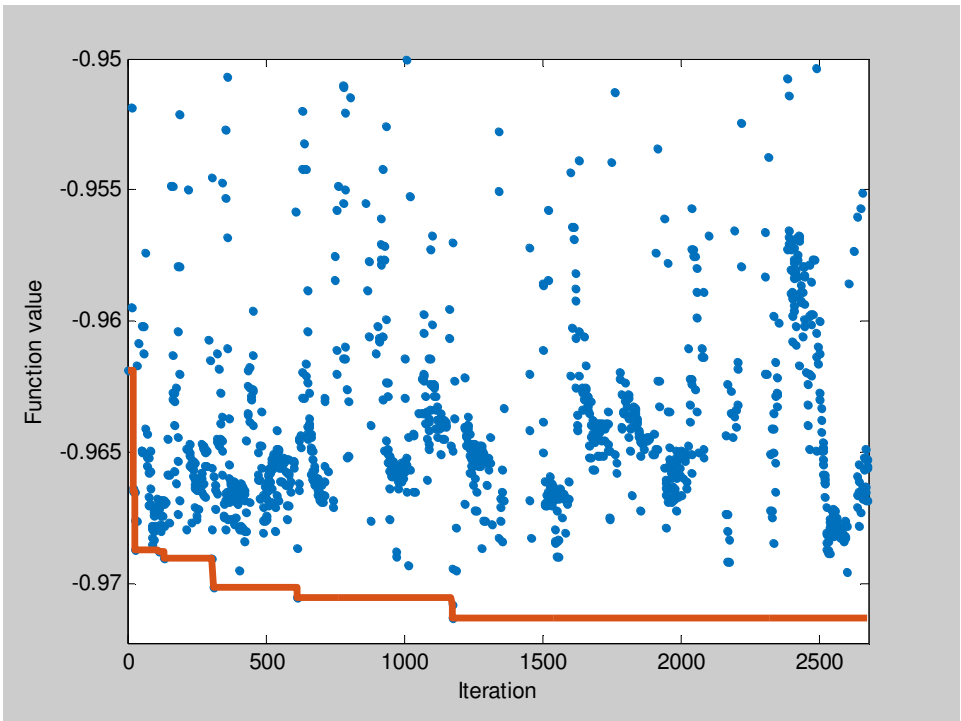

Figure S4.6 Progress of third optimisation using SA for Case 3

1.2. Optimisation using GS

Figures S4.7 to S4.12 illustrate the progress of the optimisations using GS. GS combines both stochastic and deterministic optimisation: scatter search [2] is used to generate multiple starting points and fmicon, a gradient-based solver from the MATLAB optimisation toolbox, runs for each point to generate different basins of attraction (i.e. steepest descent paths that tend to the same minimum point [3]). Once the termination criterion is met, the algorithm generates a vector containing all the minima and finds the global minimum from these values. Figures S4.7 to S4.12 show the best value found on each evaluation by fmincon.

The termination criteria used in this work is:

- the average change for the objective function value or for the optimisation variables should be less than $1x10^{-4}$.

Tables S4.3 and S4.4 summarise the most important features of the optimisations. In average for each iteration, between 6400 and 7600 points were analysed. From these points, between 39 to 67 points showed basin of attraction (i.e. fmincon ran for these points).

Even though GS needed more time to find a solution, the quality of the results is very similar to the ones of SA. Thus, GS is also suitable for the optimisation of these types of systems.

Table S4.3 History of the optimisations using GS for Case 2

Parameter	First optimisation	Second optimisation	Third optimisation
No. of iterations	7646	6559	6804
Number of solver calls	67	53	60

Table S4.4 History of the optimisations using GS for Case 3

Parameter	First optimisation	Second optimisation	Third optimisation
No. of iterations	6881	6428	7144
Number of solver calls	39	50	58

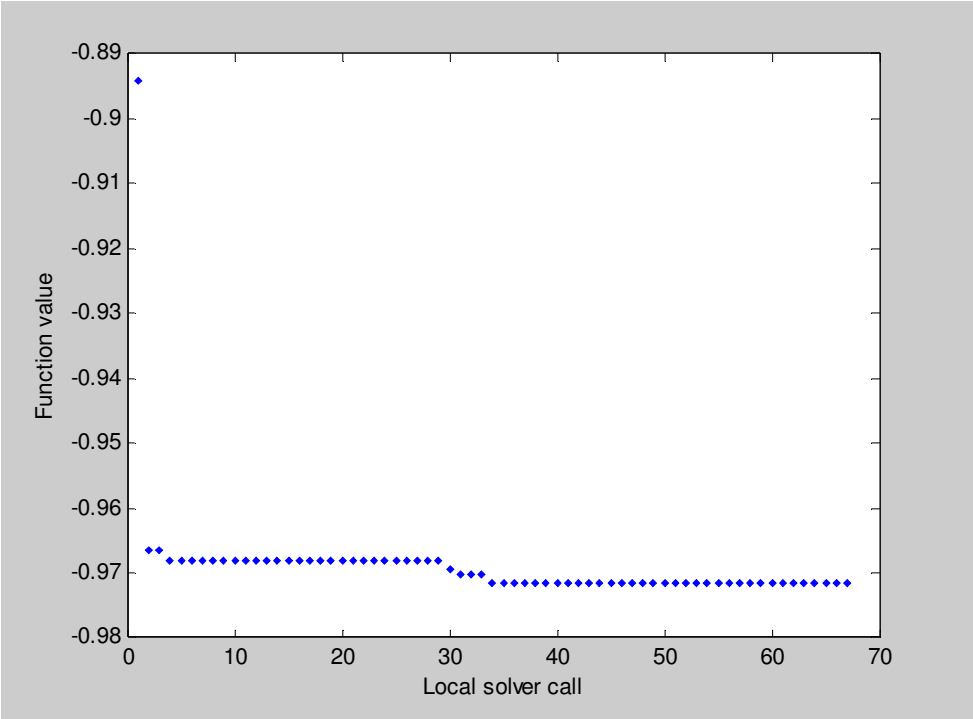

Figure S4.7 Progress of first optimisation using GS for Case 2

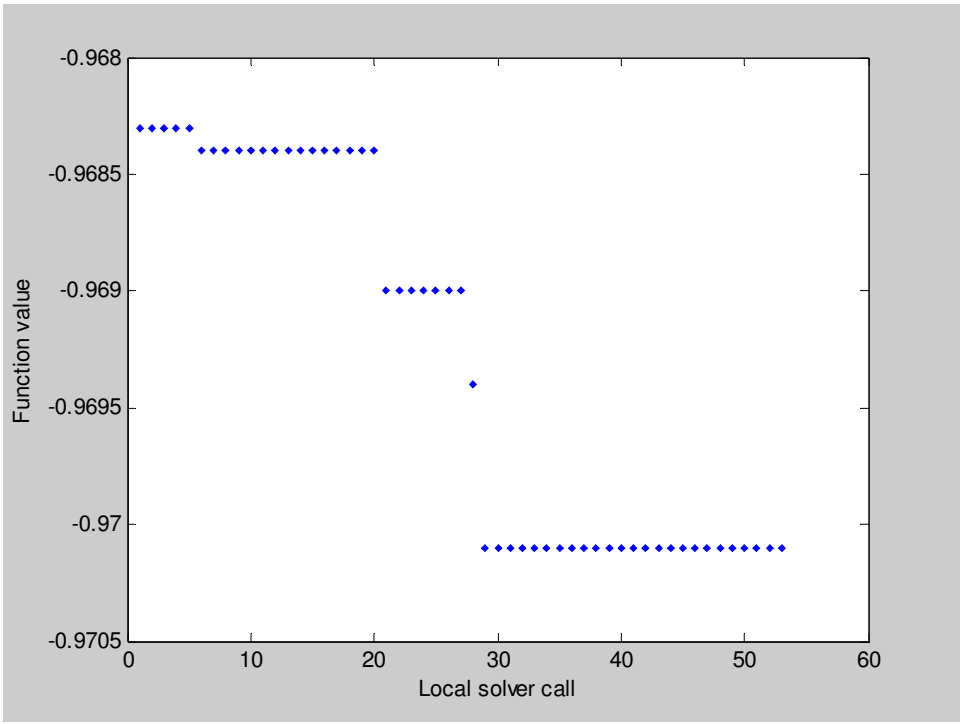

Figure S4.8 Progress of second optimisation using GS for Case 2

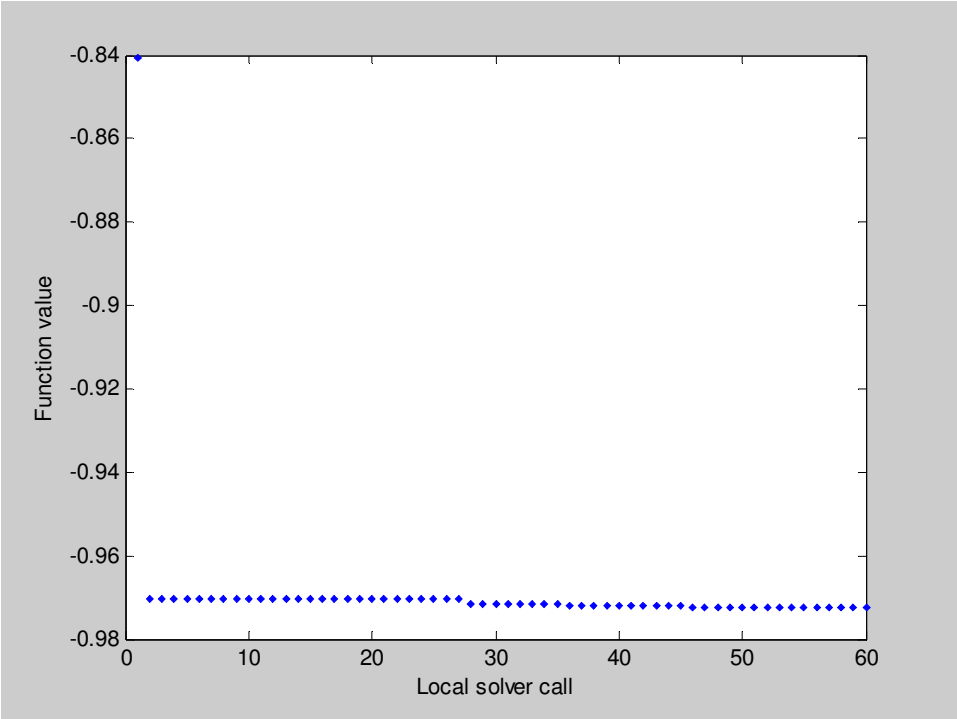

Figure S4.9 Progress of third optimisation using GS for Case 2

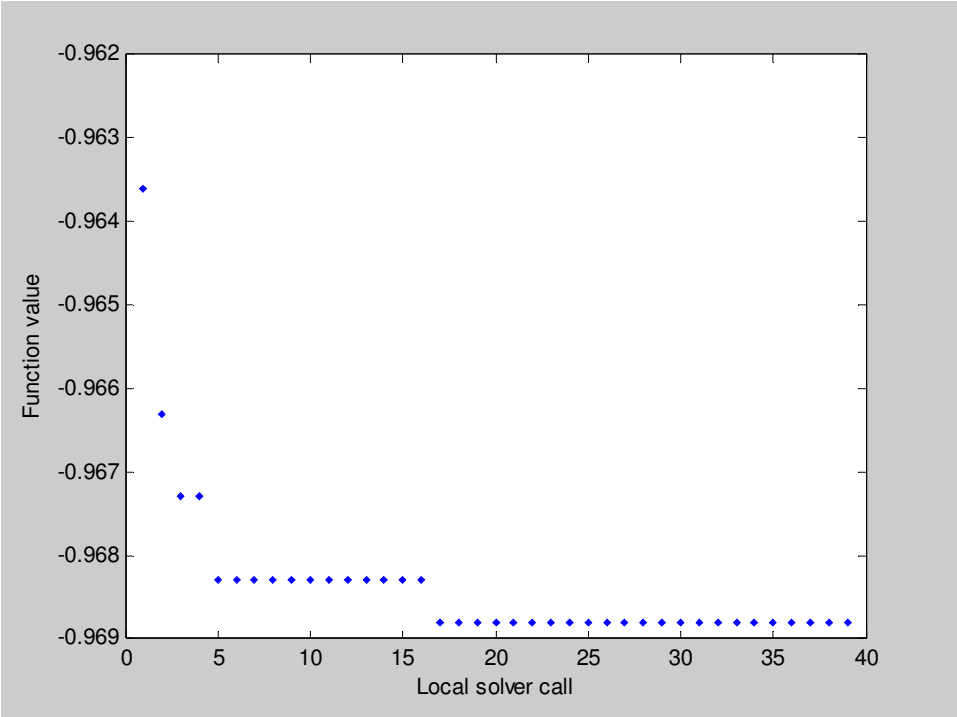

Figure S4.10 Progress of first optimisation using GS for Case 3

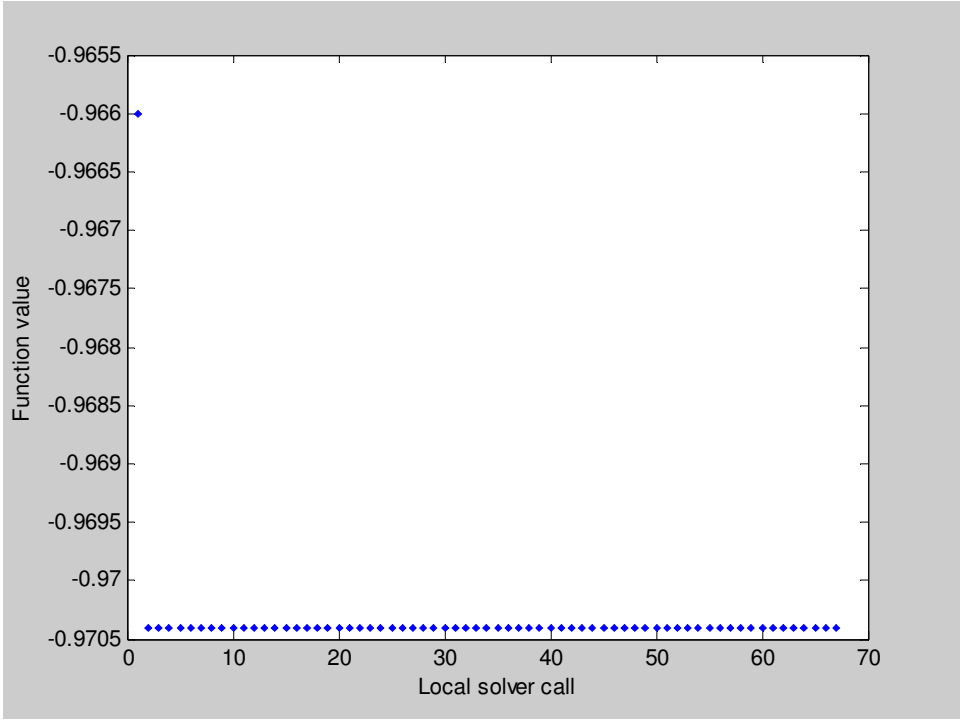

Figure S4.11 Progress of second optimisation using GS for Case 3

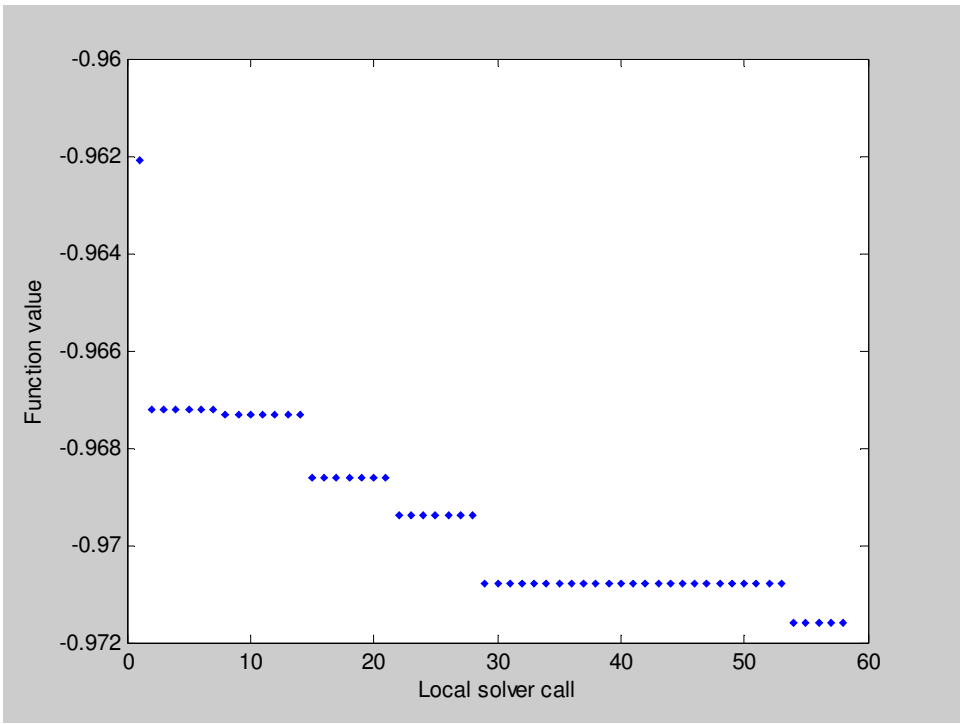

Figure S4.12 Progress of third optimisation using GS for Case 3

References

1. Enríquez-Gutiérrez, V.M. and Jobson, M., An optimisation-based retrofit approach for increasing the processing capacity of heat-integrated crude oil distillation systems. *Chemical Engineering Research & Design*, **2016**. *submitted May 2016*.
2. Ugray, Z., Lasdon, L., Plummer, J., Glover, F., Kelly, J., and Martí, R., Scatter search and local NLP solvers: a multistart framework for global optimization. *INFORMS Journal on Computing*, **2007**. *19*(3): p. 328-340.DOI: 10.1287/ijoc.1060.0175.
3. MATHWORKS. *Basins of attraction*. 2015 [access date October 2015]; Available from: http://uk.mathworks.com/help/gads/what-is-global-optimization.html#bsbalkx-1.

B.2 Supporting Information for Publication 3

Enríquez-Gutiérrez, V. M., Jobson, M., 2016, An optimisation-based retrofit approach for the assessment of structural and flowsheet modifications for heat-integrated crude oil distillation systems. Part 1.- Replacing column internals, Industrial & Engineering Chemistry Research, under preparation.

Supporting information

This document presents supporting information for the paper entitled: *An optimisation-based retrofit approach for the assessment of structural and flow sheet modifications for heat-integrated crude oil distillation systems. Part 1. Replacing column internals* [1].

S1. Case 1 — supporting information and tables

In Case 1, retrofit of column internals and HEN is addressed, but column operating conditions are simply increased pro rata by 30%.

1.1. Product quality specifications for Case 1

Table S1.1 Product quality specifications results for Case 1

Specification	Product	Base Case	Case 1	
		Value	Value	Diff*
T5 (°C, volume)	LN	3	2	-1
	HN	117	117	0
	LD	190	190	0
	HD	285	285	0
	RES	353	353	0
T95 (°C, volume)	LN	122	122	0
	HN	210	209	1
	LD	310	310	0
	HD	364	363	1
	RES	804	803	1

Diff* = difference relative to base case values

1.2. Distillation column hydraulic results for Case 1

Table S1.2 Hydraulic results for Case 1

	Section	Base case	Case 1
Jet flooding, %	**Section 1**	68	79.8
	Section 2	66	79.9
	Section 3	66	76.7
	Section 4	58	73.4
	Section 5	59	58.1
	Top SS	53	42.9
	Mid SS	63	61.2
	Btm SS	44	55.8
Weir load, $m^3\ m^{-1}\ h^{-1}$	**Section 1**	88	—
	Section 2	71	85.7
	Section 3	69	87.1
	Section 4	53	66.2
	Section 5	77	—
	Top SS	42	42.9
	Mid SS	64	63.8
	Btm SS	29	35.8
DC exit velocity, $m\ s^{-1}$	**Section 1**	0.45	—
	Section 2	0.38	0.3
	Section 3	0.37	0.4
	Section 4	0.31	0.3
	Section 5	0.41	—.
	Top SS	0.27	0.2
	Mid SS	0.35	0.3
	Btm SS	0.21	0.1
DC flooding, %	**Section 1**	67	—
	Section 2	62	37.1
	Section 3	62	39.1
	Section 4	59	36.9
	Section 5	60	—.
	Top SS	44	22.1
	Mid SS	61	30.5
	Btm SS	42	26.5

— = parameter non applicable for the packed sections of the column
Limit for approach to jet flooding (conventional trays and high-capacity trays) = 80%
Limit for liquid weir load = 90 $m^3\ m^{-1}\ h^{-1}$
Limit for downcomer exit velocity = 0.46 $m\ s^{-1}$
Limit for approach to downcomer flooding = 80%
Limit for approach flooding (structured packings) = 80%

1.3. Required additional heat transfer area for Case 1

Table S1.3 HEN required heat transfer area for Case 1

Heat exchanger number	Existing area	Additional area required m^2
	Base case	Case 1
h1	975	96
h2	332	1003
h3	112	111
h4	196	220
h5	58	138
h6	105	121
h7	684	0
h8	312	244
h9	260	0
h10	46	48
h11	555	254
h12	22	0
h13	67	0
h14*	106	15
h15*	11	2
h17*	59	16
h18*	99	0
h19*	122	39
h20*	61	28
h21*	1036	306
h22*	179	47
h24*	56	0
Total additional heat transfer area, m^2	—	2689
No. of heat exchangers needing modifications	—	16

* = Utility heat exchangers

— = Not applicable

S2. Case 2 — supporting information and tables

In Case 2, the optimisation algorithm selects the column and HEN modifications as well as the optimal operating conditions.

1.1. Operational optimisation results for Case 2

Table S2.1 Optimisation results for Case 2 using SA

Parameter	First optimisation	Second optimisation	Third optimisation
Main steam flow rate, kmol h^{-1}	1258.1	1108.4	1092.7
Btm SS steam flow rate, kmol h^{-1}	351.0	364.4	345.6
Furnace outlet temperature, ℃	353.6	357.7	364.6
PA1 heat flow, MW	17.6	12.2	12.2
PA2 heat flow, MW	20.8	20.9	20.1
PA3 heat flow, MW	12.6	11.4	15.3
PA1 ΔT, ℃	23.6	20.1	21.8
PA2 ΔT, ℃	72.4	50.7	40.2
PA3 ΔT, ℃	55.5	49.6	46.0

Table S2.2 Optimisation results for Case 2 using GS

Parameter	First optimisation	Second optimisation	Third optimisation
Main steam flow rate, kmol h^{-1}	1192.6	1397.1	1357.1
Btm SS steam flow rate, kmol h^{-1}	377.9	380.4	385.5
Furnace outlet temperature, ℃	356.6	350.6	353.5
PA1 heat flow, MW	17.3	14.2	14.6
PA2 heat flow, MW	19.9	21.0	22.2
PA3 heat flow, MW	16.0	11.3	16.0
PA1 ΔT, ℃	24.6	22.9	22.7
PA2 ΔT, ℃	48.2	76.6	50.2
PA3 ΔT, ℃	56.6	46.7	43.5

1.2. Product quality results for Case 2

Table S2.3 Product quality results for Case 2 using SA

Specification	Product	Base Case	First optimisation		Second optimisation		Third optimisation	
		Value	Value	Diff*	Value	Diff*	Value	Diff*
T5 by volume (℃)	LN	3	2	-1	2	-1	2	-1
	HN	117	117	0	117	0	117	0
	LD	190	190	0	190	0	190	0
	HD	285	285	0	285	0	285	0
	RES	353	353	0	353	0	353	0
T95 by volume (℃)	LN	122	124	2	122	0	122	0
	HN	210	210	0	210	0	210	0
	LD	310	310	0	305	-5	309	-1
	HD	364	369	5	369	5	365	1
	RES	804	805	1	805	1	804	0

Diff* = difference relative to base case values

Table S2.4 Product quality results for Case 2 using GS

Specification	Product	Base Case	First optimisation		Second optimisation		Third optimisation	
		Value	Value	Diff*	Value	Diff*	Value	Diff*
T5 by volume (℃)	LN	3	2	-1	2	-1	2	-1
	HN	117	117	0	117	0	117	0
	LD	190	190	0	190	0	190	0
	HD	285	285	0	285	0	285	0
	RES	353	353	0	353	0	353	0
T95 by volume (℃)	LN	122	123	1	122	0	122	0
	HN	210	210	0	210	0	211	1
	LD	310	310	0	309	-1	311	1
	HD	364	368	4	368	4	367	3
	RES	804	805	1	805	1	805	1

Diff* = difference relative to base case values

1.3. Distillation column hydraulic results for Case 2

Table S2.5 Hydraulic results for Case 2 using SA

	Section	First optimisation	Second optimisation	Third optimisation
Jet flooding, %	**Section 1**	76.1	78.0	77.8
	Section 2	72.0	76.1	76.8
	Section 3	71.9	73.6	76.4
	Section 4	60.8	61.4	66.1
	Section 5	61.5	58.6	45.8
	Top SS	42.9	43.0	43.0
	Mid SS	60.9	60.0	60.4
	Btm SS	59.6	63.1	60.6
Weir load, $m^3\ m^{-1}\ h^{-1}$	**Section 1**	—	—	—
	Section 2	65.6	79.8	87.4
	Section 3	51.1	53.2	65.6
	Section 4	46.1	48.8	57.7
	Section 5	89.7	89.5	89.9
	Top SS	42.9	42.9	43.0
	Mid SS	63.6	62.4	62.9
	Btm SS	39.3	41.4	39.2
DC exit velocity, $m\ s^{-1}$	**Section 1**	—	—	—
	Section 2	0.3	0.3	0.3
	Section 3	0.2	0.2	0.3
	Section 4	0.2	0.2	0.2
	Section 5	0.4	0.4	0.4
	Top SS	0.2	0.2	0.2
	Mid SS	0.3	0.2	0.2
	Btm SS	0.2	0.2	0.2
DC flooding, %	**Section 1**	—	—	—
	Section 2	28.4	34.5	37.8
	Section 3	22.9	23.9	29.5
	Section 4	25.7	27.2	32.2
	Section 5	34.8	34.7	34.9
	Top SS	22.2	22.2	22.2
	Mid SS	30.4	29.8	30.1
	Btm SS	29.0	30.6	29.0

— = parameter non applicable for the packed sections of the column
Limit for approach to jet flooding (conventional trays and high-capacity trays) = 80%
Limit for liquid weir load = 90 $m^3\ m^{-1}\ h^{-1}$
Limit for downcomer exit velocity = 0.46 $m\ s^{-1}$
Limit for approach to downcomer flooding = 80%
Limit for approach flooding (structured packings) = 80%

Table S2.6 Hydraulic results for Case 2 using GS

	Section	First optimisation	Second optimisation	Third optimisation
Jet flooding, %	**Section 1**	73.7	75.7	69.4
	Section 2	71.3	73.5	70.8
	Section 3	71.9	73.1	72.8
	Section 4	61.7	60.9	62.0
	Section 5	45.1	47.7	48.0
	Top SS	43.5	42.9	44.2
	Mid SS	60.4	60.7	60.5
	Btm SS	62.1	61.9	60.8
Weir load, $m^3\ m^{-1}\ h^{-1}$	**Section 1**	—	—	—
	Section 2	75.1	65.1	76.5
	Section 3	56.8	51.9	63.4
	Section 4	48.4	44.9	47.2
	Section 5	89.8	88.9	89.7
	Top SS	43.6	42.9	44.2
	Mid SS	63.1	63.3	63.3
	Btm SS	39.2	39.5	37.4
DC exit velocity, $m\ s^{-1}$	**Section 1**	—	—	—
	Section 2	0.3	0.3	0.3
	Section 3	0.2	0.2	0.3
	Section 4	0.2	0.2	0.2
	Section 5	0.4	0.4	0.4
	Top SS	0.2	0.2	0.2
	Mid SS	0.3	0.3	0.3
	Btm SS	0.2	0.2	0.1
DC flooding, %	**Section 1**	—	—	—
	Section 2	32.5	28.2	33.1
	Section 3	25.5	23.3	28.4
	Section 4	27.0	25.0	26.3
	Section 5	34.6	34.9	34.7
	Top SS	22.5	22.1	22.9
	Mid SS	30.2	30.2	30.3
	Btm SS	29.0	29.2	27.6

— = parameter non applicable for the packed sections of the column

Limit for approach to jet flooding (conventional trays and high-capacity trays) = 80%
Limit for liquid weir load = 90 $m^3\ m^{-1}\ h^{-1}$
Limit for downcomer exit velocity = 0.46 $m\ s^{-1}$
Limit for approach to downcomer flooding = 80%
Limit for approach flooding (structured packings) = 80%

1.4. Required additional heat transfer are for Case 2

Table S2.7 HEN required additional heat transfer area for Case 2 using SA

Heat exchanger number	**Additional area required m^2**		
	Fist optimisation	**Second optimisation**	**Third optimisation**
h1	0	41	0
h2	291	745	856
h3	130	126	100
h4	997	76	400
h5	143	162	140
h6	302	183	288
h7	162	259	237
h8	163	123	212
h9	0	53	52
h10	67	85	100
h11	67	48	309
h12	0	0	0
h13	0	0	0
h14*	11	13	9
h15*	2	2	2
h17*	16	17	17
h18*	0	0	0
h19*	39	39	39
h20*	52	38	34
h21*	123	236	235
h22*	63	8	24
h24*	7	0	0
Total additional area, m^2	2634	2253	3054
No. of heat exchangers needing modifications	17	18	17

* = Utility heat exchangers

Table S2.8 HEN required additional heat transfer area for Case 2 using GS

Heat exchanger number	**Additional area required m^2**		
	Fist optimisation	**Second optimisation**	**Third optimisation**
h1	0	161	0
h2	623	240	895
h3	98	124	112
h4	940	858	300
h5	122	56	158
h6	575	37	291
h7	153	29	296
h8	213	216	81
h9	0	0	72
h10	100	108	0
h11	248	34	268
h12	6	43	0
h13	0	0	0
h14*	5	14	3
h15*	2	2	2
h17*	16	16	16
h18*	0	0	0
h19*	42	39	45
h20*	33	35	57
h21*	106	253	162
h22*	84	53	12
h24*	0	20	0
Total additional area, m^2	3364	2339	2768
No. of heat exchangers needing modifications	17	19	16

* = Utility heat exchangers

S3. Overview of the optimisations

Figures S3.1 to S3.6 illustrate the overview of the optimisations for Case 2 in the paper [1]. In these figures, the values for the best function value and current function value are negative numbers because the optimisation algorithms used, simulated annealing (SA) and global search (GS) both from the MATLAB optimisation toolbox, are designed to find the minimum of the objective function and this work aims to maximise the net profit of a crude oil distillation system by doing retrofit. Thus, the objective function is formulated using the negative of the net profit. In order to avoid large numbers, the net profit is multiplied by 10^{-9} \$ y^{-1}. Large numbers are more difficult to analyse and handle. Also, it was observed that when the objective function was formulated using large numbers, the optimisation times increased and sometimes the 'CPU memory' ran out of space, stopping the optimisation without giving any output.

1.1. Optimisation using SA

Figures S3.1 to S3.3 illustrate the progress of the optimisations for the cases that were simulated using SA. In Figures S3.1 to S3.3, the dots represent the actual value found in a given iteration, the continuous line represents the best function value found so far.

Table S3.1 presents the results of the optimisation. In all cases, the maximum number of iterations permitted (i.e. 3000 iterations) is not reached. The best function value criterion is met in less than 3000 iterations, which helps to confirm that the optimisation was not terminated prematurely.

Note that the percentage of iterations that results in unconverged simulations or that did not meet with the product quality specifications is relatively low (i.e. less than 1%). This confirms that the lower and upper bounds selected are appropriate. Lower convergence rates in previous optimisation runs showed the importance of choosing these bounds based on sensitivity analysis.

SA took around 5 to 6 hours in finding the best solution on a computer with an Intel Core processor of 3.3 GHZ and 8 GB of installed RAM memory

Table S3.1 Results of the optimisations using SA for Case 2

Parameter	First optimisation	Second optimisation	Third optimisation
No. of iterations	1518	1771	1858
Best function value, $\$\cdot 10^{9}$ a^{-1}	0.973375	0.973550	0.973360
Unconverged simulations	0	1	0
Function values with penalties	78	147	160
Optimisation time, h	5.1	5.7	6

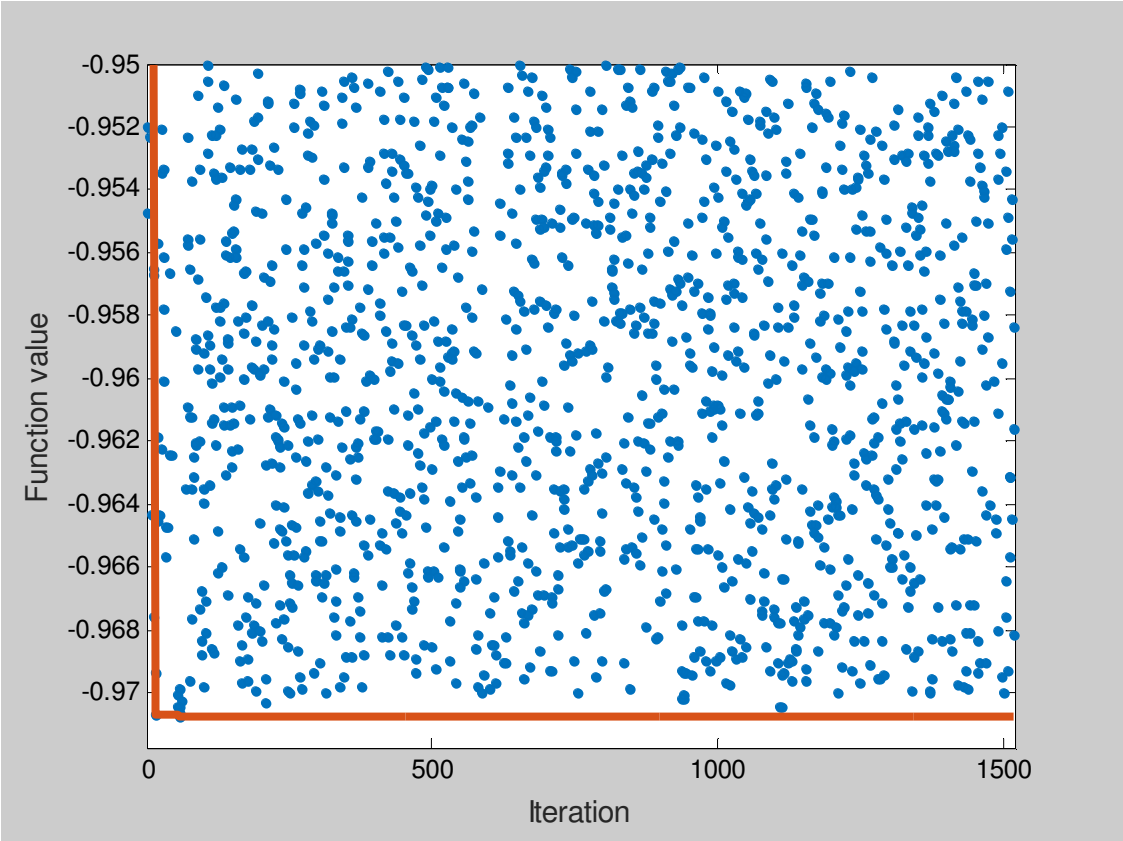

Figure S3.1 Progress of first optimisation using SA for Case 2

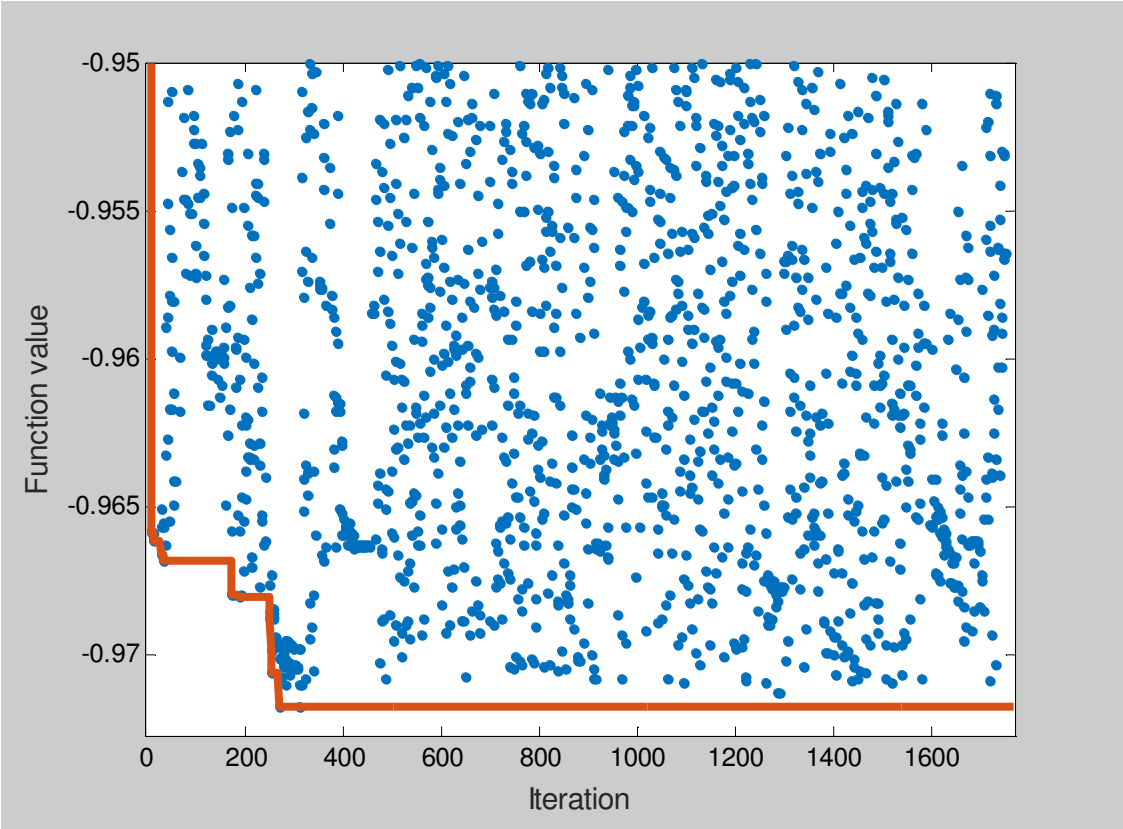

Figure S3.2 Progress of second optimisation using SA for Case 2

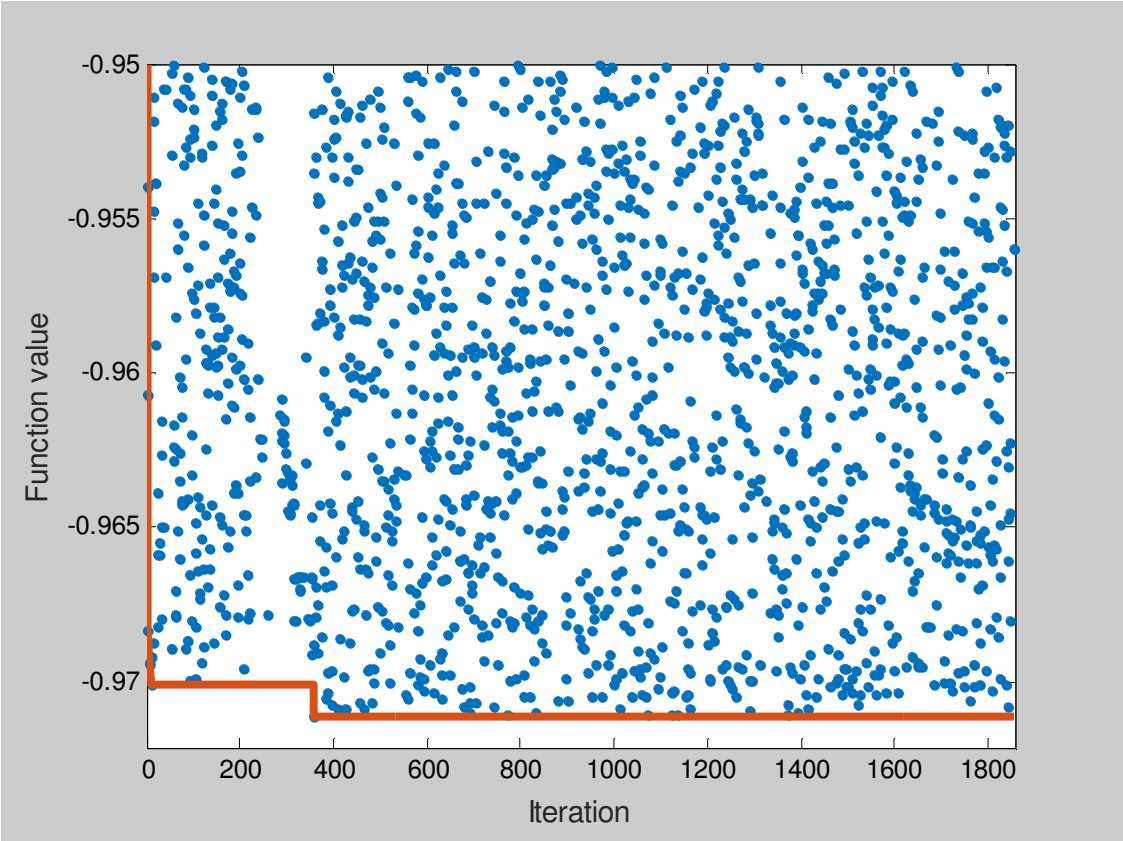

Figure S3.3 Progress of third optimisation using SA for Case 2

1.2. Optimisation using GS

Figures S3.4 to S3.6 illustrate the history of the optimisations using GS. These figures show the best function value found on each solver call (i.e. fmincon). The paper [1] notes that GS combines both stochastic and deterministic optimisation: scatter search [2] is used to generate multiple starting points and fmicon, a gradient-based solver in the MATLAB optimisation toolbox, runs for each point to generate different 'basins of attraction' (i.e. steepest descent paths that tend to the same minimum point [3]). Once the termination criterion is met, the algorithm generates a vector containing all the minima and finds the global minimum from these values.

Table S3.2 summarises the most important features of the optimisations. Over 6000 points were analysed in each optimisation run. From these iterations, around 60 points presented basins of attraction.

GS took more time than SA to find a solution (i.e. around 11 to 12 hours) because more GS analysed more points.

Table S3.2 History of the optimisations using GS for Case 2

Parameter	First optimisation	Second optimisation	Third optimisation
No. of iterations	6201	6468	6360
Number of solver calls	64	60	57
Best function value, $\$\cdot 10^{9}\ a^{-1}$	0.973860	0.972778	0.972929
Optimisation time, h	11.2	11.8	10.9

Both algorithms found similar results. The best function value is found in the first optimisation using GS (i.e. 0.973860 $\$M\cdot 10^{-3}\ a^{-1}$) and the lowest values is found in the third optimisation using GS (i.e. 0.972929 $\$M\cdot 10^{-3}\ a^{-1}$). The difference between both values is of around 0.0008. The difference between the values found by SA is smaller, around 0.0002.

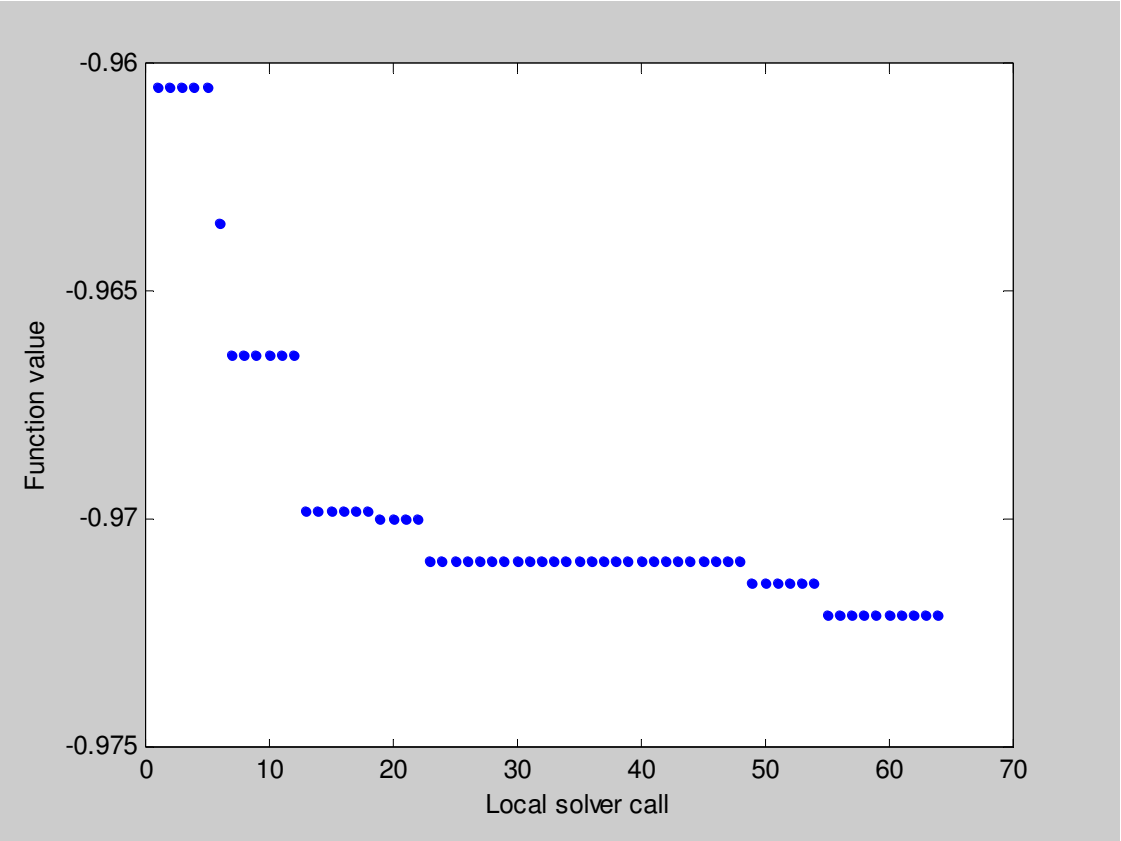

Figure S3.4 Progress of first optimisation using GS for Case 2

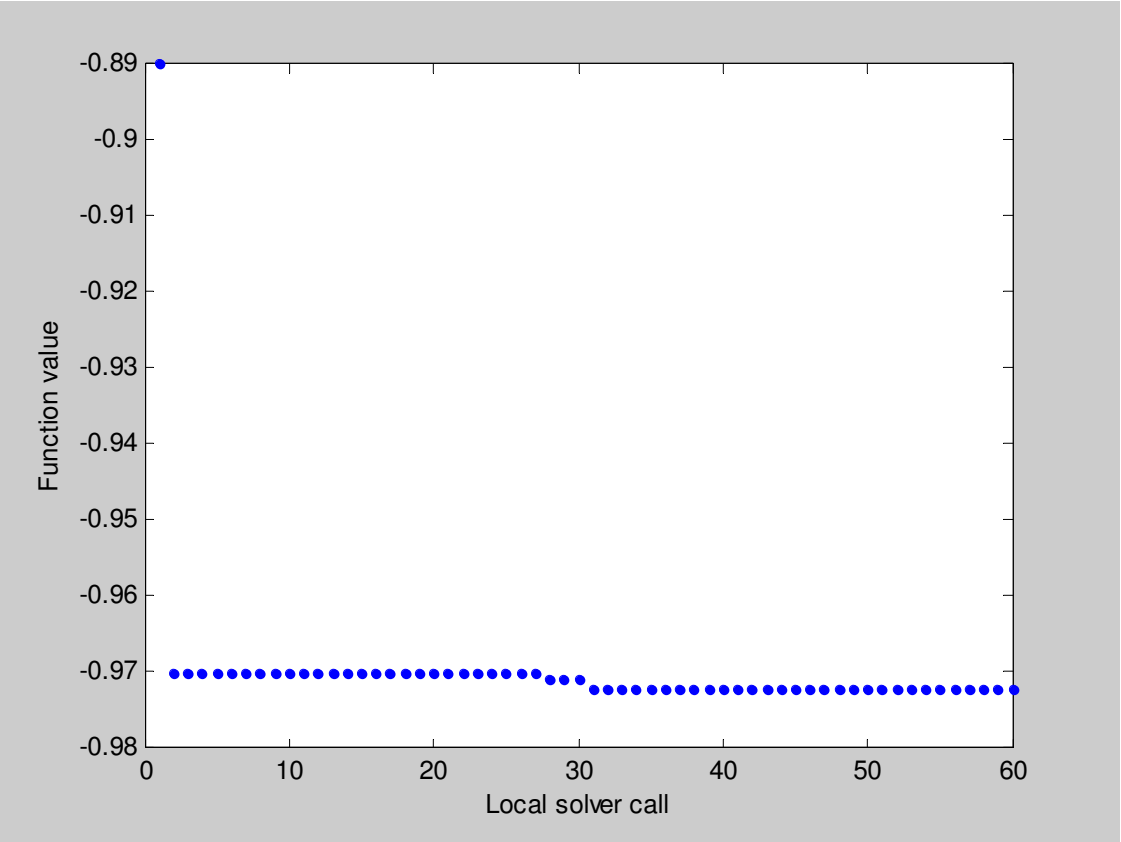

Figure S3.5 Progress of second optimisation using GS for Case 2

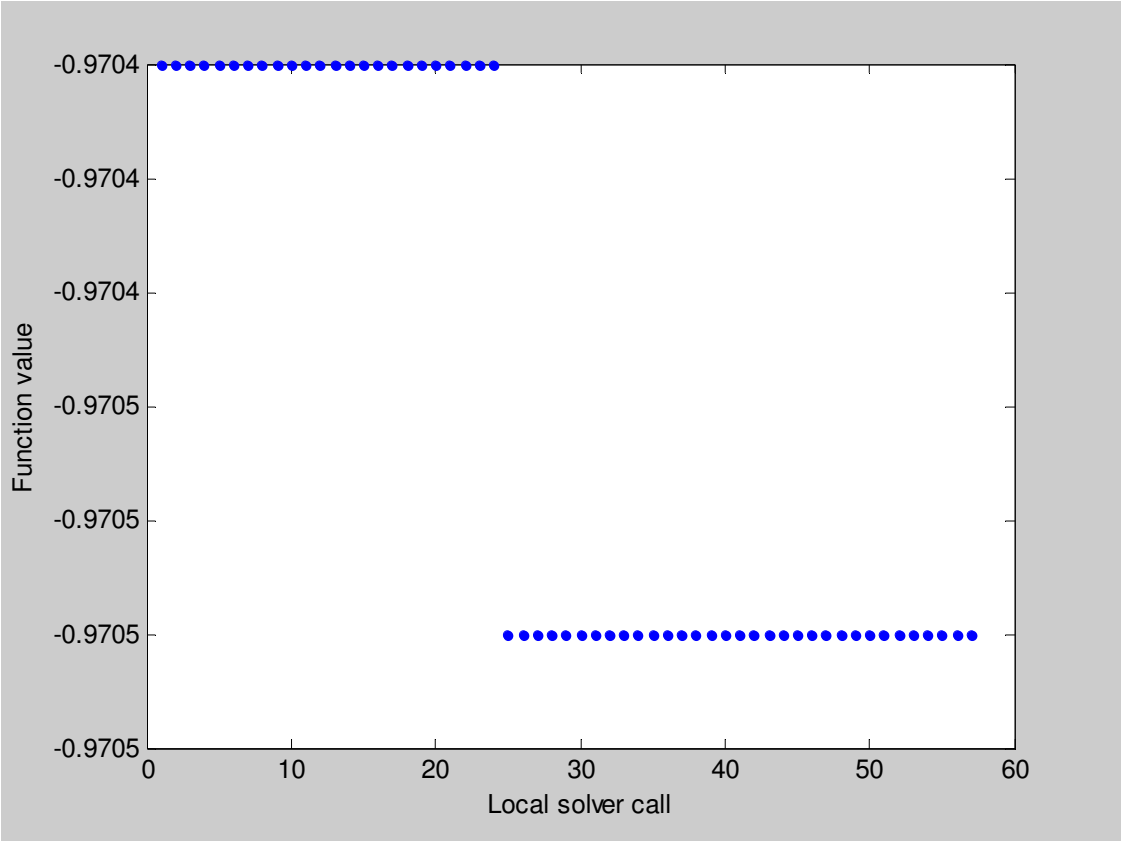

Figure S3.6 Progress of third optimisation using GS for Case 2

References

1. Enríquez-Gutiérrez, V.M. and Jobson, M., An optimisation-based retrofit approach for the assessment of structural and flowsheet modifications for heat-integrated crude oil distillation systems. Part 1.- Replacing column internals. *Chemical Engineering Research & Design*, **2016**. *submitted May 2016*.
2. Ugray, Z., Lasdon, L., Plummer, J., Glover, F., Kelly, J., and Martí, R., Scatter search and local NLP solvers: a multistart framework for global optimization. *INFORMS Journal on Computing*, **2007**. *19*(3): p. 328-340.DOI: 10.1287/ijoc.1060.0175.
3. MATHWORKS. *Basins of attraction*. 2015 [access date October 2015]; Available from: http://uk.mathworks.com/help/gads/what-is-global-optimization.html#bsbalkx-1.

B.4 Supporting Information for Publication 4

Enríquez-Gutiérrez, V. M., Jobson, M., 2016, An optimisation-based retrofit approach for the assessment of structural and flowsheet modifications for heat-integrated crude oil distillation systems. Part 2.- Adding a preflash unit, Industrial & Engineering Chemistry Research, under preparation.

Supporting information

This document presents supporting information for the paper entitled: *An optimisation-based retrofit approach for the assessment of structural and flow sheet modifications for heat-integrated crude oil distillation systems. Part 2. Adding a preflash unit [1]*.

S1. Optimisation runs to select lower and upper bounds

This section aims to find the lower and upropper bounds for the optimisation variables that guarantee converged simulations and products within quality specifications.

The optimisation runs are carried out using the retrofit approach presented in the paper [1]. Simulated annealing (SA) is used to vary the optimisation variables within the lower and upper bounds listed in Table S1.1.

The main and Btm SS steam flow rates and the pumparound heat flows are allowed to vary by 30%, the furnace outlet temperature between 350 and 370℃, the pumparound temperature drops between 10 and 100℃ and the preflash temperature between the desalter outlet temperature and the base case furnace inlet temperature (i.e. 148 and 257℃, respectively).

Table S1.1 Lower and upper bounds used for optimisation runs

Parameter	Lower bound	Upper bound
Main steam flow rate, kmol h^{-1}	1092	2028
Btm SS steam flow rate, kmol h^{-1}	227.5	422.5
Furnace outlet temperature, ℃	350	370
PA1 heat flow, MW	10	19
PA2 heat flow, MW	16	31
PA3 heat flow, MW	11	22
PA1 ΔT, ℃	10	100
PA2 ΔT, ℃	10	100
PA3 ΔT, ℃	10	100
Preflash temperature	148	257

The optimisation is repeated three times in order to observed trends.

1.1. Optimisation runs — results

Figure S1.1 illustrates the results of the optimisation runs and Table S1.1 show the values used to build this graph. Figure S1.1 shows that: i) the main and Btm SS steam flow rates and the pumparound temperature drops tend to increase; ii) the heat duties of PA2 and PA3 tend to decrease; iii) the PA1 heat flow varies between the upper and

lower bounds iv) the furnace outlet temperate do not vary from the base case value (see Part 1 [2]); v) the preflash temperate is lower than the furnace inlet temperature of the base case (i.e. 257℃).

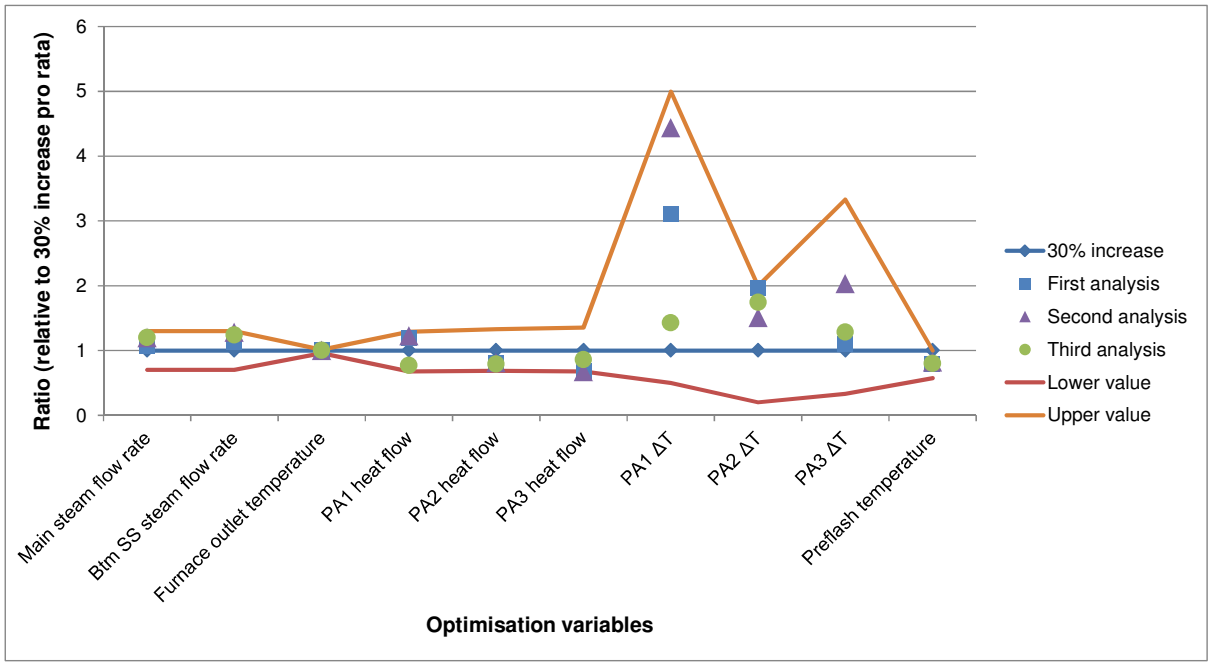

Figure S1.1 Results for optimisation runs

Table S1.2 Results of sensitivity analysis

Parameter	First analysis	Second analysis	Third analysis
Main steam flow rate, kmol h^{-1}	1678.6	1868.4	1871.4
Btm SS steam flow rate, kmol h^{-1}	366.5	415.9	403.4
Furnace outlet temperature, ℃	365.0	365.0	365.0
PA1 heat flow, MW	17.5	18.1	11.4
PA2 heat flow, MW	18.8	19.0	18.5
PA3 heat flow, MW	11.0	11.0	14.0
PA1 ΔT, ℃	62.1	88.9	28.5
PA2 ΔT, ℃	98.8	75.5	87.3
PA3 ΔT, ℃	32.8	61.1	38.5
Preflash temperature, ℃	203.2	211.9	204.8

Based on these observations, lower and upper for the optimisations are chosen. Table S1.3 lists the new lower and upper bounds used for the optimisations presented in the paper [1].

Table S1.3 Lower and upper bounds selected

Parameter	30% increase [2]	Lower bound	Upper bound
Main steam flow rate, kmol h^{-1}	1560.0	1678	1872
Btm SS steam flow rate, kmol h^{-1}	325.0	366	416
Furnace outlet temperature, ℃	365.0	365	365
PA1 heat flow, MW	14.7	11	19
PA2 heat flow, MW	23.4	18	20
PA3 heat flow, MW	16.3	11	14
PA1 ΔT, ℃	20.0	28	90
PA2 ΔT, ℃	50.0	75	100
PA3 ΔT, ℃	30.0	30	60
Preflash temperature	257	200	220

Table S1.4 presents the history of the optimisations. Note that in every case, the percentage of unconverged simulations and simulations that do not meet product quality specifications (i.e. where a penalty is applied to the objective function) are very high in comparison with the number of iterations. For this reason, using suitable constraints and bounds are important to find. Section S3 presents the history of the optimisation, in which it can be observed that after adjusting the upper and lower bounds, the probability of getting converged simulations and products within *specs* increases significantly.

Table S1.4 History of the optimisations

Parameter	First sensitivity	Second sensitivity	Third sensitivity
No. of iterations	1423	3000	913
Unconverged simulations, %	65	60	35
Function values with penalties, %	26	30	66
Optimisation time, h	1.7	2.4	1

S2. Case study — supporting information and tables

1.1. Operational optimisation results for case study

Table S2.1 Results for the optimisations using SA

Parameter	First optimisation	Second optimisation	Third optimisation
Main steam flow rate, kmol h^{-1}	1680.0	1688.2	1683.7
Btm SS steam flow rate, kmol h^{-1}	415.6	414.4	415.5
Furnace outlet temperature, ℃	365.0	365.0	365.0
PA1 heat flow, MW	11.2	11.4	14.4
PA2 heat flow, MW	18.0	18.2	18.0
PA3 heat flow, MW	11.0	11.0	11.1
PA1 ΔT, ℃	29.5	30.0	66.1
PA2 ΔT, ℃	88.5	98.4	99.7
PA3 ΔT, ℃	59.8	59.8	59.4
Preflash temperature, ℃	200.3	201.2	211.6

Table S2.2 Results for the optimisations using GS

Parameter	First optimisation	Second optimisation	Third optimisation
Main steam flow rate, kmol h^{-1}	1680.4	1685.6	1716.3
Btm SS steam flow rate, kmol h^{-1}	410.8	395.0	409.5
Furnace outlet temperature, ℃	365.0	365.0	365.0
PA1 heat flow, MW	11.6	11.2	12.9
PA2 heat flow, MW	18.1	19.0	18.7
PA3 heat flow, MW	11.2	11.4	11.1
PA1 ΔT, ℃	40.9	31.0	59.9
PA2 ΔT, ℃	97.4	93.2	86.2
PA3 ΔT, ℃	55.5	58.4	56.9
Preflash temperature, ℃	200.0	200.0	207.7

1.2. Product quality specifications for case study

Table S2.3 Product quality specifications results for the optimisations using SA

Specification	Product	Base Case	First optimisation		Second optimisation		Third optimisation	
		Value	Value	Diff*	Value	Diff*	Value	Diff*
T5 (°C, volume)	LN	3	2	-1	2	-1	2	-1
	HN	117	117	0	117	0	117	0
	LD	190	190	0	190	0	190	0
	HD	285	285	0	285	0	285	0
	RES	353	353	0	353	0	353	0
T95 (°C, volume)	LN	122	120	-2	120	-2	119	-3
	HN	210	209	-1	209	-1	210	0
	LD	310	305	-5	305	-5	306	-4
	HD	364	366	2	366	2	368	4
	RES	804	805	1	805	1	805	1

Diff* = difference relative to base case values

Table S2.4 Product quality specifications results for the optimisations using GS

Specification	Product	Base Case	First optimisation		Second optimisation		Third optimisation	
		Value	Value	Diff*	Value	Diff*	Value	Diff*
T5 (°C, volume)	LN	3	2	-1	2	-1	2	-1
	HN	117	117	0	117	0	117	0
	LD	190	190	0	190	0	190	0
	HD	285	285	0	285	0	285	0
	RES	353	353	0	353	0	353	0
T95 (°C, volume)	LN	122	119	-3	120	-2	119	-3
	HN	210	209	-1	209	-1	210	0
	LD	310	305	-5	306	-4	306	-4
	HD	364	366	2	366	2	367	3
	RES	804	805	1	805	1	805	1

Diff* = difference relative to base case values

1.3. Distillation column hydraulic results for case study

Table S2.5 Hydraulic results for optimisations using SA

	Section	First optimisation	Second optimisation	Third optimisation
Jet flooding, %	Section 1	74	74	68
	Section 2	75	75	73
	Section 3	74	74	72
	Section 4	62	62	60
	Section 5	52	52	69
	Top SS	43	43	43
	Mid SS	61	61	61
	Btm SS	64	64	63
Weir load, $m^3\ m^{-1}\ h^{-1}$	Section 1	72	72	56
	Section 2	58	58	55
	Section 3	46	46	45
	Section 4	44	44	41
	Section 5	90	90	90
	Top SS	43	43	43
	Mid SS	63	63	64
	Btm SS	39	39	39
DC exit velocity, $m\ s^{-1}$	Section 1	0.3	0.3	0.2
	Section 2	0.2	0.2	0.2
	Section 3	0.2	0.2	0.2
	Section 4	0.2	0.2	0.2
	Section 5	0.4	0.4	0.4
	Top SS	0.2	0.2	0.2
	Mid SS	0.3	0.3	0.3
	Btm SS	0.2	0.2	0.2
DC flooding, %	Section 1	27	27	21
	Section 2	25	25	24
	Section 3	21	21	20
	Section 4	25	25	23
	Section 5	35	34	35
	Top SS	22	22	22
	Mid SS	30	30	30
	Btm SS	29	29	29

Limit for approach to jet flooding (conventional trays and high-capacity trays) = 80%
Limit for liquid weir load = 90 $m^3\ m^{-1}\ h^{-1}$
Limit for downcomer exit velocity = 0.46 $m\ s^{-1}$
Limit for approach to downcomer flooding = 80%
Limit for approach flooding (structured packings) = 80%

Table S2.6 Hydraulic results using GS

	Section	First optimisation	Second optimisation	Third optimisation
Jet flooding, %	**Section 1**	72	72	69
	Section 2	74	74	74
	Section 3	74	74	73
	Section 4	62	62	61
	Section 5	52	52	52
	Top SS	43	43	43
	Mid SS	61	61	61
	Btm SS	63	62	63
Weir load, $m^3\ m^{-1}\ h^{-1}$	**Section 1**	63	70	55
	Section 2	56	58	59
	Section 3	48	47	46
	Section 4	44	44	42
	Section 5	90	90	90
	Top SS	43	43	43
	Mid SS	63	64	63
	Btm SS	39	38	39
DC exit velocity, m s^{-1}	**Section 1**	0.3	0.3	0.2
	Section 2	0.2	0.2	0.2
	Section 3	0.2	0.2	0.2
	Section 4	0.2	0.2	0.2
	Section 5	0.4	0.4	0.4
	Top SS	0.2	0.2	0.2
	Mid SS	0.3	0.3	0.3
	Btm SS	0.2	0.2	0.2
DC flooding, %	**Section 1**	24	26	21
	Section 2	24	25	25
	Section 3	22	21	21
	Section 4	25	25	24
	Section 5	35	34	35
	Top SS	22	22	22
	Mid SS	30	30	30
	Btm SS	29	28	29

Limit for approach to jet flooding (conventional trays and high-capacity trays) = 80%
Limit for liquid weir load = 90 $m^3\ m^{-1}\ h^{-1}$
Limit for downcomer exit velocity = 0.46 m s^{-1}
Limit for approach to downcomer flooding = 80%
Limit for approach flooding (structured packings) = 80%

1.4. Required additional heat transfer are for Case 2

Table S2.7 HEN required additional heat transfer area for optimisations using SA

Heat exchanger number	Additional area required m^2		
	Fist optimisation	**Second optimisation**	**Third optimisation**
h1	0	0	0
h2	181	9	0
h3	112	61	134
h4	125	200	278
h5	222	29	183
h6	862	936	818
h7	149	7	237
h8	0	35	31
h9	0	0	0
h10	50	99	126
h11	0	0	0
h12	0	0	0
h13	0	58	0
h14*	0	0	0
h15*	2	2	2
h17*	16	16	16
h18*	0	0	0
h19*	38	38	39
h20*	31	25	26
h21*	481	471	387
h22*	87	71	42
h24*	0	35	39
Total additional area, m^2	2355	2092	2357
No. of heat exchangers needing modifications	13	16	14

* = Utility heat exchangers

Table S2.8 HEN required additional heat transfer area for optimisations using GS

Heat exchanger number	Additional area required m^2		
	Fist optimisation	**Second optimisation**	**Third optimisation**
h1	0	0	0
h2	233	210	78
h3	12	23	45
h4	0	105	546
h5	0	0	238
h6	946	942	862
h7	656	597	212
h8	0	0	1
h9	0	0	0
h10	51	0	0
h11	0	0	0
h12	162	0	0
h13	0	117	0
h14*	0	0	0
h15*	2	2	2
h17*	16	16	16
h18*	10	0	0
h19*	38	38	39
h20*	18	47	50
h21*	469	357	427
h22*	35	84	65
h24*	10	24	16
Total additional area, m^2	2659	2562	2597
No. of heat exchangers needing modifications	14	13	14

* = Utility heat exchangers

S3. Overview of the optimisations

Figures S3.1 to S3.6 illustrate the overview of the optimisations for the case study [1]. Following previous work [2, 3], the best function value and current function value must be expressed as negative numbers, since simulated annealing (SA) and global search (GS), both from the MATLAB optimisation toolbox, are designed to find the minimum of the objective function. Therefore, the objective function is the negative net profit. Also, in order to avoid large numbers, the net profit is multiplied by 10^{-9} \$ y^{-1}. Large numbers are more difficult to analyse and handle. Also, it was observed that when the objective function was formulated using large numbers, the optimisation times increased and sometimes the 'CPU memory' ran out of space, stopping the optimisation without giving any output.

1.1. Optimisation using SA

Figures S3.1 to S3.3 illustrate the progress of the optimisations for the cases that were simulated using SA. In every figure, the continuous line represents the best function value found on each iteration; the dots represent the actual value found.

Note that compared to the optimisation runs presented in Section S1, the number of unconverged simulations and of penalties applies to the objective function is very low (i.e. less than 0.05%). This suggests that the lower and upper bounds chosen are appropriate.

Table S3.1 History of the optimisations using SA for Case 2

Parameter	First optimisation	Second optimisation	Third optimisation
No. of iterations	2786	2341	2362
Unconverged simulations, %	0	0	0
Function values with penalties, %	0.02	0.03	0.03
Optimisation time, h	6.1	5.2	5.4

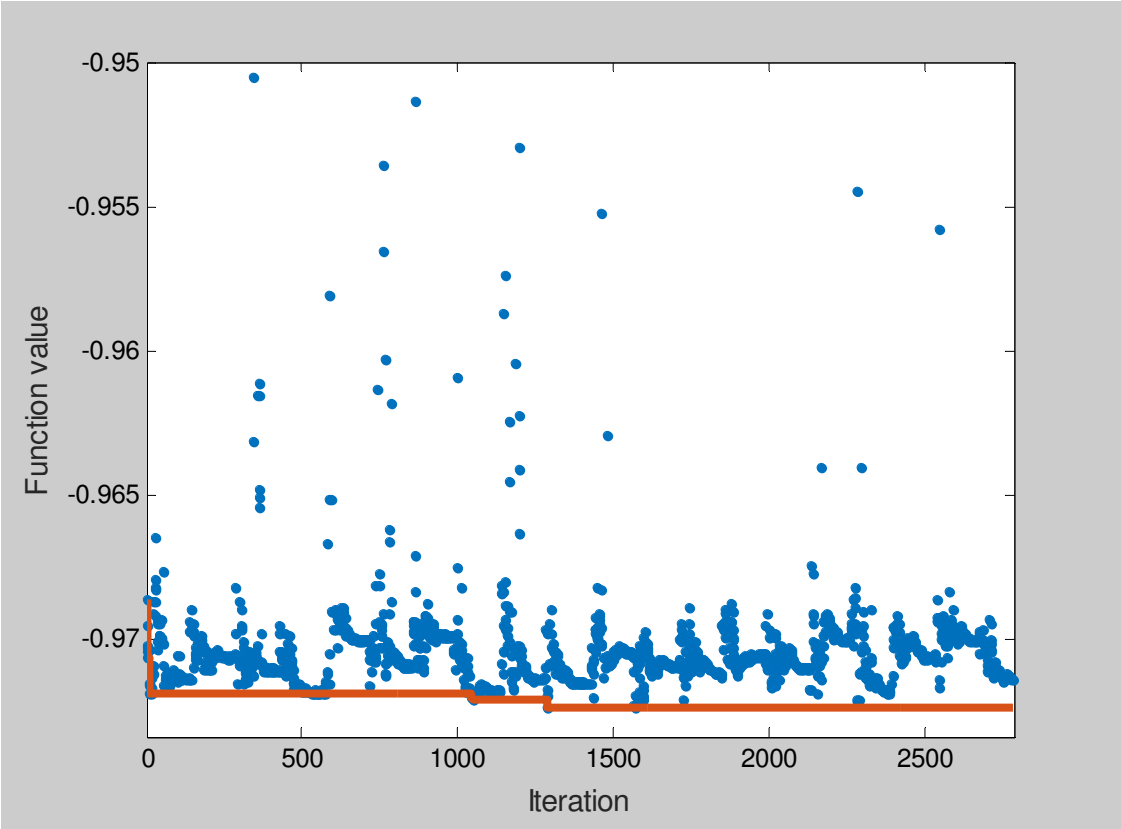

Figure S3.1 Progress of first optimisation using SA for Case 2

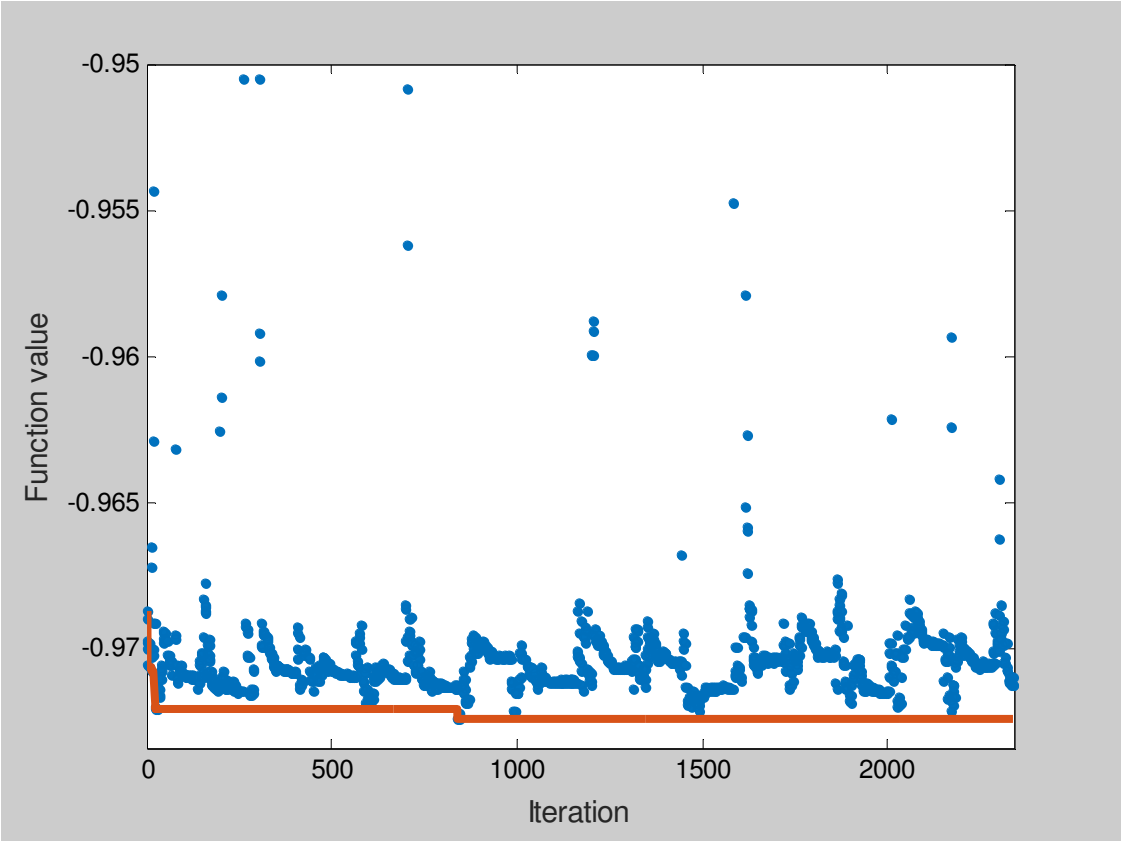

Figure S3.2 Progress of second optimisation using SA for Case 2

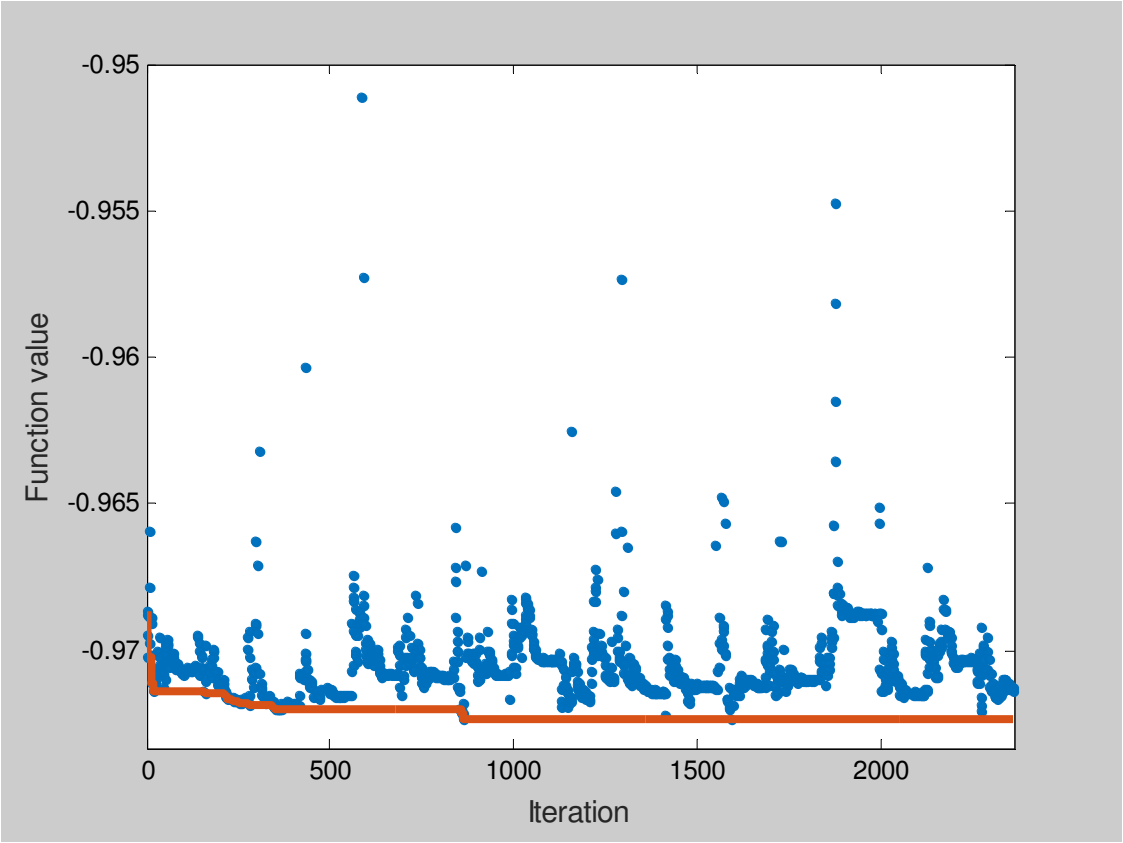

Figure S3.3 Progress of third optimisation using SA for Case 2

1.2. Optimisation using GS

Figures S3.4 to S3.6 illustrate the history of the optimisations using GS. This plot shows the best function value found for every solver call (i.e. fmincon).

Table S3.2 summarises the history of the optimisations. The number of points analysed is between 6500 and 8500, of which around 75 points showed basins of attractions (i.e. steepest descent paths that tend to the same minimum point [4]), which is around 0.01% of all the points analysed.

Note that the optimisation time is almost three times longer than the optimisation times using SA. However, the quality of the solutions is very similar.

Table S3.2 History of the optimisations using GS for Case 2

Parameter	First optimisation	Second optimisation	Third optimisation
No. of iterations	7693	6616	8427
Number of solver calls	77	72	74
Optimisation time, h	19	17	21

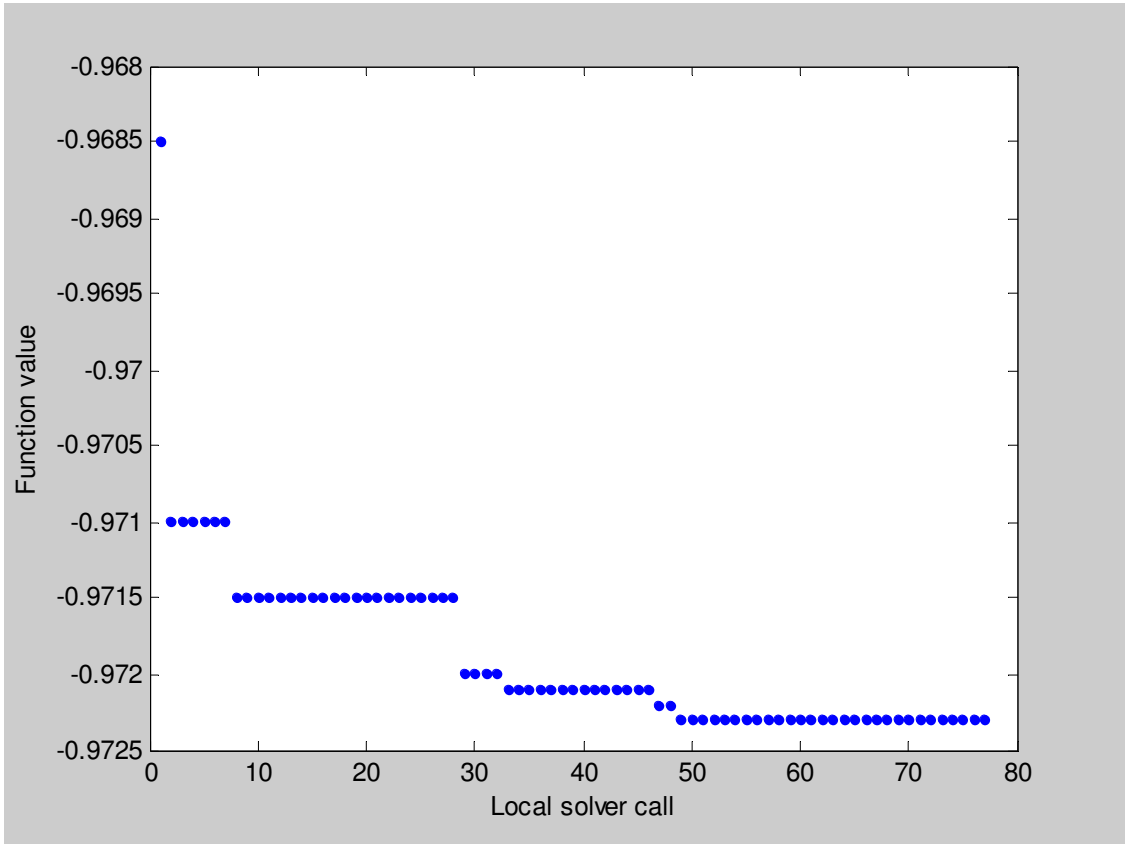

Figure S3.4 Progress of first optimisation using GS for Case 2

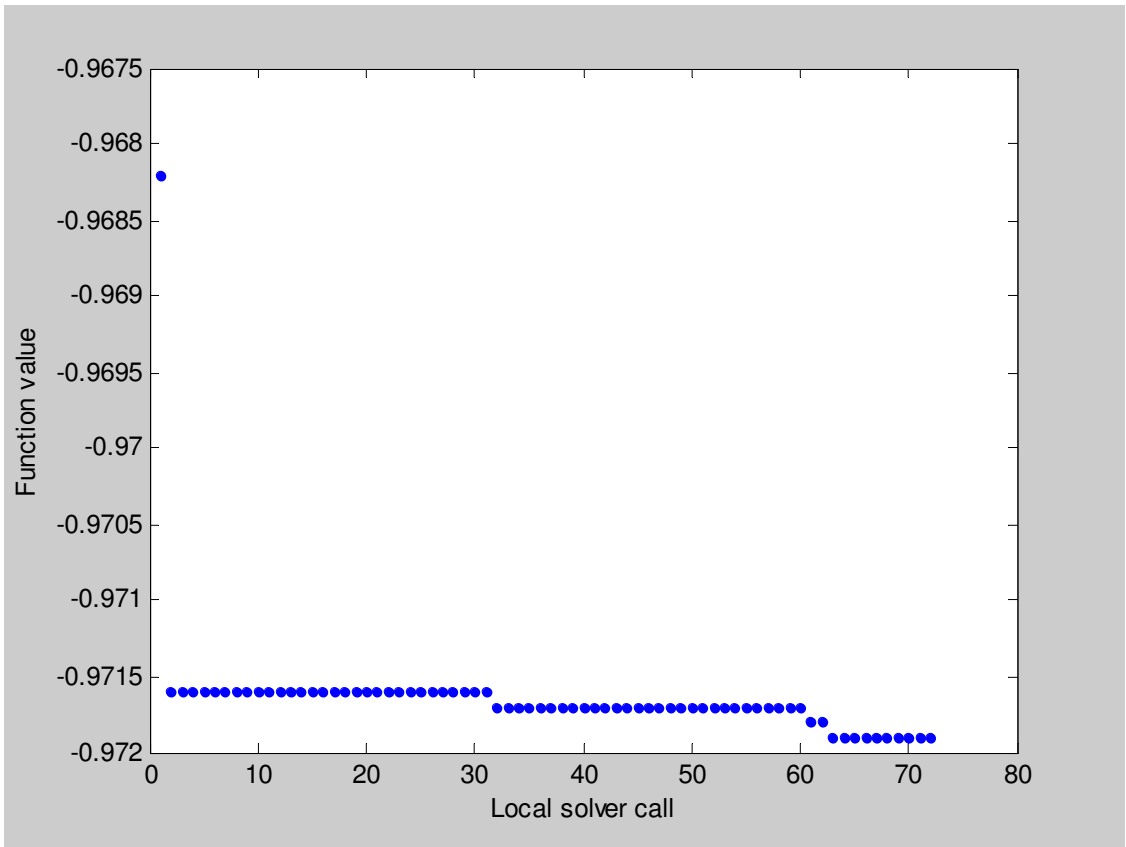

Figure S3.5 Progress of second optimisation using GS for Case 2

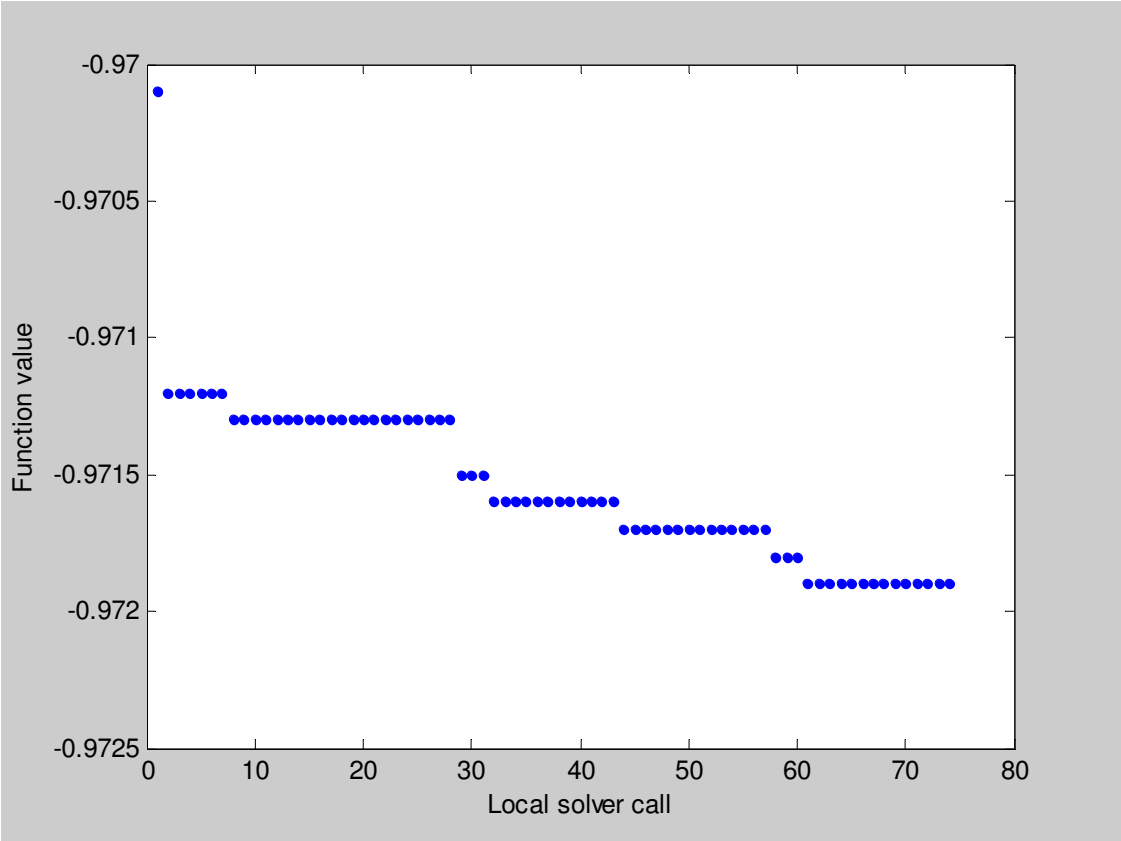

Figure S3.6 Progress of third optimisation using GS for Case 2

References

1. Enríquez-Gutiérrez, V.M. and Jobson, M., An optimisation-based retrofit approach for the assessment of structural and flowsheet modifications for heat-integrated crude oil distillation systems. Part 2.- Adding a preflash unit. *Chemical Engineering Research & Design*, **2016**. *submitted May 2016*.
2. Enríquez-Gutiérrez, V.M. and Jobson, M., An optimisation-based retrofit approach for the assessment of structural and flowsheet modifications for heat-integrated crude oil distillation systems. Part 1.- Replacing column internals. *Chemical Engineering Research & Design*, **2016**. *submitted May 2016*.
3. Enríquez-Gutiérrez, V.M. and Jobson, M., An optimisation-based retrofit approach for increasing the processing capacity of heat-integrated crude oil distillation systems. *Chemical Engineering Research & Design*, **2016**. *submitted May 2016*.
4. MATHWORKS. *Basins of attraction*. 2015 [access date October 2015]; Available from: http://uk.mathworks.com/help/gads/what-is-global-optimization.html#bsbalkx-1.